PREPARATION, PROPERTIES, AND APPLICATIONS OF BENZOXAZINES

Thesis submitted to the Delhi Technological University

for the award of the Degree of

DOCTOR OF PHILOSOPHY

By

PRATIBHA SHARMA
(2K14/PhD/AC/04)

DEPARTMENT OF APPLIED CHEMISTRY

DELHI TECHNOLOGICAL UNIVERSITY

BAWANA ROAD, DELHI-110042

JANUARY 2018

PREPARATION, PROPERTIES, AND APPLICATIONS OF BENZOXAZINES

Thesis submitted to the Delhi Technological University

For the award of the Degree of

DOCTOR OF PHILOSOPHY

By

PRATIBHA SHARMA
(2K14/PhD/AC/04)

DEPARTMENT OF APPLIED CHEMISTRY

DELHI TECHNOLOGICAL UNIVERSITY

BAWANA ROAD, DELHI-110042

JANUARY 2018

Dedicated

To

My Parents

DECLARATION

I hereby declare that this PhD thesis entitled "**Preparation, Properties and Applications of Benzoxazines**" was carried out by me for the degree of Doctor of Philosophy under the joint guidance and supervision of Prof. Devendra Kumar, Department of Applied Chemistry, Delhi Technological University and Dr. Prasun Kumar Roy, Centre for Fire, Explosive and Environment Safety, Delhi.

This thesis is a presentation of my original research work. Wherever contributions of others are involved, every effort has been made to indicate this clearly.

For the present thesis, which I am submitting to the University, no degree or diploma has been conferred on me before, either in this or in any other University.

Pratibha Sharma

Delhi Technological University

I

CERTIFICATE

This is to certify that the thesis entitled **"Preparation, Properties and Applications of Benzoxazines"** submitted by **Ms. Pratibha Sharma** to **Delhi Technological University**, for the award of the degree of "Doctor of Philosophy" is a record of bonafide work carried out by her. Ms. Pratibha Sharma has worked under our guidance and supervision and has fulfilled the requirements for the submission of this thesis, which to our knowledge has reached requisite standards.

The results contained in this thesis are original and have not been submitted to any other university or institute for the award of any degree or diploma.

<table>
<tr><td>**Dr. P. K. Roy**</td><td>**Prof. D. Kumar**</td></tr>
<tr><td>Scientist 'F'
Centre for Fire, Explosive and
Environment Safety (CFEES, DRDO)
Delhi-110054</td><td>Professor
Department of Applied Chemistry
Delhi Technological University (DTU)
Bawana Road, Delhi-110042</td></tr>
</table>

Prof. Archna Rani

Head of Department
Department of Applied Chemistry
Delhi Technological University (DTU)
Bawana Road, Delhi-110042

ACKNOWLEDGEMENT

ABSTRACT

The motivation behind the present research work is to develop low temperature curing sustainable benzoxazines which exhibit enormous potential to compete with the existing petro-based advance performance. This can be achieved through two approaches i.e., structural modification and physical blending of curing accelerator in the resin. Cardanol was chosen as renewable alternative of petro-based phenol which acts as a reactive diluent and aids solventless synthesis of benzoxazine resins.

A microwave assisted synthetic (MAS) route was explored as a sustainable tool for the preparation of benzoxazine resins. In comparison to the conventional methodology, the reaction completion time could be significantly reduced using MAS technique and the sustainability of the procedure was improved. Microwave active bifunctional amines were prepared by the condensation reaction of p-aminobenzoic acid and poly(ethylene glycol)s of different chain lengths to yield amine terminated poly(ethylene glycol)s (ATPEGs). Cardanol, an agro-waste was chosen as the phenolic source, which was reacted with ATPEG to undergo Mannich like condensation resulting in a reactive thermoplastic of telechelic nature. The structure of the resulting monomer was confirmed through Fourier transform infrared (FT-IR) and proton nuclear magnetic resonance (^{1}H-NMR) spectroscopy. Benzoxazine moieties present at the terminals undergo thermally accelerated ring opening polymerization to form cross-linked networks which was studied using non-isothermal differential scanning calorimetry (DSC). The rheological behavior of the resulting polymer suggests that the viscosity of the benzoxazine-endcapped telechelic poly(ethylene glycol)s is sufficiently low to permit solventless processing which can be credited to the presence of flexible polyether linkages. The adhesive properties of

the cross-linked benzoxazine endcapped telechelic poly(ethylene glycol)s have also been studied.

Sustainable bis-benzoxazine resins with amide linkages were synthesised where the effect of inclusion of amide linkages in the monomer is expected to result in a monomer with lower polymerisation temperature and better adhesive properties. Polyethylene terephthalate (PET) was chosen as a sustainable feedstock for the amine fraction used to prepare benzoxazine monomer containing amide linkages. Microwave assisted aminolysis of PET was performed to obtain bis-(amino-ethyl) terephthalamide (BAET) and α,ω-aminoligo(ethylene terephthalamide) (AOET), which were employed as the difunctional amine for the preparation of bis-benzoxazines. In comparison to traditional method, microwave assisted aminolysis of PET was found to be significantly faster and the reaction completion time could be brought down appreciably. Mannich like condensation of cardanol with PET derived terephthalamides and paraformaldehyde led to the formation of bis-benzoxazines with amide linkages, the structure of which was confirmed through FT-IR and ^{1}H-NMR spectroscopy. The curing behavior of bis-benzoxazines was studied using non-isothermal differential scanning calorimetry. The presence of amide linkages in addition to the polar group formed during the ring opening of benzoxazines led to the improvement in adhesive strength which was quantified in terms of lap shear strength. In addition, urea linkages were introduced in the polybenzoxazine network through ring opening polymerisation of a benzoxazine monomer containing urea linkages. The amine co-reactant for the synthesis of benzoxazine monomer was derived by the additive rearrangement of 4,4'-methylenebis(phenyl isocyanate) (MDI) with ethylene diamine, which underwent Mannich like condensation with cardanol and

VI

paraformaldehyde to yield bio-based benzoxazine monomer containing urea linkages. The structure of the amine and the benzoxazine monomer was characterized by FT-IR and ^{1}H-NMR. Benzoxazine monomer undergoes thermally accelerated ring opening polymerization to form cross-linked networks, which has been demonstrated using rheometry and non-isothermal differential scanning calorimetry. The presence of alternating urea linkages in the benzoxazine network improves the adhesive properties of the resin, which was quantified in terms of Lap shear strength. Thermal degradation of the cross-linked copolymer has also been studied by thermogravimetric analysis (TGA).

Curing accelerators were also explored to lower the polymerisation temperature of the bio-based benzoxazine resins. A representative bio-based benzoxazine resin was synthesized by mannich type condensation of cardanol and aniline with formaldehyde under solventless conditions, the structure of which was confirmed using FTIR and ^{1}H-NMR. The curing behaviour of the synthesized resin has been systematically investigated using non-isothermal differential scanning calorimetry. Metal organic frameworks, in view of their high surface area and catalytic activity, are potential candidates for curing accelerators. MOFs have been solvothermally synthesized and characterized using different techniques including powder X-ray diffraction (PXRD), Scanning Electron Microscopy (SEM), TGA, FT-IR and nitrogen physisorption measurements. Introduction of MOFs led to a shift in the curing profile to lower temperature, the extent of which was proportional to the amount of MOFs in the formulation. The activation energy associated with the curing of the resin, has been calculated using Kissinger Akahira Sunose method, was found to concomitantly decrease from 98 to 58 kJ/mol upon addition of MOF-5 (5% w/w).

Most of the curing accelerators are moisture sensitive, which adversely affect the end performance of the polymer. In this context, the potential of stearates based on transition metals as curing accelerators for the polymerization of cardanol based benzoxazine resin has been demonstrated. Metal stearates were formulated with bio-based monomer which leads to significant lowering of the curing profiles, the extent of which was proportional to the amount of accelerator. The hydrophobicity associated with the long alkyl chain in stearate bestows it hydrolytic stability, which allows its use under ambient conditions without special caution. Kinetic parameters associated with polymerization of the resin were established using Kissinger Akahira Sunose method.

Cardanol-aniline benzoxazine resin was microencapsulated in different polymeric shell walls for temperature triggered healing applications following two approaches. The very first approach which was adopted is solvent evaporation, a "physical" entrapment of monomer and is relatively less complex methodology which is routinely employed for the encapsulation of drugs for pharmaceutical applications. The monomer was encapsulated in poly(styrene) (PS) shells by solvent evaporation technique to obtain spherical microcapsules. The procedure was optimized by studying the effect of operating parameters, particularly stirring speed and PS concentration on microcapsule dimensions and core content. Spherical microcapsules with a core content of ~39 % were obtained when the reaction was carried out at 500 rpm, while maintaining the reaction medium at 60°C with 2 % w/v concentration of PS in feed solution. In addition, the resin is successfully microencapsulated in cross-linked epoxy microspheres through interfacial engineering. The encapsulation process relies on the preferential reaction of polydimethylsiloxane immiscible epoxy resin and

amine based hardener to form a crosslinked spherical shell at the interface.The microcapsule dimensions and core content could be tailored by modulating the operating parameters, particularly stirring speed and Bz-C:epoxy ratio. Spherical microcapsules with a core content of ~37% were obtained when the reaction was carried out at 600 rpm, while maintaining the reaction medium at 70°C with Bz-C: epoxy ratio of 2.3:1.

CONTENTS

X

XI

XIII

LIST OF FIGURES

XV

230 °C

XVI

benzoxazine molecule and the pore size of MOF-5.

XVIII

XIX

LIST OF TABLES

ABBREVIATIONS

a	aniline
C	cardanol
BA	Bisphenol-a
CNSL	Cardanol nut shell liquid
DSC	Differential scanning calorimetry
MAS	Microwave assisted synthesis
PEG	Polyethylene glycol
ATPEG	Amine terminated polyethylene glycol
PET	Polyethylene terephthalate
BAET	bis(2-amino ethyl) terephthalamide
AOET	α,ω-aminoligo(ethylene terephthalamide)
ED	Ethylene diamine
LSS	Lap shear strength
MDI	4,4'-Methylenebis(phenyl isocyanate)
AMDI	4,4′-Methylenebis(3-ethylamine-1-phenylurea)
MOF	Metal organic framework
PDMS	Polydimethylsiloxane
TETA	Triethylenetetramine
PS	polystyrene
SEM	Scanning electron microscopy
FST	Fire smoke toxicity
T_g	Glass transition temperature
PABA	Para-aminobenzoic acid
ppm	parts per million
ROM	Ring opening polymerisation
TGA	Thermogravimetric analysis
δ	Chemical shift

Chapter 1
Introduction
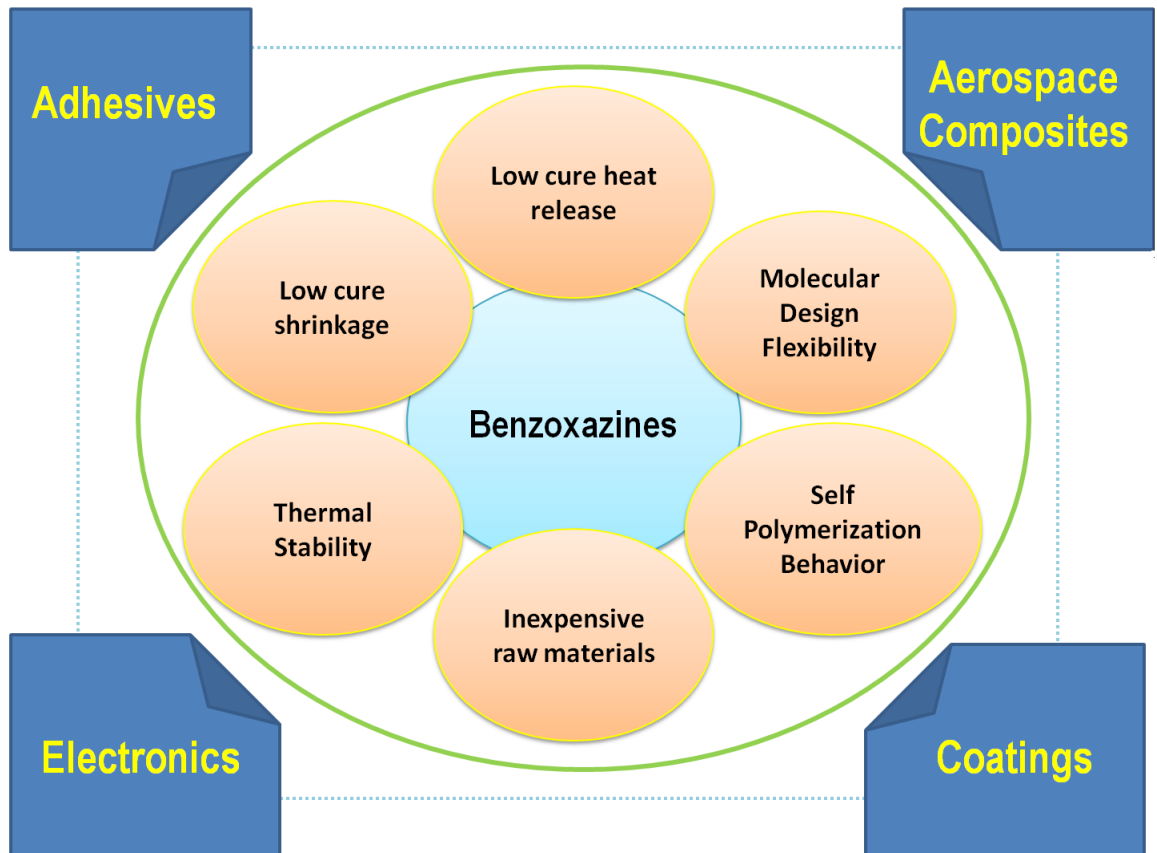
1.1 Polybenzoxazines

Polybenzoxazines are an emerging class of phenolic thermosetting resins and are strong contenders of imides and epoxies. Polybenzoxazines are one of the rarely existing non-halogenated materials that satisfy all the performance requirements for structural composites. Subsequent to its discovery in 1940s, Huntsman Advanced Materials started working with it in 1980s, followed by Henkel AG & Co. KGaA. Polybenzoxazines qualified as materials for printed-circuit boards (PCBs) in the year 2000 and is being used for structural composites in 2008. LOCTITE series of benzoxazines developed by Henkel specifically for the aerospace industry, offers performance, storage, processing, health and safety benefits over commonly employed epoxies, phenolics and BMIs. Consequently, tests to qualify benzoxazines prepegs according to OEM programs and material system baselines are in progress for the Airbus A380 and Comac C919. Polybenzoxazines are potential candidates for both primary and secondary structure applications in all ranges of service temperatures and toughness. These resins are formulated and supplied in prepreg format, where these are produced solventlessly using hotmelt processing.

Ever since Holly and Cope presented the first paper on the synthesis of a heterocyclic compound termed benzoxazine in 1944[1], many papers on this class of compounds have been published. Burke et al. in 1950-60s made significant contribution in the fundamental understanding of the chemistry of benzoxazine molecules[2-9]. In the early 1970s, Schreiber patented the synthesis of small benzoxazine oligomers, which could be employed as a modifier for epoxy resins. Higginbottom, in 1980s, was the first to report the synthesis of cross-linked polybenzoxazines from multifunctional benzoxazines, however the properties of developed polybenzoxazine were not

reported[10-12]. Riese et al. studied the kinetics of oligomerization in monofunctional benzoxazines and reported that the polymerization of monofunctional benzoxazines result in linear polybenzoxazines with molecular weights in the range of few hundreds to a few thousands[13]. Turpin and Thrane, in their patent reported self-polymerizable benzoxazine formulations functionalized with cathodic electrocoat resin[14]. Interestingly, ever since the discovery of benzoxazines in the early 1940s, the mechanical properties of the resin were first studied and reported in 1994 by Ishida et.al[15]. Benzoxazines can be broadly classified as shown in **Figure 1.1**.
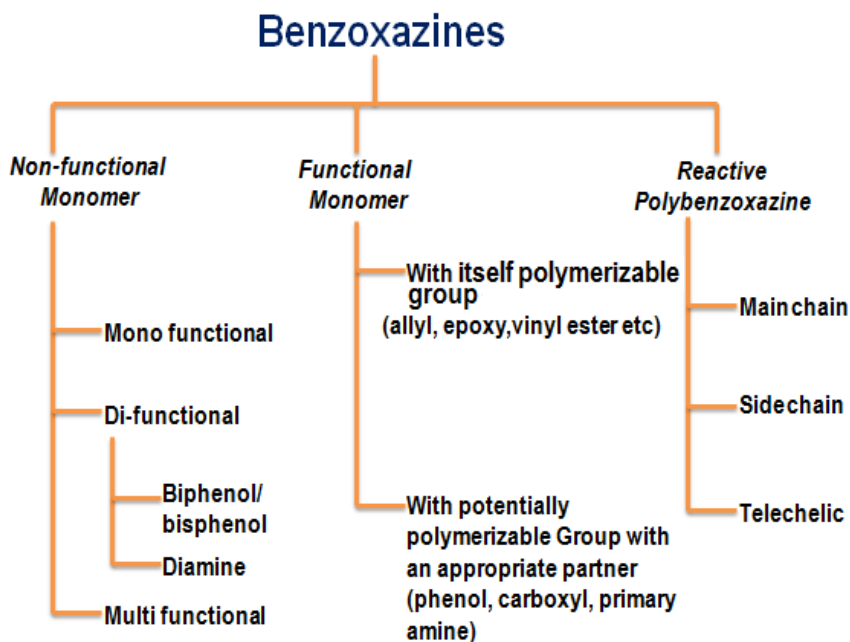
Figure 1.1: Classification of benzoxazines

Benzoxazines are relatively inexpensive materials with handling and processing advantages and exhibit interesting properties given as follows:

- These resins exhibit negligible shrinkage post polymerization and are ideal from the perspective of demolding and diminishing of residual stress[16-18].

2

- Polybenzoxazines exhibit lower water absorption than polyesters, epoxies, bismaleimides and polyimides resins, although the structure comprises of polar groups such as –OH groups and mannich base linkages $-CH_2NCH_2-$ in each repeating unit. The property is advantageous in the context of dielectric applications of polymer. Moreover, the difference in the glass transition temperatures in dry and wet conditions is rather negligible[19].

- Polybenzoxazines possess high glass transition temperatures (T_g) ranging from approximately 150 to 400°C, which do not coincide with the polymerization temperature (T_{cure}) of the resin thereby offering a significant processing advantage[20, 21]. For example, 4,4'-dihydroxybenzophenone and aniline-based benzoxazine exhibits a T_g of 350°C, when polymerized at 290°C for 1h. Post curing at this temperature leads to further increase in T_g (~385°C), in view of the possibility of local motions in polymer chains and structural rearrangements[20].

- Unlike condensation polymers, polybenzoxazines develop their mechanical and thermal properties rapidly as the polymerization proceeds and exhibit excellent mechanical properties at even lower degree of polymerization[22, 23].

- Higher char yield is an essential criterion in the context of flame retardance of any material. Polybenzoxazines, although having a high aliphatic content, leave behind high char yield (35-75 %), which bestow flame retardant properties to the polymer[20].

These interesting properties of benzoxazine resins open up new vistas of applications. Benzoxazines based on phenolphthalein, exhibit high glass transition temperatures,

3

which make them a potential candidate for use in the production of high-temperature performance adhesives[24]. In addition to this, good moisture resistance of benzoxazines improves their adhesive performance for industrial applications as well as in the manufacturing of aerospace components[19].

Benzoxazines exhibit sufficiently low viscosity during processing conditions which allows formulation of prepregs desired in fabrication of aerospace composites as well as systems for resin transfer molding. High-performance benzoxazine resins can survive exposure to challenging environments and high temperature conditions for hard-hitting industrial applications suggesting their use for retro-fitting coating applications. As already mentioned, polybenzoxazines laminates based on dicyclopentadiene and phenolphthalein are used in printed wiring boards in view of their good FST and electrical properties[25].

1.2 Chemistry of benzoxazines

Benzoxazine is a heterocyclic molecule, which comprises of an oxazine ring attached to a benzene ring. Depending on the relative positions of the heteroatoms in the oxazine ring, various benzoxazine structures[21] are possible and are presented in **Figure 1.2**.
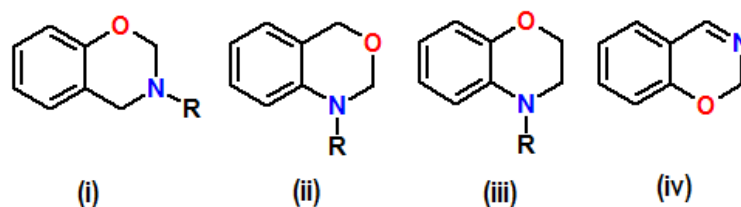
Figure 1.2: Structures of benzoxazine molecules. (i) 3-methyl-2H,4H benzo[e]1,3oxazine; (ii) 1-methyl-2H,4H-benzo[d]1,3-oxazine;(iii) 4-methyl-2H,3H-benzo[e]1,4-oxazine; and (iv) 2H-benzo[e]1,3-oxazine.

3-methyl-2H,4H benzo[e]1,3-oxazazine(**Figure 1.2(i)**), commonly abbreviated as 1,3-benzoxazine undergo cationic ring opening polymerization resulting in a value added industrially significant polymeric material. 1,3-benzoxazine monomer can be readily synthesized by Mannich like condensation of a phenolic derivative, formaldehyde, and a primary amine (**Figure 1.3**), where R and R$^{'}$ are substituents.
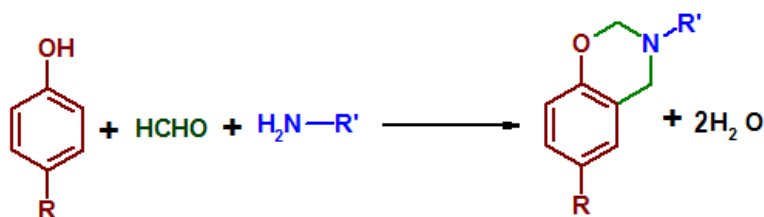
Figure 1.3: Synthesis of benzoxazine resin

The yield of the benzoxazines monomer is ~70-90% and depends on the reactants, temperature, time, solvent, and synthetic methodology. Solvent-less approach for the preparation of the benzoxazine monomer has been reported to be more efficient[26, 27] in comparison to the conventional method using a solvent[28]. Solvent-less approach is usually employed for the reaction systems, where at least one of the co-reactants is liquid or the combination reduces the liquefaction temperature of all the reactants. Several studies have been performed to understand the role of reaction conditions, especially reaction temperature on the purity of the monomer. In general synthesis of the monomer at T<150°C has been reported to minimize oligomerization[21, 29]. When prepared in the presence of solvent, benzoxazine monomers have a propensity to retain small amounts of solvent and impurities, which are difficult to purify. The resultant benzoxazines thus exist as liquids at room temperature, unlike the purest form of benzoxazines which tend to crystallize.

The 1,3-benzoxazine monomer undergoes thermally accelerated cationic ring opening polymerization (ROP) which can be initiated both in the presence or absence of an

5

external initiator. Labile proton initiators such as phenol, traces of which are present in the form of impurity, lead to a thermally stable phenolic structure of the cross-linked polymer. On the other hand, a non labile proton initiator (e.g. lewis acids) results in a thermally unstable aryl ether structure of the polybenzoxazine. However at elevated temperatures, the aryl ether structure of the polybenzoxazine rearranges to give phenolic structure[21](**Figure 1.4**).
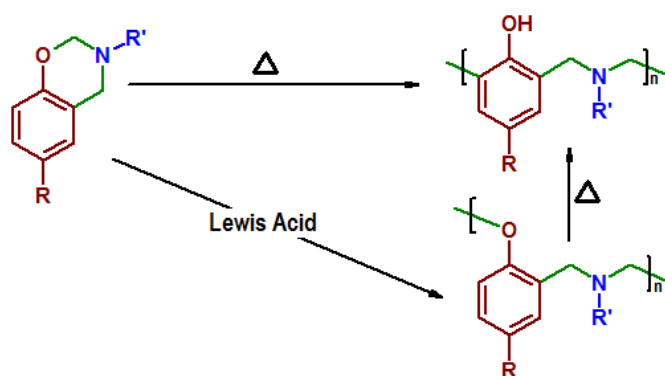
Figure1.4: Cationic ring opening polymerization of benzoxazine

It is to be noted, that the thermally accelerated ring opening polymerization in 1,3-benzoxazines is not to be confused with thermal polymerization, as the latter is initiated by the homolytic scission of a bond generating free radicals, which subsequently undergo polymerization through free radical mechanism. On the other hand, heating accelerates the rate of polymerization and is more appropriately referred to as thermally accelerated or activated ring opening polymerization. Crystal studies of the monomeric and multifunctional benzoxazine compounds are indicative of the presence of ring strain in the six-membered heterocyclic oxazine ring, which appears to have an irregular chair structure. The ring strain acts as a driving force for the polymerization reaction. Any structural modifications in the monomer which

6

increases the ring strain, is therefore expected to form resins which are curable at lower temperatures[30-33].

The auto-catalytic ring opening polymerization of benzoxazine monomers leads to the formation of polybenzoxazines[34]. The structure of two representative benzoxazine monomers: phenol-aniline (P-a) and bisphenol A-aniline (BA-a) and the polybenzoxazines formed (poly(P-a) and poly(BA-a)) by thermally accelerated ring opening polymerization are presented in **Figure1.5.**
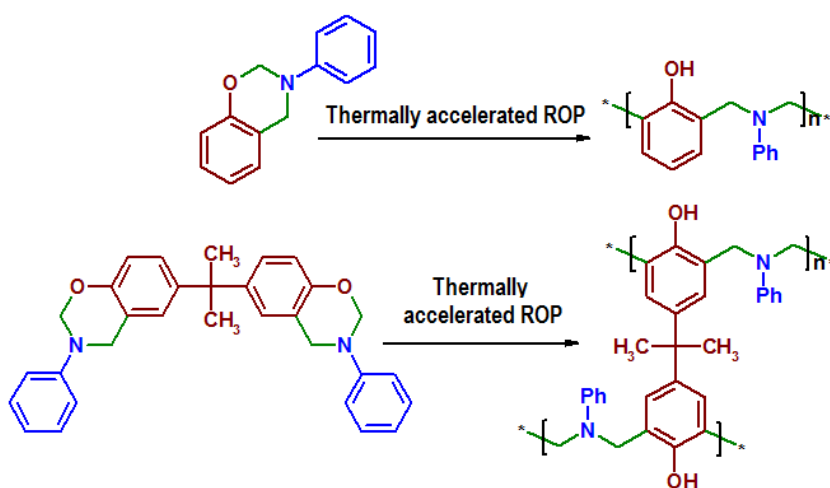
Figure 1.5: Polymerization of benzoxazine monomers (P-a and BA-a).

Several attempts have been reported towards studying the mechanism of polymerization of benzoxazine monomers and several ionic mechanisms have been proposed[13, 35-41]. By monitoring the reactive intermediates generated, several approaches for polymerization have been proposed, which are discussed in the following section. The polymerization in benzoxazine monomer can be initiated at any of the basic sites i.e., oxygen or the nitrogen of the oxazine ring; therefore, it has been proposed that the ring-opening polymerization of the benzoxazine proceeds through a cationic mechanism[35].

7

Wang and Ishida[39] proposed that either the nitrogen or the oxygen associated with the oxazine ring is attacked by a cationic initiator resulting in a cyclic tertiary oxonium ion. This is followed by an insertion step where the monomer, in view of its basicity, attacks the electrophilic site leading to the formation of a Mannich base like product. The repetition of these steps result in a thermally stable phenoxy type polybenzoxazine structure as illustrated in **Figure 1.6.**

Figure 1.6: i) Nitrogen initiator mechanism, and ii) Oxygen initiator mechanism

The polymerization of a benzoxazine monomer having an unobstructed ortho position has been reported to propagate via the insertion of the monomer by the reaction of ortho position at the cyclic tertiary oxonium ion generating a phenolic type Mannich base as shown in **Figure 1.7**[39]**.**
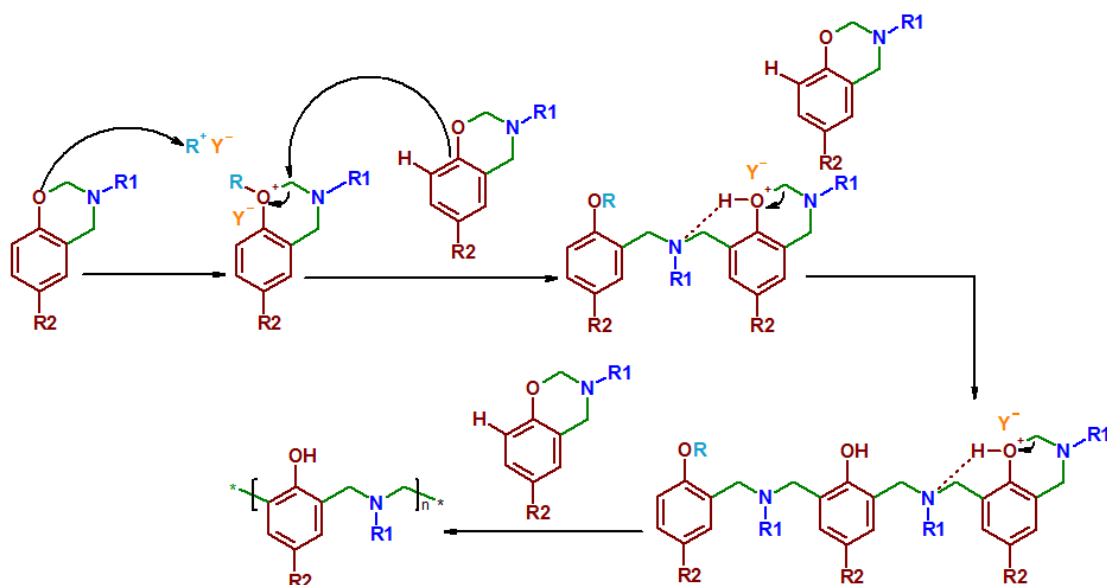
Figure 1.7: The reaction mechanism of the unobstructed benzene ortho-position

As already mentioned, the ring opening polymerization is initiated by the protonation of either the nitrogen or the oxygen atom. It was observed that the resulting oxygen protonated species is relatively more reactive whereas the nitrogen protonated species is stable, as indicated in **Figure 1.8**[41]. Hence, the polymerization propagates through oxygen protonation followed by the repetitive monomer insertion steps. Polybenzoxazines with phenolic structure are known for their excellent thermal properties, regardless of the presence of usual Mannich bridge ($-CH_2-N(R)-CH_2$) in every repeating unit of polymeric network. Majority of polybenzoxazines exhibit thermal degradation at high temperatures (>300ºC), as evidenced by their thermogravimetric analysis (TGA). It is to be mentioned that the usual Mannich linkages degrades at lower temperature and undergoes reverse Mannich reactions[42].

9
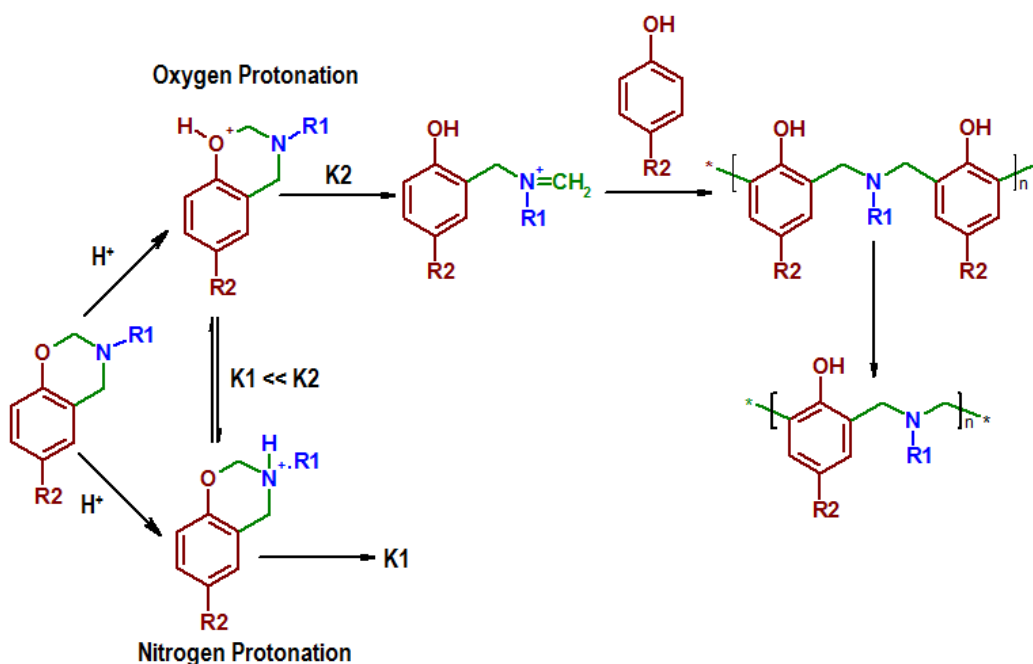
Figure 1.8: Protonation initiation proposal of benzoxazine monomers by Chutayothin and Ishida.

However, in polybenzoxazine network, these Mannich bridges are stabilized by the very stable six-membered inter- and intramolecular hydrogen bonding as shown in **Figure 1.9.** It is this hydrogen bonding which is to be credited for most of the unique features of polybenzoxazine network[43, 44].
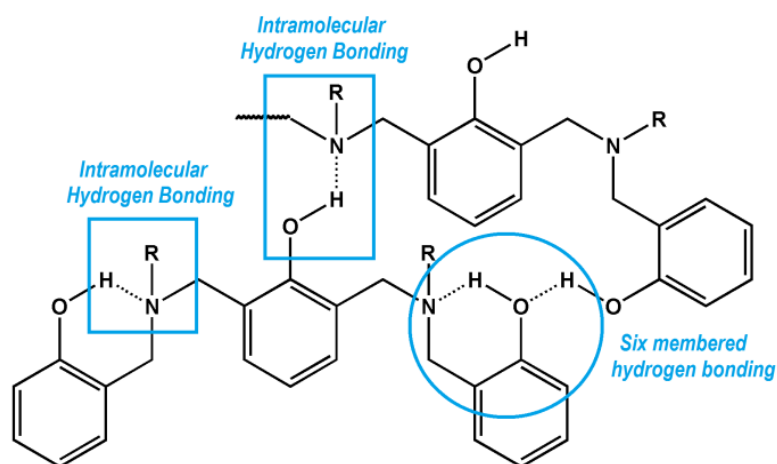
Figure 1.9: Hydrogen bonding formation in polybenzoxazine network.

1.3 Polybenzoxazines based on natural sources

In view of the increasing oil prices, global warming, and other environmental concerns, a lot of attention has been directed towards the exploration of sustainable raw materials, which can effectively substitute or replace petro-based chemicals. The current challenge for researchers is to improve the sustainability of the procedures, desired to maintain the balance between the growing requirements of today's world while preserving the nature. Advancement in polybenzoxazine technology has been limited to petro-based feed-stocks since 1940s. The flexibility offered by the benzoxazine chemistry, which involves phenols and amines as co reactants, allows the conversion of natural resources into readily advanced polymers. It is worth mentioning, that formaldehyde is already within the area of influence of biomethanol[45]. The first attempt to derive bio-based benzoxazines was reported in 1999, and ever since, both the academies as well as industry have focused their energies towards exploration of renewable resources to obtain sustainable alternatives of phenols and amines.

Naturally derived amines are relatively fewer in number, due to their lesser availability in nature's stock. However phenols, which are the secondary metabolites of plants, are widely distributed in plant kingdom in the form of single-ring molecules or highly polymerized substrates[46]. In plants, phenolics are genetically synthesized following two main pathways: the shikimate, and the polyketide (acetate) pathway. In shikimate path, phenyl propanoids such as hydroxycinnamic acids and coumarins are obtained directly, whereas the polyketide path leads to simple phenols and quinones. Largest fraction of natural phenols is obtained from flavonoids, which are the biogenetic resultant of the combination of these two pathways. It is to be noted that

easily derivable phenols present in nature can act as effective substitutes of petro based phenolic compounds. Taking into consideration the abundance and the economically feasible extraction methods, few of the naturally occurring phenols which have been used for the synthesis for benzoxazine monomers are listed in **Figure 1.10.**
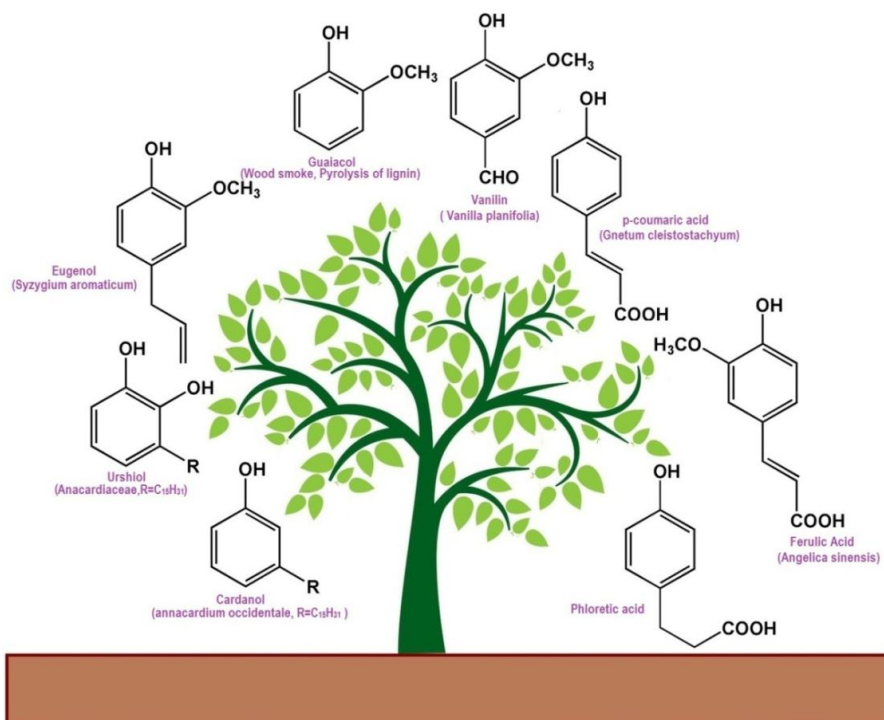
Figure 1.10: Plant derived phenols used for the synthesis for benzoxazine

monomer[46]

Numerous publications have reported the utilization of bio-origin phenols such as eugenol[47-49],vanillin[50-52], urushiol[53, 54], rosin[55] and lignin based phenols such as guaiacol[56], ferulic, coumaric, phloretic acid[57] in the context of their potential for benzoxazine synthesis. However, their food based origin, latent toxicities, complex structure and a major challenge in terms of mass scale production has led to innovative exploration of cardanol as a phenolic substitute. The advantages of cardanol include its non-food agro waste origin, commercially viable extraction

process and huge tonnage production at cheaper exportable prices (US$1232.33/metric tonne)[58]. Cardanol is obtained by vacuum distillation of "cashew nut shell liquid" (CNSL), which is an alkyl phenolic oil contained in the spongy mesocarp of the cashew nut shell from the cashew tree Anacardium occidentale L. However, natural CNSL contains other three components: anacardic acid, cardol, and 2-methyl cardol, being anacardic acid the main component (~75%). Nevertheless, cardanol is the main component of commercial grade CNSL because anacardic acid decarboxylates to cardanol during the roasting process used industrially to extract the oil from cashew nuts. The use of cardanol based benzoxazines as the matrix material for fiber-reinforced composites is well reported [59, 60]. The long alkyl chain present in cardanol acts as an intramolecular plasticizer [61, 62], which reduces the viscosity of the resin and renders it suitable as a reactive diluent for commercial benzoxazine resin[63, 64]. The alkyl chain also increases the flexibility of molecular segments which reflects in their lower glass transition temperature (T_g)[65], however the same leads to higher curing temperatures[63].

Calo et. al was first to report the solvent-less synthesis of monofunctional benzoxazine resin (C-a) employing cardanol and aniline as starting materials. The resin is commercially available with Huntsman & Co. under the name of XU 35500. In this thesis, C-a resin has been considered as a reference for comparing the properties of the newly developed bio-based benzoxazine monomers. To prepare the resin for the present study, a mixture of cardanol (5.00 g, 16.6 mol), paraformaldehyde (1.00 g, 33.2 mmol) and aniline (1.51 mL, 16.6 mmol) was gradually heated to 80°C and stirred for an hour, followed by heating at 90°C for 2 h. The reaction led to the evolution of water and the colour of the reaction medium

13

changed from yellow to red brown. Upon cooling, water (10 mL) was added and organic layer was extracted with chloroform (20 mL). The organic layers were combined and washed with aqueous NaOH solution (0.5 N, 100 mL) followed by washing with water (3 x 30 mL), drying over sodium sulphate and filtration. The solvent was removed under reduced pressure to give C-a as a red oil with a yield of ~95 %. The detailed characterization of the synthesized resin is presented in **Figure 1.11**.
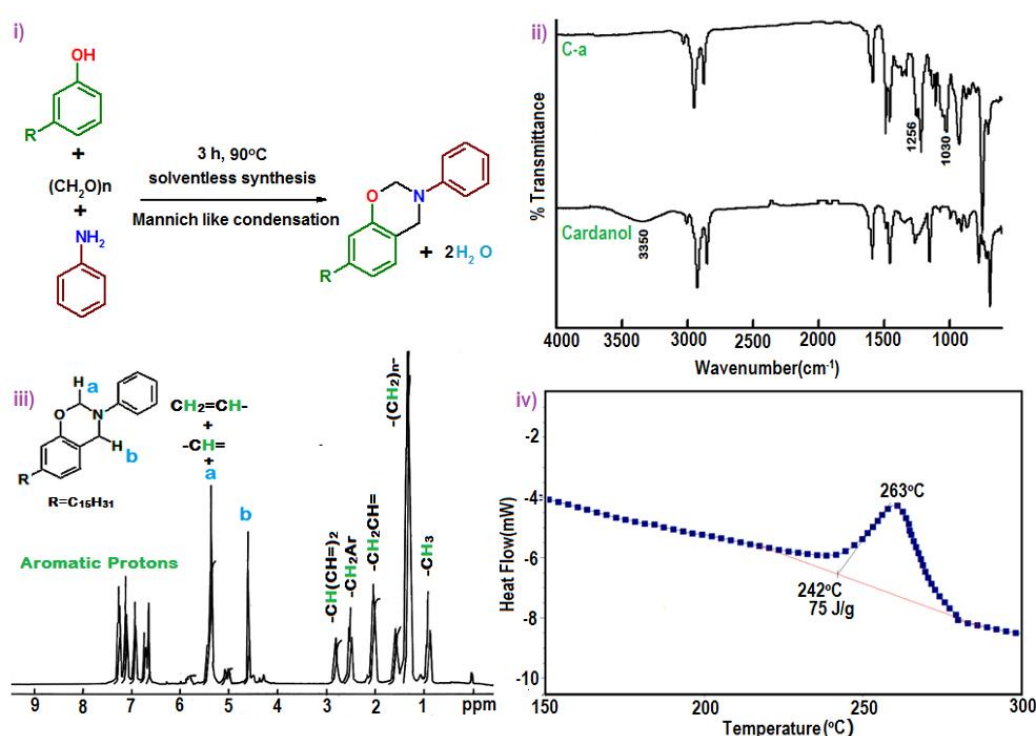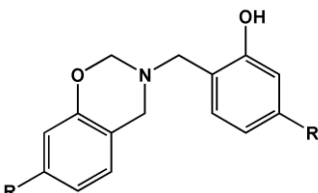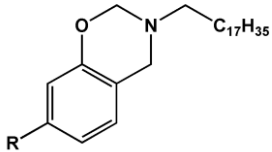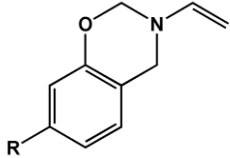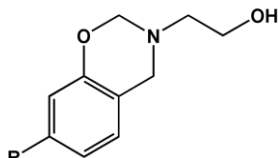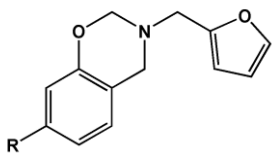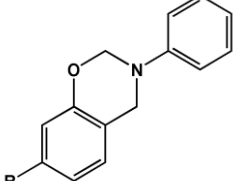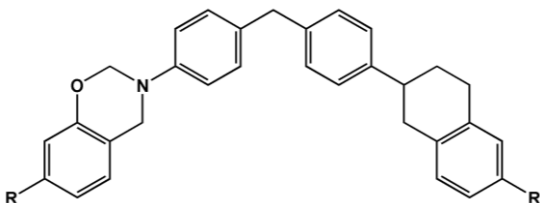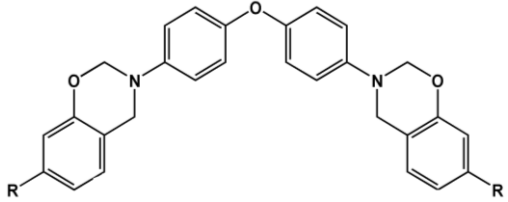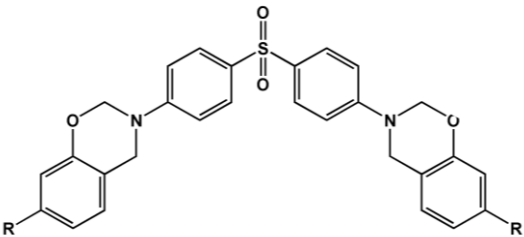
Figure 1.11: i) Reaction scheme showing the synthesis of cardanol based benzoxazine monomer (C-a) ii) FT-IR and iii) ^{1}H-NMR and iv) DSC of C-a monomer

The resin is synthesized in a single step Mannich like condensation of cardanol, aniline and paraformaldehyde taken in stoichiometric amounts (1:1:2) under solvent less condition (**Figure 1.11(i)**), followed by the purification steps. The FT-IR of the C-a monomer reveal the appearance of new absorption bands at ~1250 and ~1030 cm^{-1} which can be attributed to the Ar-C-O oxazine asymmetric and symmetric stretch

respectively[66]. The absence of absorption bands due to N-H stretching (3360-3442 cm^{-1}) and N-H bending (1619 cm^{-1}) in the spectra of C-a further suggests the absence of unreacted aniline in the Bz monomer, thereby indicating completion of the reaction(**Figure 1.11(ii)**). ^{1}H-NMR spectrum of C-a using CDCl$_3$ is presented in **Figure 1.11(iii)**. The formation of oxazines from hydroxyl functionalities was further confirmed by the presence of characteristic resonances at ~5.3 ppm (s, ArOC**H**$_2$N) and ~4.6 ppm (s, ArC**H**$_2$N) in the ^{1}H-NMR spectra.DSC traces presented in **Figure 1.11 (iv)** shows that the resin undergoes polymerization which initiates at T$_{onset}$ ~242ºC and reaches its peak at T$_{peak}$ ~263ºC. As can be seen, cardanol based benzoxazine monomers mandate high temperature curing, which may limit their potential and applicability to a certain extent. The temperature associated with polymerization of benzoxazines can be reduced either by physical blending with curing accelerators or by making structural modifications. On the basis of literature survey, the various attempts towards lowering the polymerization temperature of cardanol based benzoxazine resins by making structural modifications in the monomer have been summarized in **Table 1.1**.

Table 1.1: Thermal characteristics of cardanol based benzoxazine monomers

Cardanol based resins (R=C$_{15}$H$_{31}$)	Thermal Properties (ºC)		Ref.
	T$_{onset}$	T$_{peak}$	
	160	243	[60]

Structure			
$C_{17}H_{35}$ ... R	219	248	[67]
R	190	233	[68]
OH ... R	120*	220*	[69]
R	214	237	[67]
R	242	263	[60]
R ... R	273	373	[70]
R ... R	277	351	[70]
R ... R	268	285	[70]

	195	233	[71]
	245	267	[71]

curing temperatures are obtained from reported curing cycle.

To enhance the processibility of benzoxazine resins, various curing accelerators have been explored and are usually preferred over structural modifications in view of the economic viability. Commercially, curing accelerators for high temperature curing benzoxazines are available with Huntsman (DT300 and DT310); however their chemical composition is not available in public domain. Organic acids[34, 72] and lewis acids[73, 74] have been reported to accelerate the polymerization, but their presence in the cured resin reduces the chemical resistance of the polymer and adversely affect the physical properties of the resulting polymer[75]. Organic base such as amines[76], and imidazoles[77] have also been explored as curing accelerators and the effectiveness of acid-base combination has also been reported[78]. Recently, Sudo et.al[79] studied the efficiency of acetylacetonato complexes of 4th period transition metals as catalysts for the ring opening polymerization of benzoxazine. The examination revealed that acetylacetonato complexes of manganese, iron, cobalt and zinc exhibited the highest activity.

1.4 Research Objective

Based on the literature survey, following potential research gaps were identified:

1. Sustainable synthetic methodologies for benzoxazine synthesis need to be explored.

2. Cardanol based benzoxazine resins exhibit high temperature of curing, which need to be reduced.

3. To further broaden the scope of benzoxazines by exploring hitherto unreported applications.

The main goal of this research is to develop low curing benzoxazine resins using renewable and petro based resources and explore their potential in the field of adhesives and healing systems.

More specifically, the objectives of this research include:

- Synthesis and characterization of sustainable benzoxazines.

- Exploring alternative routes to improve the sustainability of the synthetic process.

- Evaluation of the adhesive strength of the resins.

- Exploring curing accelerators for reducing the curing temperatures of benzoxazines

- Microencapsulation of benzoxazine monomers for temperature triggered healing applications and evaluation of healing efficiency

1.5 Implementation of work plan

A systematic methodology was adopted for the proposed work which involves following steps:

- Synthesis of bio based benzoxazines resins with different functionalities.

- Structural and thermal characterization of synthesized resins by techniques including FT-IR, ^{1}H-NMR, TGA, DSC.

- Determination of adhesive strength of the resin by Lap Shear strength testing using ASTM D1002.

- Preparation and evaluation of curing accelerators for benzoxazine resin.

- Encapsulation of the monomer in fragile micro containers for temperature triggered healing applications.

1.6 Thesis organization

The work is mainly centered on lowering the curing temperature of cardanol based benzoxazine monomers. In this thesis, we have synthesized low curing bio-based benzoxazines with functionalities which are capable of improving the end performance of the polymeric materials. Alternative approach to lower the curing temperature i.e., blending of resins with curing accelerators has also been attempted. The details of the research work are organized into seven chapters. Majority of the work are manuscripts that have either been published, or have been communicated to peer-reviewed international journals.

Background of benzoxazines is summarized in Chapter 1. It gives an insight of the benzoxazine chemistry and its various applications. Renewable sources which can act as effective substitutes for petro based raw materials in the synthesis of benzoxazines are elaborately discussed.

Chapter 2 demonstrates the feasibility of microwave assisted synthesis (MAS) for benzoxazine monomer preparation. The work is proposed to serve as a sustainable methodology which reduces the energy requirements and can be utilized to synthesize various monomers in shorter reaction times.

Chapter 3 discusses the synthesis and characterization of bio-based benzoxazines with amide linkages where the co-reactants are derived by tertiary recycling of discarded bottles of polyethylene terephthalate (PET).

Chapter 4 discusses the synthesis and characterization of bio-based benzoxazines with urea linkages where the co-reactants are derived by stochiometrically unbalanced additive rearrangement of diisocyanates and diamines.

Chapter 5 deals with two different classes of curing accelerators for high temperature benzoxazine resin and the details are elaborated under two headings 5A and 5B. Chapter 5A describes the investigation results of exploring metal organic frameworks as curing accelerators for cardanol-aniline benzoxazine (C-a) resin. Chapter 5B discusses the outcomes of using metal stearates as curing accelerators.

Chapter 6 discusses the details of microencapsulation of the cardanol-aniline benzoxazine monomer in different polymeric shell walls for temperature triggered healing applications, following two distinct approaches i.e., solvent evaporation and interfacial polymerization.

Chapter 7 summarizes the data and the important conclusions, which were drawn from this thesis and provide suggestions for future work.

Chapter 2
Microwave assisted synthesis Sustainable Tool for Synthesis of Benzoxazines

Cardanol + Formaldehyde + Microwave active amine

Microwave Energy

Microwave 250 watts

25 mins Solvent-less

Benzoxazine- endcapped Telechelic poly(ethylene glycol)

Network Configuration

Ladder Configuration

Regular Architecture

Random Configuration
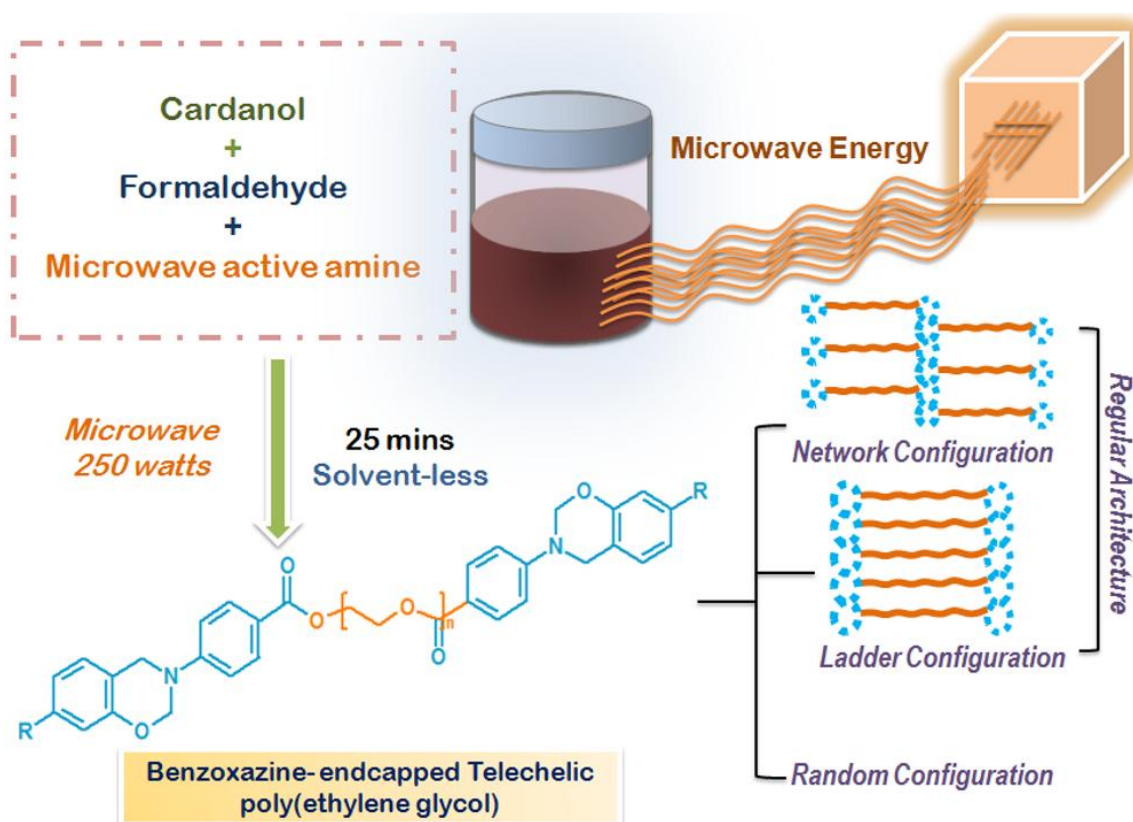
2.1 Introduction

In this chapter, the feasibility of Microwave assisted synthesis (MAS) towards synthesis of benzoxazine monomers has been demonstrated. MAS has emerged as a sustainable tool for organic synthesis which offers a simple, efficient and economic route towards the preparation of industrially important chemicals[80]. Microwave assisted heating is a rather rapid process, which does not mandate any contact between the energy source and the reaction vessel. The acceleration in the rate of reaction is primarily due to thermal effects, which is essentially due to rapid heating of the reactants[81]. Possible existence of "non-thermal microwave effects" that could rationalize the difference in 'thermal' and 'microwave assisted' heating has always been a topic of much debate[81]. In general, the essential criterion behind the success of MAS technique is the polarity of the reaction media. In the field of polymers, the application of microwaves for process development has led to apt solutions for several intriguing technical problems[82]. For example, MAS has been adopted for the synthesis of several industrially important polymeric resins like unsaturated polyesters[83], polyamides[84], polyethers[85], polyimides[86, 87] etc. and microwave radiation has also been reported to facilitate the curing process of various polymeric systems[88-94].

Several benzoxazine derivatives have also been prepared using MAS [95-97], which are generally used in the field of pharmacological sciences. Inan et. al.[98] reported the microwave synthesis of polybenzoxazine precursor using humic acid as a source of phenol from coal. However, literature on the exploration of MAS technique towards synthesis of polymeric benzoxazine resins is relatively scarce, the reason probably being the low microwave activity of the reactants involved, i.e. amine,

21

formaldehyde and phenol. 1,3-benzoxazine monomer is synthesized by Mannich like condensation of these reactants in solution or through melt processing. Polybenzoxazines, formed by the thermal curing of this monomer, exhibit interesting properties, particularly negligible volume shrinkage during curing[16], low water absorption[99] and excellent thermal stability in combination with excellent mechanical performance[100, 101]. As is clear, there is enormous design flexibility in benzoxazine synthesis, due to the large library of precursors available. In view of the potential of benzoxazines in different areas, all endeavours towards reduction in the reaction time for the preparation of these resins are highly desirable.

Development of benzoxazines, especially those based on renewable raw materials using alternative sustainable processes, has been receiving the attention of academicians and industrialists[47, 48, 102-104]. In the quest to derive sustainable benzoxazines, replacing petro-based raw material with CNSL (cardanol nut shell liquid) for the chemical industry appears to be an extremely attractive proposition, in view of its low cost, relative abundance, and chemically reactivity, amongst other attributes[62]. CNSL being a non edible oil, its use as a chemical raw material does not impose any significant pressure on the food-chain. CNSL is primarily composed of anacardic acid (74-77%), the rest being cardanol, cardol, and 2-methyl cardol. However, commercial-grade CNSL is obtained through roasting which results in the decarboxylation of anacardic acid into cardanol[105]. The use of cardanol based benzoxazines as the matrix material for fibre-reinforced composites is well reported [59, 60]. The long alkyl chain present in cardanol acts as an intramolecular plasticizer [61, 62], which reduces the viscosity of the resin and renders it suitable as a reactive diluent for commercial benzoxazine resin[63, 64]. The alkyl chain also increases the

flexibility of molecular segments which reflects in their lower glass transition temperature (T_g)[65], however the same leads to higher curing temperatures[63].

The Mannich like condensation reaction of cardanol with amines and formaldehyde has been extensively studied[102, 103, 106-108], which reveal that the reaction requires about 3 h at 90°C. The sustainability of this process can be further improved by using MAS technology, which has the additional advantage of reducing the reaction time.

As already mentioned, both the raw materials for benzoxazine synthesis i.e. phenols and amines, are not sufficiently microwave active to ensure rapid reaction under microwave irradiation. Poly(ethylene glycol)s (PEGs), on the other hand, are considered effective solvents for the microwave assisted synthesis[109]. It is worth mentioning that PEGs are employed as green solvents for sustainable organic synthesis as they are relatively inexpensive, nontoxic and biodegradable[110, 111]. Terminal functionalization of PEGs yields microwave active amine-terminated poly(ethylene glycol)s (ATPEGs), which can subsequently be used as a reactant for the preparation of monomer. The resulting benzoxazine is expected to contain repeating ether functionalities, and the length of the polyether chain affects the flexibility of the resultant polymer[112, 113]. The presence of oxazine moieties at the terminal positions lead to the formation of benzoxazine-endcapped telechelic poly(ethylene glycol)s, which are cross-linkable macro-monomers combining the thermoplastic properties associated with the flexible segment in addition to the dimensional, high-temperature stability and chemical resistance offered by the benzoxazine units[114].

The intention of this chapter is to improve the sustainablity of the procedure by performing the microwave assisted synthesis of cross-linkable telechelic poly(ethylene glycol)s with benzoxazine end groups under solventless conditions. The chapter discusses the synthesis and characterization of benzoxazine endcapped telechelic polymer and evaluation of their adhesive characteristics. The rheological behavior of the synthesized resin was studied in order to investigate the effect of flexible polyether chains on the viscosity of the resin.

2.2 Experimental

2.2.1 Materials

Polyethylene glycol (PEG 200, PEG 400, PEG 600, PEG 1000, and PEG 1500) (E. Merck) was used without any further purification. Sodium sulphate, paraformaldehyde, sodium bicarbonate, chloroform, p-toluene sulfonic acid (p-TSA), xylene, p-amino benzoic acid (PABA) was obtained from CDH was used as such. Cardanol (ρ =0.9272-0.9350 g cm^{-3}; iodine value 250; Acid Value Max 5; Hydroxyl Value 180-190) was obtained from Satya Cashew Chemicals Pvt. Ltd. (India). Double distilled water was used throughout the course of this work.

2.2.2 Preparation of amine terminated poly(ethylene glycol)s (ATPEGs)

The amine derivatives of poly(ethylene glycol)s were prepared by the condensation of the poly(ethylene glycol)s with stoichiometric amount of PABA in the presence of p-TSA[115]. The reaction mixture of PEG (0.16 moles), PABA (0.33 moles) and p-TSA as catalyst were refluxed in the presence of xylene in a three-necked reaction flask fitted with a stirrer, thermometer pocket and Dean-Stark apparatus. The reaction was continued till no more condensable liquid could be collected (~8 h). Excess xylene was subsequently removed through distillation and the reaction mixture was dissolved

in chloroform, followed by washing with sodium bicarbonate solution (10% w/v) to remove residual reactants and catalyst. The product was dried over anhydrous sodium sulfate, subsequent to which, chloroform was removed under reduced pressure. The amine derivative will be referred to as ATPEG followed by the molecular weight of the polyol used for its synthesis, in the subsequent text, e.g. amine derivative of PEG 200 and PEG 1500 will be referred to as ATPEG200 and ATPEG1500 respectively. The sample designation and the respective yield of amine are presented in **Table 2.1.**

Table 2.1: Designations and yield of amine terminated poly(ethylene glycol)s

Poly(ethylene glycol) used	Designation of amine	Yield of amine (%)
PEG200	ATPEG200	94
PEG400	ATPEG400	90
PEG600	ATPEG600	88
PEG1000	ATPEG1000	86
PEG1500	ATPEG1500	90

2.2.3 Synthesis of poly(ethylene glycol)s endcapped benzoxazines

Solventless synthesis using conventional approach

A mixture of cardanol (0.0165 moles), ATPEG (0.0082 moles) and paraformaldehyde (0.032 moles) was gradually heated to 80°C and stirred for an hour, followed by heating at 90°C for 2 h. The reaction led to the evolution of water and the color of the reaction medium changed from yellow to red brown. Upon cooling, water (10 mL) was added and organic layer was extracted with chloroform (20 mL). The organic layers were combined and washed with aqueous NaOH solution (0.5 N, 100mL) followed by washing with water (3 x 30 mL), drying over sodium sulphate and filtration. The solvent was removed under reduced pressure to give benzoxazine endcapped poly(ethylene glycol) as red oil. The synthesized resin will be referred to

25

as C-ATPEG followed by the molecular weight of the polyol used, in the subsequent text, e.g. benzoxazine resin prepared using ATPEG200 will be referred to as C-ATPEG200 **(Table 2.2).**

Table 2.2: Designations and yield of poly(ethylene glycol)s endcapped benzoxazines

Amine Used	Designation of benzoxazines	Yield of benzoxazines (%)
ATPEG200	C-ATPEG200	95
ATPEG400	C-ATPEG400	89
ATPEG600	C-ATPEG600	85
ATPEG1000	C-ATPEG1000	85
ATPEG1500	C-ATPEG1500	87

Solventless synthesis using MAS technique

For microwave assisted synthesis, a mixture of cardanol (0.0165 moles), ATPEG (0.0082 moles) and paraformaldehyde (0.032 moles) was sealed under nitrogen atmosphere and allowed to react in the microwave reactor (Anton Paar Monowave 300 equipped with a digital temperature controller and pressure monitoring system in a 30 mL teflon coated silicone sealed borosilicate glass reaction tube) under isothermal conditions at 150°C temperature for 25 mins. The methodology adopted for the purification of the resin obtained is similar to that used in the conventional process and has already been mentioned above.

2.2.4 Adhesive strength

The adhesive strength of the resin was quantified in terms of Lap shear strength, which was determined as per ASTM D1002. For this purpose, ~ 0.05 g of the liquid resin was coated on steel plates (15×15 mm^2) while maintaining the thickness of the resin between 0.23-0.46 mm. The assembly was clamped with paper clips and initially maintained at 80°C for 30 mins, and cured in an air oven at 80 to 180 °C (30 mins)

followed by heating at 240°C (1h) for C-ATPEG1500, 236°C (1h) for C-ATPEG1000, 228°C (1h) for C-ATPEG600, 223°C (1h) for C-ATPEG400 and 219°C (1 h) for C-ATPEG200. A total of 6 replicates were tested per sample and the average value is reported.

2.2.5 Characterization

FT-IR spectra of samples were recorded using a Thermo scientific FT-IR (NICOLET 8700) analyzer with an attenuated total reflectance (ATR) crystal accessory. The spectra were obtained by maintaining 45° as the angle of incidence of the germanium ATR over the wavelength range 4000-500 cm^{-1}, with a resolution of 4 cm^{-1}. Bruker AC 500 MHz FT-NMR spectrometer was used to record the ^{1}H-NMR of the samples. The spectrum was recorded in CDCl$_3$ and DMSO using tetramethylsilane as the internal standard. Thermal behavior was investigated using Perkin Elmer Diamond STG-DTA under N$_2$ atmosphere (flow rate = 50 ml min^{-1}) in the temperature range 50-700°C. A heating rate of 10 °C/min and sample mass of 5.0 ± 0.5 mg was used for each experiment. Calorimetric studies were performed on a differential scanning calorimeter (TA instruments Q 20). For dynamic DSC scans, samples (10 $\pm$2 mg) were sealed in aluminum pans, and heated from 0 to 300°C at 10°C min^{-1} under Nitrogen atmosphere to minimize oxidative degradation of the sample during curing. Prior to the experiments, the instrument was calibrated for temperature and enthalpy using standard Indium and Zinc. Thermal equilibrium was regained within 1 min of sample insertion, and the exothermic reaction was considered to be complete when the recorder signal levelled off to the baseline. Lap shear strength (LSS) of bonded steel plates (Roughness, R$_a$ 0.42–0.51μm) was measured in accordance with ASTM standard D1002 using Universal Testing System (International equipments) at a

crosshead speed of 1.3 mm min^{-1}. Anton Paar Rheometer MCR-CTD620 was used to study the rheological behavior of the benzoxazines in three intervals of temperature profile by keeping constant strain of 0.5% and constant angular frequency of 10 rad/s in each interval.

2.3 Results and Discussion

The potential of MAS technology towards the sustainable synthesis of telechelic poly(ethylene glycol) endcapped with benzoxazine moieties has been explored. Microwave active amines ATPEG were prepared, which were reacted with cardanol and formaldehyde under solventless conditions to result in telechelic polymer with terminal benzoxazine moieties, which are capable of undergoing ring opening polymerization to form cross-linked polymers with excellent thermal stability.

2.3.1 Amine terminated poly(ethylene glycol) (ATPEG)

The most common approach for the conversion of hydroxyl functionality into primary amine involves a multiple stage protocol, where the hydroxyls are first converted to sulphonates or halides followed by the nucleophilic substitution by azide anion, which are subsequently reduced[116]. It is to be noted that, commercially, only high molecular weight amines terminated poly(ethylene glycol) (M_w >2000) are available, which too are rather expensive. A single step process for the amine termination of poly(ethylene glycol), which involves condensation reaction with PABA in the presence of catalyst as per **Figure 2.1** has been previously reported[115].
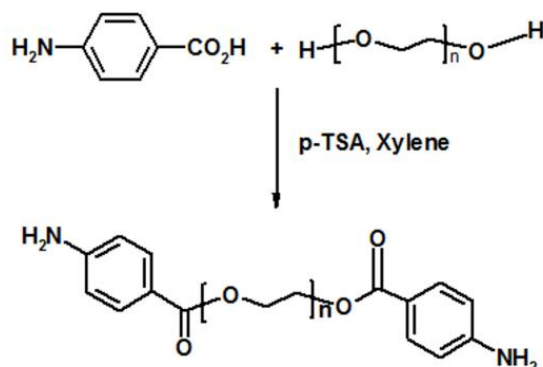
Figure 2.1: Amine fictionalization of poly(ethylene glycol).

The FT-IR spectra of amine-terminated poly(ethylene glycol)s (ATPEGs) is presented in **Figure 2.2(i).**
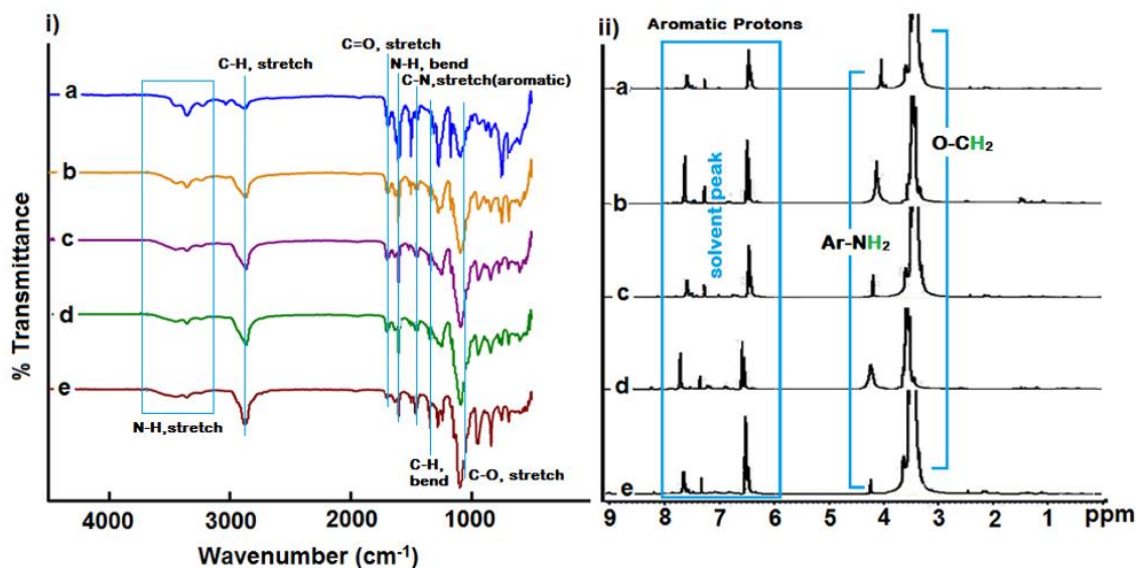
Figure 2.2 i) FT-IR and ii) ^{1}H-NMR spectra of a) ATPEG200 b) ATPEG400 c) ATPEG600 d) ATPEG1000 e) ATPEG1500

The spectra of ATPEG exhibit characteristic peaks associated with $v_{C-H, stretch}$ at ~ 2875 cm^{-1}, $v_{C-H, bend}$ at ~ 1466 cm^{-1} and $v_{C-O, stretch}$ at ~ 1060 cm^{-1} which can also be seen in the spectra of PEG (**Figure 2.3**). The amine derivative exhibits additional peaks associated with $v_{N-H, stretch}$ at ~ 3357 cm^{-1}, $v_{N-H, bend}$ at ~ 1603 cm^{-1}, $v_{C=O, stretch}$ at ~ 1698 cm^{-1}, and $v_{C-N, stretch}$ at ~ 1341 cm^{-1}.

29
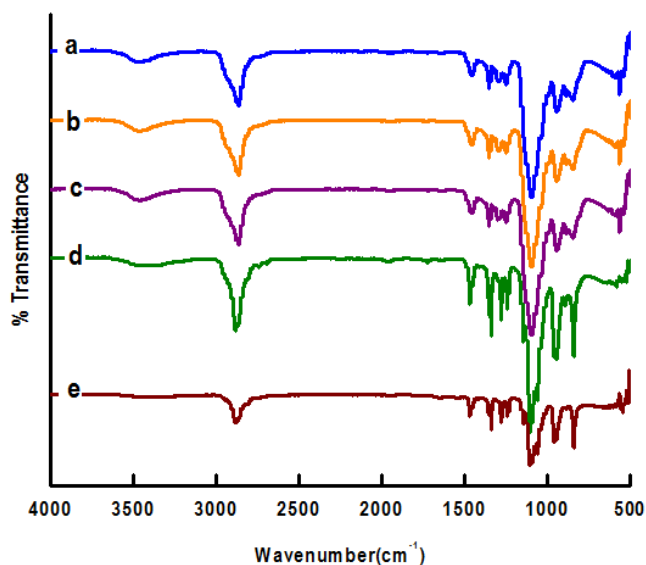
Figure 2.3: FT-IR spectra of Poly(ethylene glycol)s a) PEG 200 b) PEG 400 c) PEG 600 d) PEG 1000 e) PEG 1500

The ATPEGs were also characterized using ^{1}H-NMR spectroscopy using CDCl$_3$ solvent and the ^{1}H-NMR spectra of the amines are also presented in **Figure 2.2(ii).** As expected, the spectra of all the amines were found to be similar irrespective of the molecular weight of the polyether glycol used for synthesis. Characteristic resonances at ~6.5 ppm (4H, aromatic), 7.5ppm (4H, aromatic), 4.2 ppm (4H, s, ArNH$_2$) and 3.4 ppm (m, OCH$_2$CH$_2$O) can be seen in spectra of ATPEG.

Poly(ethylene glycol) are microwave active species with PEG 200 having a loss factor of ~7.08 (2GHz and 25°C)[117]. Since, it is the terminal hydroxyl groups, which contribute towards the polarity of PEG, the microwave activity of the reactants decreases with increasing molecular mass. The presence of ethereal oxygen and terminal –NH$_2$ is also expected to confer microwave activity to ATPEGs, which form the basis of selection of the latter for microwave assisted synthesis of benzoxazines. The ability of the reactants to convert microwave energy into heat was evidenced in terms of increase in the temperature of the ATPEG, upon being exposed to uniform

30

microwave radiation. The temperature-time profiles for a few representative reactants are presented in **Figure 2.4**.

Figure 2.4: Rise in temperature for a) ATPEG200 b) ATPEG1500 c) Cardanol d) C-ATPEG200 e) C-ATPEG1500 with time under constant microwave radiation (900 watts)

2.3.2 MAS for synthesis of telechelic poly(ethylene glycol)s endcapped with benzoxazine

Thermally cross-linkable telechelic poly(ethylene glycol)s with benzoxazine end groups were synthesized through solvent-less Mannich like condensation reaction of cardanol with the ATPEG using conventional as well as microwave route as per the reaction presented in **Figure 2.5**. The microwave assisted synthesis of benzoxazine-endcapped telechelic polymers was relatively easy, and more energy efficient than the conventional route without compromising on the performance, properties and application of the end product. In view of the suitable viscosity of cardanol (145 mPa.s)[108], solventless synthesis was feasible[102, 103, 107, 118]. However, under conventional heating, the reaction took approximately 180 mins (at 90°C) to reach completion (yield ~90±5%). As with most chemical reactions, raising the reaction

31

temperature increases the reaction rate and the extent of acceleration was evidenced in terms of the reduction in reaction completion time. At 150°C, the reaction completion time concomitantly reduced to 120 mins, without affecting the reaction yield (~90±5%), however the elevated temperature leads to oligomerization of the monomer, which was observed in the ^{1}H-NMR spectra.
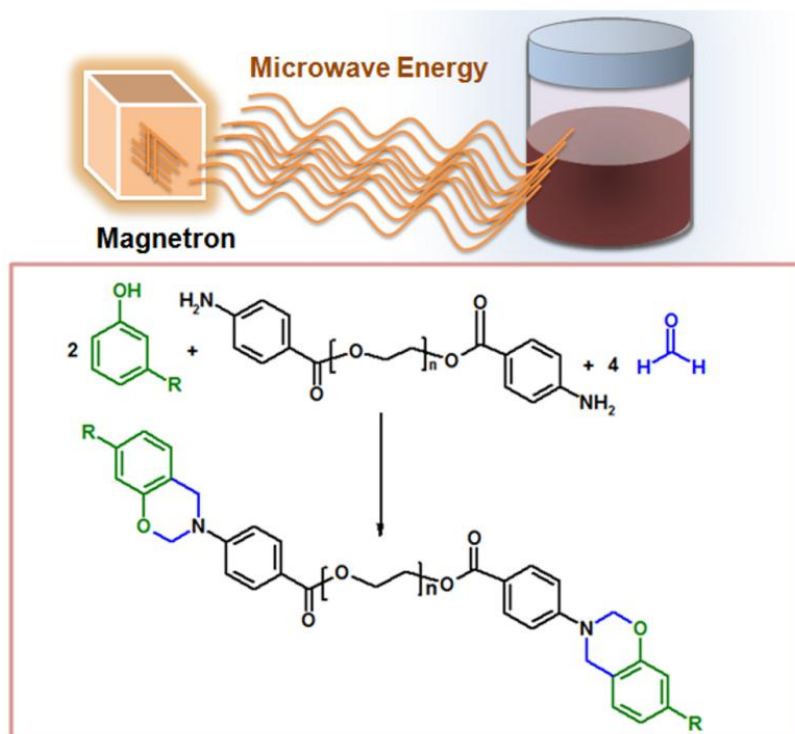
Figure 2.5: Telechelic poly(ethylene glycol) endcapped with benzoxazines from cardanol and amine terminated poly(ethylene glycol) (ATPEG)

The ^{1}H-NMR spectra of the benzoxazine-endcapped polymer is presented in **Figure 2.6**, where the reaction was performed at 90°C and 150°C. In view of the presence of alkylene protons associated with cardanol (m, **CH=**, **CH₂=CH–**), which resonates at the same position as ArO**CH₂**N (~5.4 ppm), the intensity ratio of the signals associated with the oxazine moiety in cardanol based benzoxazines at 4.6 (singlet) and 5.4 ppm (multiplet) is expected to be 1:3[107].
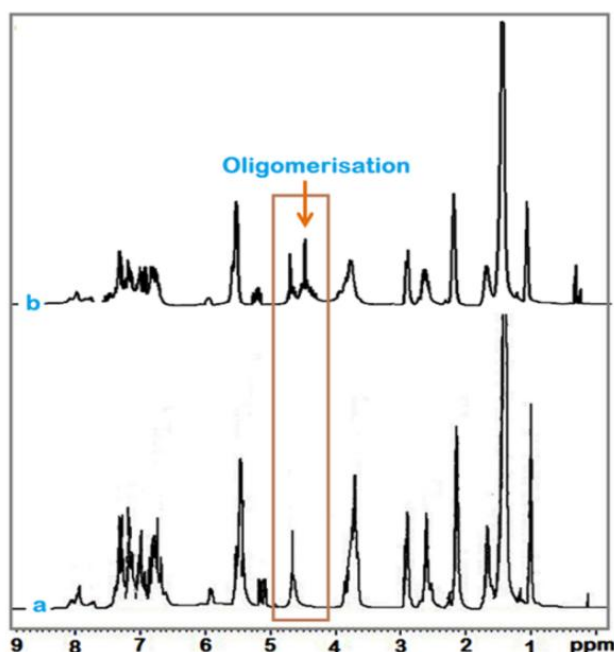
Figure 2.6: ^{1}H-NMR spectra of C-ATPEG200 prepared at a) 90°C and b) 150°C

However, it can be seen that the ratio of intensities of the signals was found to deviate largely in the product obtained when the reaction was performed at 150°C. This deviation from 1:3 can be ascribed to the oligomerization in the oxazine moiety. This leads to the appearance of an additional peak in the region 3.5-4.5 ppm, which is associated with -**CH$_2$**- protons of mannich base formed during the ring opening of the oxazine moiety **(Figure 2.6).**

Liu and Ishida have proposed the mechanism and studied the kinetics of the solventless synthesis of Bisphenol A and toluidine based benzoxazine[29]. It has been suggested that at temperatures between 90-100°C, the overall reaction rate is controlled by the formation of mannich base, which follows third order kinetics. With the progress of the reaction, the concentration of mannich base reaches maxima, which subsequently convert to benzoxazine. On increasing the temperature further, and/or with extended time, the 1,3-benzoxazine undergoes ring opening to form

33

oligomers. In view of the possibility of oligomerization, it is suggested that under conventional heating, it is not advisable to increase the reaction temperature beyond 90°C, in congruence with previous studies[21].
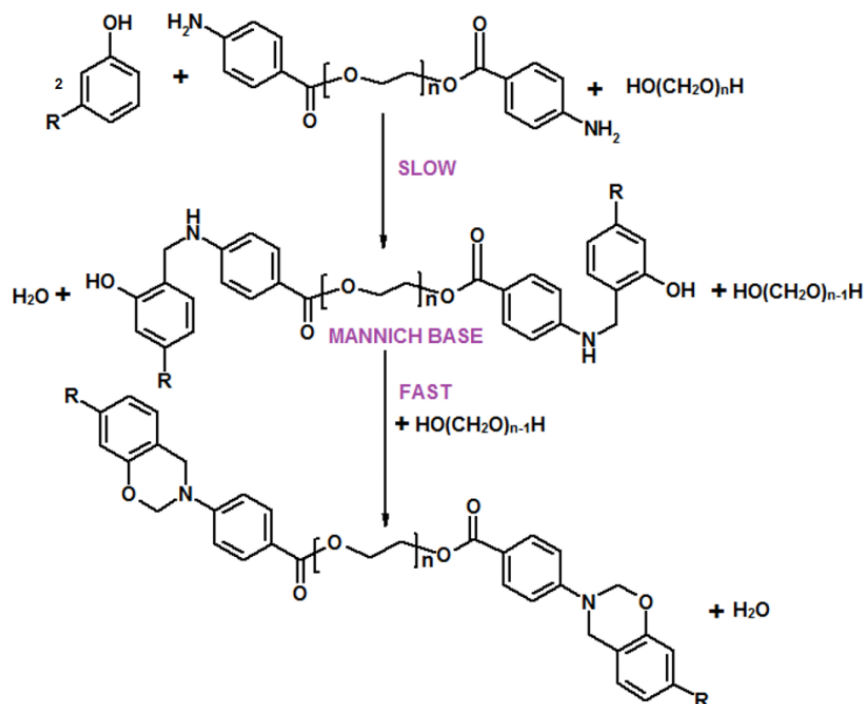
Figure 2.7: Possible mechanism of benzoxazine formation using solvent-less route at higher temperature

It is to be noted that under conventional conditions, paraformaldehyde remains in the solid phase, which renders this reaction practically diffusion controlled. Under microwave conditions, it is possible to increase the reaction temperature beyond the melting point of paraformaldehyde (120°C), leading to the formation of a homogeneous media, where the reaction is expected to proceed at much faster rate. The reaction can also be maintained isothermally at higher temperatures for adequate time durations resulting in formation of benzoxazines monomer avoiding the formation of oligomers, as shown in **Figure 2.7**.

In view of the microwave activity of ATPEG and cardanol[119], it was observed that the reaction took significantly lesser periods (25 min as opposed to 120 mins at 150°C) to reach completion (yield ~95±5%) under microwave assisted conditions. The microwave profile is presented in **Figure 2.8.** It can be seen that the reactants reach 150°C in less than a minute under microwave irradiation, a phenomenon unaccomplishable using conventional heating. This rapid heating of the reactants is primarily responsible for the reduction in the reaction time under microwave conditions. In view of the possibility of opening of the oxazine moiety at higher temperatures (T > 150°C), the temperature of the reaction media was not increased further.
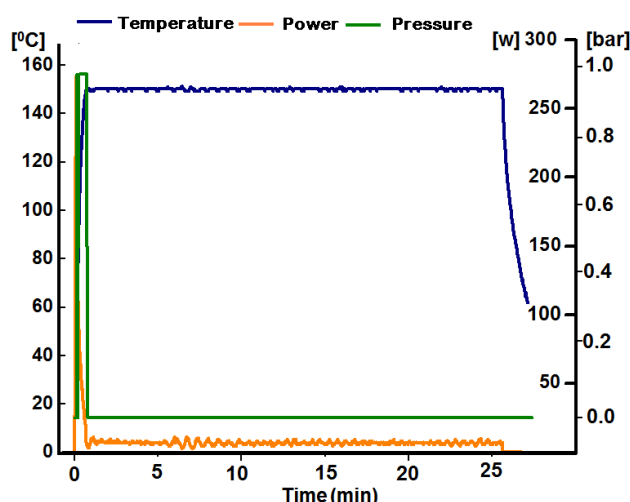
Figure 2.8: Representative microwave profile of the synthesis of C-ATPEG at 150°C for 25 mins.

The FT-IR spectra of the benzoxazine monomers are presented in **Figure 2.9(i)**. The absence of absorption due to O-H and N-H stretching at >3161 cm^{-1} suggests that the unreacted amine terminated poly(ethylene glycol) and cardanol are completely removed from the resin. The appearance of absorption bands at ~1250 and ~1030 cm^{-1} can be attributed to the Ar-C-O oxazine asymmetric and symmetric stretch

35

respectively[66]. In addition to the stretching bands associated with the alkene and aromatic groups (3008 cm^{-1}), aliphatic C–H vibrations (2926 and 2854 cm^{-1}), other characteristic absorption bands include C=C (~1600 cm^{-1}), CH$_2$ wagging (1370 cm^{-1}), and asymmetric stretching vibrations of C-N-C (1116 cm^{-1}) respectively. A bimodal peak centered at 990 and 960 cm^{-1} associated with the out-of-plane bending vibrations of C-H bond due to alkylene double bond and oxazine ring respectively is also present[58].
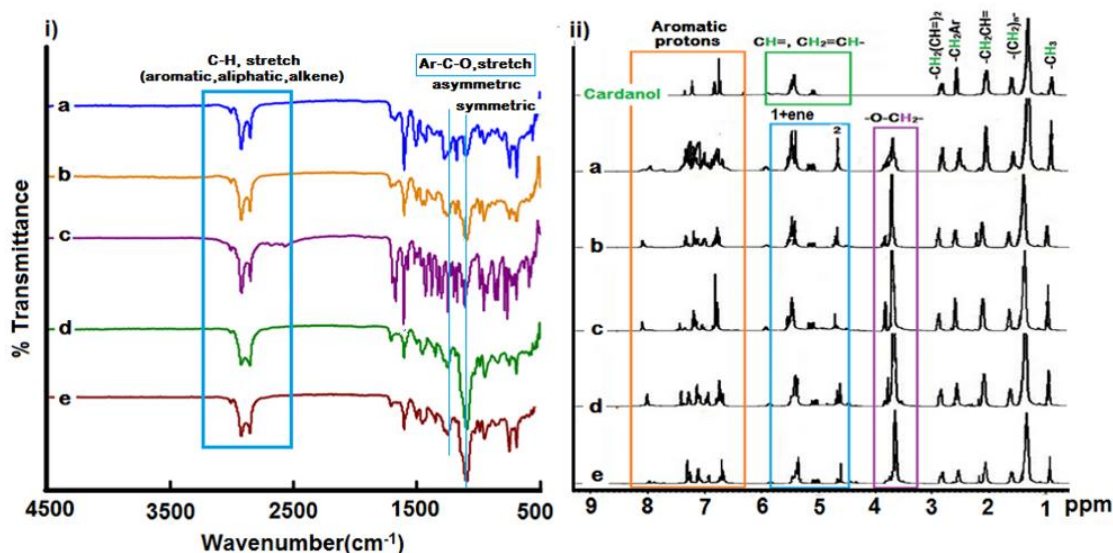
Figure 2.9 :i) FT-IR and ii) ^{1}H-NMR spectra of a) C-ATPEG200 b) C-ATPEG400 c) C- ATPEG600 d) C-ATPEG1000 e) C-ATPEG1500

The ^{1}H-NMR spectra of benzoxazine-endcapped polymer prepared is presented in **Figure 2.9(ii).** C-ATPEG exhibit characteristic resonances at ~ 5.3 ppm (m, ArO**CH$_2$**N) and ~ 4.7 ppm (s, Ar**CH$_2$**N), which confirms the formation of oxazine functionality. Interestingly, oligomerization is practically absent, when the reaction is performed under microwave conditions. This can be attributed to the lower residence time available with the resin under the experimental conditions maintained during microwave synthesis.

The curing behavior was studied using non-isothermal calorimetry, and the DSC profiles are presented in **Figure 2.10.** The polymerization of benzoxazine, being autocatalytic in nature is strongly influenced by the adjacency of the reactive oxazine terminals. The temperature associated with the cross linking of benzoxazine-endcapped polymer was found to increase with increasing chain length of the ATPEG used for its preparation; a feature attributable to the dilution of the oxazine functionalities[113]. The broad exothermic peaks as observed in the DSC profiles are a result of the dispersity associated with the polyether chains of ATPEGs. In addition, the molar enthalpy associated with the polymerization of C-ATPEG was found to decrease with increasing chain length, which can again be credited to the lower oxazine ring concentration per unit mass.
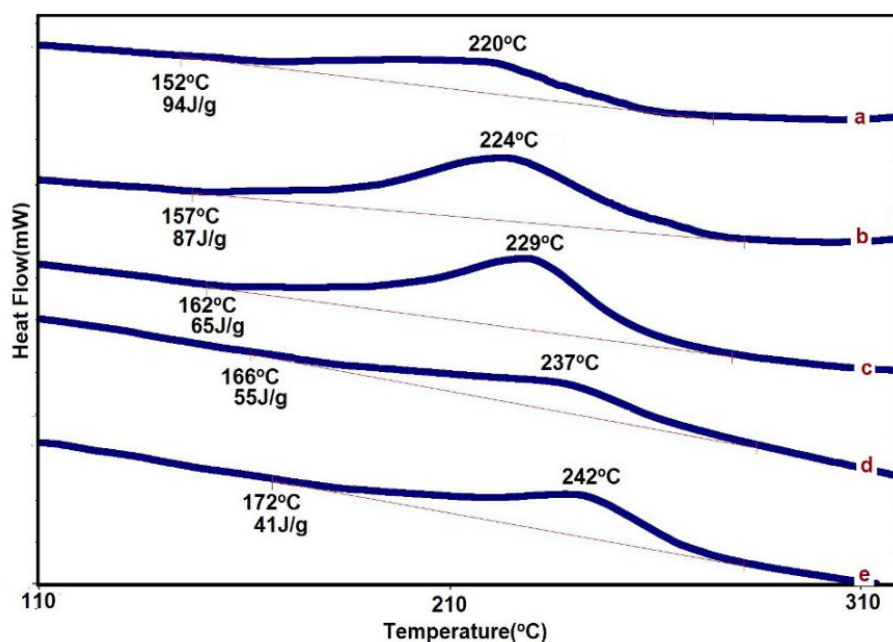
Figure 2.10: DSC traces a) C-ATPEG200 b) C-ATPEG400 c) C-ATPEG600 d) C-ATPEG1000 e) C- ATPEG1500

In view of the telechelic nature of the synthesized benzoxazine-endcapped poly(ethylene glycol)s, several possibilities in terms of molecular architecture can be

37

envisaged in the cross-linked polymer, the extreme ones being pictorially represented in the **Figure 2.11.**

Ladder Configuration   Network Configuration
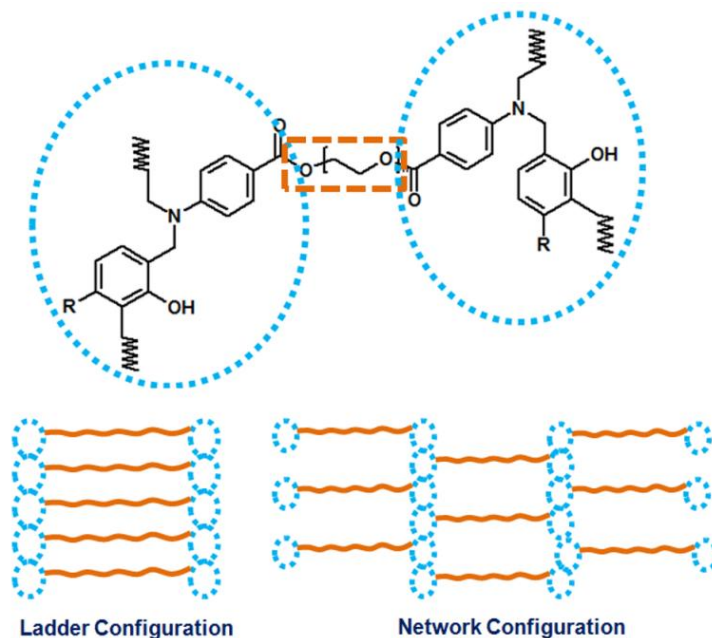
Figure 2.11: Probable arrangement of repeating unit in telechelic polybenzoxazines

However, their formation mandates the alignment of reactive species. The telechelics prepared in the present work exhibit low liquefaction temperatures, suggestive of the absence of strong molecular interactions, thereby eliminating the possibility of formation of regular structures.

The practical applicability of a polymer is governed by its ease of processibility, where viscosity turns out to be a controlling parameter. The difference in the liquefaction and gelation temperatures is indicative of the processing window available with the polymer, as it is only within this range that the polymer can be molded or compounded. Rheological behavior of C-ATPEG was analyzed to study the effect of increasing flexible segments of amines on processibility of resin (**Figure 2.12**) and studies indicated that the viscosity of the resin was sufficiently low to allow solventless processing. Cardanol based benzoxazine precursors are liquids at room

temperature, and therefore liquefying point is not observed in the complex viscosity curve. As expected, telechelic polymers with relatively smaller flexible segment exhibit marginally higher viscosity, which is noticeable only at the gelation point (**Inset, Figure 2.12**).
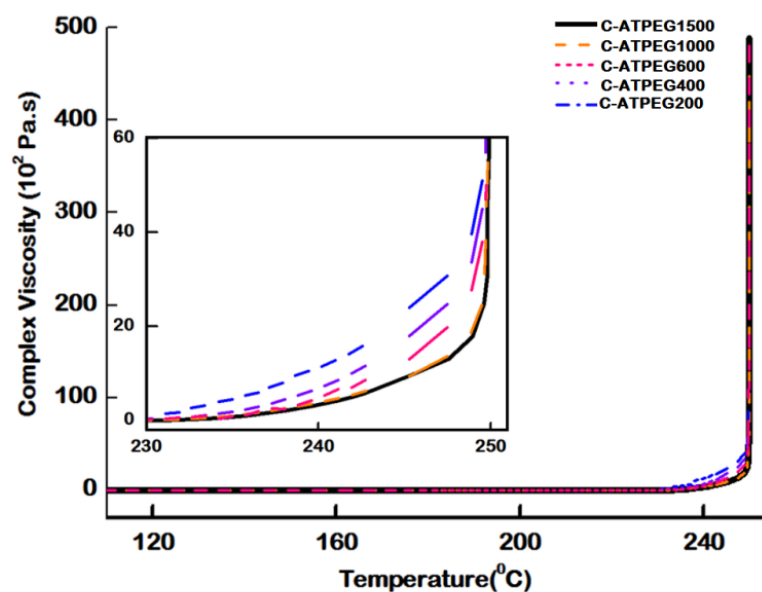
Figure 2.12: Variation of complex viscosity with temperature of the monomer

Due to early onset of oligomerization, the benzoxazine-endcapped polymers with lower cross-linking temperature exhibited higher viscosity build-up at gelation temperature. It is interesting to note that the complex viscosity of the C-ATPEG200 (~7.28 Pa.s at 30°C) is substantially lower than that of cardanol-aniline monofunctional benzoxazine (~ 26.4 Pa.s under the same conditions)[107]. This decrease in the complex viscosity can be credited to the presence of flexible ether linkages, in addition to the long alkyl chain in cardanol.

The TG-DTG traces of the cured benzoxazines are presented in **Figure 2.13.** The polybenzoxazine were found to exhibit excellent thermal stability with the

39

temperature associated with 5% mass loss to be higher than 300°C, suggesting their application in demanding areas requiring high thermal stability.
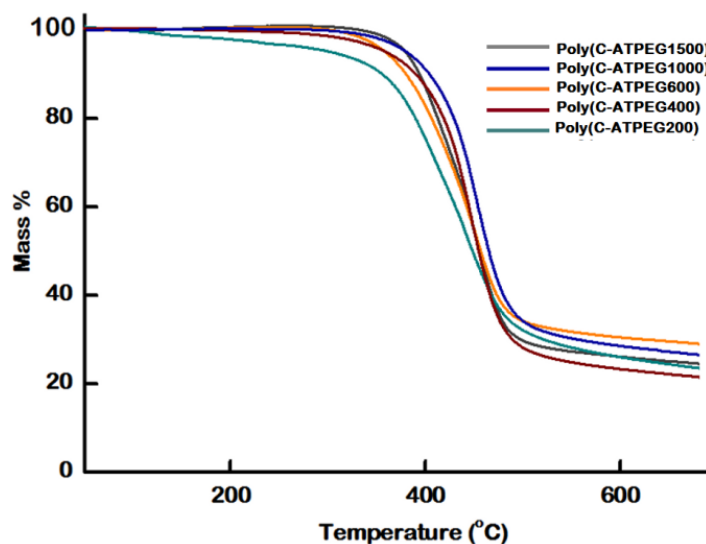
Figure 2.13: TGA traces of polybenzoxazines

2.3.3 Adhesive Property

The adhesion of the cross-linked telechelic poly(ethylene glycol)s endcapped with benzoxazine over stainless steel coupons was quantified as per the standard procedure. The results in terms of lap shear strength (LSS) are presented in **Table 2.3**, and the representative load−displacement curve is presented in **Figure 2.14**.

Table 2.3: Lap shear Strength of polybenzoxazines

Benzoxazine-endcapped poly(ethylene glycol)s	Lap Shear Strength (kgcm^{-2})
Poly(C-ATPEG1500)	9.98±0.09
Poly(C-ATPEG1000)	14.98±0.09
Poly(C-ATPEG600)	17.94±0.09
Poly(C-ATPEG400)	20.90±0.19
Poly(C-ATPEG200)	37.72±0.29

40
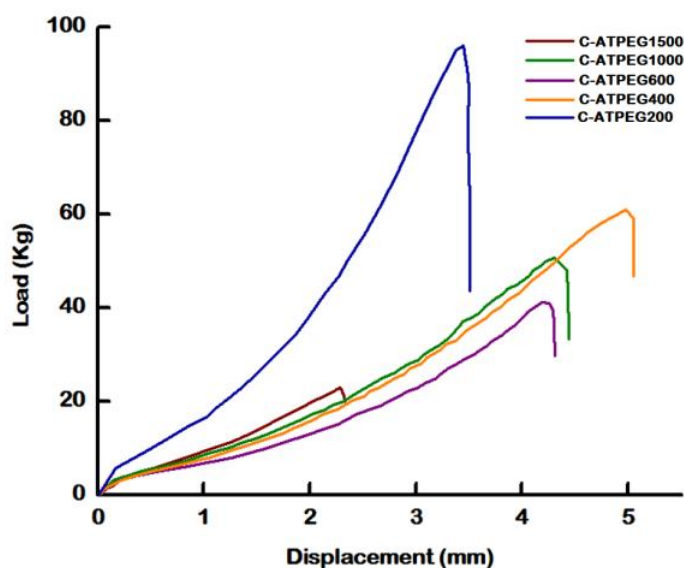
Figure 2.14: Load Displacement curve of polybenzoxazines and FT-IR of a) poly(C-ATPEG1500) b) poly(C-ATPEG1000) c) poly(C-ATPEG600

It can be seen from the table that cross-linked benzoxazine-endcapped polymer with shortest chain length (poly(C-ATPEG200) exhibit highest LSS, which can be attributed to the relatively larger number of cross-links in the polybenzoxazine network and highlight the potential of these resins as adhesives and healants for healing applications[120-122].
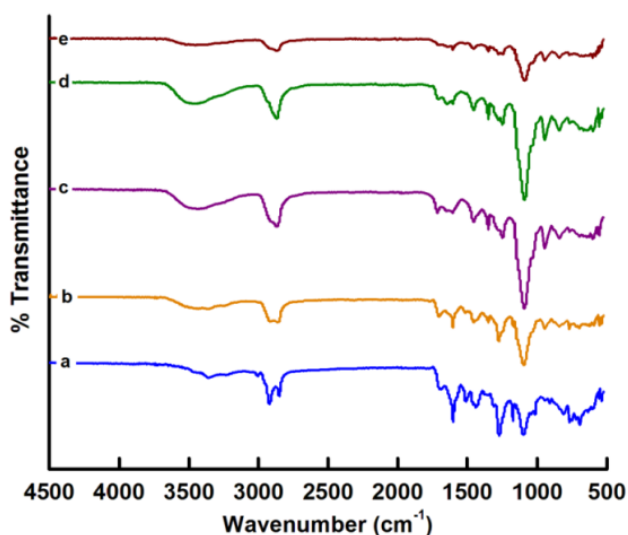
Figure 2.15: FT-IR of a) poly(C-ATPEG200) b) poly(C-ATPEG400) c) poly(C-ATPEG600) d) poly(C-ATPEG1000) e) poly(C-ATPEG1500)

Benzoxazine moiety undergoes thermally accelerated ring opening polymerization to form cross-linked networks on metal surfaces[123], resulting in functional groups that are capable of undergoing H-bonding, such as−OH and >N−, as shown in the FT-IR of cured resin (**Figure 2.15**).

Chapter 3

Structural Modification in Cardanol Based Benzoxazine by introducing amide linkages
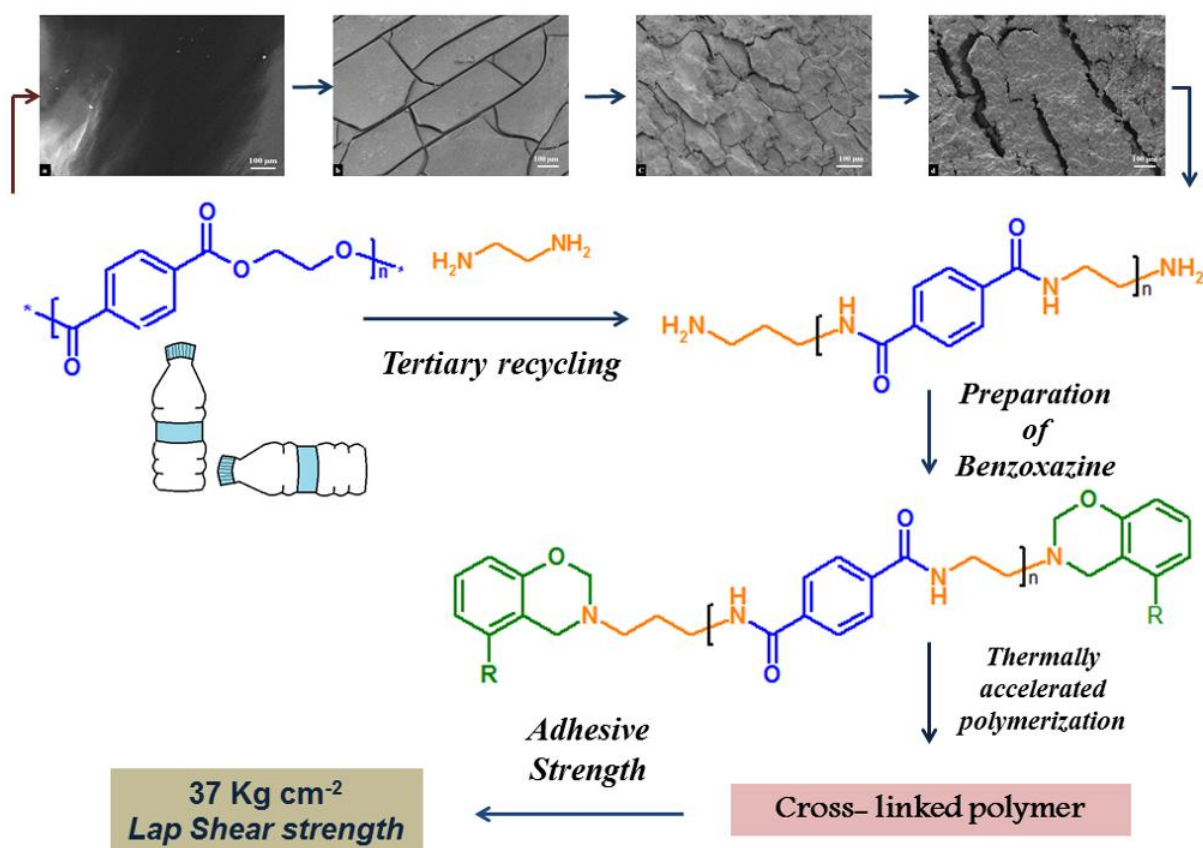
3.1 Introduction

Polybenzoxazines are bridging the gap between the mechanically strong polyepoxies and thermally stable maleimides. Polybenzoxazines exhibit interesting properties, notably negligible volume shrinkage during curing[16], low water absorption[99] and thermal stability without compromising on the excellent mechanical performance, as elaborated in previous chapters[100, 101]. In addition, the flexibility in molecular designing, made possible through the astute choice of the amine and phenolic components permit structure tunability, which further open up new vistas of application[48, 60, 124, 125]. However, certain drawbacks like high polymerisation temperature, low cross link density, brittle nature of the cross linked polymer restrict the use of polybenzoxazines in widespread applications. Several methodologies, such as structural modifications[126, 127], introduction of curing acclerators[128, 129] and blending[130], have been adopted to deal with these issues. Benzoxazine monomers have been structurally functionalised with electron donating or releasing groups at their respective active positions, where they destabilise the oxazine ring or stabilise the intermediates formed during the polymerisation, thereby lowering the curing temperature of the resin[131]. Increasing the oxazine functionality in benzoxazine monomer has also been attempted[132, 133].

Exploring alternative renewable feedstock's to meet the ever-increasing demands of the chemical industry is an essential step towards sustainable development. In the quest to derive sustainable benzoxazines, replacing petro-based raw material with CNSL (cardanol nut shell liquid) for the chemical industry appears to be an extremely attractive proposition, in view of its low cost, relative abundance, and chemically reactivity, amongst other attributes[62]. The properties of bio-based benzoxazines

43

derived from cardanol can further be improved by introduction of additional functional groups[134]. In this context, amide linkages have been reported to bestow flame retaradance, chemical resistance and excellent mechanical properties, due to which polyamides find extensive application in fiber and film technology. It is therefore of interest to design benzoxazine monomers containing amide groups in the chain[135, 136]. Terephthalamides obtained by aminolysis of polyethylene terephthalate(PET) offer interesting candidacy to prepare diamines with amide groups for possible application as a precursor for synthesizing such bis-benzoxazines.Tertiary recycling of PET using diamines leads to terephthalamides terminated with amine functionalities[137, 138]. The kinetics of PET aminolytic depolymerisation is a rather slow process[139, 140] due to the heterogeneous nature of the reaction medium[141]. Literature, however supports microwave assisted aminolysis as a propitious route towards tertiary recycling of PET wastes[142].

This chapter deals with the synthesis and chracterisation of sustainable bis-benzoxazine monomers containing amide linkages where the amine co-reactants are derived from microwave assisted tertiary recycling of PET. The monomers are polymerized via thermally accelerated ring-opening polymerization to obtain polybenzoxazines with amide linkages. The effect of amide linkages on the curing profile of monomer has been studied and is expected to improve the adhesive characteristics of the cross-linked polymer. The present approach involves the use of microwave energy source for the preparation of amines, instead of the conventional heating process, thereby reducing the energy requirements as suggested in previous chapter.

44

3. 2 Experimental

3.2.1 Materials

Cardanol was obtained from Satya Cashew Chemicals Pvt. Ltd. (India). Paraformaldehyde, ethylene diamine; sodium sulphate and chloroform from CDH were used as received. Post-consumer plastic bottles were used as the source of PET. Disposed off bottles were collected, washed, dried and used after removing the caps and labels. Bottles were cut into small pieces (6 mm x 6 mm), before microwave assisted aminolysis in the presence of ethylene diamine (ED). Double distilled water was used throughout the course of this work.

3.2.2 Aminolysis of PET: Microwave assisted synthesis of terephthalamides

PET depolymerisation was performed in a microwave reactor (Anton Paar Monowave 300) equipped with a digital temperature control and pressure monitoring system using 30 mL teflon coated silicone sealed borosilicate glass reaction tube. PET flakes (1 g) together with requisite amounts of ethylene diamine were sealed under nitrogen atmosphere and allowed to react under isothermal conditions at different temperatures (100-250 °C) in a microwave synthesiser. The PET:ED molar ratio was varied from 1:2 to 1:16 to investigate the effect of the same on the PET conversion. The reaction vessel was cooled to room temperature and the mixture was filtered through a copper wire mesh (0.5 x 0.5 mm pore size). The remaining PET flakes were weighed and the extent of PET conversion was determined gravimetrically as follows [141, 143]:

$$\text{PET conversion (\%)} = \frac{M_{PET, Initial} - M_{PET, residual}}{M_{PET, Initial}} \times 100 \qquad \ldots\ldots\ldots\ldots(3.1)$$

where, $M_{PET, Initial}$ and $M_{PET; residual}$ refer to the initial mass of PET and the mass of PET flakes remaining unreacted in the reaction medium respectively. The white product

formed as a result of PET aminolysis is a mixture of terephthalamides, which can be separated on the basis of their solubility difference in ethanol[138]. For separation purposes, the aminolysed product was refluxed in ethanol for 2 h, followed by filtration after cooling to room temperature. The ethanol insoluble residue (Part A) was washed with acetone and dried at 50°C for 24 h. The filtrate was concentrated and placed in an ice bath to yield crystalline powder (Part B) which was filtered, washed with acetone to remove unreacted ethylene diamine and ethylene glycol, prior to drying at 40-45 °C for 6 h.

Mass spectrometry (discussed later), suggest that the ethanol soluble fraction (part B) is bis-(amino ethyl) terephthalamide

(**BAET**, $NH_2CH_2CH_2(NHCOC_6H_4CONHCH_2CH_2)_nNH_2$, where n=1), while the ethanol insoluble fraction (Part A) comprised of α,ω-aminoligo(ethylene terephthalamide) (**AOET**,$NH_2CH_2CH_2(NHCOC_6H_4CONHCH_2CH_2)_nNH_2$ where n $\geq$ 2).

3.2.3 Preparation of bis-benzoxazine monomer containing amide groups (C-BAET and C-AOET)

A mixture of cardanol (5 g, 16.4 mmol) BAET (2.06 g, 8.2 mmol), and paraformaldehyde (1 g, 32.9 mmol), was slowly heated to 80°C under constant stirring for 1 h, followed by heating at 90°C for 2 h. The reaction led to the evolution of water and the color of the reaction medium changed from yellow to red brown. Upon cooling, water (10 mL) was added and organic layer was extracted with chloroform (20 mL). The organic layers were combined and washed with aqueous NaOH solution (0.5 N, 100mL) followed by washing with water (3 x 30 mL), drying

over sodium sulphate and filtration. The solvent was removed under reduced pressure to give C-BAET as red sticky oil. Yield ~88%.

The method for the preparation of C-AOET is similar to that of C-BAET, except the amount of reactants used: cardanol (5 g, 16.4 mmol), paraformaldehyde (1 g, 32.9 mmol), AOET (3.62 g, 8.2 mmol) was slowly heated to 80°C and maintained under stirring for a period of one hour, followed by heating at 90°C for 4 h. C-AOET was obtained as red sticky oil. Yield ~83%.

3.2.4 Adhesive strength

To quantify the adhesive nature of the bis-benzoxazines, ~ 0.05 g of the liquid benzoxazine was coated on steel plates (15×15 mm^2). The assembly was clamped with paper clips and kept at 80°C for 30 mins, and cured in an air oven at 80 -180 °C (30 mins) followed by heating at 214°C (1 h) for the C-BAET and 238°C (1 h) for C-AOET. The thickness of adhesive layer was maintained at ~ 0.23-0.46 mm. A total of 6 replicates were tested per sample and the average value has been reported.

3.2.5 Characterization

Structural (FT-IR, ^{1}H-NMR, MS) and thermal (TGA and DSC) characterizations of amines and bis-benzoxazine monomers were performed. The surface morphology of PET during its aminolysis was monitored. The adhesive strength of the cross-linked polybenzoxazines was determined using ASTM D002. The detailed procedure has already been discussed in Chapter 2.

3.3 Results and Discussion

Microwave assisted aminolysis of PET in the presence of ethylene diamine was performed to yield terephthalamides which were used to synthesize sustainable bis-

benzoxazine containing amide groups by reacting with cardanol as a renewable source of phenol.

3.3.1 Aminolysis of PET

Detailed characterization of PET is presented in **Figure 3.1.**
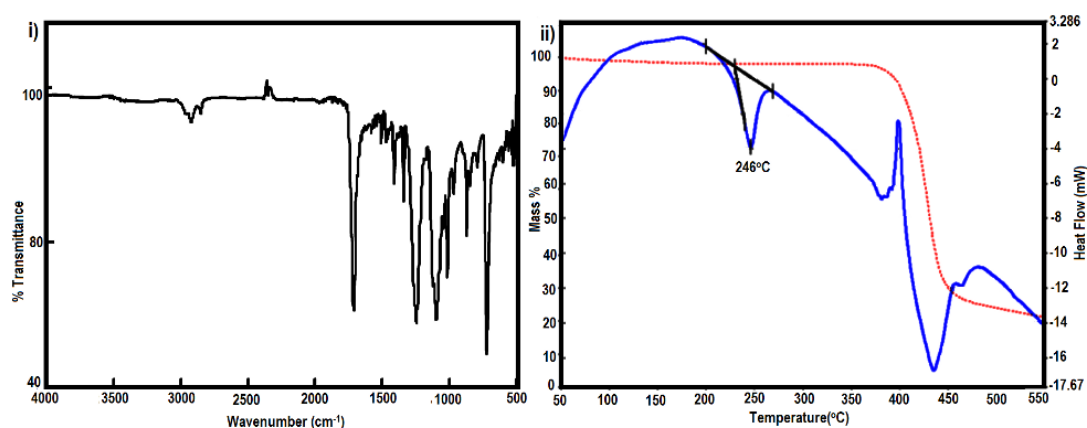
Figure 3.1: i) FT-IR and ii) DSC and TG traces of PET

The FT-IR spectra (**Figure3.1(i)**) shows characteristic absorption at ~1340 and ~1370 cm^{-1}, associated with the -CH$_2$- wagging in trans and gauche conformations respectively[144]. As is apparent from the DSC and TG traces (**Figure 3.1(ii)**) PET exhibits a sharp melting at ~246°C (crystallinity ~27.2 %) and undergoes a single step pyrolytic degradation commencing at 400 °C. The viscosity average molecular weight of PET was determined by solution viscometry. Samples were dissolved in a mixture of phenol and 1,1,2,2-tetrachloroethane(60/40 w/w) under heating and the intrinsic viscosity[143] was measured using ubbelohde suspension level viscometer at 25 C. the viscosity average molecular weight of PET was calculated as 27,431±162 g/mol using the following equation,

$$[\eta] = 75.5 \times 10^{-3} \text{ mL/g } M_v^{0.685} \quad \ldots\ldots\ldots \text{ (3.2)}$$

48

Aminolytic depolymerization of PET was performed under microwave irradiation with an aim to reduce the reaction time and energy as compared to the conventional process. The reaction is expected to result in the formation of terephthalamides of different molecular weights as per the reaction scheme presented in **Figure 3.2A,** the product composition being dependant on the relative quantities of PET and ethylene diamine in the reaction medium. In the presence of excess ethylene diamine, formation of bis(2-amino ethyl) terephthalamide (BAET) is expected, as shown in **Figure 3.2B(c).** However, the condensation of the half-aminolysed moiety with the terminal ester group of PET, followed by its further aminolysis results in the formation of higher oligomers i.e α,ω-aminoligo(ethylene terephthalamide) (AOET) as per the reaction (b)-(f) in **Figure 3.2B**[145-147], which was separated from BAET based on solubility differences in ethanol[138]. Higher molecular weight terephthalamide (AOET) is ethanol insoluble, while BAET, being ethanol soluble was recovered through solvent evaporation. The designated names, structural representation and masses of the products are given in **Table 3.1.** The terephthalamides obtained through PET aminolysis were characterized using mass spectrometry.

Table 3.1: Designation, molecular formula and expected molecular masses of the terephthalamides.

Designation	Molecular Formula	Expected Molecular Mass (amu)
BAET *(ethanol soluble fraction)*	$NH_2CH_2CH_2NHCOC_6H_4CONHCH_2CH_2NH_2$	250
AOET *(ethanol insoluble fraction)*	$NH_2CH_2CH_2(NHCOC_6H_4CONHCH_2CH_2)_nNH_2$	440 (n=2) 880 (n=4)
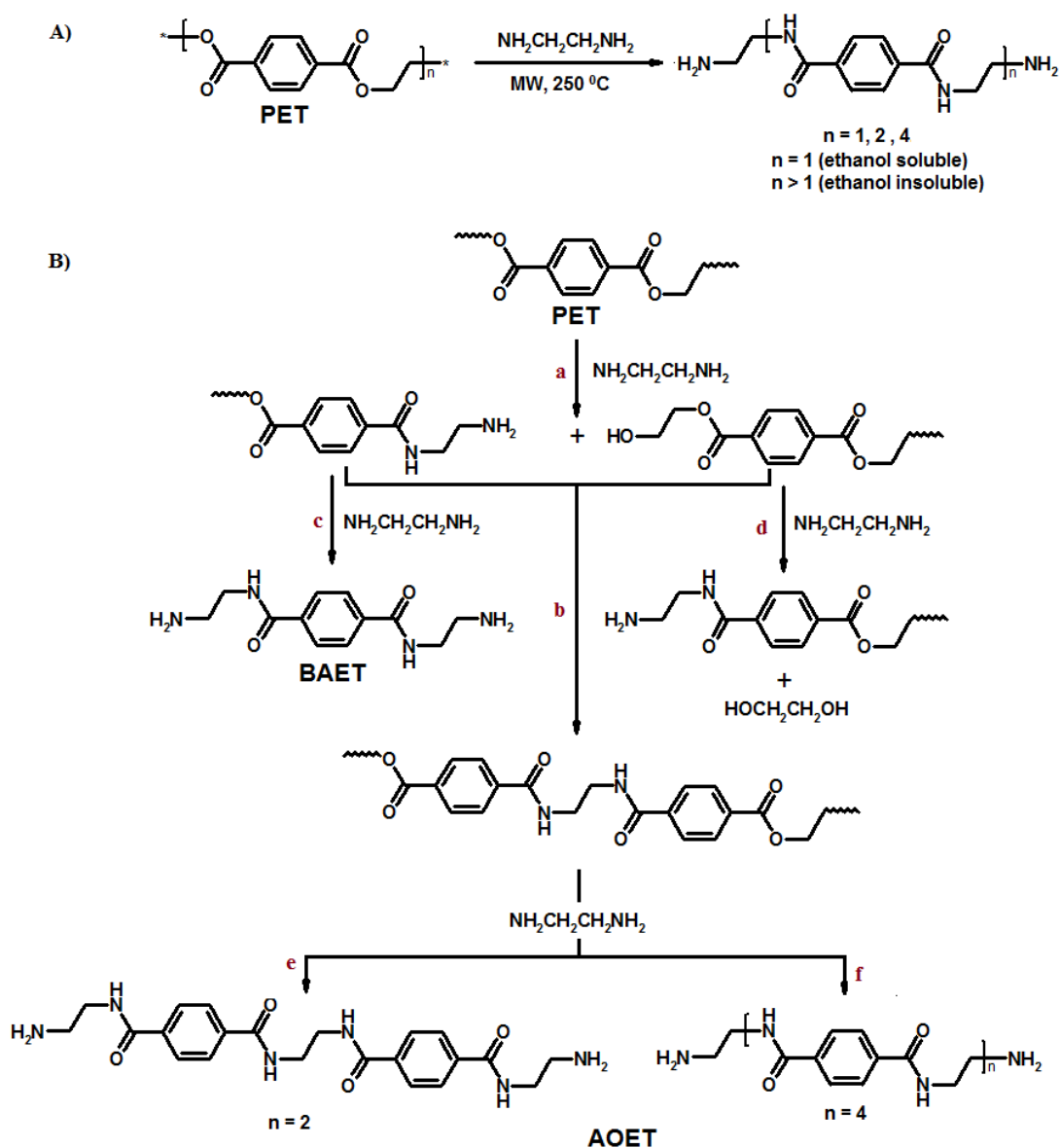
Figure 3.2: A) Aminolysis of PET B) Oligomers formation during PET aminolysis.

The mass spectrum of ethanol soluble terephthalamide fraction (Part B) eluted at 0.389-0.649 min is presented in **Figure 3.3.** The associated chromatogram is presented in the inset. The appearance of peak at m/z 251.1510 in the spectrum is attributed to the presence of BAET ionized by H^+. The other peaks at 273.1210 is due to BAET ionized by Na^+ and fragments for $[BAET-NH_2]^+$ at m/z 234.1263, $[BAET-2NH_2]^+$ at m/z 215.1297, suggest the molecular formula of BAET to be $NH_2CH_2CH_2NHCOC_6H_4CONHCH_2CH_2NH_2$.

50
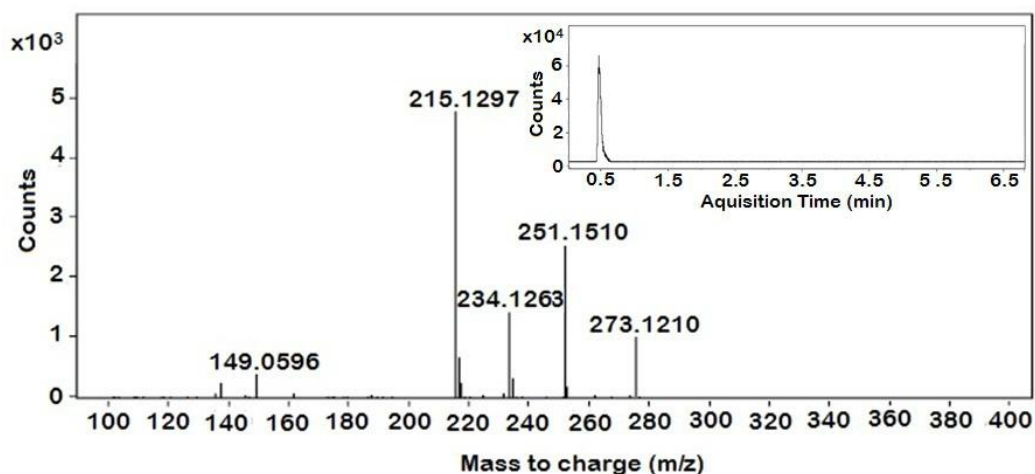
Figure 3.3: Mass spectra of ethanol soluble terephthalamide fraction eluted at 0.389-0.649 min.

The mass spectrum of ethanol insoluble fraction (Part A) eluted at 0.116 min is presented in **Figure 3.4** and the associated chromatogram is presented in the inset.
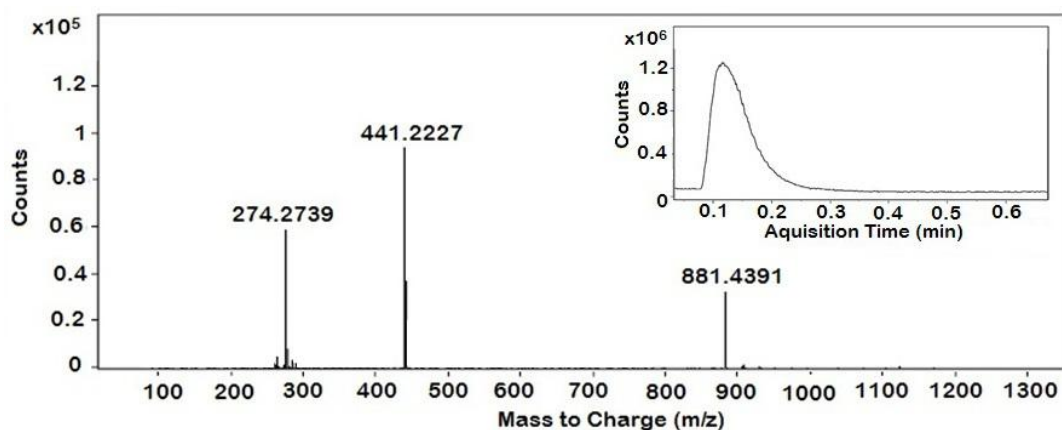
Figure 3.4: Mass spectra of ethanol insoluble terephthalamide fraction eluted at 0.116 min.

The peak profile is suggestive of the presence of more than a single component. The principal constituent terephthalamide in part A, $NH_2CH_2CH_2(NHCOC_6H_4CONHCH_2CH_2)_nNH_2$, is the dimer (n=2) which is confirmed by the appearance of peak at m/z 441.2227. However, the presence of tetramer (n = 4) is also confirmed by the appearance of peak at m/z 881.4319 (n=4) ionized by H^+ (**Table 3.1**).

51

3.3.1.1. Effect of reaction temperature on PET conversion

The effect of increasing temperature on PET aminolysis was studied by following the extent of PET conversion, the results of which are presented in **Figure 3.5**. As expected, an increase in the reaction temperature led to an increase in PET conversion. At lower temperatures (T ≤ 150 °C), PET conversion is rather negligible (≤ 2 %). However, as the temperature is raised to 250°C, complete conversion can be effected within 10 mins. The notable increase in the rate can be attributed to the melting of the solid PET flakes at 246°C, which leads to the formation of a homogenous reaction medium. On the other hand, the solid-liquid reaction remains largely diffusion controlled, which accounts for the slower rates of reaction at lower temperatures[138].
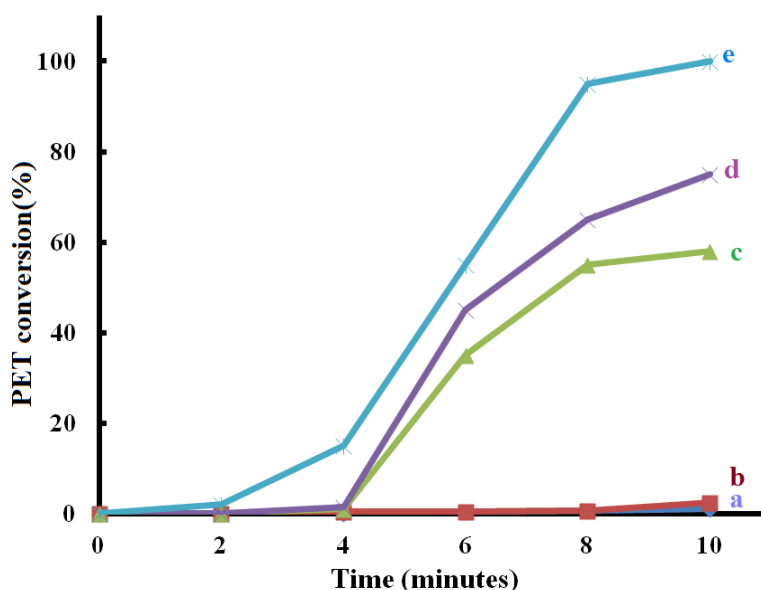
Figure 3.5: PET conversion as a function of the reaction temperature and time a) 100 b) 150 c) 220 d) 230 e) 250 °C (PET:ED::1:6)

Aminolysis initiates at the solid-liquid interface with the diffusion of the amine into the solid PET, resulting in the swelling of the polymer followed by its

52

depolymerization into terephthalamides of lower molecular weight. Amorphous regions are expected to be more susceptible to degradation[141, 148] which was confirmed by morphological investigations. The SEM images of the surface of recovered PET are presented in **Figure 3.6**. It can be seen, the smooth surface of neat PET develops cracks, with the extent of corrugation increasing with time. The crystallinity of PET flakes was found to increase from 27.2 to 37.2 % due to diffusion of lower terephthalamides from PET[149].
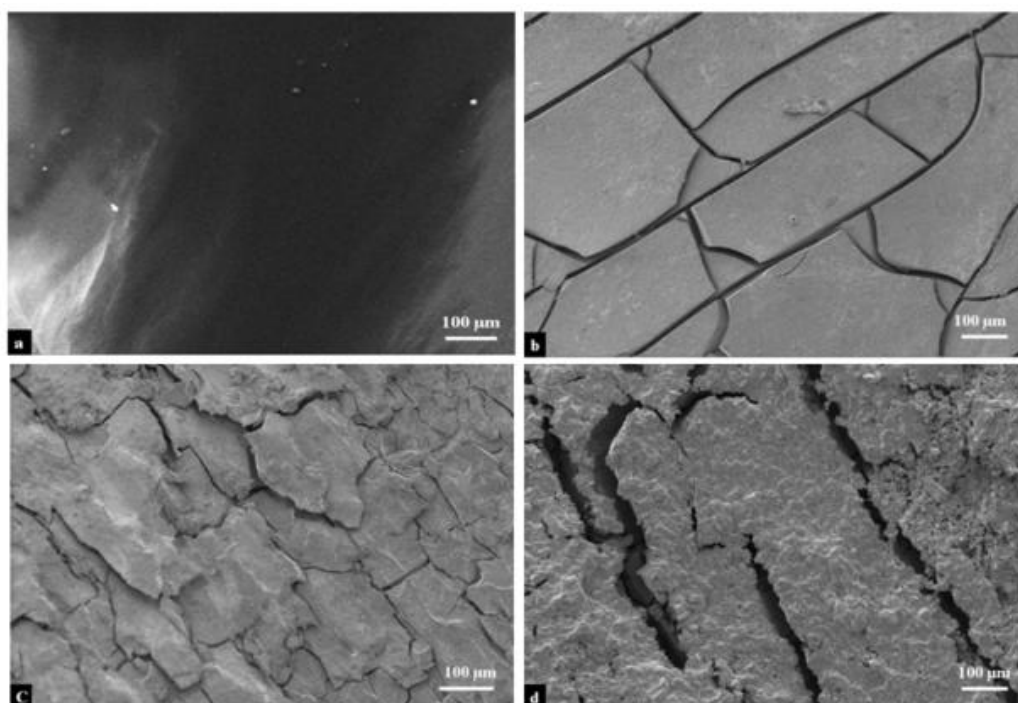
Figure 3.6: Scanning electron micrographs of PET films (a) Neat PET films and residual PET after reacting with ethylene diamine for duration of (b) 4 (c) 6 (d) 8 mins.(reaction temperature 230°C, PET:ED :: 1:6)

Representative plots showing the variation of operating parameters during microwave assisted PET aminolysis at two different temperatures (230 and 250 °C) is presented in **Figure 3.7**. It can be seen that the temperature and pressure increase initially and remain practically constant thereafter, while the microwave power drops significantly after the rapid initial increase. PET aminolysis has been reported to be a slow process

53

requiring extended time periods for completion. A recent study revealed that the unanalysed aminolytic depolymerization of PET under electrical heating required more than 17 h, in the presence of excess ED (PET:ED::1:8)[138]. The studies are clearly suggestive of the advantages associated with microwave assisted PET aminolysis. The same is attributed to the high loss factor of ED (δ= 0.573), which is indicative of the strong ability of the diamine to convert electromagnetic energy to heat[150, 151].
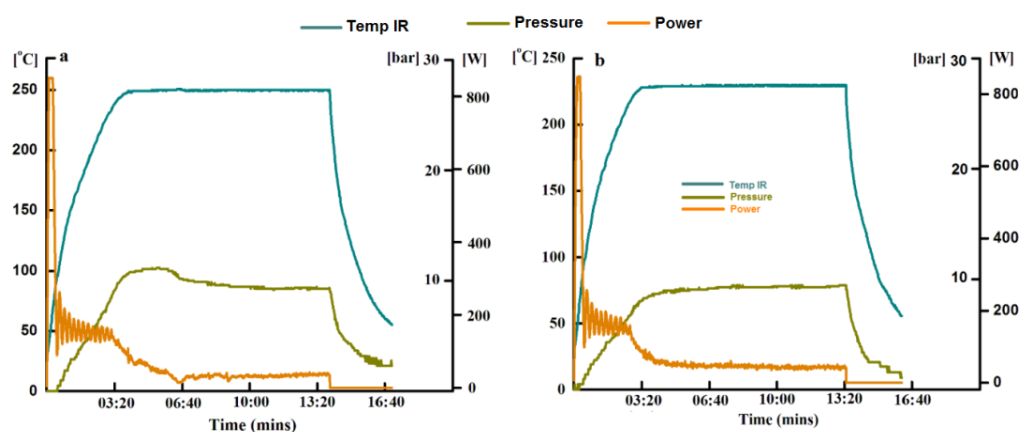
Figure 3.7: Microwave profile of PET aminolysis at a) 250 and b) 230 °C.

3.3.1.2. Effect of reactant ratio on PET conversion and product composition

The effect of increasing PET:ED on the extent of PET conversion is presented in **Figure 3.8(i)**. It is to be noted that stochiometrically, PET:ED of 1:2 is sufficient to effect complete depolymerization of PET. However, under these conditions, only 30 % conversion could be effected, which increased with increasing amounts of ED in the reactant medium. Complete PET conversion could only be effected as the PET:ED ratio increased to 1:6, under the experimental conditions employed. The effect of varying PET: ED ratio on the relative fraction (%) of AOET and BAET is presented in **Figure 3.8(ii).**
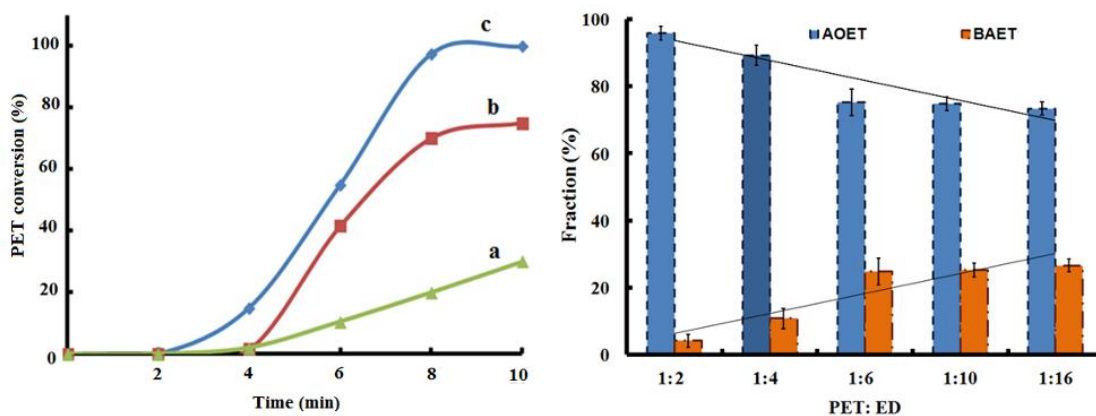
Figure 3.8: i) PET conversion as a function of reaction time and PET : ED ratio a) 1:2 b) 1:4 and c) 1:6 ii) Relative fraction (%) of AOET & BAET as a function of PET:ED ratio (reaction temperature 250 °C, time 10 mins)

As per Carothers relation, increasing the stoichiometric imbalance between the reactants in the system precludes the formation of higher molecular weight species[152]. Assuming that all the ester linkages in PET have equal probability of undergoing aminolysis, regardless of their position in the chain and the molecular weight of the polymer, the extent of depolymerization resulting in the formation of lower molecular weight terephthalamides is expected to increase with higher amounts of ED in the reaction medium. It can be seen that the product mixture obtained at lower PET:ED comprise primarily of higher species (AOET) with lesser amounts of BAET, the amount of which increases with increasing ED. Interestingly, increasing the amount of ED in the medium beyond PET:ED:: 1:6 did not exert any pronounced effect on the product composition.

The variation in BAET yield (%) with PET:ED ratio, as quantified in terms of the ratio of amount of BAET experimentally obtained to the theoretical prediction is presented in **Figure 3.9,** which shows that maximum BAET yield can be obtained under PET:ED ::1:6 at a reaction temperature of 250°C.
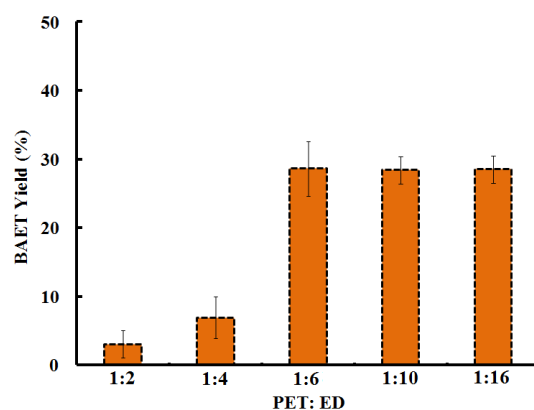
Figure 3.9: BAET yield as a function of PET:ED ratio (reaction temperature 250 °C, reaction time 10 min)

As expected, the FT-IR spectra of AOET and BAET in **Figure 3.10** is rather similar, with characteristic $v_{C=O,amide}$ at 1626 cm^{-1}, $v_{N-H,1°}$ at 3342 cm^{-1} and $v_{N-H,2°}$ at 3280 cm^{-1} [153]. The relative intensity of the peaks associated with NH stretching of 1° and 2° amines in BAET was higher as compared to AOET, which was quantified in terms of the ratio of their absorbance. This ratio (0.57, BAET and 0.49 AOET) clearly indicates that the concentration of 1° amine in BAET is greater than in AOET, in line with the structure presented in **Figure 3.2**.
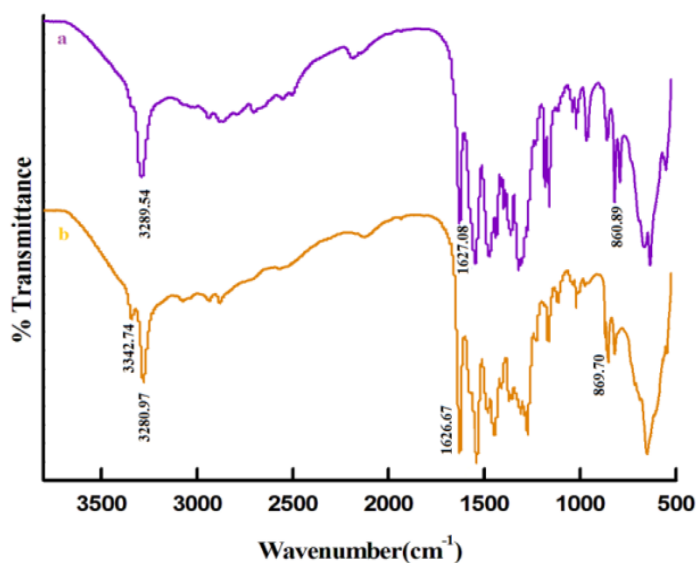
Figure 3.10: FT-IR of a) AOET b) BAET

56

The terephthalamides fractions were also characterized using ^{1}H-NMR spectroscopy using DMSO as a solvent (**Figure 3.11**). The ^{1}H-NMR spectrum of BAET (**Figure 3.11a**) shows resonances at 8.0 ppm (4H, s, aromatic), 3.2 ppm (4H, t, CONH**CH₂**CH₂NH₂) and 2.7 ppm (4H, t, CONHCH₂**CH₂**NH₂). The ^{1}H-NMR spectrum of AOET (**Figure 3.11b**) shows resonances at 8.0 ppm (8H, s, aromatic), 3.4 ppm (4H, t, CONH**CH₂**), 2.7 ppm (4H, t, CONHCH₂**CH₂**NH₂), 4.3 ppm (4H, s, CONH**CH₂CH₂**NHCO). The appearance of a singlet centered at 4.3 ppm in the spectra of AOET is due to the symmetrical ethylene group in between two amide groups in addition to the peaks of asymmetrical ethylene group in between an amide and an amine group at 3.4 and 2.7 ppm of part B.
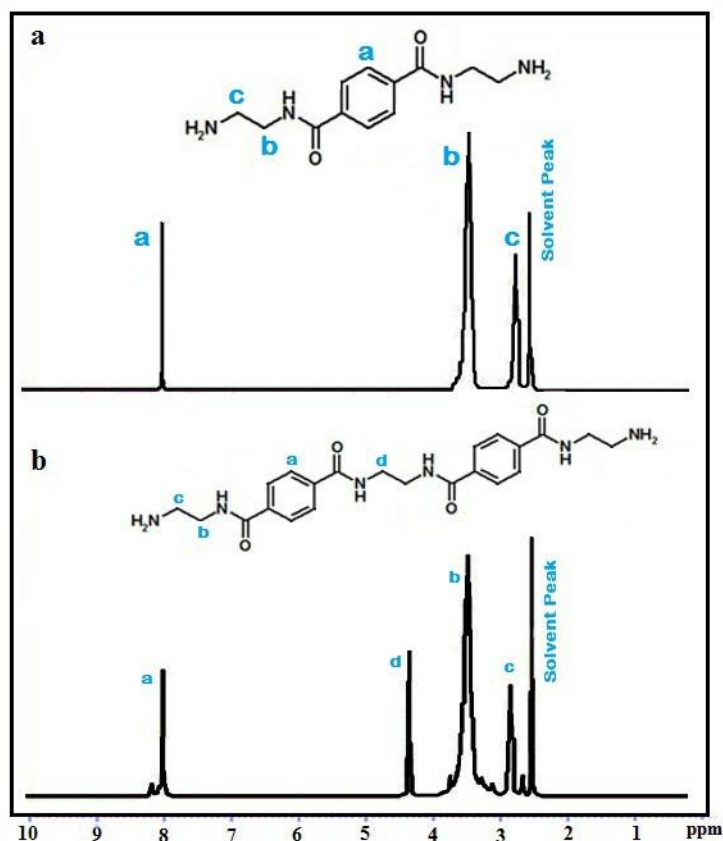
Figure 3.11: ^{1}H-NMR of a) AOET b) BAET

The DSC traces of BAET and AOET are presented in **Figure 3.12**. The sharp endotherm appearing at 181 and 298 ºC are associated with the melting of BAET and AOET respectively. It is to be noted that the melting point of the terephthalates obtained by glycolysis of PET in the presence of ethylene glycol is much lower; 110 and 160ºC for bis-(hydroxyethyl) terephthalate (BHET) and oligomers respectively[143]. This difference in the melting points of PET glycolysates and aminolysates can be attributed to the strong intermolecular H –bonding between the amide groups in terephthalamide which is absent in the analogues esters.
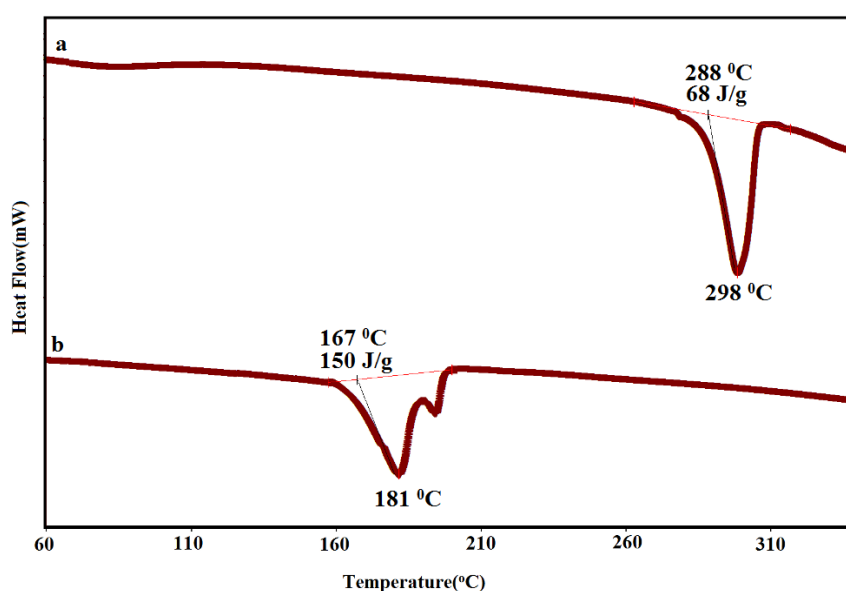
Figure 3.12: DSC traces a) AOET b) BAET

3.3.2 Synthesis of bis-benzoxazines (C-BAET and C-AOET)

Bis-benzoxazines containing amide linkages were prepared using a solventless route by reacting cardanol with the PET derived terephthalamides obtained by PET aminolysis as per the reaction scheme presented in **Figure 3.13**. The oxazine ring formed by Mannich like condensation of cardanol with terephthalamide and paraformaldehyde (2:1:4) is capable of undergoing ring opening polymerization

58

leading to the formation of a cross-linked network. The presence of amide linkage in view of the H-bonding is expected to alter the properties of the resin appreciably. The benzoxazine resins obtained by the reaction of cardanol and formaldehyde with BAET and AOET have been referred to as C-BAET and C-AOET respectively.
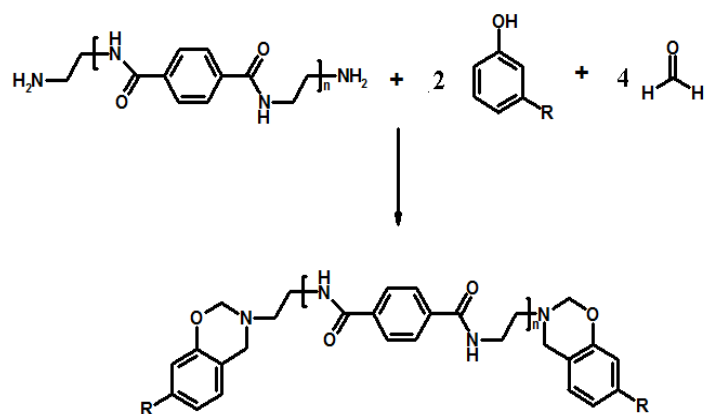
Figure 3.13: Bis-benzoxazine formation by reaction of terephthalamide with cardanol and formaldehyde

The FT-IR spectra of cardanol, C-BAET & C-AOET is presented in **Figure 3.14**. The benzoxazine monomers, showed the absence of O-H and N-H at ~3335, >3161 cm^{-1}, suggestive of complete utilization of cardanol and amine towards formation of oxazine ring. In addition to the stretching bands associated with the aromatic and alkene (3008 cm^{-1}), and aliphatic (2926 and 2854 cm^{-1}) C–H vibrations, other characteristic absorption bands observed in the spectra can be attributed to the C=C (~1600 cm^{-1}), asymmetric and symmetric stretching vibrations of C-O-C (~1245 cm^{-1} and ~1030 cm^{-1}), CH$_2$ wagging (1370 cm^{-1}), and asymmetric stretching vibrations of C-N-C (1116 cm^{-1}) respectively supporting the presence of double bonds and oxazine ring in Bz monomers. In cardanol, the peak at 990 cm^{-1} can be attributed to the C=C-H vinylene C-H out-of-plane bend associated with the alkylene chain. Benzoxazine monomers showed a bimodal peak centered at 990 and 960 cm^{-1} associated with the

out-of-plane bending vibrations of C-H bond due to alkylene double bond and oxazine ring respectively[58].

Figure 3.14: FT-IR spectra: a) cardanol b) C-BAET c) C-AOET

The ^{1}H-NMR of both the bis-benzoxazine resins was recorded using CDCl$_3$ as solvent and presented in **Figure 3.15**. C-BAET exhibit characteristic resonances at ~5.3 ppm (4H, m, ArO**CH$_2$**N) and ~4.7 ppm (4H, s, Ar**CH$_2$**N) suggesting the conversion of hydroxyl to oxazine functionality (**Figure 3.15a**). Similarly, C-AOET formation was confirmed by the appearance of resonance at ~5.4 ppm (4H, m, ArO**CH$_2$**N) and ~4.6 ppm (4H, s, Ar**CH$_2$**N) (**Figure 3.15b**). The intensity ratio of the signals associated with the oxazine moiety at 4.6 (singlet) and 5.4 ppm (multiplet) is expected to be 1:1. However, the same was found to be higher in the present study, which can be attributed to the resonance of alkylene protons present in cardanol (m, CH=, CH$_2$=CH–) at the same position as ArO**CH$_2$**N (~5.4 ppm). In cardanol based benzoxazines this ratio has been reported to be 1:3[126]. This deviation from 1:1 can

60

also be ascribed to the oligomerization of the benzoxazine resin. The protons associated with the >CH$_2$ in the Mannich base formed as a result of ring opening appear in the region 3.5-4 ppm which overlap with the peaks associated with the amine protons (BAET and AOET) in the same region as can be seen in the NMR spectra.
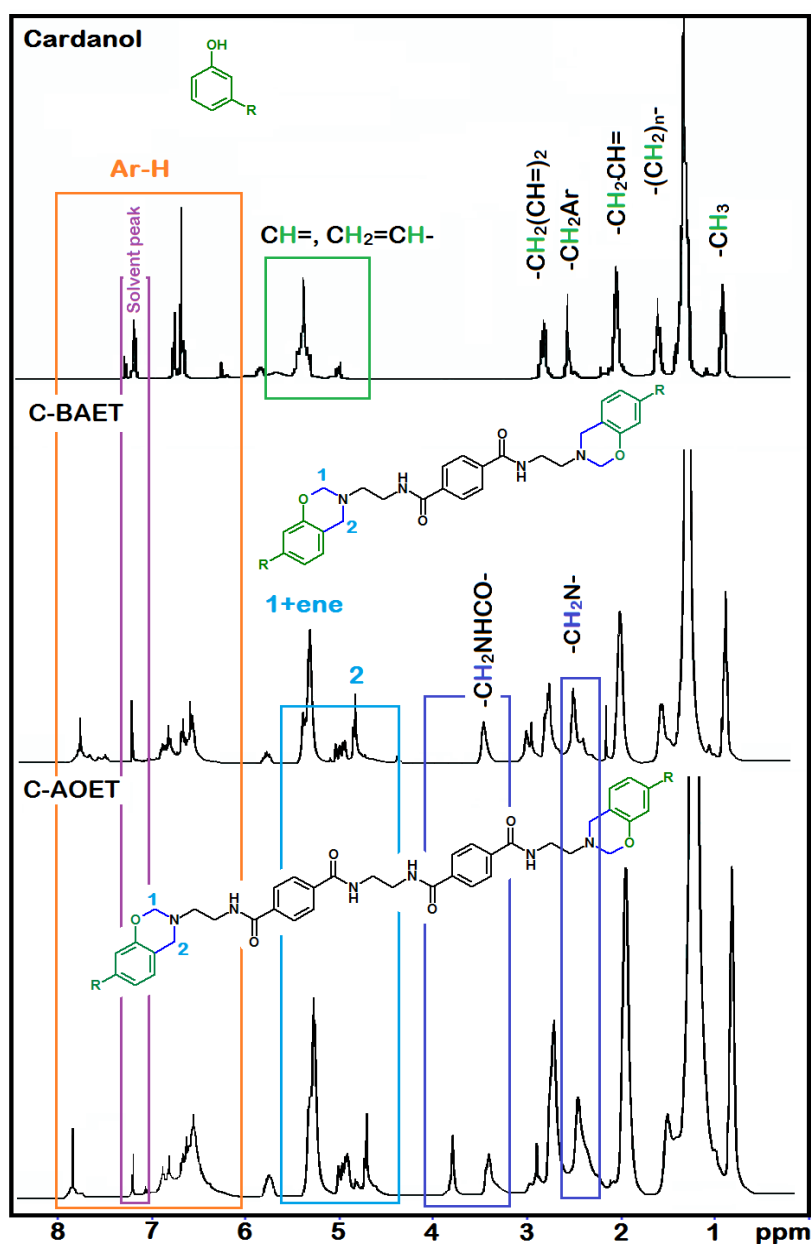
Figure 3.15: ^{1}H-NMR spectra a) Cardanol b) C-BAET c) C-AOET

61

To investigate the curing behavior of the benzoxazine resins, non-isothermal calorimetric studies were performed and the curing profiles are presented in **Figure 3.16**. It can be seen that the temperature associated with the curing of C-BAET (T_{peak} = 214 ºC) is relatively lower than C-AOET (T_{peak} = 238ºC). This is in accordance with studies reported[113], where increasing the chain length between benzoxazine moieties leads to a increase in curing temperature. In chapter 1, the curing behavior of cardanol-aniline based mono-benzoxazine (C-a) is presented and shows that the ring opening polymerization in C-a initiates at relatively higher temperature (T_{onset} ~242ºC and T_{peak} ~263ºC)[154]. The studies clearly suggest that increasing the functionality can lead to substantial lowering of the curing temperature [126, 130]. Further, the molar enthalpy associated with the polymerization for C-AOET is lower than C-BAET, which can again be credited to the larger number of oxazine rings per unit mass in the latter.
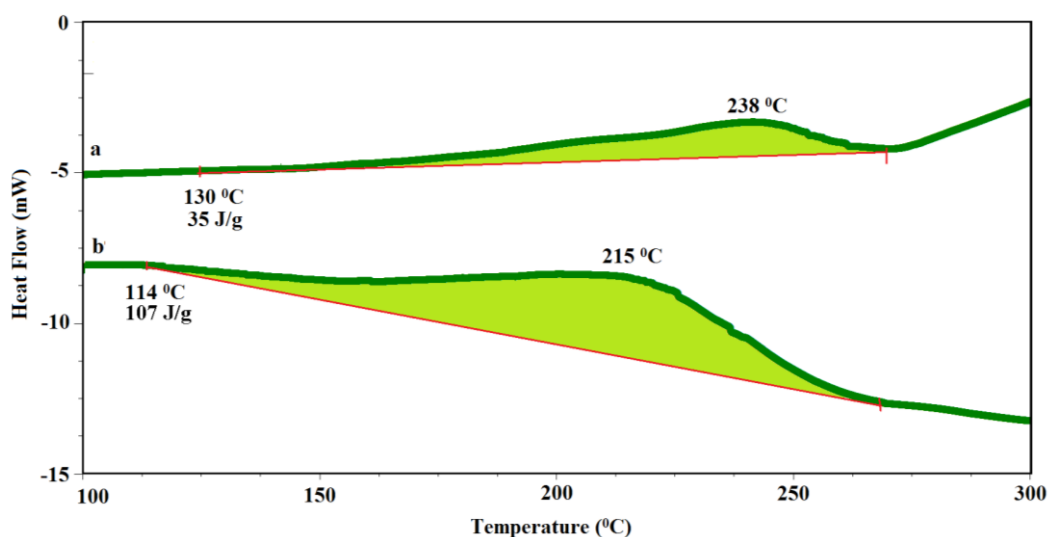
Figure 3.16: DSC Traces: a) C-AOET b) C-BAET

The TG-DTG traces of the cured benzoxazines are presented in the **Figure 3.17.** The benzoxazine resins prepared in the present work were found to exhibit excellent

thermal stability with the temperature associated with 5 % wt. loss being 298 and 380 °C for poly(C-BAET) and poly(C-AOET) respectively, suggesting their application in demanding areas requiring high thermal stability.
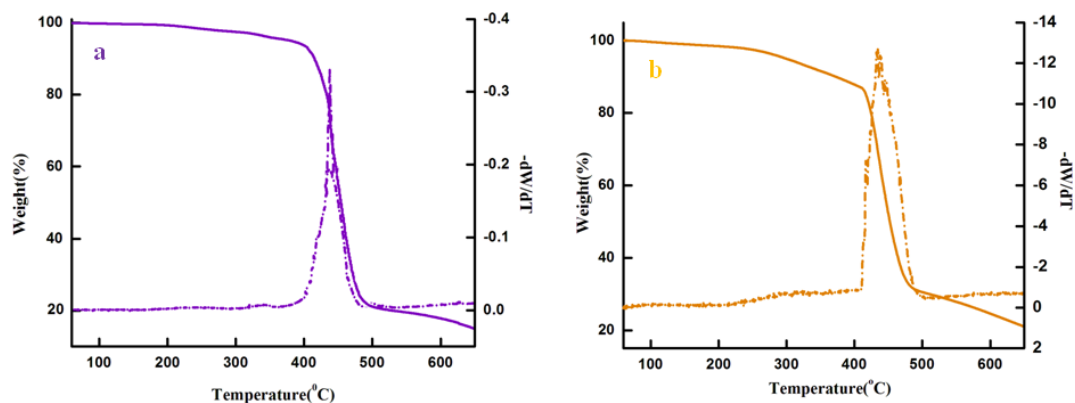
Figure 3.17: TGA traces of a) poly(C-AOET) b) poly(C-BAET)

3.3.3 Adhesive property

The adhesive nature of the bis-benzoxazine resin was quantified as per the standard procedure. The results in terms of lap shear strength (LSS) are presented in **Table 3.2** and the representative load-displacement curve is presented in **Figure 3.18.**

Table 3.2: Lap Shear Strength of benzoxazine resins

Benzoxazine Resin	Lap Shear Strength (kgcm^{-2})
C-BAET	38.2 ± 3.9
C-AOET	28.3 ± 3.1
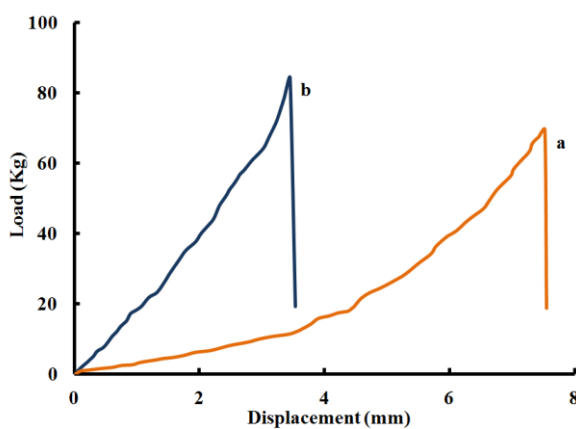
Figure 3.18: Representative load displacement curve of cured resins of a) C-AOET and b) C-BAET

63

It is to be noted that the LSS is dependent on several factors, particularly the ability of the resin to wet the substrate, its inherent adhesive nature, temperature, thickness of the resin and type of failure. The presence of larger number of polymerizable molecules in benzoxazines which undergo thermally activated ring opening polymerisation in the absence of catalyst form cross linked networks on metal surfaces[123]. The ring opening of oxazine moieties generates specific groups which are capable of undergoing H-bonding, such as –OH and >N- as shown in FT-IR of cured resin **Figure 3.19**, in addition to the amide linkages which are already available in the main chain.
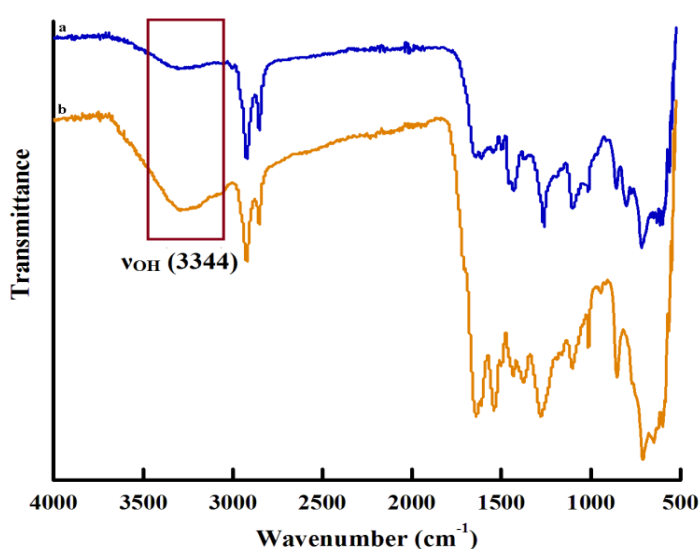
Figure 3.19: FT-IR Spectra of a) poly(C-AOET) b) poly(C-BAET)

Due to the presence of larger number of polymerizable benzoxazine in C-BAET as compared to C-AOET, the lap shear strength of the former was found to be relatively higher which advocate the use of these resins as healants for self healing applications[155-157].

Chapter 4
Structural Modification in Cardanol Based Benzoxazine with Urea Linkages
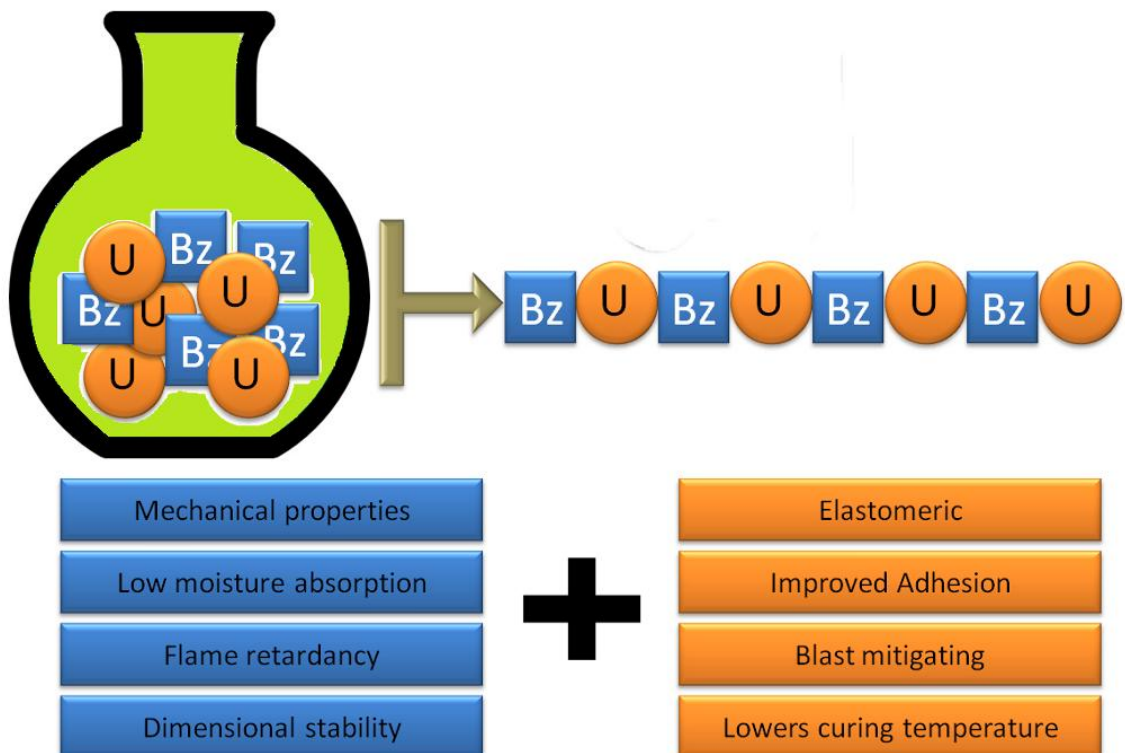
4.1 Introduction

Blending and copolymerization has been attempted by academicians to prepare low curing benzoxazine systems without compromising on the performance of the product. In this context, the functionalities which are intrinsically capable of lowering the polymerisation temperature of benzoxazines such as nitriles[158], ester[159], epoxy[160], urethanes[161], maleimides[162, 163], siloxane[164], acetylene[165], have been explored. The integration of benzoxazines moieties in other polymeric networks have been reported to be advantageous for the co-monomer as the copolymerization improves the thermal and mechanical performance of the latter. Surprisingly, the potential of urea linkages has not been explored towards lowering of the curing temperature of benzoxazines, the former being reported of exhibiting exceptional blast resistance[166], but relatively inferior thermal stability.

A general flow chart, illustrating possible routes for preparation of benzoxazine copolymers is presented in **Figure 4.1**. Self polymerizable monomers can be integrated in the polymeric network by functionalizing the benzoxazine with the co-monomer, followed by thermal treatment (**Figure 4.1, Approach 1**)[158]. Blending/reaction of benzoxazine with co-monomer is usually performed, where the monomer mandates a curing agent (**Figure 4.1, Approach 2**)[167]. The phenols generated as a result of benzoxazine polymerisation acts as curing agents for the co-monomer and, thus are blocked from participating in intramolecular six-membered ring hydrogen bonding, responsible for bestowing unique properties of polybenzoxazines[40, 168]. Baqar et al.[161], addressing the above said issue, reported a route where benzoxazine is first substituted and subsequently reacted with the curing agent of the co-monomer, followed by the thermal polymerization of

oxazine moiety, resulting in cross-linked alternating copolymer (**Figure 4.1, Approach 3**).

A is self polymerizable	A requires curing agent (C)	
Difunctionalize Bz by A	Blending of Bz with prepolymer	Difunctionalize Bz by A/C
Approach 1	*Approach 2*	*Approach 3*

Thermal Polymerization — Main chain benzoxazine copolymer

-OH generated during polymerisation acts as a curing agent — Thermal Polymerization

Reaction with C/A — Main chain benzoxazine copolymer — Thermal Polymerization

Poly(benzoxazine-co-A)

Thermal Polymerization | Ring opening polymerisation

Present Approach

Functionalize A with one of the reactants for benzoxazine (phenol/amine termination)
NH$_2$-A-NH$_2 \longrightarrow$ Bz-A1-Bz

Bz : benzoxazine monomer	A : co-monomer	C: curing agent for A

Figure 4.1: Varied approaches behind benzoxazine copolymer preparation

Here we make an attempt to functionalize a model compound containing urea linkages with amine terminals and utilizing the same as a co-reactant for the preparation of bis-benzoxazine monomer containing urea linkages. The monomer is prepared by solventless Mannich like condensation of cardanol with amine terminated model compound containing urea linkages. The terminal oxazine moieties are expected to undergo ring-opening polymerisation leading to the formation of cross-linked polymer with alternating benzoxazine-urea linkages. The effect of amalgamating urea linkages with benzoxazine moieties is expected to alleviate the curing profile and improve the adhesive properties of the resin.

4.2. Experimental

4.2.1 Materials

Cardanol was obtained from Satya Cashew Chemicals Pvt. Ltd. (India). 4,4'-Methylenebis(phenyl isocyanate)/MDI (AR, Aldrich) was used without purification. Sodium sulphate, paraformaldehyde, chloroform, ethylene diamine, obtained from CDH was used as such. Double distilled water was used throughout the course of this work.

4.2.2 Synthesis of 4,4′-Methylenebis(3-ethylamine-1-phenylurea)(AMDI)

4,4′-Methylenebis(3-ethylamine-1-phenylurea) was prepared by the additive rearrangement of ethylene diamine with MDI. For this purpose, a reaction mixture of MDI (1 g, 4 mmol) with excess of ethylene diamine (1.44 g, 24 mmol) was sealed under nitrogen atmosphere and allowed to react at room temperature for ~15 mins. The white precipitate obtained upon addition of chloroform, was washed repeatedly and finally dried under vacuum at 50°C.

3.2.3 Synthesis of bio-based benzoxazine monomer containing urea linkages (C-amdi)

A mixture of cardanol (5 g, 16.4 mmol), AMDI (2.06 g, 8.2 mmol), and paraformaldehyde (1 g, 32.9 mmol), was slowly heated to 80°C under constant stirring for 1 h, followed by heating at 90°C for 2h. The reaction led to evolution of water and the colour of the reaction medium changed from yellow to red brown. Upon cooling, water (10 mL) was added and the organic layer was extracted with chloroform (20 mL). The organic layers were combined and washed with aqueous NaOH solution (0.5 N, 100 mL) followed by washing with water (3 x 30 mL) and

67

drying over sodium sulphate and filtration. The solvent was removed under reduced pressure to give C-amdi as red sticky oil. Yield ~85%.

4.2.4 Adhesive property

To quantify the extent of adhesion of the developed copolymer, Lap shear strength was estimated for which ~ 0.05 g of the liquid resin was coated on steel plates (15×15 mm^2) as per ASTM D1002 standard. The assembly was clamped with paper clips and maintained at 80°C for 30 mins, and cured in an air oven at 80-180°C (30 min) followed by heating at 202°C (1 h). The thickness of adhesive layer was maintained at ~ 0.23-0.46 mm. A total of 6 replicates were tested for sample and the average value has been reported.

4.2.5 Characterization

Structural (FT-IR, ^{1}H-NMR, MS) and thermal (TGA and DSC) characterizations of amine and benzoxazine monomer were performed. The adhesive strength of the cross-linked polybenzoxazines was determined using ASTM D1002. The fractured samples were analysed through SEM to study the fractography. The characterisation techniques have been discussed extensively in previous chapters. The rheological behavior was analysed to study the processing window of the developed resin. Anton Paar Rheometer MCR102 was used to study the rheological behavior of the benzoxazines in three intervals of temperature profile by keeping constant strain of 0.5% and constant angular frequency of 10 rad/s in each interval.

4.3 Results and Discussion

4.3.1 AMDI, 4,4′-Methylenebis(3-ethylamine-1-phenylurea)

The additive rearrangement of diisocyanate with diamine exhibit rapid reaction kinetics, and under stoichiometric conditions (1:1) leads to the formation of polyurea

as shown in **Figure 4.2**. However, performing the reaction in the presence of excess of any one of the reactants, a drastic reduction in degree of polymerization is expected **(Inset, Figure 4.2),** as predicted by the Carothers relation[152].
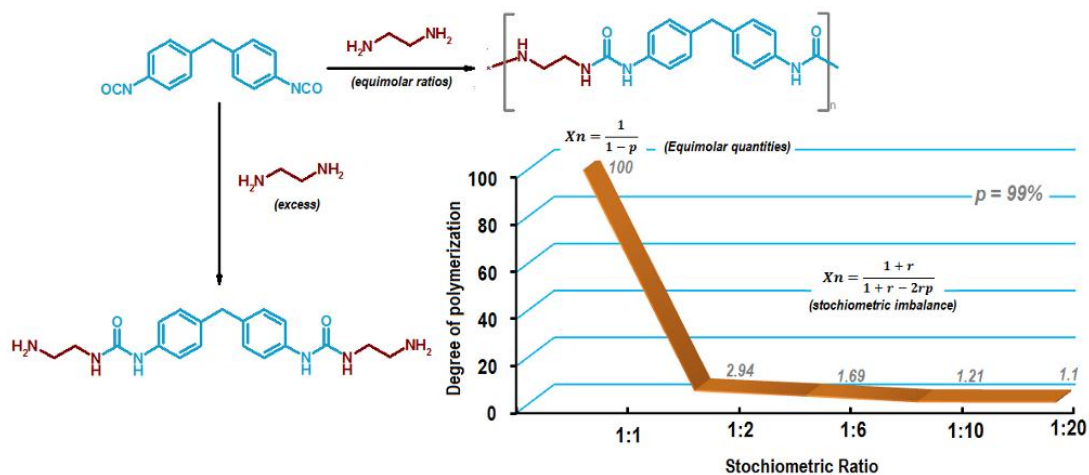
Figure 4.2: Preparation of 4,4′-methylenebis(3-ethylamine-1-phenylurea) (AMDI)

Since polyurea is prepared from step-growth polymerization of diisocyanates and diamines under stoichiometric conditions (1:1), Carothers equation can be used to predict the degree of polymerization (X_n) for a given fractional monomer conversion, p (eq 4.1).

$$Xn = \frac{1}{1-p} \quad ....(4.1)$$

Stoichiometric imbalance is expected to lower the degree of polymerisation (X_n) as denoted by eq (4.2).

$$Xn = \frac{1+r}{1+r-2rp} \quad ....(4.2)$$

where **r** is the stoichiometric ratio of the reactants.

The reaction of diisocyanate with diamine exhibits rapid reaction kinetics and high monomer conversion (p ~99%). The degree of polymerisation $X_n,$ can be theoretically estimated for different values of **r** and is tabulated in **Table 4.1**.

Table 4.1: Degree of polymerisation X_n, for different values of r

MDI: ED	Stoichiometric ratio (r)	Degree of polymerization (X_n)
1:1	1	100
1:2	0.5	2.94
1:6	0.16	1.69
1:10	0.1	1.21
1:20	0.05	1.1

It can be seen that the reactant ratio has a pronounced effect on the degree of polymerization. At isocyanate: amine::1:6, X_n drops down to 1.69, which is sufficiently low to arrive at 4,4′-methylenebis(3-ethylamine-1-phenylurea) required for the synthesis of polybenzoxazine containing urea linkages.

HPLC-MS of the obtained product was performed and the mass spectrum of amine eluted at 0.37 min is presented in **Figure 4.3.** The appearance of peak at m/z 372.4580 in the spectrum is due to the presence of AMDI ionized by $2H^+$. The other peaks at m/z 398.2002 and 355.3349 can be attributed to AMDI ionized by Na^+ and fragments for $[AMDI-NH_2]^+$, which suggest the formation of AMDI with molecular formula of $NH_2CH_2CH_2NHCONHC_6H_4CH_2C_6H_4NHCONHCH_2CH_2NH_2$.
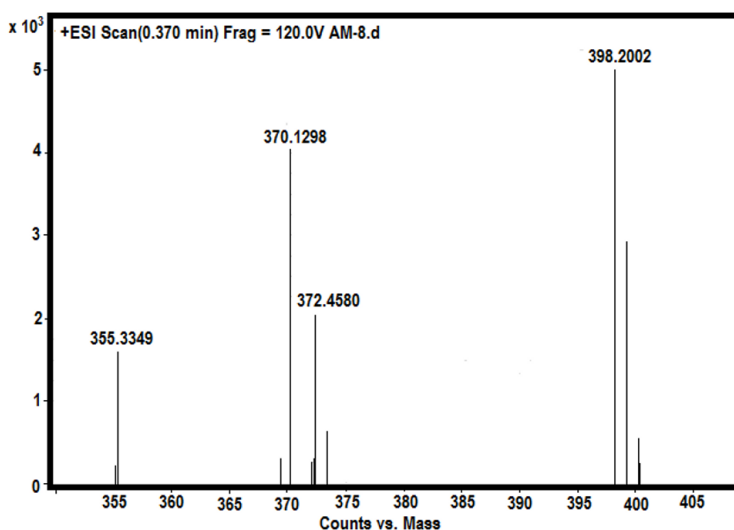
Figure 4.3: Mass spectra of AMDI eluted at 0.370 min

The FT-IR spectra of AMDI and MDI is presented in **Figure 4.4(i(a,b)).** The presence of a sharp absorption band at 3298 cm^{-1} ($v_{N-H,1°}$), 1633 cm^{-1} ($v_{C=O, urea}$) and the absence of $v_{N=C=O}$ at 2274 cm^{-1} in the spectra of AMDI indicate complete conversion of isocyanate to form urea linkages[153].
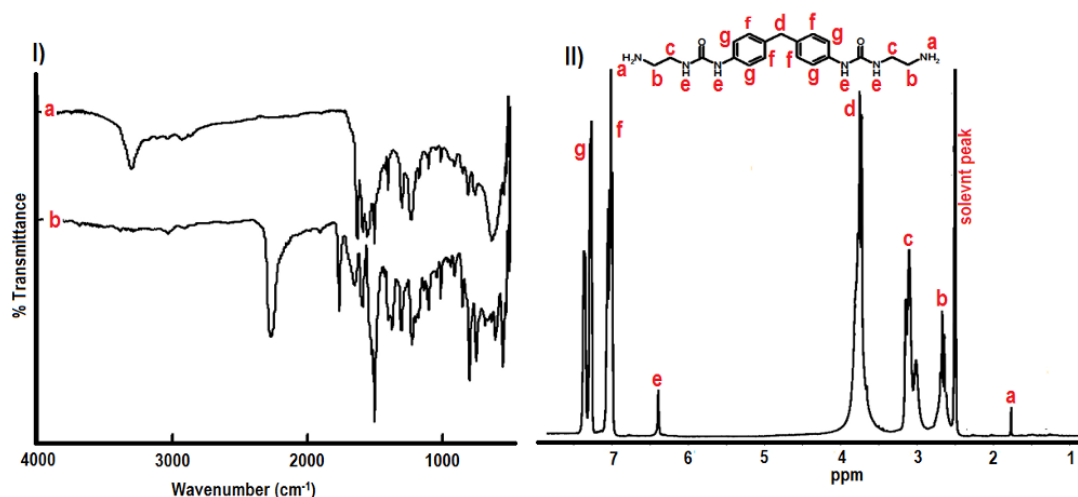
Figure 4.4: i) FT-IR and ii) ^{1}H-NMR of AMDI

The structure of AMDI was further confirmed using ^{1}H-NMR spectroscopy where DMSO is used as the solvent (**Figure 4.4(ii)**). The spectrum shows resonances at ~ 7.1 ppm (4H, aromatic), 7.5 (4H, aromatic), 6.3 ppm (4H, t, -N**H**CON**H**-CH$_2$CH$_2$NH$_2$), 3.8 ppm (2H, -C$_6$H$_4$-**CH$_2$**-C$_6$H$_4$-), 3.2 ppm (4H, -NHCONH-**CH$_2$**CH$_2$NH$_2$) and 1.8 ppm (4H, CONHCH$_2$**CH$_2$**NH$_2$).

A sharp endothermic peak at 129ºC, associated with the melting of AMDI was observed in the DSC trace (**Figure 4.5**). The difference in the melting point of AMDI and MDI from which it is derived (42-45ºC), can be attributed to the strong intermolecular H–bonding between the urea linkages.
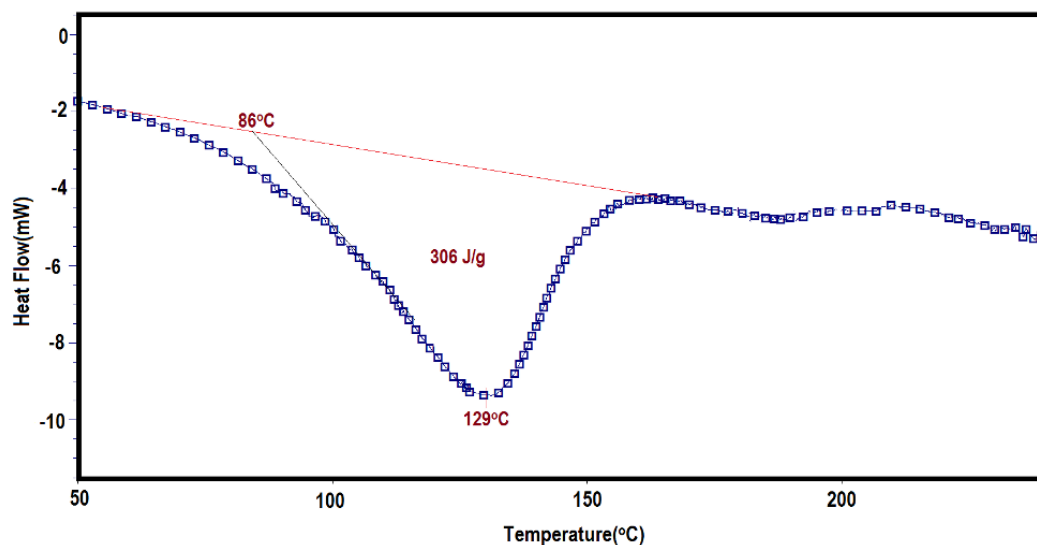
Figure 4.5: DSC trace of AMDI

TG-DTG trace of AMDI is presented in **Figure 4.6.** The amine exhibits negligible mass loss at T <200°C, which confirms the stability of the structure under the conditions employed for the synthesis of benzoxazine.
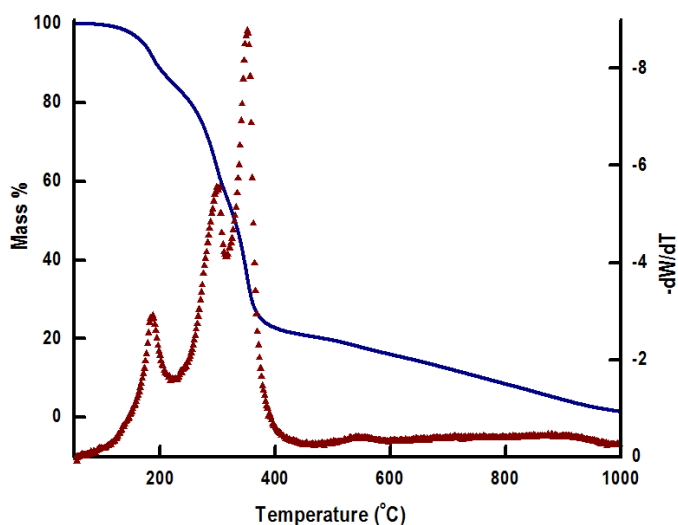
Figure 4.6: TG-DTG of 4,4'-methylenebis(3-ethylamine-1-phenylurea)

4.3.2 Cardanol bis-benzoxazine with urea linkages, C-amdi

Benzoxazine monomer possessing urea linkages was derived through Mannich like condensation of cardanol AMDI and paraformaldehyde (2:1:4), which resulted in the formation of a red brown liquid in high yields (>80 %) as per the reaction sequence

72

presented in **Figure 4.7.** Cardanol, an agricultural source of phenol, exhibit sufficiently low viscosity (145 mPa.s)[108], acting as a reactive diluent, so as to permit solventless synthesis of the benzoxazine[102, 107, 169, 170]. The oxazine moieties available at the terminal position can undergo ring opening polymerization reaction resulting in the formation of a polymeric network with alternating benzoxazine/urea linkages.
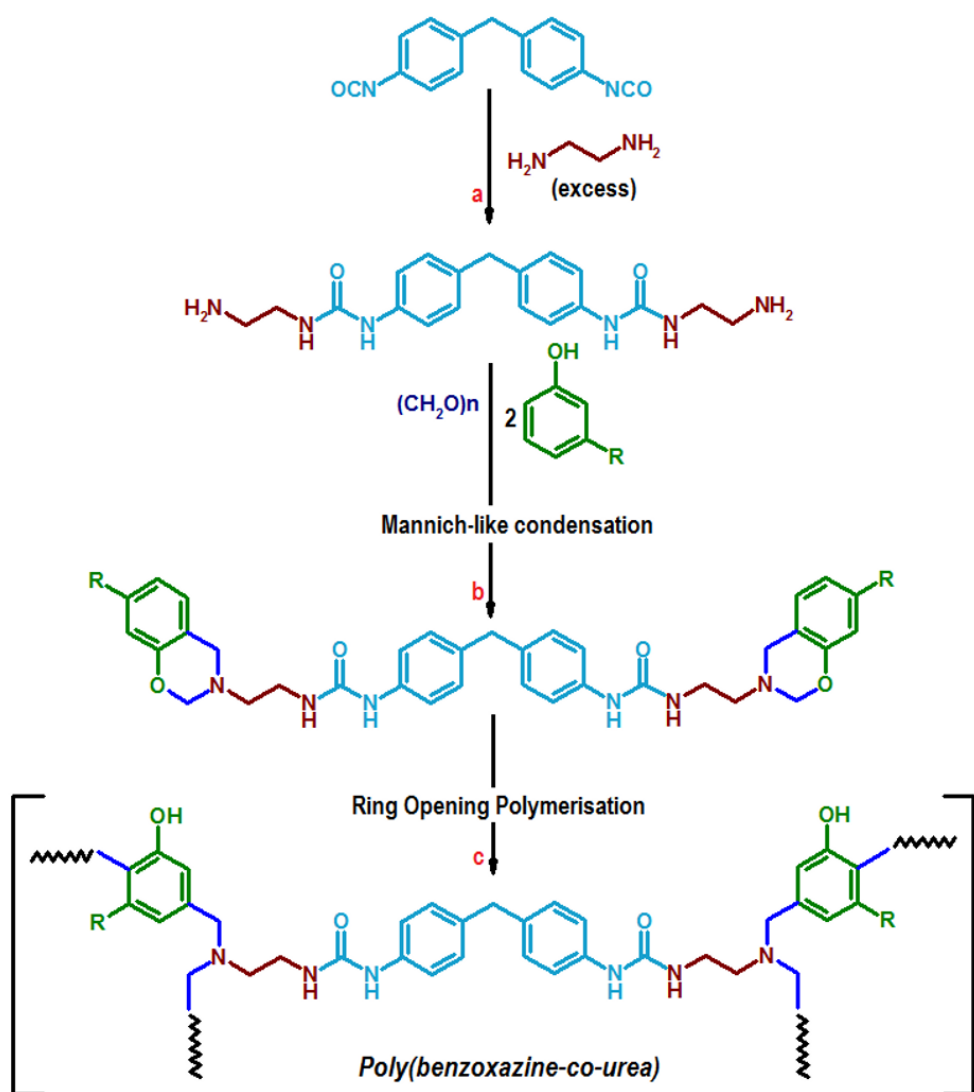
Figure 4.7: Bis-benzoxazine formation by reaction of AMDI with cardanol and paraformaldehyde

73

The FT-IR and ^{1}H-NMR spectrum of the bis-benzoxazine resin (C-amdi) is presented in **Figure 4.8**. The absence of peaks due to O-H and N-H at ~3335 and 3298 cm^{-1} in the FT-IR of the monomer is indicative of complete utilization of cardanol and amine towards formation of the oxazine ring. The characteristic absorption bands associated with asymmetric and symmetric stretching vibrations of C-O-C (~1270 cm^{-1} and ~1030 cm^{-1}), CH_2 wagging (1368 cm^{-1}), and asymmetric stretching vibrations of C-N-C (1117 cm^{-1}) supports the formation of oxazine ring in the monomer. Stretching bands associated with the aromatic and alkene (3008 cm^{-1}), and aliphatic (2852 cm^{-1}) C–H vibrations, C=C (~ 1583 cm^{-1}) were also observed[58]. (**Figure 4.8(i)**).
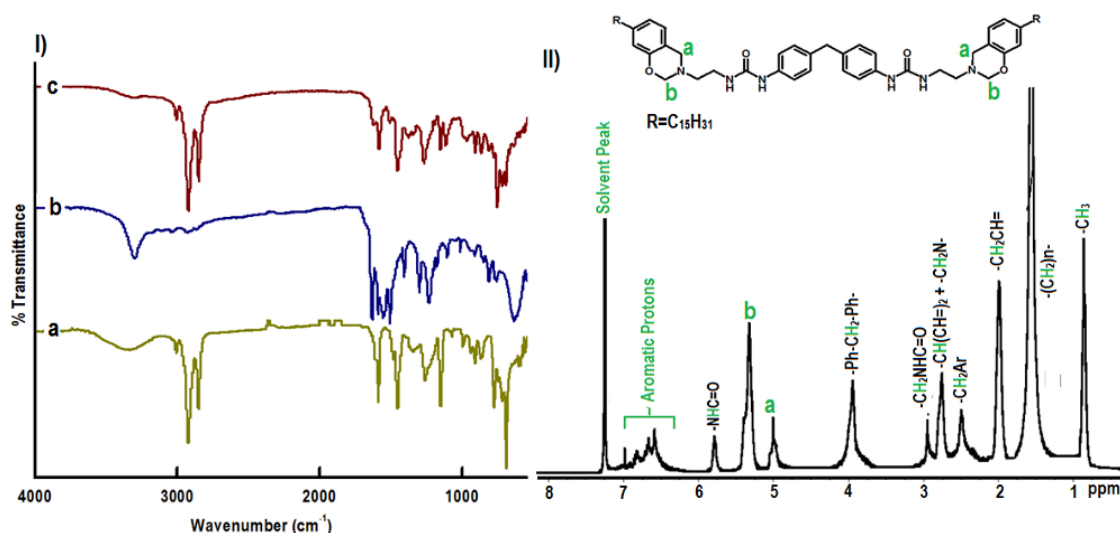
Figure 4.8: i) FT-IR of a) Cardanol, b) AMDI, c) C-amdi and ii) ^{1}H-NMR of C-amdi

The formation of oxazine was further confirmed by the presence of characteristic resonances at ~5.3 ppm (s, $ArOCH_2N$) and ~4.6 ppm (s, $ArCH_2N$) in the ^{1}H-NMR spectra of the resin using $CDCl_3$ as a solvent **(Figure 4.8(ii)).**

Understanding the rheological response of C-amdi is essential in order to gain insight into the conditions required for processing of the resin. During polymerization, structural changes take place as the material gradually builds up and converts from

monomers to oligomers and finally into a rigid cross-linked polymer. Temperature sweep experiments is the most conventional techniques for studying the rheological behavior of any resin during polymerization, and the variation in terms of complex viscosity and loss-storage modulus is presented in **Figure 4.9.**
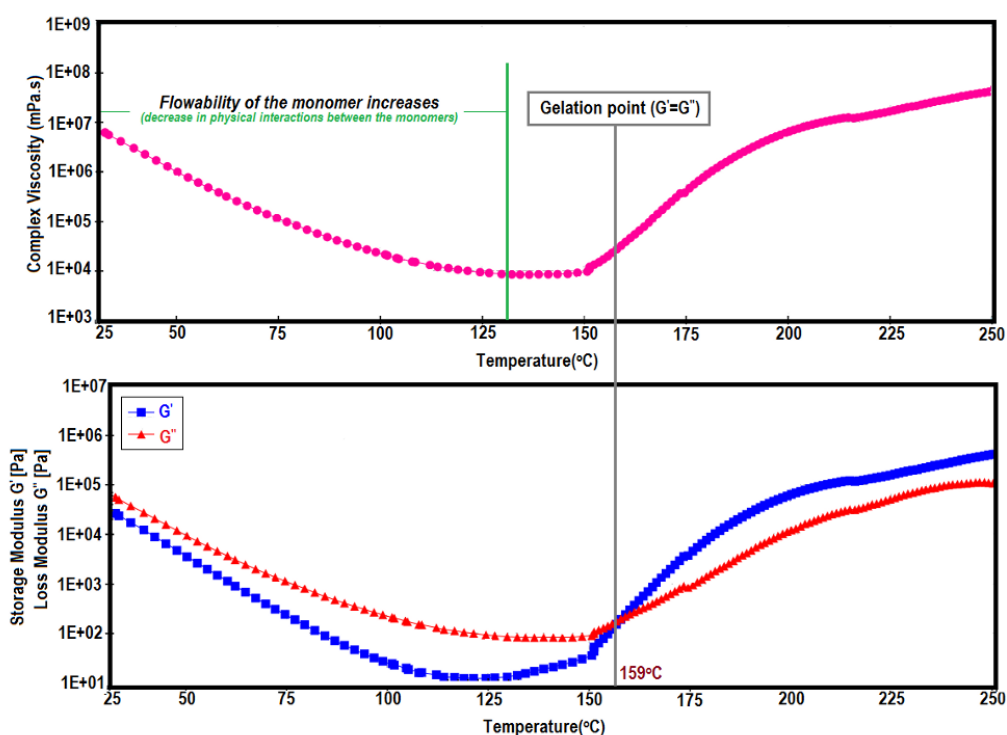
Figure 4.9: Rheological behavior of C-amdi during polymerization

It can be seen that an increase in the temperature lead to a continuous decrease in the viscosity of the resin which is expected in view of the reduced hydrogen bonding interactions between urea linkages available in the monomer. The ring-opening of oxazine moieties leads to the formation of opened Mannich bases, having hydrogen bonding interactions. At this stage, the degree of polymerization and the viscosity build-up is practically negligible[171]. Subsequently, polymerization is initiated where the linear chains associate with each other leading to a build-up of viscosity. The phenolic hydroxyl groups generated act as polymerization catalysts and gelation

is achieved at ~159°C where a crossover of loss and storage modulus can be seen[171, 172]. Further increase in temperature leads to an increase in the viscosity as well as the moduli which finally levels off.
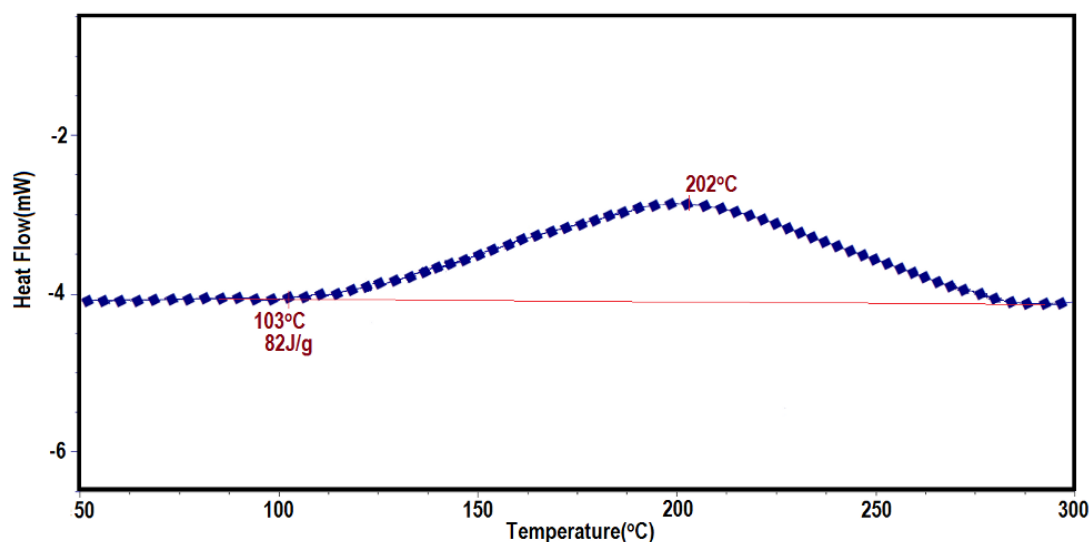
Figure 4.10: DSC trace of C-amdi

Non-isothermal calorimetry was also performed to understand the enthalpy associated with the curing of the benzoxazine resin, and the resulting curing profiles are presented in **Figure 4.10.** The curing profile of cardanol based bis-benzoxazines containing amide linkages has been presented in Chapter 3. The polymerization in the resin with amide linkages initiates at T_{onset} ~114°C and reaches its peak at T_{peak} ~ 215°C [169]. It is interesting to observe that the introduction of urea linkages lead to further decrease in the curing temperature, with the initiation temperature being reduced to T_{onset} ~103°C and peak temperature at T_{peak} ~202°C. The bidentate hydrogen bonds within the urea linkages in the resin, is responsible for bringing the benzoxazine moieties closer to each other and the proximity of the oxazine rings tend to accelerate the ring opening polymerization.

TG-DTG trace of the poly(C-amdi) is presented in **Figure 4.11.**
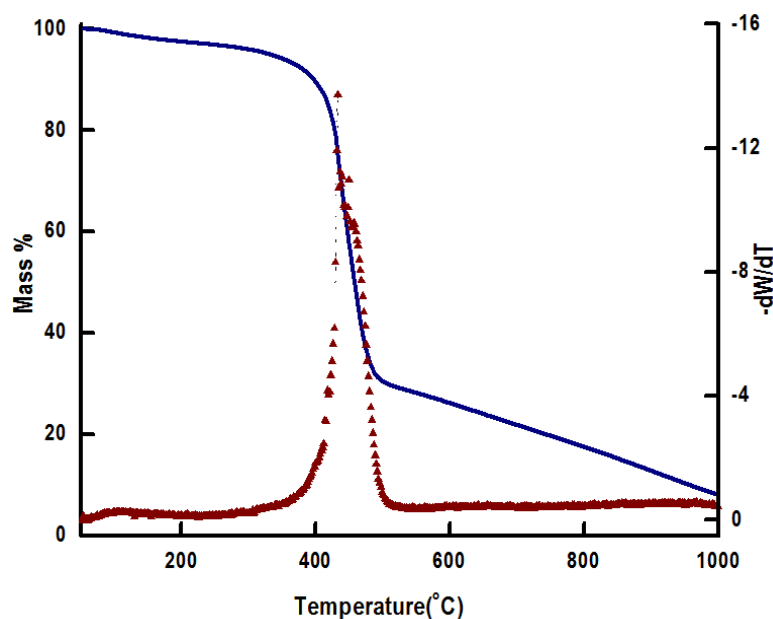
Figure 4.11: TG-DTG of poly(C-amdi)

The benzoxazine resins prepared in the present work was found to exhibit excellent thermal stability with the temperature associated with 5 and 10% mass loss being ~322 and 369 °C respectively. Polyurea, due to the presence of urea linkages, degrades at relatively lower temperatures[166, 173]. It can be seen that copolymerization with benzoxazine tends to improve the thermal stability of the polyurea, thereby suggesting its use in applications mandating thermal stability.

4.3.3 Adhesive Property

The adhesive property of the poly(C-amdi) was quantified as per the standard procedure and a representative load-displacement curve obtained is presented in **Figure 4.12.** The lap shear strength (LSS) of the developed bis-benzoxazine resin is 71 ± 0.29 kgcm^{-2} which is relatively higher than the bi-functional benzoxazine resin containing amide linkages[169].

77
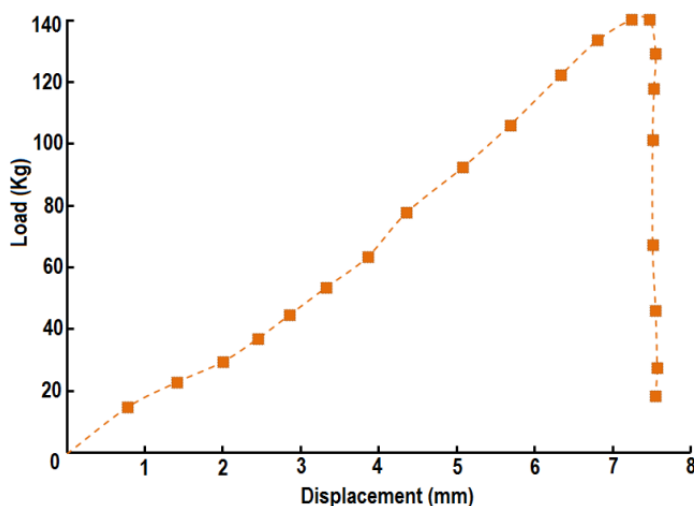
Figure 4.12: Load-displacement curve for poly(c-amdi)

It has already been mentioned that the adhesive strength is a function of several parameters, particularly wetting ability of the substrate with the resin, its inherent adhesive nature, temperature, thickness of the resin, mode of failure, hydrogen bonding interactions and cross link density. The ring opening polymerisation of oxazine moieties generate functional group which are capable of undergoing H-bonding, such as –OH and >N- as shown in the FT-IR spectra of poly(C-amdi) presented in the **Figure 4.13.**

Figure 4.13: FT-IR of poly(C-amdi)

Moreover, the three dimensional network formed herein comprises of urea linkages, which exhibit bi-dentate hydrogen bonding (bond strength ~21.8 kJ/mol)[174] as shown in **Figure 4.14,** which is an additional factor responsible for the adhesive strength of the resin.
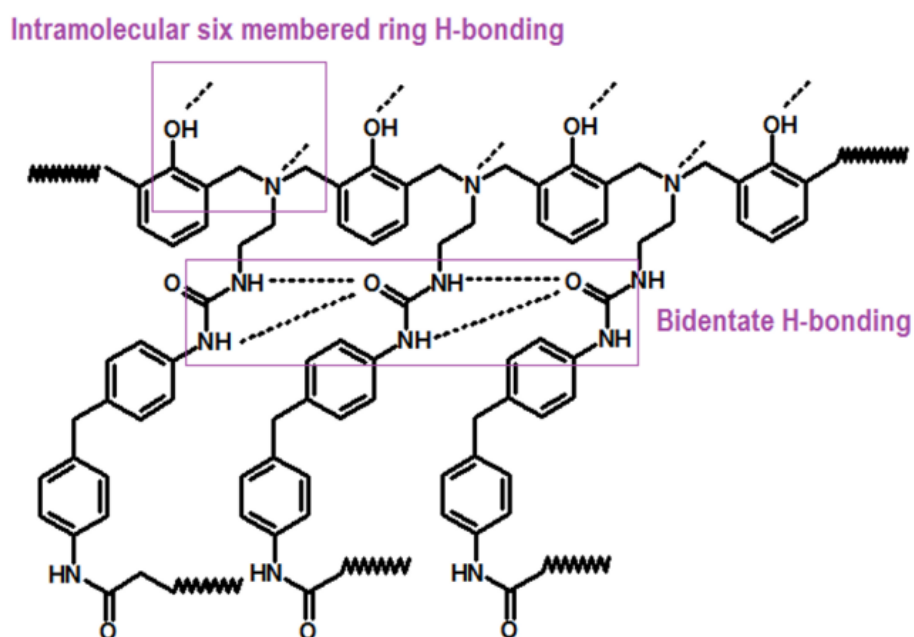
Figure 4.14: Hydrogen bonding in the poly(C-amdi)

Fractographic analysis on the cracked surface (obtained post-lap shear strength studies) was performed to gain an insight into the micro-mechanisms behind the failure of sample. For this purpose, the fracture surface of the sample was examined by SEM and a representative SEM image is presented in **Figure 4.15**.

The fracture surface of benzoxazine shows uninterrupted crack propagation, which in turn is characteristic of brittle failure.
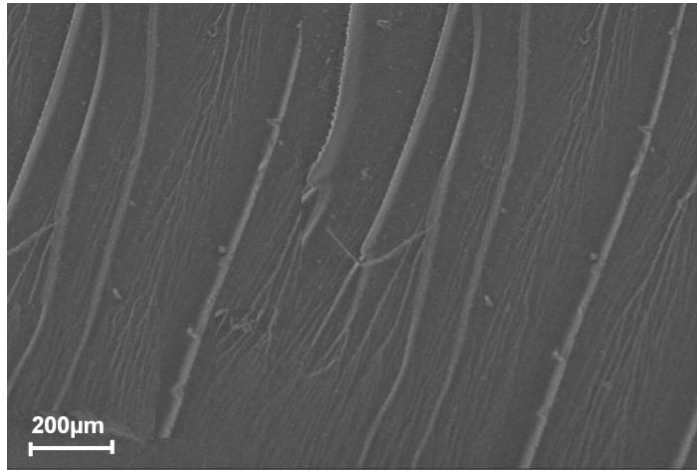
Figure 4.15: SEM image of fractured poly(C-amdi)

Chapter 5A

Curing Accelerator for Benzoxazine: Metal Organic Frameworks
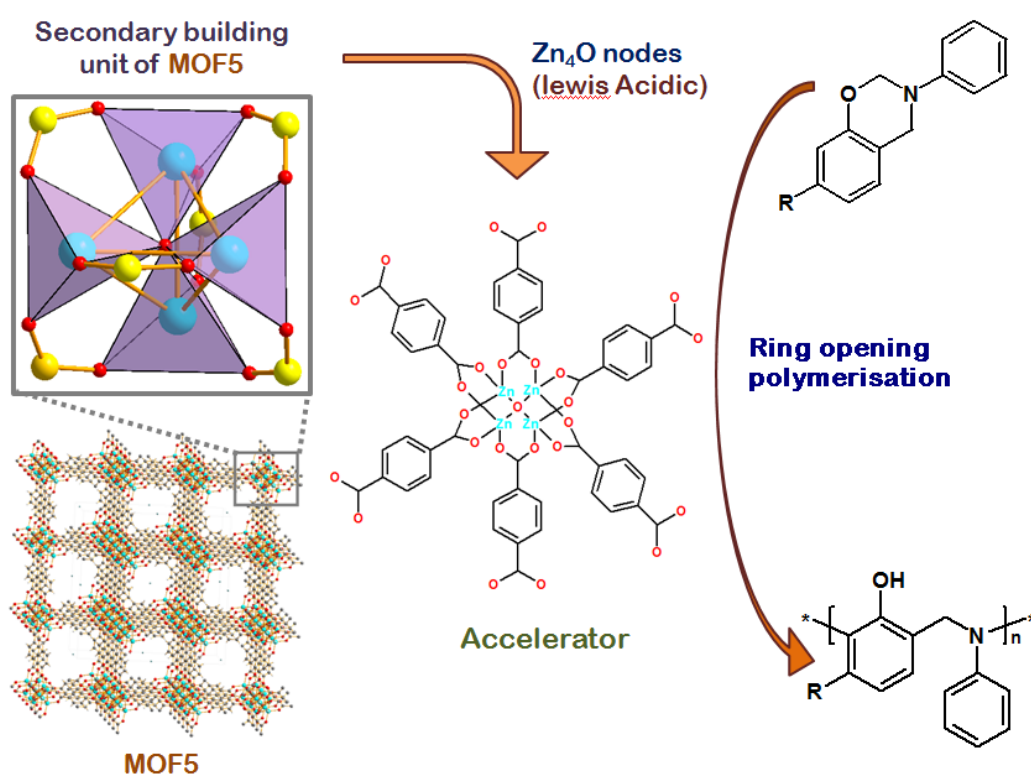
5A.1 Introduction

The present chapter focuses on the exploration of Metal Organic Frameworks (MOF) as accelerators for curing of benzoxazine resin, with an aim to lower the curing temperature. Metal Organic Frameworks are microporous polymeric material which comprises of metal ions linked together by organic linkers. MOFs are finding increasing applications in varied fields including gas adsorption[175], separation, chemical sensing and catalysis[176-178]. Inherent characteristic properties of MOFs, particularly in terms of their ultra-high surface areas, possibility of pore structure modification and a high degree of chemical and thermal stability bestow them excellent candidature for the aforementioned applications[120, 122, 156]. The possibility of tailoring the chemical environment around the metal centre along with the exceptionally high surface area of MOFs leaves enormous scope for these materials in the context of catalysis.

Benzoxazines undergo ring-opening polymerization reaction[124, 179, 180] to form cross-linked networks with exceptional thermal stability as already elaborated in previous chapters[99, 180, 181]. However, majority of benzoxazine resins undergo curing at elevated temperatures[34, 79] which creates a processing issue during practical applications. To overcome this drawback, several accelerators have been explored. In this context, organic acids[34, 72] and lewis acids[73, 74] are of particular interest, but their presence in the cured resin has been reported to reduce the chemical resistance of the polymer and adversely affect the physical properties of the resulting polymer[75]. Organic base such as amines,[76] and imidazoles[77] have also been explored as curing accelerators and the effectiveness of acid-base combination has also been reported[78]. It is to be noted that commercially, proprietary

accelerators for high temperature curing benzoxazines are available with Huntsman (DT300 and DT310); however their chemical composition is not available in public domain and necessitate special caution while handling. Sudo et.al[79] studied the efficiency of acetylacetonato complexes of 4th period transition metals as catalysts for the ring opening polymerization of benzoxazine, which revealed that acetylacetonato complexes of manganese, iron, cobalt and zinc exhibited the highest activity.

MOF-5, is an archetypal robust three dimensional zinc carboxylate framework ([$Zn_4O(BDC)_3$], BDC = 1,4-benzenedicarboxylate),reported by Yaghi et.al[182]. The crystal structure of MOF-5 is comprised of oxo-centered Zn_4O nodes, connected through linear BDC units forming an extended 3D cubic network with interconnected pores of 0.9 nm (**Figure 5.1**).
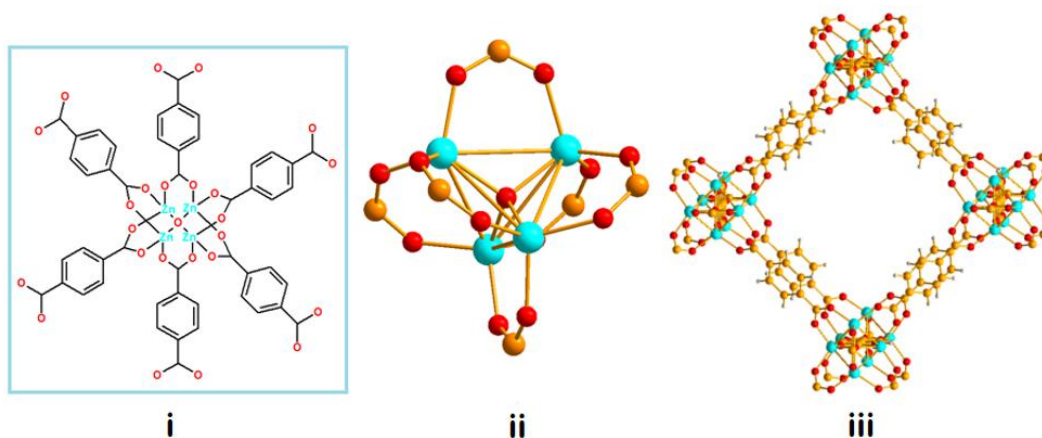
Figure 5A.1: i) Chemical structure of secondary building unit, ii) structure of Zn_4O node and iii) 3D structure of the framework of MOF-5 (Zn: cyan; C:grey; H:White and O:red)

Zinc oxide clusters (Zn_4O) of atomic precision, which are available throughout the framework confer it excellent candidature for applications where acidic catalysis is desirable which has led researchers to explore its potential in representative applications e.g. Friedel craft reaction[183-185]. Although applications of MOF's as

heterogeneous catalysts has been well reported[186-189], studies concerning their ability to accelerate the polymer curing reactions are virtually absent. Interestingly, the introduction of MOF-5 in polymeric matrices, both thermosetting as well as thermoplastics lead to significant improvement in their mechanical properties[190].

The present chapter discusses the potential of MOF-5 towards accelerating the ring opening polymerization of cardanol based mono-functional benzoxazine resin. Differential Scanning Calorimetric (DSC) analysis was performed to quantify the extent of acceleration in the ring opening polymerization behaviour. To validate the role of chemical environment towards the acceleration of benzoxazine curing, calorimetric studies were also performed in the presence of ZIF-8 ($Zn (MeIm)_2$), another zinc based MOF with high surface area but differ in the organic linker. To exclude the possible role of ligands towards acceleration of the curing process, the efficacy of another set of MOFs prepared using BDC and BTC as the acidic ligands, i.e. $Cu(BDC).DMF$ and $[Cu_3(BTC)_2(H_2O)_3]_n$, was also investigated.

5A.2 Experimental

5A.2.1 Materials

Zinc acetate dihydrate ('AR', E. Merck), Copper nitrate trihydrate ('AR', E. Merck), Copper acetate trihydrate ('AR', E. Merck), 1,4-benzenedicarboxylic acid (BDC) ('AR', Aldrich), Benzene-1,3,5-tricarboxylic acid (BTC)(Aldrich) and N,N-dimethyl formamide(DMF) ('HPLC', Aldrich), 2-methylimidazole (MeIm) ('AR', Aldrich) was used without further purification. Zinc dust and zinc oxide from CDH were used as received. Double distilled water was used throughout the course of this work.

5A.2.2 Supramolecular assembly of Metal Organic frameworks

Zinc terephthalate [Zn$_4$O(BDC)$_3$, MOF-5]: MOF-5 was prepared as per the procedure reported earlier[148, 191]. In brief, separate solution of BDC (5.06 g, 30.5 mmol) and zinc acetate dihydrate (16.99 g, 77.4 mmol) were prepared in DMF, which were mixed and allowed to react for 2.5 h under stirring (600 rpm). The resulting crystallites were filtered, washed repeatedly with DMF and stored under desiccation.

Zinc imidazolate [Zn (MeIm)$_2$, ZIF 8]: Zinc nitrate and MeIm and were dissolved in water (MeIm : Zn^{2+}::1:4 molar ratio, 900 mL) constant stirring at 600 rpm for 24 h at room temperature. The mother liquor was set aside for another 24 h, following which ZIF-8 crystals were obtained; the resulting crystals were filtered, washed repeatedly with water, dried and stored under desiccation.

Copper benzene tricarboxylate [Cu$_3$(BTC)$_2$(H$_2$O)$_3$]$_n$,, HKUST-1]: HKUST-1 was prepared at room temperature as per the procedure reported previously[192]. For this purpose, BTC (4.2 g) was dissolved in ethanol: DMF mixture (2:1 v/v, 750 ml) and copper acetate (5.98 g) was separately dissolved in water (1000 mL). They were mixed and maintained under continuous stirring at room temperature for 12 h. The mother liquor was set aside for another 24 h, following which a crystalline powder of HKUST-1 was obtained, which was filtered, washed repeatedly and dried before use.

Copper terephthalate [Cu-(BDC).DMF]: Copper terephthalate was synthesized using the solvothermal procedure in which equimolar quantities of copper nitrate trihydrate (2 g) and terephthalic acid (1.52 g) in 100 ml DMF was allowed to react in a sealed autoclave at 110°C for extended time periods (~36 h). Blue crystals of copper terepthalate were obtained, which were washed repeatedly with DMF, filtered and stored under desiccation for subsequent analysis.

5A.2.3 MOF-5 as curing accelerator for cardanol-aniline benzoxazine (C-a)

To an accurately weighed amount of the cardanol derived benzoxazine (C-a), varying amount of MOF-5 (1-10 %w/w) was added and stirred at room temperature; conditions under which no polymerization was perceptible. The details of the formulations prepared along with their sample designations have been mentioned in **Table 5A.1**. Neat benzoxazine has been referred to as C-a and the compositions containing MOF-5 will be referred to as MXC-a where X indicates the mass percent of MOF-5 present in the sample. For C-a containing 5% w/w MOF-5 has been designated as M5C-a.

Table 5A.1 Details of formulation and designations

Sample Designation	Resin (g)	Additive	Amount of Additive(g)
C-a	100	-	-
M1C-a	100	MOF 5	1
M5C-a	100	MOF 5	5
M10C-a	100	MOF 5	10
Zn10C-a	100	Zinc	10
BDC5C-a	100	Benzenedicarboxylic acid	5
ZnO5C-a	100	Zinc oxide	5
Z5C-a	100	ZIF 8	5
CT5C-a	100	Cu-BDC	5
H5C-a	100	HKUST-1	5

Curing studies were also performed with zinc dust, zinc oxide, 1,4-benzenedicarboxylic acid, ZIF-8, Cu-(BDC).DMF and $Cu_3(BTC)_2(H_2O)_3]_n$. Sample was placed in a DSC pan and heated at a rate of 10°C /min. The curing of the resin was accompanied with evolution of heat, and from the corresponding DSC profiles, characteristic curing parameters were quantified. Of particular interest is the onset temperature (T_o), peak temperature (T_{peak}).

5A.2.4 Adhesive property

The adhesive strength of the resin was quantified in terms of Lap shear strength which was determined as per the standard procedure (ASTM D1002). For this purpose, the samples were prepared by coating ~ 0.05g of resin on steel plates of dimension 15×15 mm^2. The coated samples were kept at 100°C for 30 mins. The assembly was clamped with paper clips (15 mm) and cured in an air oven at 100-240 °C (30 mins) followed by heating at 263°C (1 h). A total of 6 replicates were tested per sample.

5A.2.5 Characterization methods

Surface area investigations were performed using N_2 adsorption-desorption studies on a Surface Area Analyzer (Micromeritics ASAP 2020). For this purpose, the sample was initially degassed under vacuum (10^{-6} Torr) at elevated temperature (200 °C) for 16 h following which nitrogen adsorbate was pulsed at -196°C. PXRD data was collected on Bruker D8 advanced diffractometer using Nickel filter Cu-K$_\alpha$ radiation. Data was collected at a step size of 0.02° and at count time of 1 s/step over the range of 2°- 60° (2Θ value) for the solid. Structural characterization (FT-IR) of accelerators was performed. The morphology of the samples was studied. The detailed procedures have already been mentioned in previous chapters.

5A.3 Results and Discussions

5A.3.1 Supramolecular assembly of Metal Organic Framework

MOF-5: Zinc ions coordinate with benzenedicarboxylate ligand [148, 190, 191] to result in the formation of cubic MOF-5 crystals as shown in **Figure 5A.2(i).** Rietveld analysis of the diffraction pattern based on the structure reported in the literature (CCDC-277428) revealed the existence of the cluster core as a regular Zn_4O tetrahedron, linked to each other through a pair of terephthalate linkers in paddle-

wheel type fashion resulting in the composition [(Zn$_4$O)(BDC)$_3$] (**Figure 5A.2(ii)**).

The nitrogen adsorption desorption isotherm at -196°C is presented in **Figure 5A.2(iii)**. Circles and triangular symbols represent adsorption and desorption data respectively. The BET surface area was found to be 1750 m^{2}g^{-1}. The TG-DTG trace of MOF-5 is presented in **Figure 5A.2(iv)**. The initial mass loss of <5% at 300°C can be attributed to the removal of DMF from the framework, which was followed by its pyrolytic decomposition at 410°C leaving behind a char content of 51 % at 600°C.
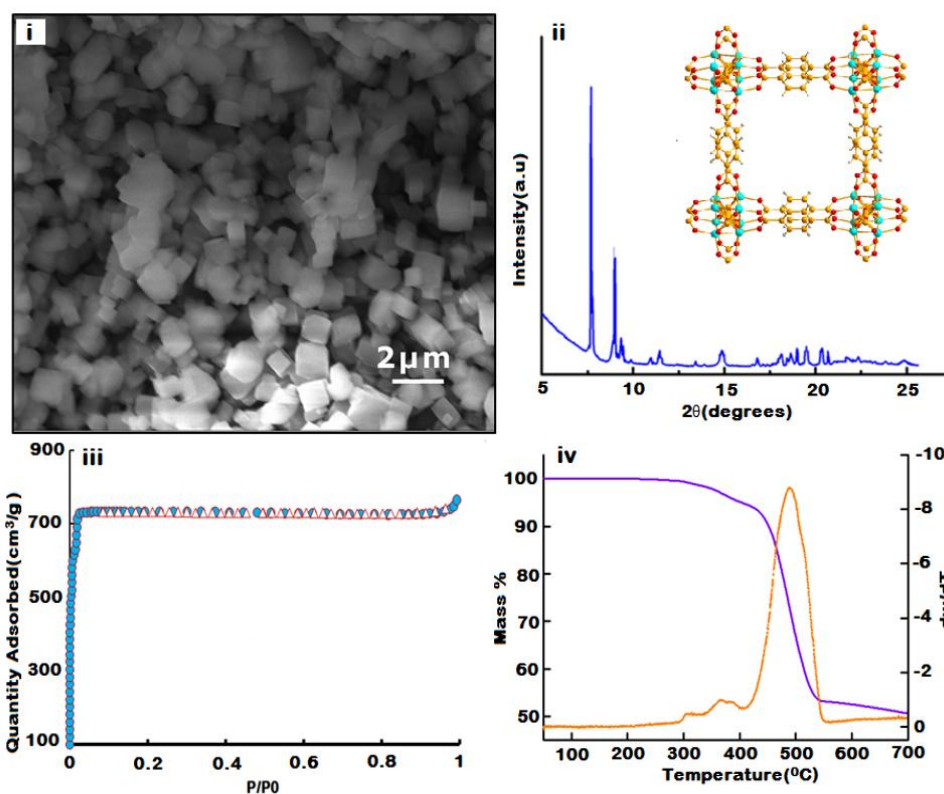
Figure 5A.2: MOF-5 i) SEM image, ii) PXRD pattern, iii) N$_2$ adsorption desorption isotherm and iv) TG-DTG traces.

It is to be noted that the particle size distribution is highly dependent on the synthetic procedure adopted for its synthesis. Under the reaction conditions used for the present

work, the average particle size is ca. 1-2 microns. Particle Size distribution of MOF-5 is presented in **Figure 5A.3.**
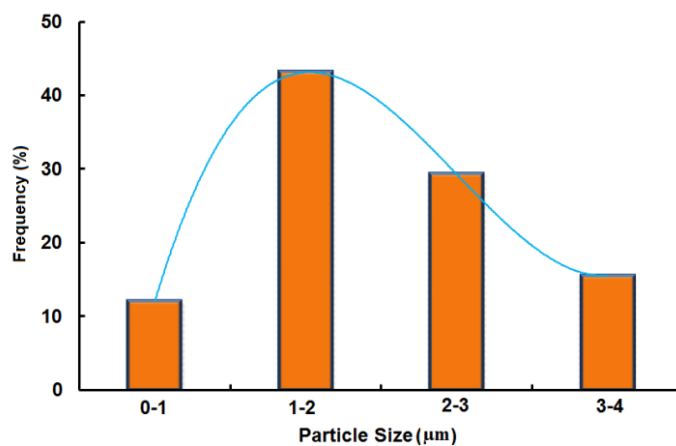
Figure 5A.3: Particle size distribution of MOF-5

ZIF-8: The peak positions match with the simulated powder pattern of ZIF-8 based on the CIF (CCDC-7201498) (**Figure 5A.4(i)**). ZIF-8 exhibits Zn-Im-Zn bonds with cavities of diameter 11.6Å, connected via 6- and 4-ring apertures. The adsorption-desorption isotherm revealed the characteristic microporous nature of ZIF-8. The N_2 adsorption–desorption isotherms of the ZIF-8 as recorded by physisorption of N_2 at -196°C, are presented in **Figure 5A.4(iii)**. The BET specific surface area of ZIF-8 was found to be $900m^2g^{-1}$. The TG traces of ZIF-8 is presented in **Figure 5A.4(iv)**, which clearly reveals the excellent thermal stability for practical applications till 500 ºC.
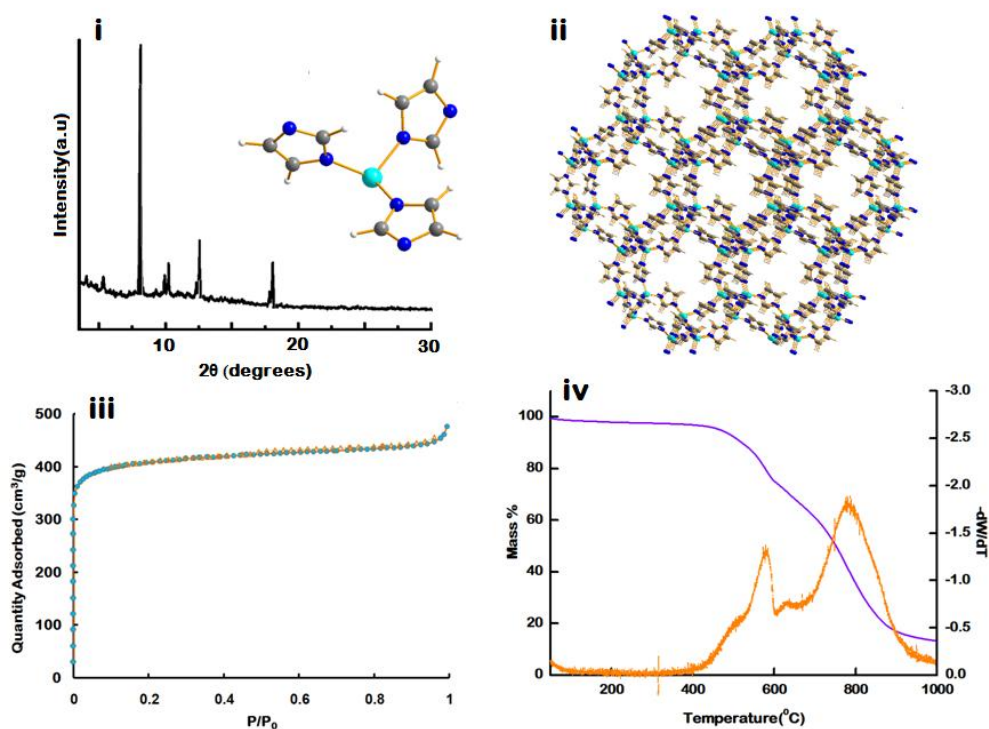
Figure 5A.4: ZIF-8 i) PXRD pattern, inset shows the three dimensional structure, ii) secondary building unit (Zn: cyan; C: grey; H: white and N: blue) iii) N_2 adsorption desorption isotherm and iv) TG-DTG traces

Copper terephthalate: Rietveld analysis of the PXRD data (CCDC 687690) (**Figure 5A.5(i)**) confirms that the structure of Cu(BDC).DMF has benzenedicarboxylate ligands coordinated in a bidentate bridging fashion to a Cu^{II} dimer, separated from each other by a distance of 2.63 Å. Each Cu^{II} atom is also coordinated to a molecule of DMF resulting in square-pyramidal coordination geometry around the Cu^{II} species (**Figure 5A.5(ii)**). This leads to a sheet type structure in which the Cu^{II} atoms are coordinated to the terephthalic acid linkers in the (201) planes which are bonded through weak stacking interactions. The N_2 adsorption–desorption isotherms of the Copper terephthalate as recorded by physisorption of N_2 at -196°C, are presented in **Figure 5A.5(iii)**. The BET specific surface area of copper terephthalate was found to be 660 m^2g^{-1}.
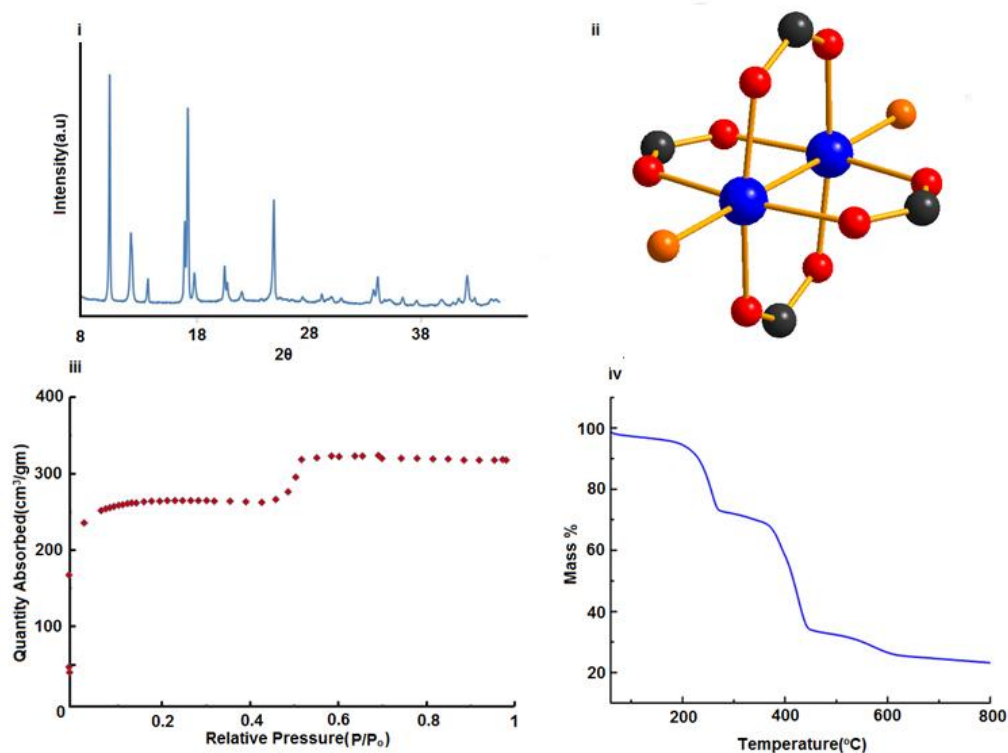
Figure 5A.5: Copper terephthalate i) PXRD pattern, ii) unit cell (Cu: blue C: black;
O: red) iii) N_2 adsorption desorption isotherm and iv) TG-DTG traces

It is apparent from the TG trace (**Figure 5A.5 (iv)**), that desolvation of DMF occurs at
~250 °C, leading to the formation of Cu(BDC) which decomposes on further heating
at 450 °C. Prior to DSC analysis, the copper terephthalate was activated to get rid of
the entrapped DMF within.

HKUST-1: Rietveld analysis of the PXRD data (CCDC 827934) (**Figure 5A.6(i)**)
confirms that the building block of HKUST-1 comprises of Cu^{2+} dimer coordinated
with four oxygen atoms of benzene tricarboxylate forming a paddle wheel type
structure (**Figure 5A.6(ii)**). The activation of the framework reportedly leads to
removal of water molecules coordinated to the exchangeable copper sites, thereby
exposing the lewis acidic positions. The N_2 adsorption–desorption isotherms of
HKUST-1 as recorded by physisorption of N_2 at -196°C, are presented in **Figure**

5A.6(iii). The BET specific surface area of HKUST-1 was found to be 750 m^{2}g^{-1}. It is apparent from the TG trace (**Figure 5A.6(iv)**), that desolvation is complete at T ~200 °C, and the resulting structure decomposes upon further heating at 390°C. Prior to DSC analysis, the MOF was activated to get rid of the entrapped solvent.
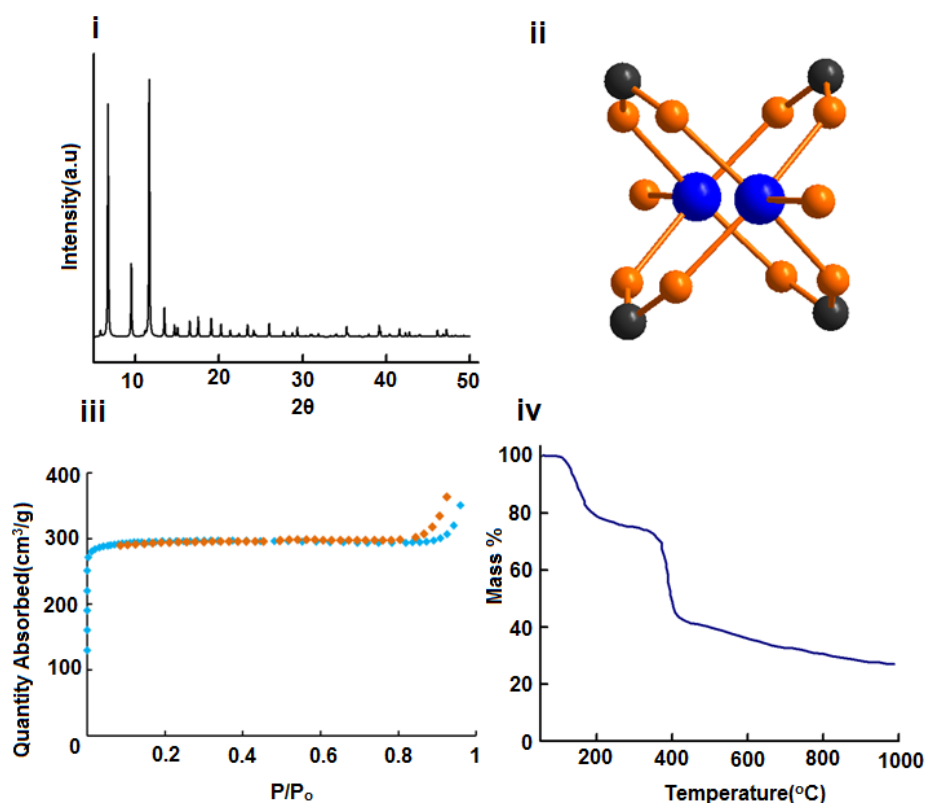
Figure 5A.6: HKUST-1 i) PXRD pattern, ii) unit cell (Cu: C: grey; N: blue and O: red) iii) N$_2$ adsorption desorption isotherm and iv) TG-DTG traces

5A.3.2 Acceleration of benzoxazine ring opening polymerization

Benzoxazine monomers undergo thermally accelerated cationic ring opening polymerization leading to the formation of a thermally stable cross-linked polymer (**Figure 5A.7**). The ring opening polymerization has been reported to be auto catalytic as the phenolic -OH generated in situ act as an additional initiator. Accelerators employed, alleviates the kinetics of the oxazine ring opening stage through several proposed mechanisms[78, 179, 193-196].

91
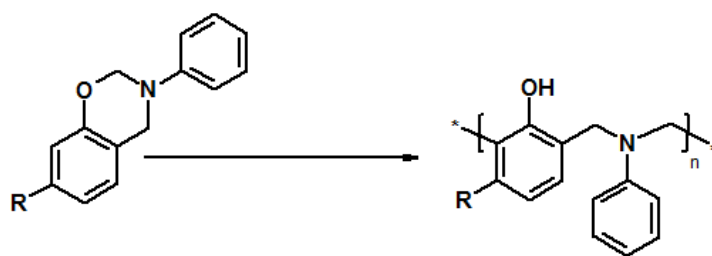
Figure 5A.7: Ring opening polymerization of 1,3-benzoxazine

To investigate the curing behaviour of the benzoxazine resins in the presence of accelerators, non-isothermal calorimetric studies were performed and the representative curing profiles of formulations containing MOF-5 are presented in **Figure 5A.8**
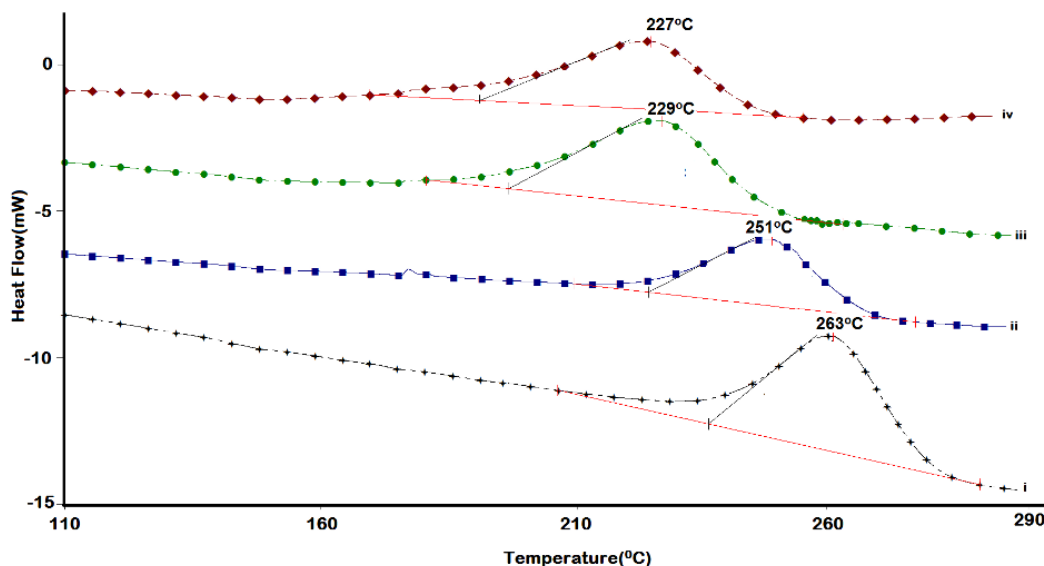
Figure 5A.8: DSC curves for i) C-a, ii) M1C-a, iii) M5C-a and iv) M10C-a

It can be seen that the curing of the synthesized cardanol based benzoxazine exhibits a peak at 263°C (**Figure 5A.8(i)**). A pronounced shift in the curing profile towards lower temperature was observed, the extent of which was found to be proportional to the amount of MOF-5 in the formulation (**Figure 5A.8(ii)-(iv)**). The ability of MOF-5 to accelerate the curing process can be credited to the acidic Zn_4O nodes of the MOF-

92

5 crystal lattice. To gain insight on the role of the chemical environment around the central zinc species, curing studies were also performed in the presence of Zn, ZnO, BDC and an another zinc based metal organic framework ZIF-8, with high surface area (900 m^2/g) but differs predominantly with respect to the chemical environment around the central zinc atom. ZIF-8 reportedly features a sodalite topology (Si-O-Si bonds in zeolites being replaced by Zn-Im-Zn bonds) with cavities of diameter 1.16 nm, connected via 6- and 4-ring apertures[197, 198].

Another set of experiment was performed using two archetypal MOFs $[Cu_3(BTC)_2(H_2O)_3]_n$, HKUST-1 and Cu(BDC).DMF. The selection of accelerators for the study is stemming from the similarity in the nature of ligand i.e. BDC for copper terephthalate and BTC for HKUST-1. Copper terephthalate exhibits a sheet type structure in which the Cu^{II} atoms are coordinated to the terephthalic acid linker's specific planes which are bonded through weak stacking interactions. HKUST-1 is made up of interconnected $[Cu_2(O_2CR)_4]$ units (where R is an aromatic ring), creating a three dimensional network. The building block of HKUST-1 comprises of Cu^{2+} dimer coordinated with four oxygen atoms of benzene tricarboxylate forming a paddle wheel type structure. The activation of the framework reportedly leads to removal of water molecules coordinated to the exchangeable copper sites, thereby exposing the lewis acidic positions. The DSC traces associated with the curing of benzoxazine in the presence of different MOFs is presented in **Figure 5A.9.** It can be seen that among all the MOFs studied, presence of MOF-5 led to the maximum decrease in the curing temperature.
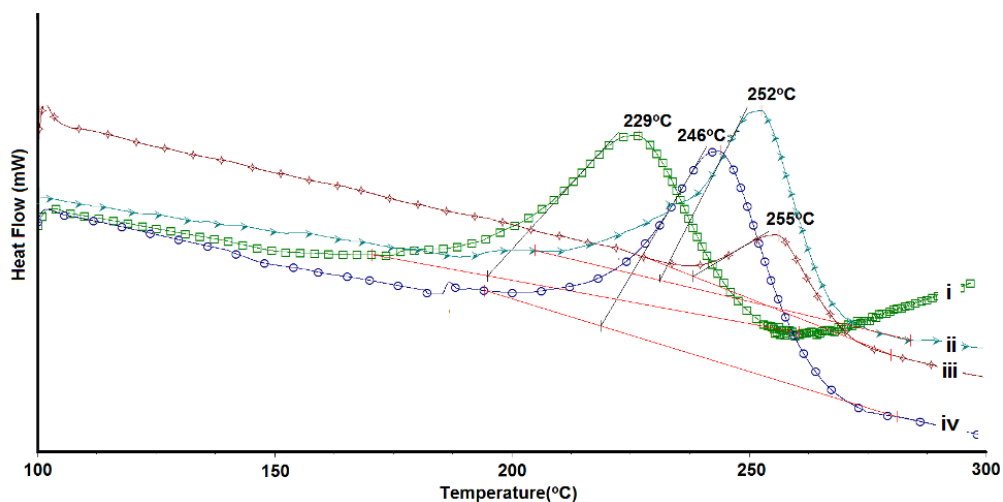
Figure 5A.9: DSC traces i) M5C-a, ii) H5C-a, iii) CT5C-a and iv) Z5C-a

The results of the DSC analyses in terms of characteristic curing temperatures are summarized in **Table 5A.2.**

Table 5A.2: Effect on introduction of accelerators on characteristic curing temperatures ($\beta=10°C/min$)

Sample designation	T_o (°C)	T_{peak} (°C)	% Decrease in terms of	
			T_{peak}	T_o
C-a	240	263	-	-
BDC10C-a	231	253	2.6	3.7
ZnO10C-a	214	237	4.9	10.8
Zn10C-a	220	244	6	8.3
Z5C-a	218	246	6.5	9.1
CT5C-a	237	255	2.7	1.2
H5C-a	230	252	4.2	4.2
M1C-a	228	251	4.8	5
M5C-a	184	229	12.8	23.33
M10C-a	178	227	13.6	25.8
M15C-a	231	248	5.7	3.7

A proposed polymerization mechanism employing various curing accelerators has been presented in **Figure 5A.10.** Acids, such as BDC have been reported to accelerate oxazine ring opening by the preferable protonation of oxygen atom generating a reactive species which undergoes condensation with the phenolate or other benzoxazine molecule resulting in phenolic structure (**Figure 5A.10(ii)**). Metal

94

centered accelerators such as metal oxides and MOFs accelerate benzoxazine polymerization through the formation of aryl ether structures (**Figure 5A.10(iii)**).
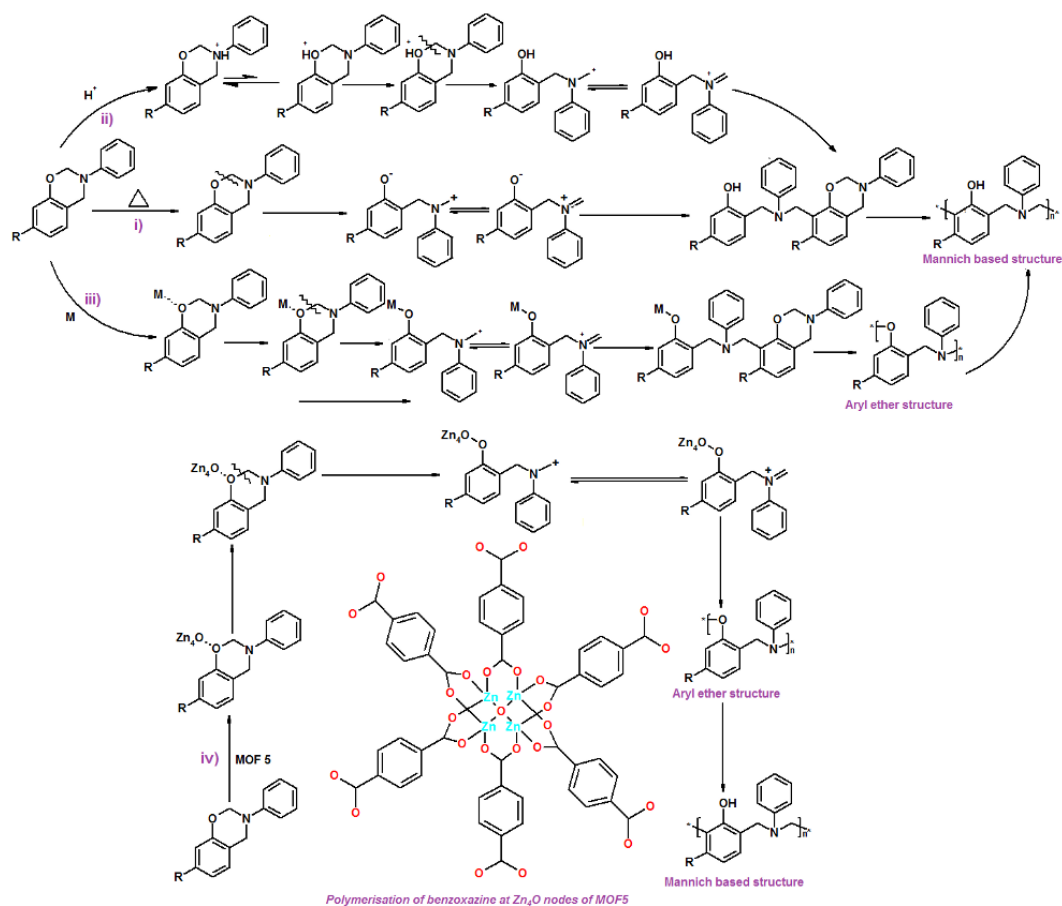
Figure 5A.10: Probable mechanisms i) thermally accelerated polymerization of benzoxazine resin ii) polymerization by protonation iii) polymerization in the presence of metal based accelerators iv) polymerization in the presence of Lewis acidic Zn_4O nodes present in MOF-5

The curing of benzoxazine in the presence of MOF-5 as accelerator is proposed to proceed through coordination of zinc present in the Zn_4O cluster with the benzoxazine oxygen atom resulting in the formation of reactive iminium species. The electrophile generated condenses with other benzoxazine molecule resulting in unstable aryl ether structure which rearranges to more stable phenolic structures at elevated temperature (**Figure 5A.10(iv)**).

As is evident from **Table 5A.2**, among all the additives studied,MOF-5 leads to the most pronounced decrease in the curing temperature of C-a, However, increasing the amount of MOF-5 beyond 5%, does not lead to any considerable decrease in the curing temperature further. In view of the same, M5C-a was chosen for establishing the kinetic parameters associated with the polymerization reaction. It is to be noted that the dimensions of the benzoxazine resin (fully extended form, ~1.25 nm) is relatively larger than the pore diameter of MOF-5 (0.9 nm) (**Figure 5A.11**), which restrict the diffusion of the resin within the pores.
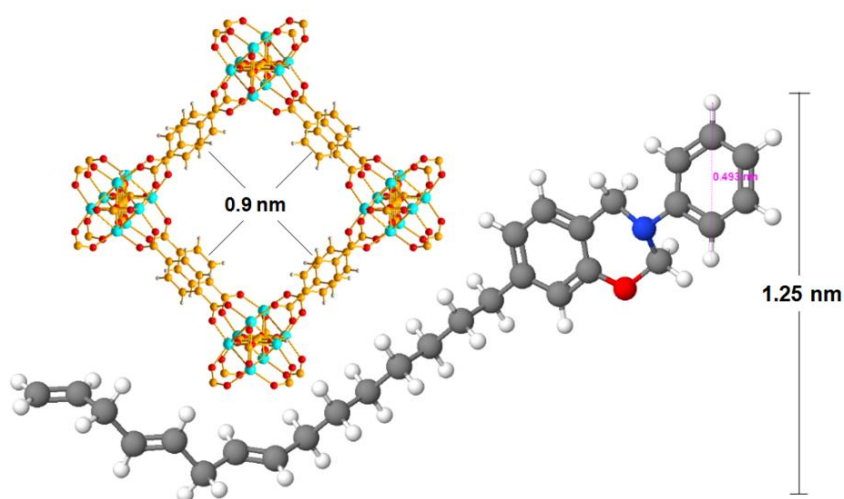
Figure 5A.11: Three dimensional representations showing the dimensions of the benzoxazine molecule and the pore size of MOF-5.

This suggests that the accelerating ability of MOF-5 can be attributed primarily to the Zn_4O nodes available largely at the surface of the framework. In view of the possibility of tailoring the pore-dimensions of MOFs by rational choice of the organic linker, suitable framework with acidic nodes and larger pores can be designed, where the monomer can diffuse into, which can lead to further reduction in the curing temperature. It is interesting to note that ZIF-8, although containing the same metal centre (Zn) and exhibiting high surface area (900 m^2/g) did not lead to any substantial

curing acceleration of the benzoxazine in terms of decrease in the curing temperature. ZIF-8, a prototypical structure with sodalite (SOD) topology comprises of individual Zn nodes as against Zn_4O nodes available throughout the MOF-5. In addition, the presence of Cu(BDC) and HKUST-1 both of which are synthesized using acidic ligands, does not lead to any substantial decrease in the curing temperature. Our studies lead us to believe that, it is primarily the availability of the acidic Zn_4O nodes in MOF-5, is responsible for the acceleration of the benzoxazine curing. One of the characteristic features of benzoxazines is "Zero- shrinkage" which implies 100% solid content. In all the cases, the benzoxazine samples exhibited high yields >99.5%, irrespective of the presence or absence of MOF.

5A.3.3 Curing Kinetics

The DSC traces of a representative formulation (M5C-a) at various heating rates viz. 5, 7 and 10 °C/min are presented in **Figure 5A.12.** Increasing the heating rate (β) leads to systematic shift in the trace towards higher temperatures, which can be attributed to the reduced time available with the reactive molecules upon being subjected to higher heating rates. The curing of benzoxazine resin is typically a multi-step process exhibiting complex kinetics. The process is accompanied with a dramatic change in the physical state of the reaction medium. At the early stages, the reaction medium is a liquid composed primarily of monomers. With the progress of the reaction, the molecular weight and viscosity of the polymer formed increases which in turn results in a decrease in the molecular mobility. The most dramatic decrease in the mobility occurs with the cross-linking of polymer chains, where the chains lose their ability to move past one another, and the medium turns from flowing liquid to a solid that can be either rubbery or glassy, depending upon the T_g of the

cured resin. Characteristic parameters associated with the curing of the resin i.e. ΔH_{cure}, T_{onset} and T_{peak} are summarized in **Table 5A.3**.

The extent of conversion, α at any particular temperature (T_α) was calculated as the ratio of the areas under the exothermic DSC peak and expressed as:

$$\alpha = \frac{\Delta H_{T_\alpha}}{\Delta H_{cure}} \ldots\ldots\ldots\ldots\ldots(5A.1)$$

where, ΔH_{T_α} is the heat of reaction of partially cured samples (till temperature T_α) and

ΔH_{cure} is the total heat of curing. The increase in the degree of conversion with temperature for C-a and M5C-a at a particular heating rate (5°C/min) is presented in **Figure 5A.13.**
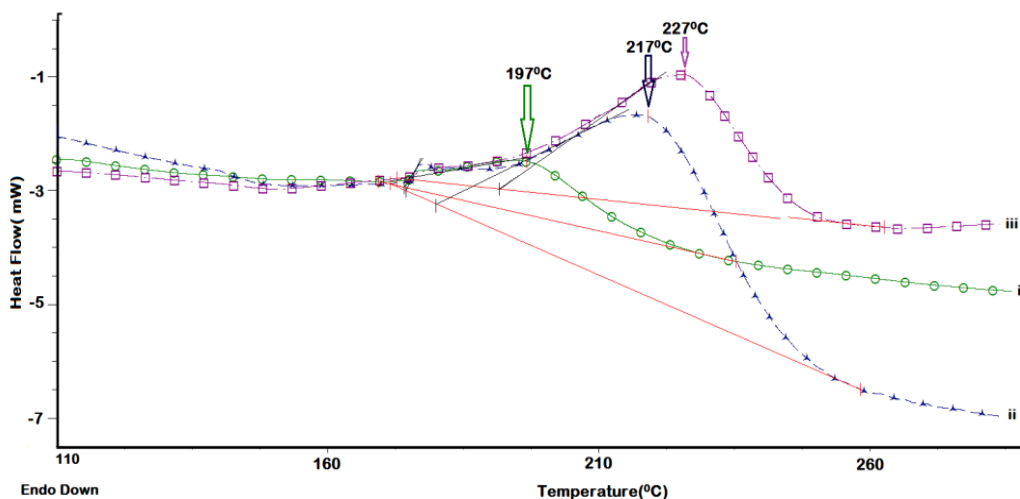
Figure 5A.12: Effect of heating rate (β) on the curing profile of M5C-a a) 5, b) 7 and c) 10 °C/min.

It can be seen that the complete curing of neat monomer is achieved at 280°C while in the presence of MOF-5 the same is attained at 230°C, which is indicative of the ability of MOF-5 as an accelerator for curing of benzoxazines.
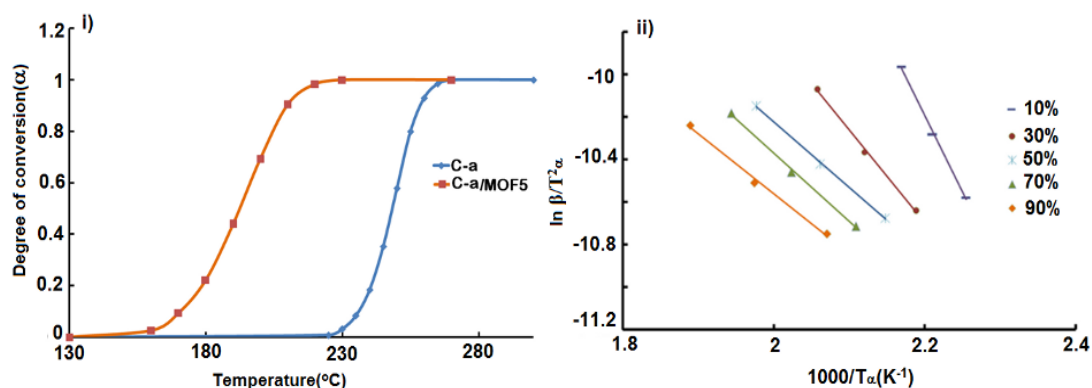
Figure 5A.13: i) Effect of temperature on the degree of conversion of cardanol based benzoxazine in the presence and absence of MOF-5 (β = 5 °C/min). ii) Iso-conversion plots.

Table 5A.3: Characteristic curing parameters of neat benzoxazine and M5C-a

Sample	β (°C/min)	T_{onset} (°C)	T_{peak} (°C)	Activation energy α= 10% (kJ/mol)
C-a	5	224	246	98
	7	236	255	
	10	241	263	
M5C-a	5	173	196	58
	7	178	217	
	10	184	229	

In view of its simplicity, Kissinger–Akahira–Sunose equation[199] was applied for determination of activation energies (E_α) from the plot of $ln\left(\dfrac{\beta_i}{T_{\alpha,i}^2}\right)$ against $1/T_\alpha$.

$$ln\left(\frac{\beta_i}{T_{\alpha,i}^2}\right) = \text{Constant} - \frac{E_\alpha}{RT_{\alpha,i}} \quad\ldots\ldots\ldots\ldots\ldots.(5A.2)$$

Where, β is the heating rate, T_α is the temperature associated with a particular conversion (α) at the corresponding heating rate, E_α is the activation energy at that α and R is the gas constant. The linear plots at few representative conversions for M5C-a (**Figure 5A.13(ii)**) were in turn used to arrive at the activation energy. The presence

of MOF-5 led to a substantial decrease in the activation energy from 98 kJ/mol for neat resin to 58 kJ/mol (M5C-a).

5A.3.4 Thermal properties

Thermogravimetric analysis was performed to investigate the effect of introducing MOF-5 on the thermal stability of polybenzoxazine. The TG and DTG traces of poly(C-a) and poly(M5C-a) in air atmosphere are presented in **Figure 5A.14**. The thermal decomposition of cardanol based benzoxazines is a multi-step process occurring through the degradation of the phenolic linkages and of the Mannich bridges in the polybenzoxazine[200, 201]. The double bond α-carbon of the cardanol undergoes scission at ~ 200°C[202]and the methylene linkages in the cured polymer have been reported to undergo cleavage at 440-500 °C[203].
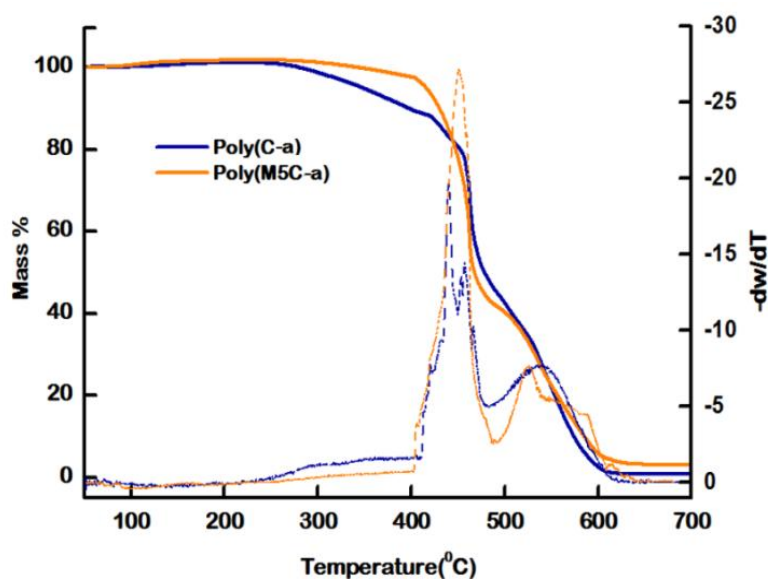
Figure 5A.14: TG-DTG traces of poly(C-a) and poly(M5C-a)

Decomposition temperatures associated with characteristic mass loss at 5%, 10% and char content (at 600°C) are presented in **Table 5A.4.** An appreciable increase in the $T_{5\%}$ and$T_{10\%}$ values is evident from the traces, and the increase in the char content can

be attributed to the presence of zinc oxide formed during the oxidative degradation of the cured formulation.

Table 5A.4: Characteristic thermo-oxidative degradation parameters

Sample Designation	$T_{5\%}(°C)$	$T_{10\%}(°C)$	Char content at 600°C (%)
Poly (C-a)	345	393	5
Poly (M5C-a)	416	429	10

5A.3.5 Adhesive property

The effect of MOF-5 inclusion on the adhesive strength of the benzoxazine resin was studied on steel plates as per the standard procedure. The results in terms of LSS are tabulated in **Table 5A.5** and the representative load−displacement curve is presented in **Figure 5A.15.** The LSS of adhesive to any substrate is dependent on several factors, particularly substrate wetting, inherent adhesive strength, temperature, resin thickness and type of failure.
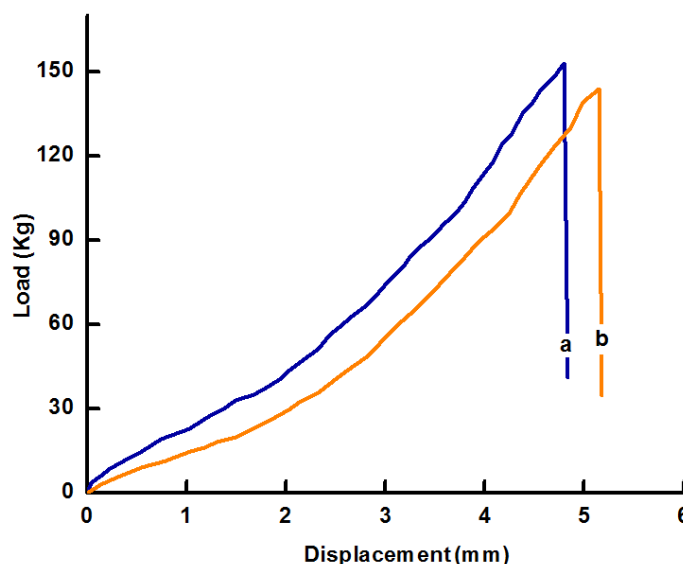
Figure 5A.15: Load displacement curve a) poly(C-a) and b) poly(M5C-a)

The thickness of the adhesive was maintained between 0.23–0.46 mm. The curing of benzoxazine lead to generation of sites which are involved in hydrogen bonding such

101

as –OH and >N-. It can be seen from the table that the presence of MOF-5 does not lead to any appreciable decrease in the LSS of the resin.

Table 5A.5: Lap Shear Strength values of benzoxazines

Resin	Lap Shear Strength(kgcm^{-2})
C-a	27± 2
M5C-a	25± 3

Chapter 5B

Curing Accelerators for Benzoxazine: Metal Stearates
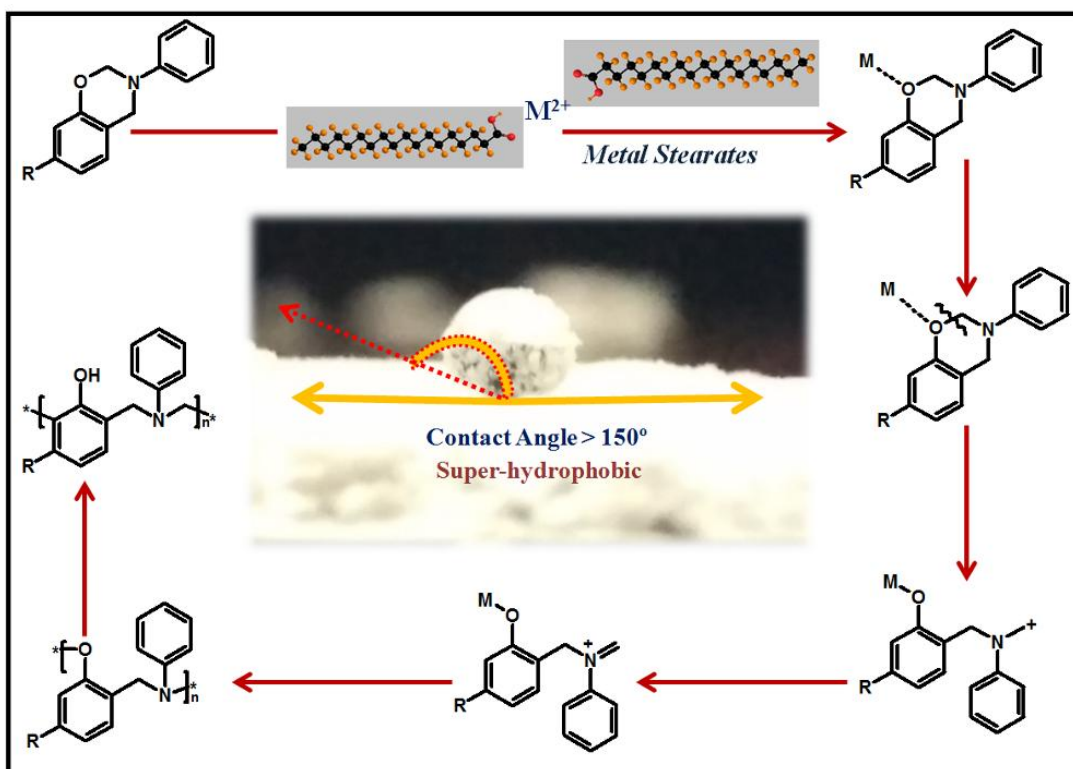
5B.1 Introduction

In the previous chapter, metal organic frameworks (MOFs) based on zinc have been explored as curing accelerators in view of their high surface area and acidic sites[204]. The lewis acidic Zn_4O nodes of atomic precision, available throughout the framework, were found to capable of reducing the temperature associated with curing of bio-based benzoxazines. Studies on transition metals complexes of acetylacetonates as curing accelerators for benzoxazines revealed that the complexes of manganese, iron, cobalt and zinc were found to exhibit the highest activity[79]. Inopportunely, metal complexes are relatively intolerant towards moisture, which deteriorate the mechanical performance of the material. Considering previous studies, hexafluoroacetylacetonate(F_6-acac) was employed as an organic ligand and the resulted acetylacetonato complexes reported as relatively more efficient accelerators, in view of their enhanced lewis acidity of the metal center due to the presence of strong electron-withdrawing group[79]. In addition, the replacement of acetylacetonate with the hexafluoroacetylacetonate reportedly improved the moisture tolerance of the accelerator. However, fluorinated compounds are toxic which imposes operability issues and are relatively expensive.

Considering the requirements, the motivation of this work is to come up with curing accelerators for bio-based benzoxazine monomer which proves to be efficient, eco-friendly and economically viable. In this context, metal stearates have not been scrutinized for catalytic curing of bio-based benzoxazines.

Metal stearates, coordination complexes of long chain fatty acids with transition metals, are of greatest commercial importance. The organic ligand, i.e. stearic acid is derived from saponification of the triglycerides obtained from natural sources (cocoa

butter and shea butter)[205]. Among the many interesting properties of metallic stearates, the most important are water repellence[206], gelling capacity, and stabilizing effect[207]. Most of the metal stearates, undergo solid to liquid transition ca ~150°C; conditions under which cardanol based benzoxazine curing is negligible[60]. In addition, metal stearates do not undergo thermal degradation during processing of the resin, rendering them excellent candidature as curing accelerators.

Zinc stearate, an industrially significant material, is used as a powerful mold realseasing agent in view of its superhydrophobicity[206]. Taking into account the environmental concers, the LD_{50} values indicative of lethal toxicity for 50% population, are high for zinc compounds (186 to 623 mg zinc/kg/day)[208]. Infrared and XAFS analysis shows that the coordination structure of zinc stearate comprises of oxo-centered Zn_4O nodes are coordinatively linked to four carboxylate moieties with a Zn-O distance of 1.95Å[209]. Lewis acidic Zn_4O nodes confer it excellent candidature for applications where acidic catalysis is desirable which has led researchers to explore its potential in representative applications e.g. lewis acid catalyzed transesterification reactions[210-212].

The present chapter discusses the potential of zinc stearate towards acceleration of ring opening polymerization of cardanol based mono-functional benzoxazine resin. Differential Scanning Calorimetric (DSC) analysis was performed to quantify the extent of acceleration in the ring opening polymerization behaviour. To validate the role of chemical environment towards the acceleration of benzoxazine curing, calorimetric studies were also performed in the presence of manganese, iron, cobalt, nickel and copper stearate, different in the coordination structure. To gain more insight of chemical environment around the central zinc species, curing studies were

104

also performed in the presence of zinc acetate anhydrous, which also has been reported to possess Zn_4O nodes.

5B.2 Experimental

5B.2.1 Materials

Aniline, paraformaldehyde was purchased from CDH chemicals. Manganous chloride, ferric chloride, cobaltous chloride, nickel sulphate, cuprous chloride, zinc sulphate, and stearic acid were purchased from CDH were used as received. Zinc acetate anhydrous ('AR', E. Merck), was used without further purification. Double distilled water was used throughout the course of this work.

5B.2.2 Synthesis of metal stearates

Transition metal stearates were synthesized using double decomposition technique of sodium stearate with metal salt as per the procedure reported in the literature[213]. Sodium stearate was prepared by the reaction of stearic acid with stoichiometric amount of sodium hydroxide. Subsequently, the temperature was increased to 75°C, and the desired aqueous metal salt solution was added drop-wise till complete precipitation of the metal stearates was observed. The metal stearates formed were filtered, washed repeatedly with hot water and finally dried under vacuum at 60°C.

5B.2.3 Polymerisation of cardanol based benzoxazine (C-a) using metal stearates.

To an accurately weighed amount of the cardanol-derived benzoxazine (C-a), varying amount of metal stearates (1-10 %w/w) were added and stirred at room temperature; conditions under which no polymerization was perceptible. The details of the formulations prepared along with their sample designations have been mentioned in **Table 5B.1**. Neat benzoxazine has been referred to as C-a and the compositions containing metal stearates have been referred to as MStXC-a where X indicates the

mass percent of metal stearate present in the sample. For e.g. C-a containing 10% w/w zinc stearate has been designated as ZnSt10C-a. A control set of curing studies were also performed on benzoxazine resin containing stearic acid and zinc acetate anhydrous. Sample was placed in a DSC aluminum pan and heated at a uniform rate of 10°C/min, while measuring the heat flow associated with polymerization. The corresponding DSC profiles of formulations were used to quantify characteristic curing parameters.

Table 5B.1: Details of formulations and sample designation

Sample Designation	Resin (g)	Additive	Amount of additive (g)
C-a	100	-	-
St10C-a	100	Stearic Acid	10
MnSt10C-a	100	Manganous Stearate	10
FeSt10C-a	100	Iron Stearate	10
CoSt10C-a	100	Cobalt Stearate	10
NiSt10C-a	100	Nickel Stearate	10
CuSt10C-a	100	Copper Stearate	10
ZnSt1C-a	100		1
ZnSt5C-a	100	Zinc Stearate	5
ZnSt10C-a	100		10
ZnAc10C-a	100	Zinc Acetate	10

5B.2.4 Characterization

Structural (FT-IR) and thermal (TGA and DSC) characterizations were carried out as discussed in previous chapters. Temperature sweep experiments were performed to study the rheological response of the resin as discussed in chapter 4.

To determine the non-volatile content of metal stearates, a weighed amount of sample was placed in a drying oven maintained at a temperature of 105°C. After 3h, the sample was removed from the oven; cooled in dessicator and reweighed the weight of the residue, consisting of solid and non volatiles was calculated as percentage of initial sample weight. For determination of ash content, the sample was heated in a

crucible over a hot plate to drive out all volatile solvents and moisture. It was subsequently transferred to a muffle furnace were the temperature was maintained at 550°C for 2 h to ensure final ignition. The remaining ash was weighed and reported as ash content. Free fatty acid content was determined chemically by titration of the unreacted carboxyl groups against a standard base. For this purpose, a known amount of metal stearate was hydrolyzed and then immersed in acetone for swelling/dissolution. After equilibrium swelling, the solution was titrated against previously standardized methanolic NaOH using phenolphthalein as indicator. The carboxyl-content was then calculated using the following equation:

$$Carboxyl\ content = \frac{(V_1 - V_2) \times N_1}{W \times 1000}$$ ....(5B.1)

Where, V_1 and V_2 are the volume of NaOH consumed by additive and blank respectively. N1 is the normality of methanolic NaOH and W is the weight (g) of the metal stearate.

5B.3 Results and Discussions

The potential of stearates based on transition metals as curing accelerator for benzoxazine resins has been explored. Non-isothermal calorimetric studies were performed to study the curing behaviour of benzoxazine in the presence of stearates.

5B.3.1 Transition metal stearates

Metallic stearates were synthesized by double decomposition process involving formation of sodium stearate followed by the replacement of the sodium cation with transition metal to form an insoluble metal stearate (**Scheme 5B.1**).

$$C_{17}H_{35}COOH + NaOH \longrightarrow C_{17}H_{35}COONa + H_2O$$
$$C_{17}H_{35}COONa + M^{2+}_{(aq)} \longrightarrow (C_{17}H_{35}COO)_2M + 2Na^+$$

Scheme 5B.1: Double decomposition method for metal stearate preparation

FT-IR spectra of all the stearates exhibited absorbance at 1545 cm^{-1}; attributable to asymmetric vibration stretching of the carboxylic group coordinated to the metal ion (**Figure 5B.1 (i)**).
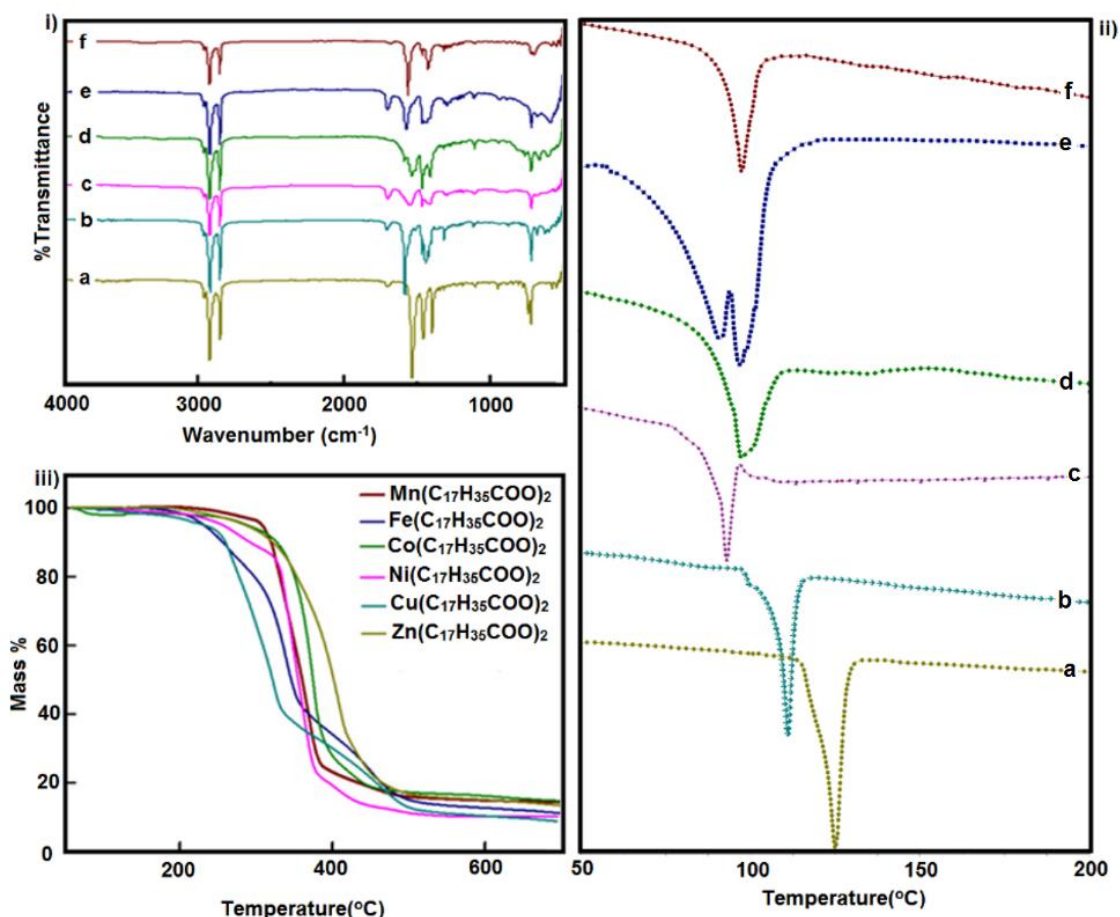
Figure 5B.1: Characterization of metal stearates i) FT-IR ii) DSC and iii) TGA traces of a) zinc(II) b) copper(II) c) nickel(II) d) cobalt(II) e) iron(II) f) manganous(II) stearate

Three intense bands in the 1300–1600 cm^{-1} regions were also observed. The 1545 cm^{-1} band is assigned to the carboxylate antisymmetric stretch and 1465 cm^{-1} to the CH$_2$ bending. The 1399 cm^{-1} band may be assigned to the C$_x$H$_{2x}$ bending and/or the carboxylate symmetric stretch, both of which should be observed in the infrared spectrum. DSC traces presented in **Figure 5B.1(ii)**, reveal that all the stearates undergo melting prior to the onset of the polymerization of the benzoxazine monomer

(~242°C). This is expected to result in homogeneous blending of the stearate with the monomer, thereby enhancing their candidature as accelerators. Thermo gravimetric analysis (**Figure 5B.1(iii)**) revealed that all metal stearates are thermally stable within the processing window of the benzoxazine monomer ca~ 250°C. All the metal stearates were found to be insoluble in water and soluble in THF, DMF, xylene and toluene. The contact angle of zinc stearate has been reported to be 154.6 ± 1.5°[206], which is a direct evidence of its super hydrophobicity. The same was confirmed from the mobile water drops over surface of zinc stearate as can be seen in digital images presented in **Figure 5B.2**. The hydrolytic stability of the metal stearates is an extremely interesting feature, which bestow them ideal candidature as curing accelerator for benzoxazine curing.
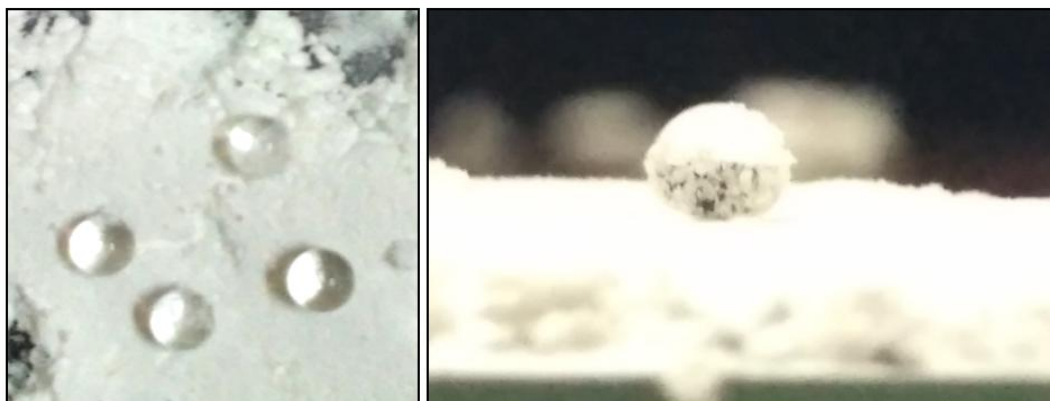
Figure 5B.2: Digital images of mobile water drop over super hydrophobic surface of zinc stearate

Characteristic thermal properties like non-volatile content (%) and ash content (%) of metal stearates were determined as per the standard procedure and the results are tabulated in **Table 5B.2**. All metal stearates exhibited a non-volatile content >95% and ash content of 12–15 %. The ash content has been reported to be dependent on the oxidation state of the central metal[213]. As per theoretical calculations, the metal content corresponding to all the stearates should be 6.25 ±0.21%. However, this

figure is not in concordance with the char content obtained during TGA, which can be attributed to the conversion of the metal to its oxide form during the thermal decomposition process. The acidic co-reactants were completely consumed during the formation of metal stearate, which was confirmed from the negligible free fatty acid content, as determined using established procedure.

Table 5B.2: Physiochemical characterization of the metal stearates

Metal Stearate	Non- Volatile Content (%)	Ash Content (%)
$Mn(C_{17}H_{35}COO)_2$	98	15
$Fe(C_{17}H_{35}COO)_2$	95	11
$Co(C_{17}H_{35}COO)_2$	95	11
$Ni(C_{17}H_{35}COO)_2$	98	14
$Cu(C_{17}H_{35}COO)_2$	99	12
$Zn(C_{17}H_{35}COO)_2$	99	13

5B.3.2 Screening of accelerators based on DSC analysis of polymerization of cardanol benzoxazine monomer

Benzoxazine monomers undergo thermally accelerated cationic ring opening polymerization and results in thermally stable cross-linked polymer. The presence of curing accelerators in the formulation is expected to shift the curing profile towards lower temperatures and alter the kinetics of the oxazine ring opening stage through several reported mechanisms[39, 78, 179, 193-195]. Non-isothermal calorimetric studies were performed to assess the potential of metal stearates towards acceleration in polymerization of benzoxazine resins. The results of the DSC analyses in terms of characteristic curing temperatures are summarized in **Table 5B.3**. The presence of metal stearates based on manganese(II), iron(II), cobalt(II) and zinc(II) in the

formulation led to a remarkable decrease in the curing parameters, with copper(II) and nickel(II)-stearate being relatively less effective. Cobalt(II) complexes have been reported to exhibit high levels of toxicity and pose adverse effect on the environment[214]. In view of these concerns, zinc stearate, was selected as the most suitable accelerator and representative curing profiles of formulations containing varying amounts of zinc stearate are presented in **Figure 5B.3.**

Table 5B.3: Effect on introduction of accelerators on characteristic curing temperatures (β=10°C/min)

Sample designation	T_o (°C)	T_{peak}(°C)	% Reduction	
			T_o	T_{peak}
C-a	242	263	-	-
St10C-a	223	244	7.8	7.2
MnSt10C-a	187	226	22.7	14.0
FeSt10C-a	206	225	14.8	14.4
CoSt10C-a	183	213	24.3	19.0
NiSt10C-a	205	236	15.2	10.2
CuSt10C-a	212	234	12.3	11.0
ZnSt1C-a	226	247	6.6	6.0
ZnSt5C-a	193	222	20.2	15.5
ZnSt10C-a	169	202	30.1	23.1
ZnAc10C-a	218	222	9.9	15.5
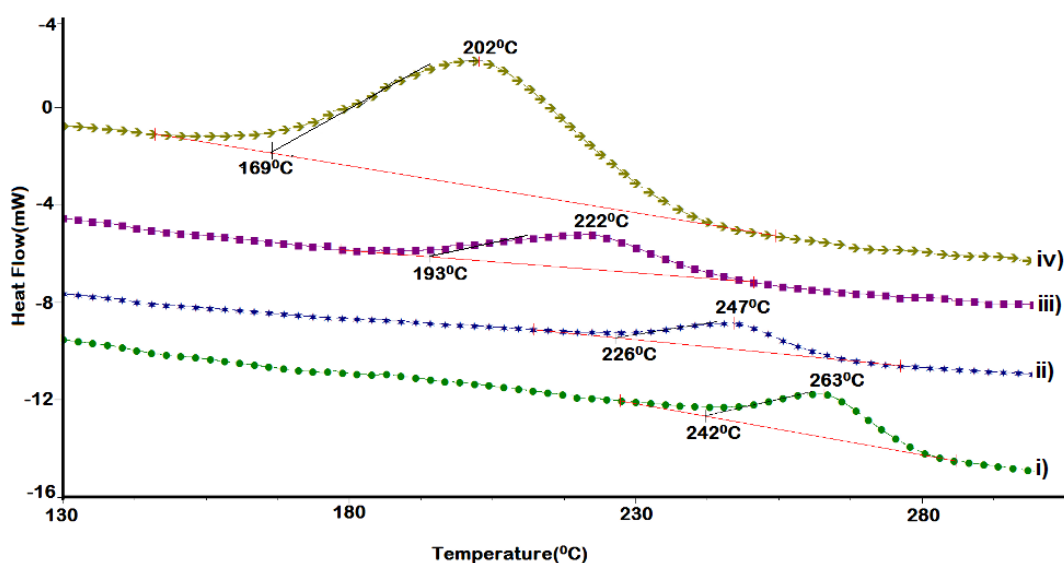
Figure 5B.3: DSC profile i) C-a, ii) ZnSt1C-a, iii) ZnSt5C-a and iv) ZnSt10C-a

It has been mentioned already, the ring opening polymerization process in cardanol based benzoxazine initiates at 242°C with a peak at 263°C (**Figure 5B.3(i)**). It can be seen from the figure that the curing profile shifts towards lower temperature in the presence of zinc stearate, the extent of which was found to be proportional to its amount in the formulation. Inclusion of 10 %w/w zinc stearate in the formulation was found to decrease the curing temperature of neat benzoxazine from ~263 to ~202 °C (23% decrease) (**Figure 5B.3(ii)-(iv)**).Acetylacetonate complexes have been previously reported to decrease the curing temperature by 23% for high temperature curing bisphenol-a based benzoxazine(BA-a)[79]. Commercially available accelerators DT310 and DT300 (Huntsman) have been reported to result in decrease of 16.8% and 7.2 % respectively for bisphenol-A benzoxazine (BA-a).

Extensive characterization studies on zinc stearate[209] confirm the presence of Zn_4O nodes, which are coordinatively linked to four carboxylate moieties with a Zn-O distance of 1.95Å. The structure of both zinc stearate and acetate are presented in **Figure 5B.4**. It is the presence of these lewis acidic Zn_4O nodes, which result in

112

accelerating activity of zinc stearate[204].As the temperature is increased, a solid–liquid phase transition occurs in zinc stearate at ~130°C, however the coordination structure reportedly remains unaffected[209].
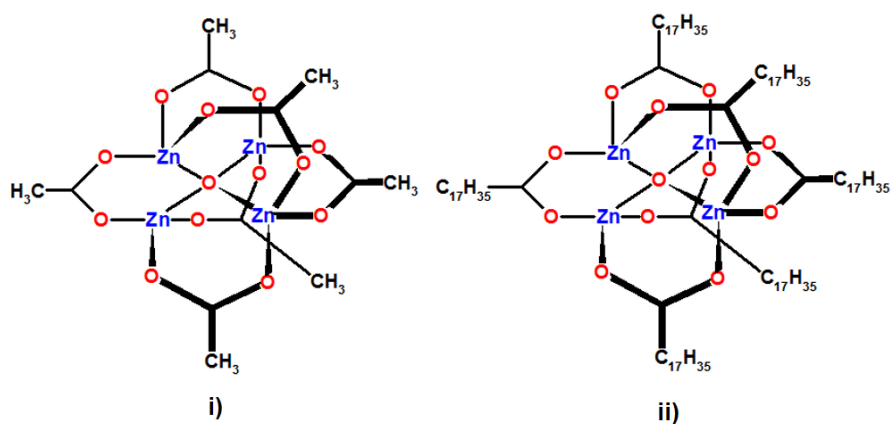
Figure 5B.4: Chemical Structures of i) anhydrous zinc(II) acetate and ii) zinc stearate

To understand the importance of the chemical environment around the central zinc species, curing studies were also performed in the presence of zinc(II) acetate anhydrous, which also has been reported to possess Zn_4O nodes[209], and the results are included in **Table 5B.3**. It can be speculated that the synergistic combination of acidic Zn_4O nodes and the uniform dispersion due to the hydrophobic stearate chains (**Figure 5B.5(i)**) result in the observed acceleration of the curing reaction. The proposed mechanism of zinc stearate accelerated polymerization of benzoxazine is presented in **Figure 5B.5(ii)**. The Zn_4O nodes available in zinc stearate interact with the oxygen to form a cyclic oxonium cationic species, which is followed by an electronic rearrangement leading to the formation of a resonance stabilized iminium cation. Subsequently, benzoxazine monomer adds to the cationic imine moiety, forming another electron deficient cyclic oxonium species. Repetitive electrophilic substitutions result in a polymeric network with thermally unstable aryl ether

113

structure, which undergoes rearrangement resulting in a polymer with phenolic structure.
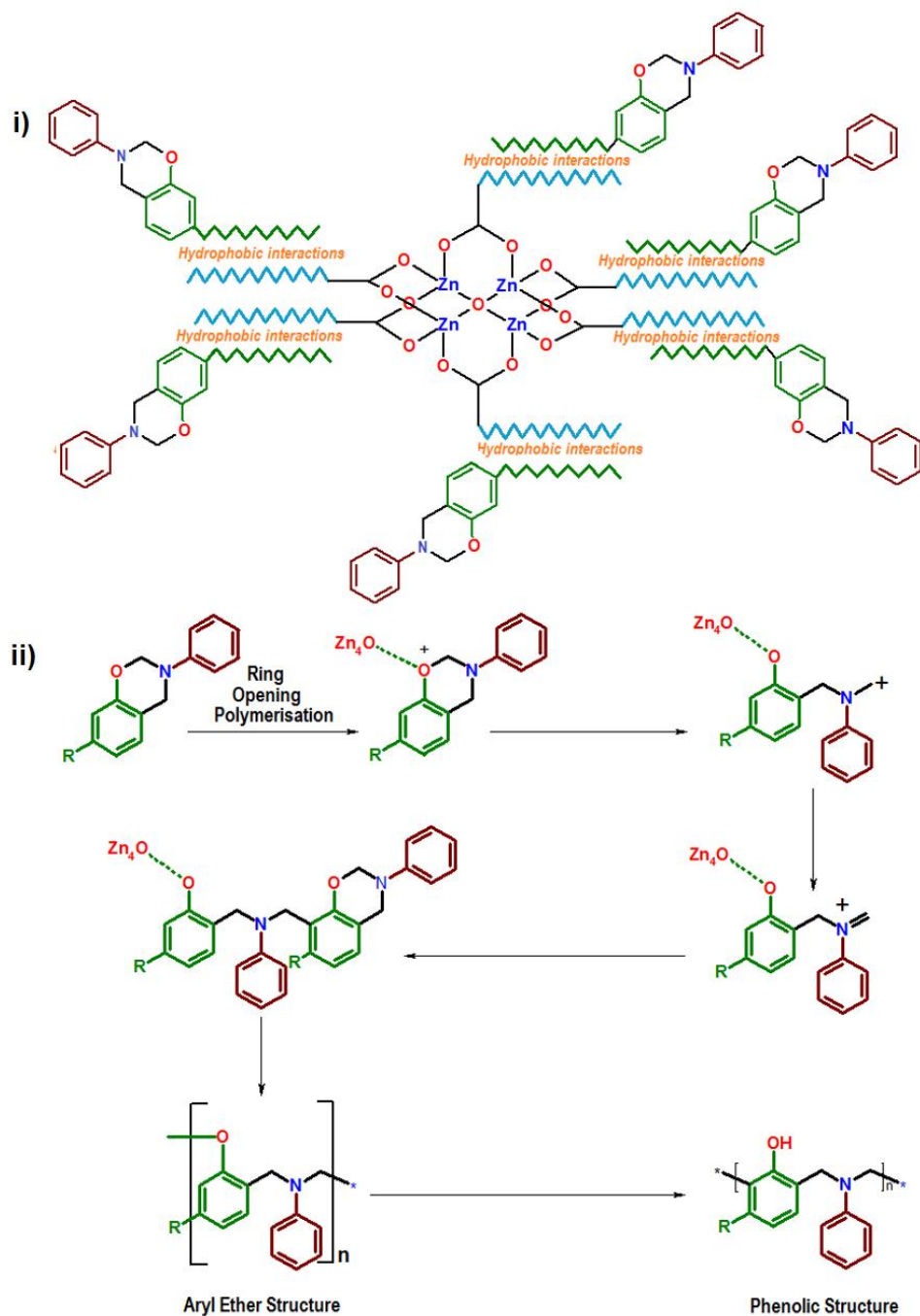
Figure 5B.5: i) Hydrophobic interactions present within zinc stearate and C-a resulting in uniform dispersion of accelerator in the resin. ii) Proposed mechanism for ring opening polymerization of C-a in the presence of zinc stearate as curing accelerator.

114

Changes in the rheological behavior of the resin due to inclusion of zinc stearate in the formulation has been investigated by temperature sweep experiments and the variation in terms of complex viscosity and loss-storage modulus is presented in **Figure 5B.6**. Increase in temperature to 100°C leads to a sudden decrease in the viscosity of the formulation, which can be attributed to the melting of zinc stearate. This is accompanied by a simultaneous decrease in storage and loss modulus. The ring-opening of oxazine moieties leads to the formation of open Mannich bases, possessing hydrogen bonding interactions, however till ~220°C, the viscosity buildup is practically negligible[171]. Subsequently, polymerization is initiated where the linear chains associate with each other leading to a sudden increase in viscosity. The phenolic hydroxyl groups generated act as polymerization catalysts and gelation is achieved at ~220°C where a crossover of loss and storage modulus is observed[171, 172] (**Figure 5B.6(ii)**), while the same is achieved at ~257°C (for the neat resin) as shown in the **Figure 5B.6(i)**, which further confirms the accelerating activity of zinc stearate. Further increase in temperature leads to an increase in the viscosity as well as the moduli, which finally levels off.
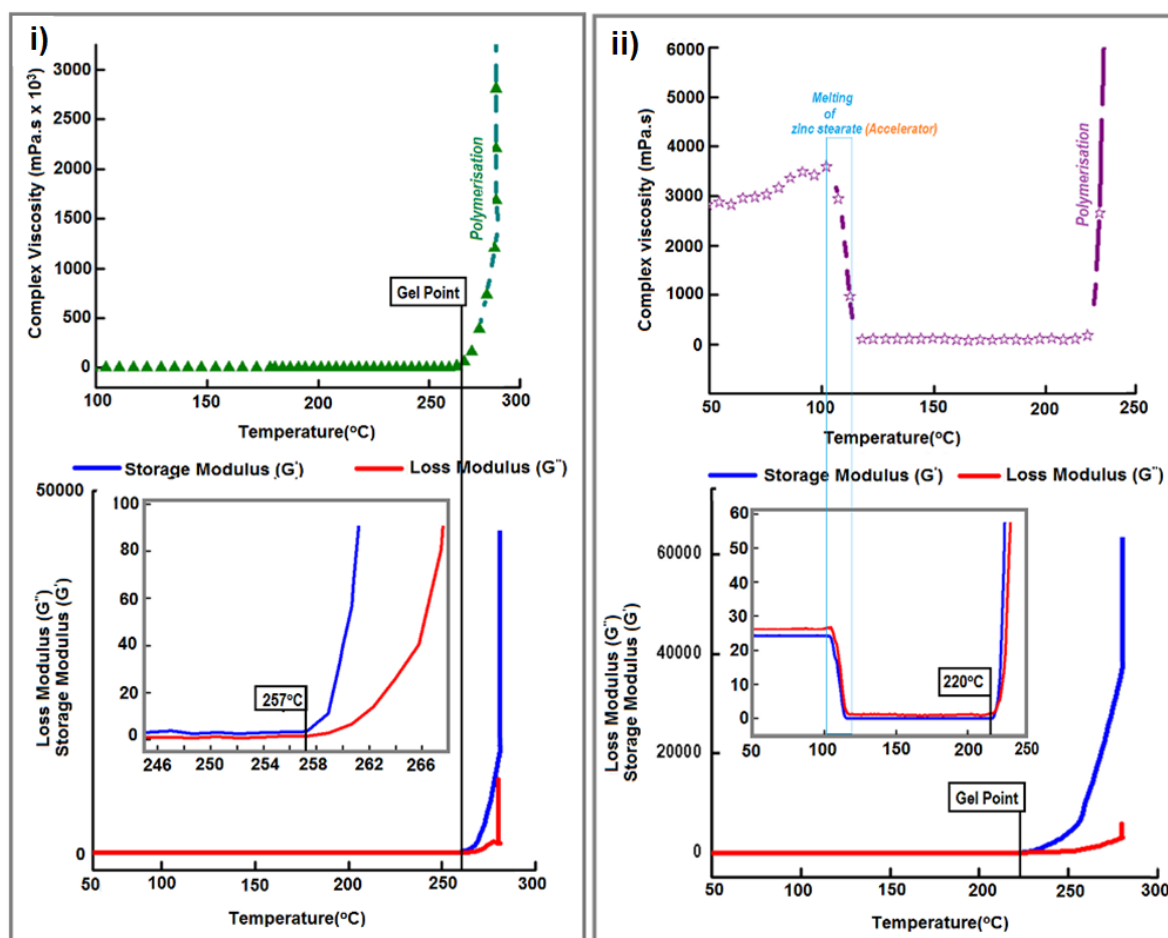
Figure 5B.6: Rheological behavior of i) C-a and ii) ZnSt10C-a during

polymerization.

5B.3.3 Kinetics of metal stearate accelerated polymerization

DSC traces of a representative formulation (ZnSt10C-a) at various heating rates viz.

5, 7 and 10 °C/min are presented in **Figure 5B.7.** Increasing the heating rate (β) leads

to systematic shift in the trace towards higher temperatures, which can be attributed to

the reduced time available with the reactants at higher heating rates. The curing of

benzoxazine resin is typically a multi-step process exhibiting complex kinetics[215-

217]. The process is accompanied with a dramatic change in the physical state of the

reaction medium. At the early stages, the reaction medium is a liquid composing

116

primarily of monomers. With the progress of the reaction, the molecular weight and viscosity of the polymer formed increases, which in turn results in a decrease in the molecular mobility. The sudden decrease in the mobility however occurs with the cross-linking of polymer chains, where the chains lose their ability to move past one another, and the medium turns to a solid that can be either rubbery or glassy, depending upon the T_g of the cured resin. Characteristic parameters associated with the curing of the resin i.e. ΔH_{cure}, T_{onset} and T_{peak} are summarized in **Table 5B.4**.

Figure 5B.7: Effect of heating rate (β) on the curing profile of ZnSt10C-ai) 5, ii) 10 and iii) 15°C/min.

The extent of conversion, α at any particular temperature (T_α) was calculated as the ratio of the areas under the exothermic DSC peak and expressed as:

$$\alpha = \frac{\Delta H_{T_\alpha}}{\Delta H_{cure}} \dots\dots\dots\dots\dots(5B.2)$$

117

where ΔH_{T_α} is the heat of reaction of partially cured samples (till temperature T_α) and ΔH_{cure} is the total heat of curing. The increase in the degree of conversion with temperature for ZnSt10C-a at a different heating rates is presented in **Figure 5B.8(i)**.
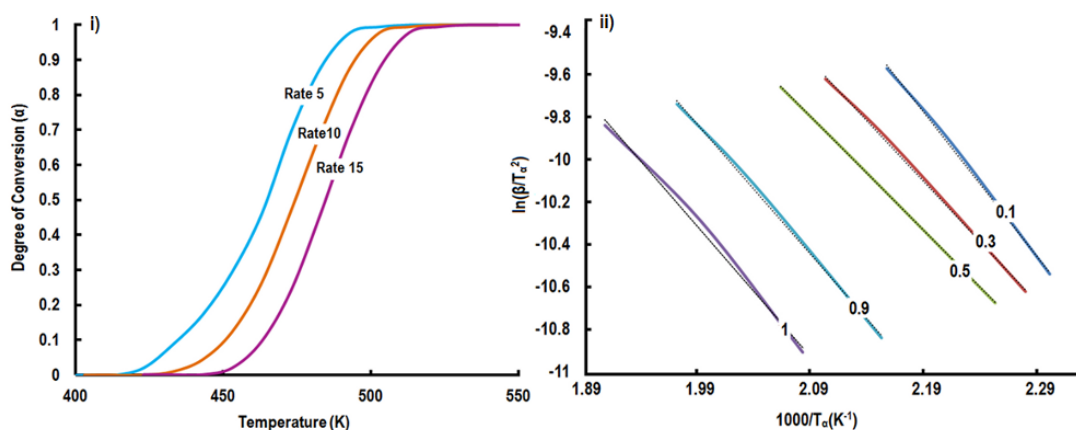
Figure 5B.8: i) Effect of temperature on the degree of conversion of cardanol based benzoxazine in the presence and absence of zinc stearate (β = 5, 10 and 15 °C/min) ii) Iso-conversion plots associated with various degree of conversions (α).

It can be seen that in the presence of zinc stearate, complete curing is attained at ~203°C while the same for a neat monomer is achieved at 280°C[218], clearly demonstrating the effectiveness of zinc stearate as an curing accelerator for benzoxazine.

Table 5B.4: Characteristic curing parameters of neat benzoxazine and ZnSt10C-a

Sample	β(°C/min)	T_{onset}(°C)	T_{peak}(°C)	Activation energy (kJ/mol) α= 10%
C-a	5	224	246	98
	10	236	255	
	15	241	263	
ZnSt10C-a	5	159	192	51
	10	170	203	
	15	179	211	

In view of its simplicity, Kissinger–Akahira–Sunose equation[199]was applied for determination of activation energies (E_α) from the plot of $ln\left(\dfrac{\beta_i}{T_{\alpha,i}^2}\right)$ against $1/T_\alpha$.

$$ln\left(\frac{\beta_i}{T_{\alpha,i}^2}\right) = \text{Constant} - \frac{E_\alpha}{RT_{\alpha,i}} \quad \ldots\ldots\ldots\ldots\ldots.(5B.3)$$

Where, β is the heating rate, T_α is the temperature associated with a particular conversion (α) at the corresponding heating rate, E_α is the activation energy at that α and R is the gas constant. The linear plots at few representative conversions for ZnSt10C-a are presented in the **Figure 5B.8(ii)** which were used to arrive at the activation energy. The presence of zinc stearate led to a substantial decrease in the activation energy from 98 kJ/mol for neat resin to 51 kJ/mol (ZnSt10C-a).

5B.3.4 Thermal Properties of Polybenzoxazines

Thermo gravimetric analysis was performed on the cured resins, to investigate the effect of introducing zinc stearate on the thermal stability of cardanol based polybenzoxazine. The TG and DTG traces of poly(C-a) and poly(ZnSt10C-a) in nitrogen atmosphere are presented in **Figure 5B.9**. The thermal decomposition of cardanol based benzoxazines is a multi-step process occurring through the degradation of the phenolic linkages and of the Mannich bridges in the polybenzoxazine[200, 201]. The double bond α-carbon of the cardanol undergoes scission at ~200°C[202] and the methylene linkages in the cured polymer have been reported to undergo cleavage at 440-500 °C[203].
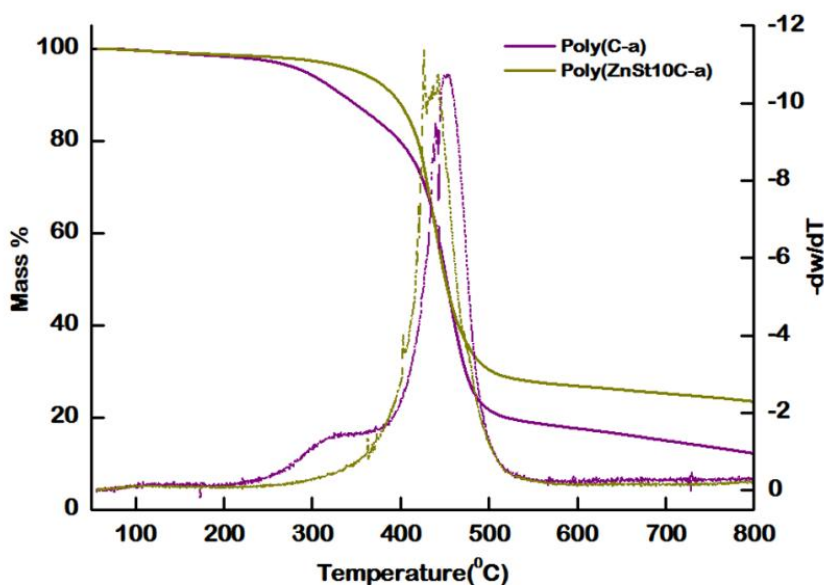
Figure 5B.9: TG-DTG traces of poly(C-a) and poly(ZnSt10C-a)

Decomposition temperatures associated with characteristic mass loss at 5%, 10% and

char content (at 600°C) are presented in **Table 5B.5**. An appreciable increase in the

$T_{5\%}$ and $T_{10\%}$ values is evident from the traces, and the increase in the char content can

be attributed to the presence of zinc oxide formed during the thermal degradation of

the cured formulation. Polybenzoxazines have been reported to exhibit excellent fire,

smoke and toxicity (FST) properties, which can be preliminarily adjudged through

Limiting oxygen index (LOI) studies. The same refers to the minimum amount of

oxygen (%) in an oxygen-nitrogen mixture that is just sufficient to maintain

combustion (post-ignition) of the material[219]. A significant correlation between the

char residue (CR) and LOI has been reported, LOI = 17.5 + 0.4×CR[220]. The LOI

for poly(C-a) was calculated to be 24, which is considered to be suitable for

application of these polymers in areas necessitating flame retardance[107]. The same

was found to increase substantially to 28 upon addition of 10 %w/w zinc stearate

indicating superior flame retardancy of the developed formulation.

Table 5B.5: Characteristic thermo-oxidative degradation parameters

Sample Designation	$T_{5\%}$ (°C)	$T_{10\%}$ (°C)	Char content at 600 °C (%)	LOI
Poly (C-a)	345	331	10	24
Poly(ZnSt10C-a)	351	390	27	28

5B.3.5 Adhesive property

The effect of zinc stearate inclusion on the adhesive strength of the benzoxazine resin was studied on steel plates as per the standard procedure. The results in terms of LSS are tabulated in **Table 5A.6** and the representative load−displacement curve is presented in **Figure 5A.10.**

Table 5A.6: Lap Shear Strength values of benzoxazines

Resin	Lap Shear Strength(kgcm^{-2})
Poly(C-a)	27± 2
Poly(ZnSt10C-a)	20± 3

The LSS of adhesive to any substrate is dependent on several factors, particularly substrate wetting, inherent adhesive strength, temperature, resin thickness and type of failure.
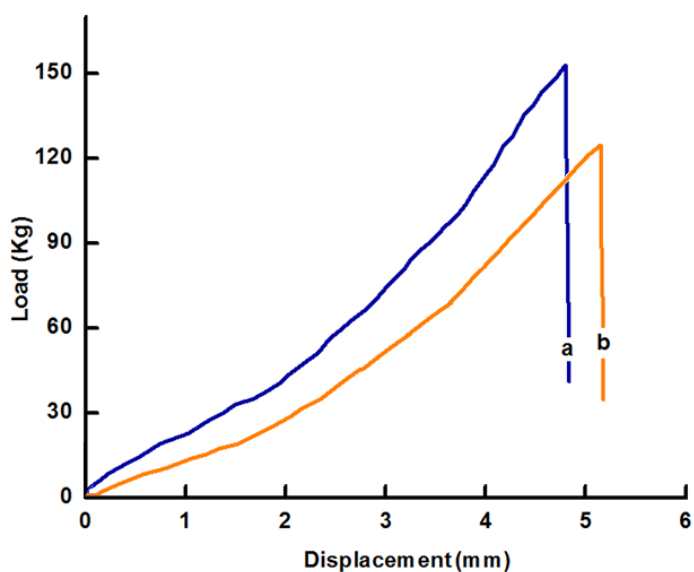
Figure 5B.10: Load displacement curve a) poly(C-a) and b) poly(ZnSt10C-a)

The thickness of the adhesive was maintained between 0.23–0.46 mm. The curing of benzoxazine lead to generation of sites which are involved in hydrogen bonding such as –OH and >N-. It can be seen from the table that the presence of zinc stearate leads to decrease in the LSS of the resin.

Chapter 6
Microencapsulation of cardanol based benzoxazines

Thermally accelerated ring opening polymerisation

Healing agent

Encapsulation

Microcapsules

Pressure
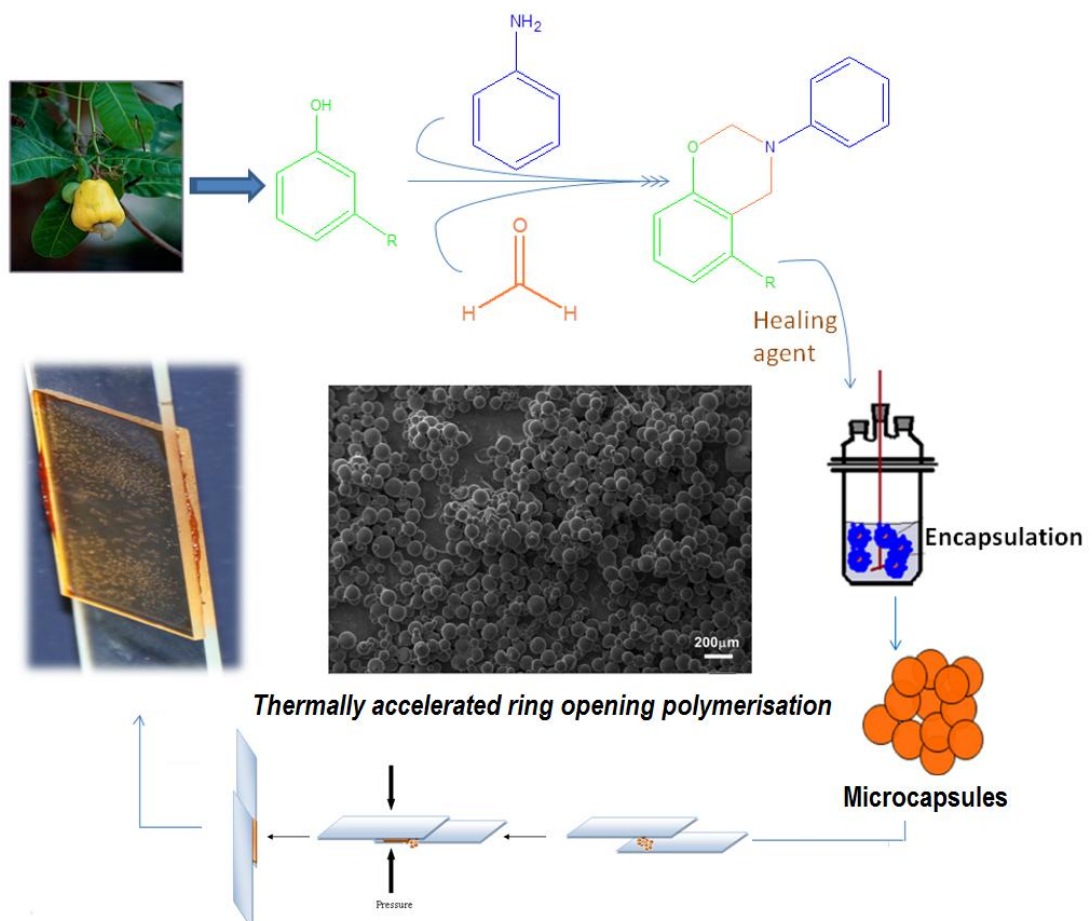
6.1 Introduction

Benzoxazine precursors hold enormous potential as healants for temperature triggered healing[221], provided they are encapsulated in fragile micro-containers, prior to their inclusion in the polymeric matrix. Surprisingly, attempts towards usage of oxazine monomers for this purpose have not been reported till date. Benzoxazines, interestingly, do not require any catalyst for their curing, and hence are ideal candidates for the aforementioned purpose. In addition, few benzoxazines have also been reported to exhibit anti-tuberculosis activity, and their encapsulation can lead to improvement in their efficiency as pharmacological agents by controlled release[222]. Microencapsulation, in simple terms refers to the entrapment of solids, liquids or gases, usually in fragile polymeric containers[223]. The protective polymeric shell wall separates the core from surroundings and is ruptured through a specific stimulus, releasing the core in the perfect place and time[224]. Microencapsulation is emerging as an industrially significant technique and has numerous applications in areas such as polymers, paints, pharmaceutical, and agricultural[225].

Unfortunately, the possibility of curing of benzoxazine monomers under acidic conditions imposes a restriction on the technique used for its encapsulation. The conventional encapsulation procedure involves in-situ emulsion polymerization of urea or melamine with formaldehyde on the surface of the hydrophobic dispersed phase of the precursor[226]. The condensation process requires low pH (<3); [227, 228] but the acidic conditions may induce curing in benzoxazine[229]. We believe that this issue can be addressed by adopting distinct approaches for encapsulation which includes solvent evaporation and interfacial polymerization, which surprisingly has not been attempted till date for benzoxazine.

Solvent evaporation is a "physical" entrapment of monomer and is relatively less complex methodology which is routinely employed for the encapsulation of drugs for pharmaceutical applications. The process involves stabilization of the dispersed healant, which is followed by the addition of a solution containing shell wall material and the evaporation of solvent results in free flowing microcapsules.

Interfacial engineering is an alternative approach adopted to perform chemical microencapsulation of liquid benzoxazine. The potential of liquid-liquid interface towards preparation of nano-crystals, thin films[230-232] and microcapsules[233, 234] has been well reported. We believe that this concept could very well be extended to prepare microcapsules with interesting morphologies. To elucidate this approach, a solution of epoxy resin and benzoxazine is dispersed in silicone medium followed by addition of a polyamine which reacts selectively with the epoxy resin. In view of the preferential reaction of oxirane with amine, we engender that the reaction would be driven to the interface, leading to the formation of cross-linked spherical shell. Conventionally, liquid paraffin is used as a dispersing phase, however, the viscosity of liquid paraffin is not high enough to maintain system stability[235], so rapid polymerization is needed to prevent the coagulation of the polymerization droplets[236]. Polydimethylesiloxane (PDMS) was chosen as the reaction medium in view of its thermal stability and solubility differences with both the resins as well as triethylenetetramine (TETA) hardener[236].

In this chapter, we report the results of microencapsulation of benzoxazine by two methodologies (i.e solvent evaporation and interfacial encapsulation) in different shell wall materials i.e, polystyrene and epoxy. Of particular interest is to investigate the

effect of operating parameters to arrive at optimized conditions for preparation of microcapsules.

6.2 Experimental

6.2.1 Materials

Styrene (Merck) was washed with 10% aqueous sodium hydroxide to remove inhibitor, followed by washing with water, till neutral pH was obtain. After drying over anhydrous sodium sulphate (CDH), styrene was further purified by vacuum distillation at 60℃. PVA (Mol. wt. 14000, CDH) was used without further purification. Epoxy resin (Ciba Geigy, Araldite CY 230; epoxy equivalent 200 eq g^{-1}) and hardener (HY 951; amine content 32 eq kg^{-1}) was used as received. Double distilled water was used throughout the course of study. Polydimethylesiloxane (CDH, kinematic viscosity 300 cSt) was used without any further purification. Double distilled water was used throughout the course of study. Resin encapsulated as healant is cardanol-aniline benzoxazine (C-a) which was synthesized and characterized as per the procedure reported in previous chapters. The detailed characterization of the resin has been already mentioned in Chapter 1.

6.2.2 Microencapsulation of benzoxazine in poly(styrene) shells

6.2.2.1 Preparation of polystyrene

Polystyrene was prepared by emulsion polymerisation according to the procedure reported in the literature[237]. A monomer premix containing sodium lauryl sulphate (2 g), styrene (20 g) in water (4 g), and aqueous solution of potassium persulphate and sodium metabisulphite (redox initiator) were prepared separately. 10% of the monomer premix was taken in a reaction vessel and was diluted with distilled water (25 mL).The temperature was raised to 60°C, after which initiator solution (1 ml) was

125

added under inert atmosphere. After seed formation, the rest of the monomer was poured slowly in 1h. After complete addition of monomer, the reaction was allowed to continue at 80°C for 4 h. Electrolyte solution (Al_2SO_4) was added to precipitate the emulsion and a soxhlet extraction was performed for duration of 12h. Yield ~87 %

6.2.2.2 Microencapsulation of benzoxazine monomer in polystyrene shells

C-a was encapsulated in PS microcapsules by solvent evaporation technique using the procedure reported in the literature[238]. A solution of benzoxazine monomer in chloroform (20% w/v) was added drop wise to 100 mL aqueous PVA solution (2.5% w/v) under continuous stirring (500 rpm). Separately, a solution of PS in chloroform (2-10% w/v) was injected through a hypodermic syringe into the reaction vessel, maintained at 60°C, at different stirring rates (400-600 rpm). Post-evaporation of chloroform, the reaction mixture was cooled, and the C-a encapsulated PS microcapsules were filtered and washed repeatedly with water followed by drying under vacuum.

6.2.3. Microencapsulation of benzoxazine in interfacially engineered epoxy shells.

Benzoxazine was encapsulated in cross-linked epoxy shell by the preferential reaction of epoxy resin with triethylenetetramine (TETA) hardener at the silicone-benzoxazine interface, while keeping the mixture suspended in silicone medium by agitation. The immiscibility of the benzoxazine and epoxy resin in PDMS was first verified by capturing the optical images using computer interfaced optical microscope at a magnification of 40 of the suspensions prepared by stirring the resins vigorously (1000 rpm) for a period of 5 mins. Subsequently, epoxy resin was first homogenized in C-a in varying ratio (2.3:1-1.0:1; 10 g). The reaction was performed in reaction vessel under inert atmosphere. Silicone oil (200 mL) was purged with nitrogen over a

period of 15 mins. The homogenized benzoxazine-epoxy resin mixture was introduced into silicone, which was maintained at 70°C under continuous stirring. Stoichiometric quantity of TETA (13 %w/w epoxy resin) was subsequently injected slowly through a hypodermic syringe and the curing reaction was allowed to continue for 8 h under varying stirring speeds (500-700 rpm), after which the reaction mixture was cooled and filtered. Epoxy microspheres were also prepared in the absence of benzoxazines under similar conditions, while maintaining a constant temperature of 70°C and a stirring speed of 600 rpm.

6.2.4. Determination of adhesive property of microcapsules

To demonstrate the potential of the C-a encapsulated microcapsule sin the context of temperature triggered healing, microcapsules (0.3 ±0.01 g) with different core content were placed between two steel plates, crushed by manual tapping and placed at 240°C for a period of 1h. A total of 5 replicates were tested per sample.

6.2.5. Characterization

Structural (FT-IR and ^{1}H-NMR) and thermal (DSC and TGA) characterization were carried out. Lap shear strength of resin was determined using standard ASTM D1002 the detailed procedure has been discussed in previous chapters.

Optical images of suspended micro droplets were captured using an optical microscope Motic, B3-223PL. The surface morphology of samples was studied using a Scanning Electron Microscope (Zeiss EVO MA15) under an acceleration voltage of 1 kV. Samples were mounted on aluminium stubs and sputter-coated with gold and palladium (10 nm) using a sputter coater (Quorum-SC7620) operating at 10-12 mA for 120 s. The microsphere size distribution was determined from SEM images. Image J software was used to measure the diameter of fifty spheres per image.

6.3. Results and Discussion

C-a was prepared using solvent less method, followed by its encapsulation in different shells. The effect of operating parameters, particularly stirring speed and polymer concentration on the microcapsule dimensions was investigated.

6.3.1. Microencapsulation of benzoxazine in polystyrene shells

6.3.1.1 Polystyrene

DSC and TG-DTG trace of the shell wall material (polystyrene) is presented in **Figure 6.1.** A glass transition phenomenon is clearly evidenced at ~98°C and single step degradation can be observed at ~400°C.
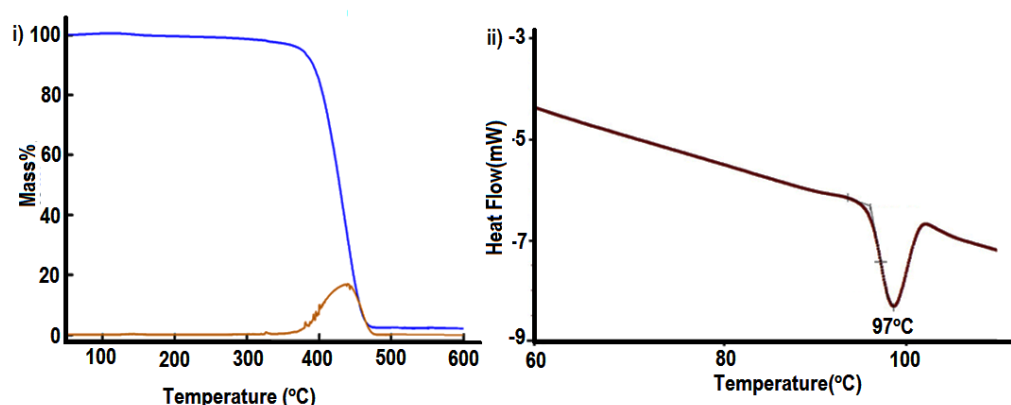
Figure 6.1:a) TG-DTG and b) DSC traces of polystyrene

The intrinsic viscosity of polystyrene in toluene was ~105 ml/g (34°C), which was used to determine the viscosity average molecular weight of the polymer (3.19 x 10^5 g/mol).

6.3.1.2 Polystyrene microcapsules encapsulating benzoxazine (C-a)

C-a was encapsulated in fragile PS containers by solvent evaporation technique to form pale yellow microcapsules, the SEM image of a representative batch is presented in **Figure 6.2.** The microcapsules are perfectly spherical, and exhibit a smooth surface

128

texture. The thickness of the shell wall was found to be ~7 ± 1μm, as can be seen in the SEM images of broken microcapsules **(Figure 6.2, Inset).**
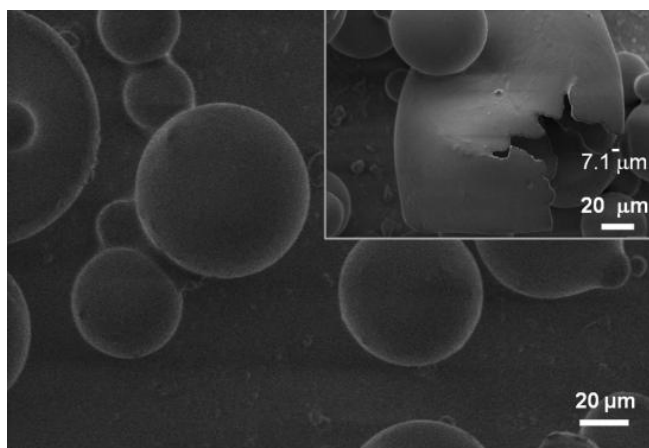
Figure 6.2: SEM image of C-a encapsulated PS microcapsules. Inset shows the magnified image of a broken microcapsule indicating its shell wall thickness.

6.3.1.2.1 Effect of stirring speed

The effect of increasing stirring speed on the microcapsule dimensions is presented in **Figure 6.3.** As expected, increasing the rate of stirring led to a decrease in the particle dimensions, which could be attributed to the shearing of the large oily droplets into smaller microspheres under higher shear rates[239].
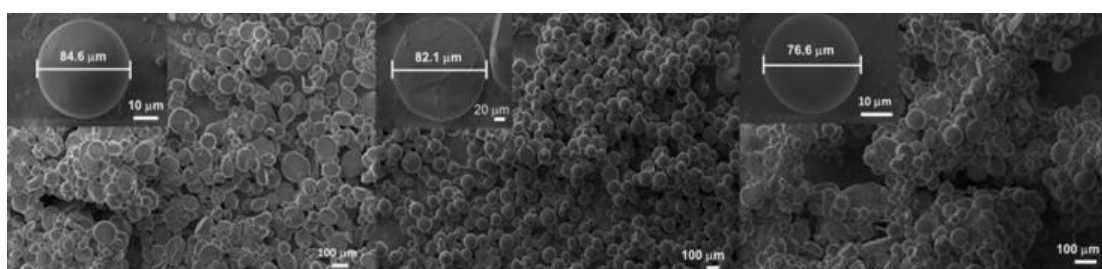
Figure 6.3: SEM image of microcapsules prepared under different stirring speeds a) 400, b) 500, c) 600 rpm. Inset shows the enlarged image of a single microcapsule.

6.3.1.2.2 Effect of encapsulating polymer concentration

Core-content is one of the most important characteristics of microcapsules. In view of the similar solubilities of C-a and PS, conventional technique of core-content quantification proved unsuccessful and the ratio of heat of curing of encapsulated

benzoxazines to that of the neat benzoxazines was used to determine the same (**Table 6.1**).

$$\text{Core content(\%)} = \frac{\Delta H_{curing,encapsulated\ C-a}}{\Delta H_{curing,C-a}} \times 100 \qquad \text{................(6.1)}$$

Where, enthalpy of curing of neat C-a ($\Delta H_{curing,\ C-a}$) is 71.1 ± 1.8 J/g.

Table 6.1: Core content of polystyrene microcapsules

Concentration of PS in feed solution (%w/v)	ΔH_{curing} (J/g)	Core content (%)
2	26.0 ± 0.7	38 ± 2.7
6	22.0 ± 0.5	31 ± 2.1
10	13.5 ± 0.5	19 ± 3.1

The core content was found to increase from 20 % to 40 % by decreasing the PS content in the feed solution from 10 % to 2 % w/v, at a constant stirring speed of 500 rpm. However, the core content could not be increased further, due to the fragile nature of the shell, which appears to be incapable of cementing higher amounts of healing agent.

The TGA traces of the resultant microcapsules in air atmosphere are presented in **Figure 6.4.** Neat PS exhibits a mass loss of ~98 % at 500°C. The thermal decomposition of PS reportedly occurs in a single step via unzipping reaction, while polybenzoxazines exhibit a bimodal mass loss distribution centered at 448 and 558 °C [154]. Similar decomposition behavior was observed in all the encapsulated microcapsules, suggesting polymerization of the C-a during heating.
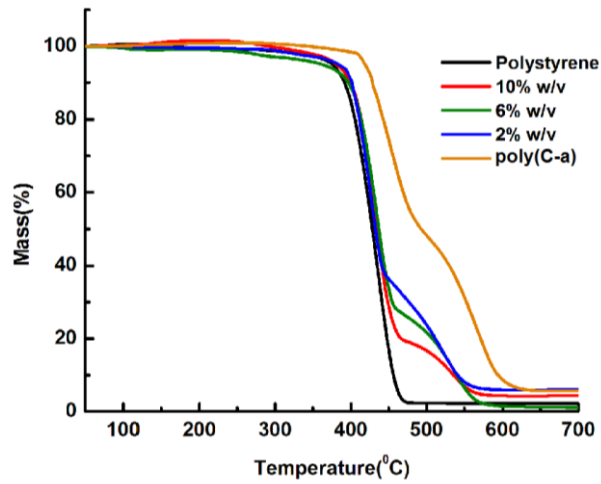
Figure 6.4: TG traces of encapsulated microcapsules prepared by varying the PS concentration in the feed.

To demonstrate the potential of the C-a encapsulated microcapsules in the field of temperature triggered healing, ~5 mg of microcapsules were placed between two stainless steel plates, crushed by manual tapping and placed at ~260°C for 30 mins. Photographs, captured at different stages of experimentation are presented in **Figure 6.5.**
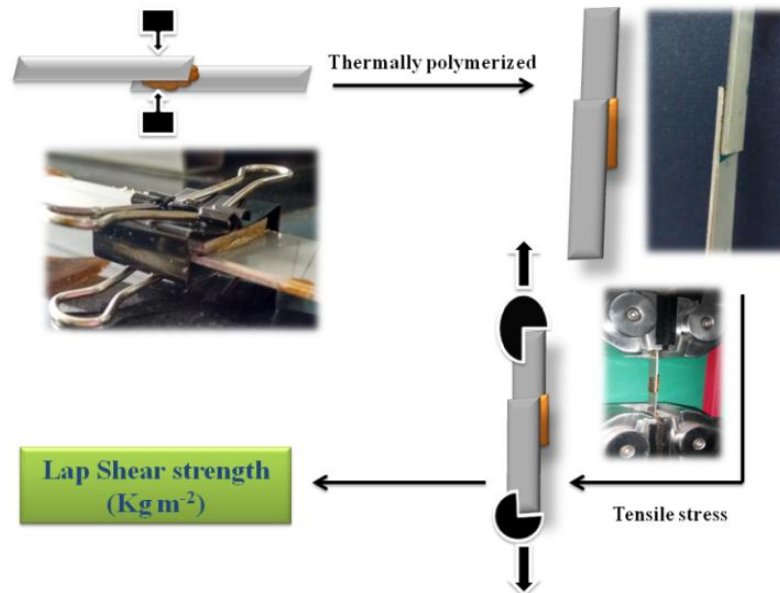
Figure 6.5: Demonstration of temperature triggered healing potential

The steel plates were found to seal completely, and could not be separated by exposure to solvents even for extended periods (72 h).The adhesive ability of the microcapsules encapsulating benzoxazine was quantified by evaluating the lap shear strength (LSS) using ASTM D1002 standard. The average values of lap shear strength exhibited by the samples are tabulated in **Table 6.2**.

Table 6.2: Lap shear strength of polystyrene microcapsules

Concentration of PS in feed solution (%w/v)	Core content (%)	LSS (kgcm^{-2})
2	38 ±2.7	28.04±1.9
6	31 ± 2.1	20.49±2.7
10	19 ± 3.1	16.05±2.1

6.3.2. Microencapsulation of cardanol aniline benzoxazine (C-a) in interfacially engineered cross-linked epoxy
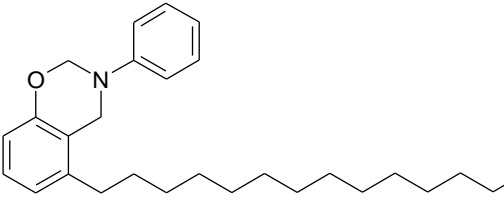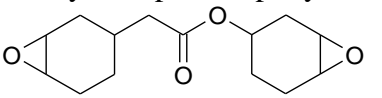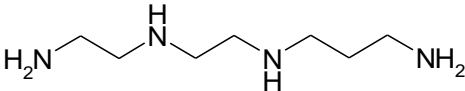
The conventional in-situ polymerization technique involves the formation of the encapsulating shell, essentially in the dispersion medium. For example, in the most commonly reported urea-formaldehyde (UF) microencapsulation process, the monomers, namely urea and formaldehyde react in the aqueous phase to form a low molecular weight prepolymer. With increasing molecular weight of the prepolymer, deposition occurs at the healant-water interface and the cross-linking process continues to form the microcapsule shell wall[227]. The smooth inner surface of the shell basically results from the deposition of low molecular weight prepolymer at the interface while the prepolymer is still soluble. The roughness observed on the outer shell surface result from the precipitation of higher molecular weight prepolymer formed in the aqueous solution, which subsequently aggregate and deposit on the capsule surface[240].

On the other hand, in the present study, epoxy microcapsules were prepared by the preferential reaction of the epoxy resin with TETA at the silicone-benzoxazine interface. The Hoy's solubility parameter(δ) of epoxy, TETA and benzoxazine have been calculated based on the group contribution models of Hoy[241] and the values are reported in **Table 6.3.** As a first approximation, and in the absence of strong interactions such as hydrogen bonding, solubility can be expected if $\delta 1 - \delta 2$ is less than 1.7-2.0 but not if appreciably larger. The easiest way to determine δ of a known structure is by the use of molar attraction constants E.

$$\delta = \frac{\rho \sum E}{M}$$ ....(6.2)

Where E values are summed over the structural configuration, with molecular weight, M and density ρ.

Table 6.3: Density, Molar attraction constants and Solubility parameter

Sample	Density (g ml^{-1})	Molar attraction constant, E, (cal cm^3)$^{1/2}$ mole$^{-1)}$	Solubility parameter(δ) cal$^{1/2}$cm$^{3/2}$ mL^{-1}
Cardanol-aniline benzoxazine	1.0	3739.5	9.0
Cycloaliphatic epoxy	1.1	2068.0	9.0
Triethylenetetramine	0.9	1602.0	10.8

133

It can be seen that the solubility parameter of cycloaliphatic epoxy, benzoxazine and TETA are in the same range, i.e. 9.0, 9.0 and 10.8 $cal^{1/2} cm^{3/2} mL^{-1}$ respectively. It was not possible to ascertain the Hoys parameter for polydimethylsiloxane in view of its inorganic-organic hybrid nature, however the Hansen solubility parameter of TETA (22.7 $MPa^{1/2}$)[66] is markedly higher than that of PDMS (14.9 $MPa^{1/2}$)[215, 242].This difference in miscibility results in their existence as phase separated droplets under agitation. To verify the same the optical images of epoxy-PDMS, benzoxazine-PDMS and epoxy-benzoxazine-PDMS mixtures were captured, where the presence of droplets in the medium is clearly indicative of its immiscibility **(Figure 6.6).**
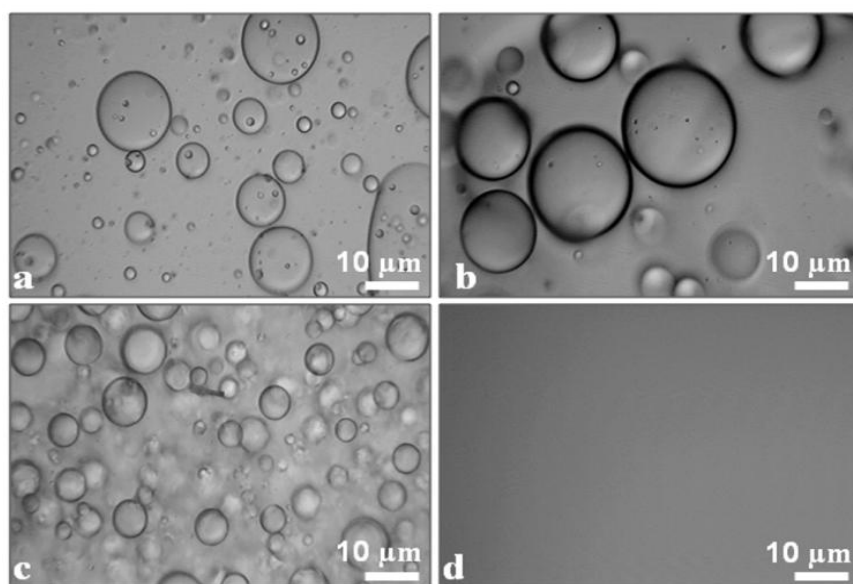
Figure 6.6: Optical images of a) epoxy-PDMS, b) epoxy-benzoxazine-PDMS mixtures c) benzoxazine-PDMS and d) epoxy-benzoxazine.

Preliminary studies were performed to arrive at the optimal reaction conditions, especially reaction time and temperature. For successful encapsulation, the rate of reaction between the epoxy and amine should exceed the rate of molecular diffusion[243]. The reaction condition should be tuned so as to allow the curing process to proceed at the reactive interface till complete exhaustion of the epoxy and

amine thereby leading to the formation of a stable cross-linked shell around the unreacted benzoxazine core. The curing behavior of the cycloaliphatic epoxy resin in the presence of TETA, as established using non-isothermal calorimetry, is presented in **Figure 6.7**[244].
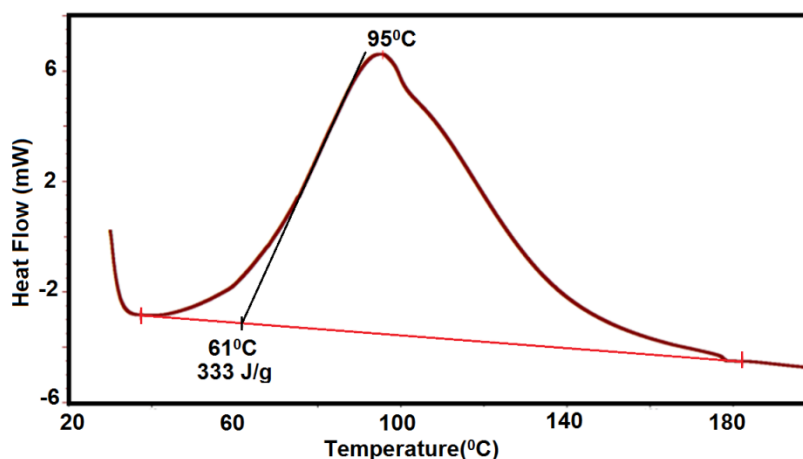
Figure 6.7: Curing profile of epoxy resin

It can be seen that the exothermic curing process initiates at 61°C and reaches a peak at 96°C. On the basis of this curing profile, studies on encapsulation were performed at temperatures as low as 60°C. However, when the reaction medium was maintained at T <65°C, complete curing necessitated prolonged periods (~36 h), which was too long to be of any practical significance. The rate of the curing reaction increased significantly with increasing temperature and free flowing microcapsules could be obtained within 10 h at 70°C. Further increase in temperature was impractical in view of the strong vapor pressure-temperature dependence of TETA[245], which led to significant vaporization of the amine, thereby leading to the formation of partially cured and tacky microcapsules. In view of the above, the effects of other operating parameters were performed while maintaining the reaction medium at 70°C.

The FT-IR of benzoxazine monomer, epoxy resin and cured microcapsules is presented in **Figure 6.8.** Characteristic band at 915 cm⁻¹ associated with the stretching of C-O due to oxirane ring is visible in the FTIR spectra of liquid epoxy resin[246]. The absence of this absorption and the peaks confirming the structure of benzoxazine in the FTIR spectra of microcapsule indicates successful encapsulation of the benzoxazine monomer in cross linked epoxy shell.
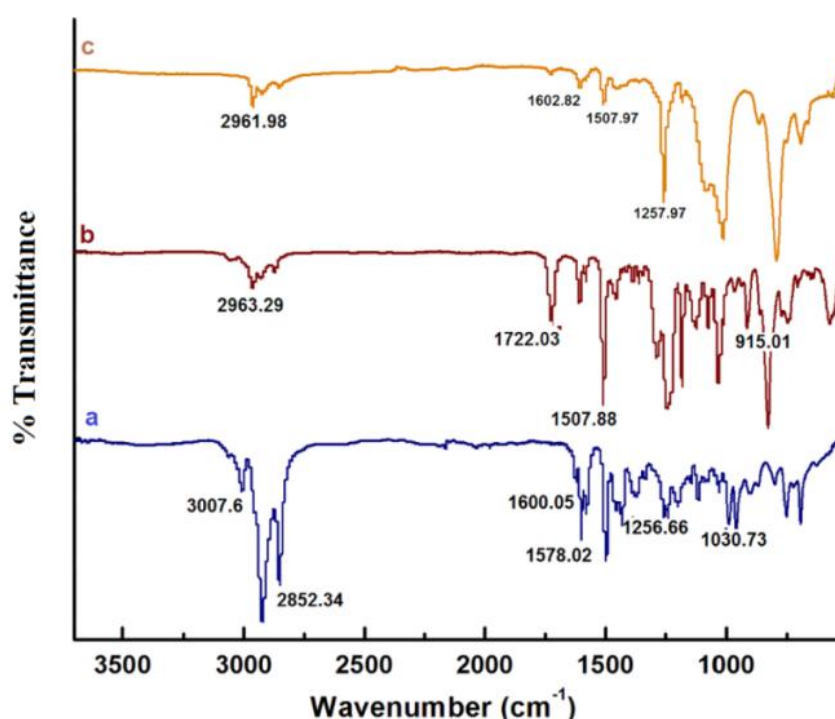
Figure 6.8: FT-IR spectra of a) C-a, b) epoxy resin and c) microcapsules

6.3.3.1 Effect of stirring speed on particle size distribution and morphology

C-a was encapsulated in interfacially engineered cross-linked epoxy shell to form microcapsules, pale yellow in color, the SEM images of a representative batch being presented in **Figure 6.9**. The thickness of the shell wall was found to be ~4.1μ, as can be seen in the SEM images of broken microcapsules **(Figure 6.9, Inset).**

136
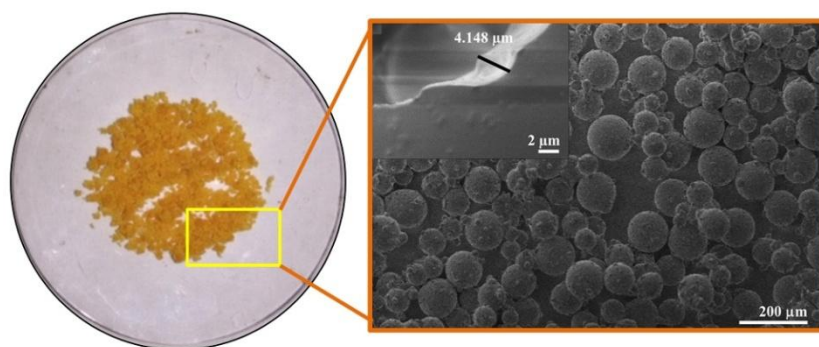
Figure 6.9: SEM image of C-a encapsulated in cross-linked epoxy shell. Inset shows the magnified image of a broken microcapsule indicating thickness of its shell wall

The SEM images of the microcapsules prepared under varying stirring speeds are presented in **Figure 6.10** and the particle size distribution is presented in **Figure 6.11.**
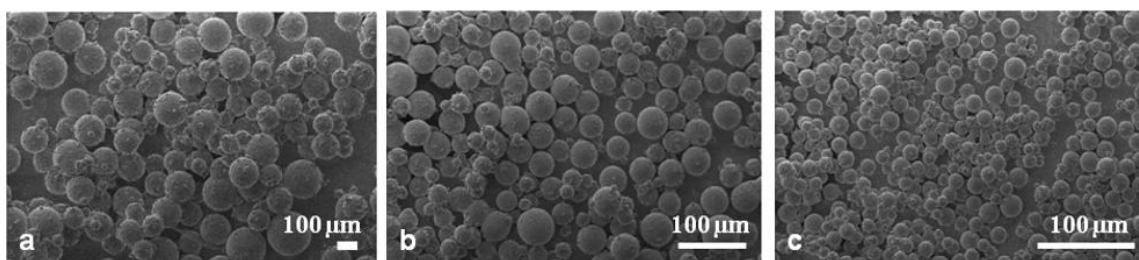
Figure 6.10: Effect of stirring speed on the surface morphology of microcapsules a) 500 b) 600 and c) 700 rpm

It is interesting to note that the high viscosity of the silicone oil employed for the purpose is proficient in stabilizing the suspended epoxy-benzoxazine micro-droplets, thereby abating the necessity of a suspending agent[236]. As expected, increasing the rate of stirring led to a shift in the average particle size towards lower dimensions, which could be attributed to the extensive shearing of the large oily droplets into smaller microspheres.
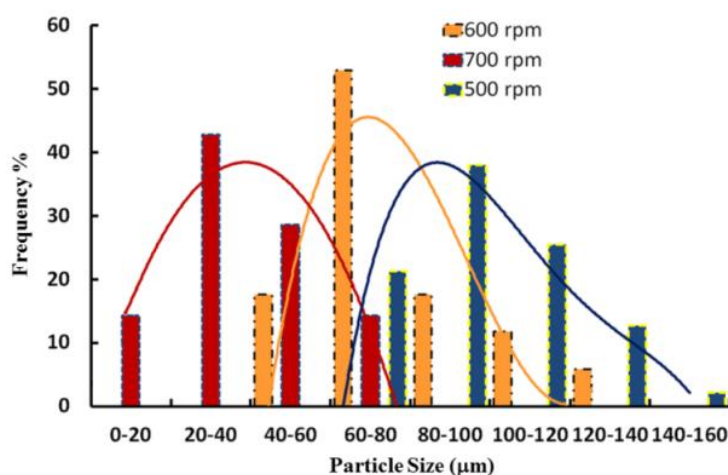
Figure 6.11: Effect of stirring speed on the average particle size distribution of microcapsules.

Among the experimental parameters: agitation rate, temperature, surfactant type and concentration, hydrodynamics, viscosity and interfacial tension of the media are primary influential parameters on the microcapsule dimension. Stirring speed, particularly, defines the equilibrium between shear forces and interfacial tension of the discrete oil droplets[247]. It was observed that free flowing microcapsules could not be obtained upon lowering the stirring speeds to <500 rpm (**Figure 6.12**).
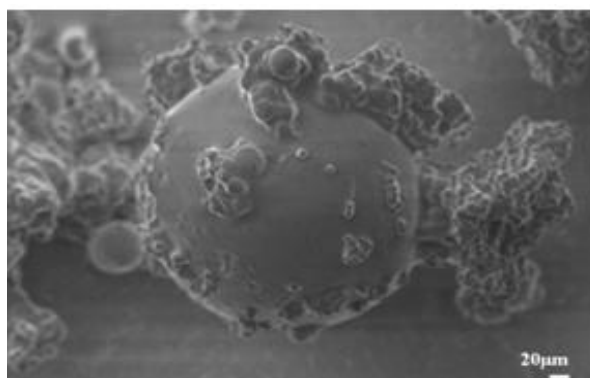
Figure 6.12: SEM image of microcapsules prepared at 400 rpm

Increasing the stirring speed to >700 rpm is expected to lead to the formation of microcapsules of significantly lower dimensions to be of any practical value. Under

optimal reactions conditions, i.e. stirring speed of 600 rpm, reaction temperature of 70°C and C-a: (2.3:1), spherical microcapsules were obtained.

6.3.3.2 Effect of concentration of encapsulating polymer

Core content, refers to a quantitative estimate of the polymerizable fraction actually available in the microcapsules, which in the present context, was quantified as the ratio of heat of curing of encapsulated benzoxazine to that of the neat monomer[248]. In view of the ring strain associated with oxazine ring, polymerizes through thermally activated ring opening polymerization and the DSC traces obtained during controlled heating are presented in **Figure 6.13.**
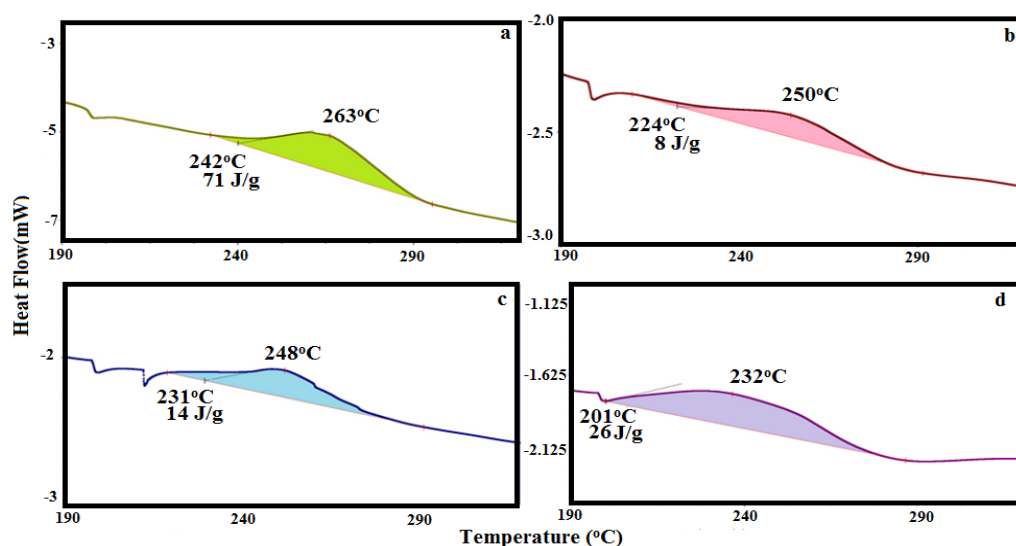
Figure 6.13: DSC traces of a) C-a and epoxy encapsulated benzoxazine microcapsules prepared using C-a: Epoxy ratio of b) 1:1, c) 1.5:1 and d) 2.3:1

The DSC trace of cured epoxy microsphere prepared in the absence of benzoxazine has been presented in the **Figure 6.14**.
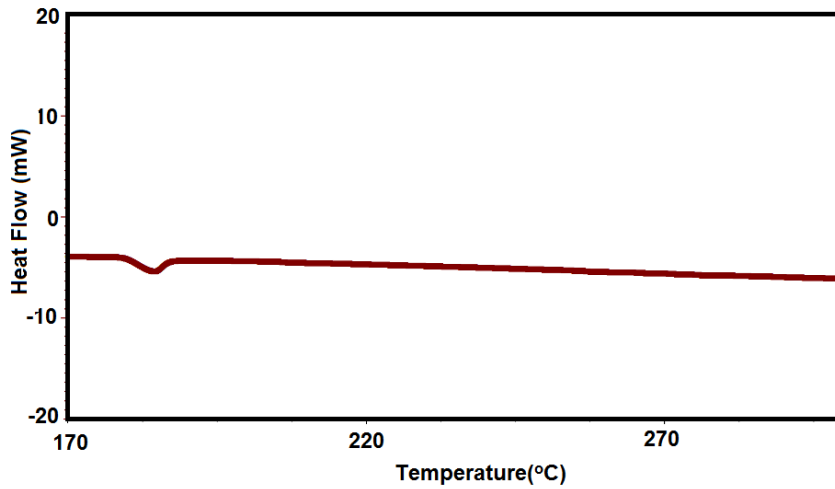
Figure 6.14: Curing profile of cured epoxy microcapsules prepared in the absence of benzoxazine

As expected, the exotherm associated with the curing of benzoxazine cannot be observed in the DSC trace. The core content of benzoxazine filled microcapsules was quantified as per the procedure reported previously and the results are tabulated in **Table 6.4**[248].

$$\text{Core content}(\%) = \frac{\Delta H_{curing,encapsulated\ C-a}}{\Delta H_{curing,C-a}} \times 100$$ .... (6.3)

Where, enthalpy of curing of neat C-a ($\Delta H_{curing,\ C-a}$) is 71.1 ± 1.8 J/g.

Table 6.4: Effect of C-a: Epoxy ratio on the core content of microcapsules

C-a: Epoxy ratio (%w/w)	ΔH_{curing} (J/g)	Core content (%)
1:1	8.5	11.9
1.5:1	14.1	19.8
2.33:1	26.3	36.0

The core content of the benzoxazine filled microcapsule increased from 12 to 37 % as the weight fraction of epoxy in the feed solution was lowered from 50 to 30 %w/w while maintaining a constant stirring speed of 600 rpm.

140

Although, attaining larger core content is a vital target of any encapsulation process, it was not possible to increase the core content further, probably due to high surface energy of microcapsules, which led to their agglomeration on increasing the benzoxazine content in the feed[242]. It was interesting to observe a lowering in the onset of curing behavior as the composition of the feed solution (epoxy resin: benzoxazine) was varied from 1:1 to 2.33:1. To gain further insight into this aspect, benzoxazine curing was also studied in the presence of liquid epoxy resin.
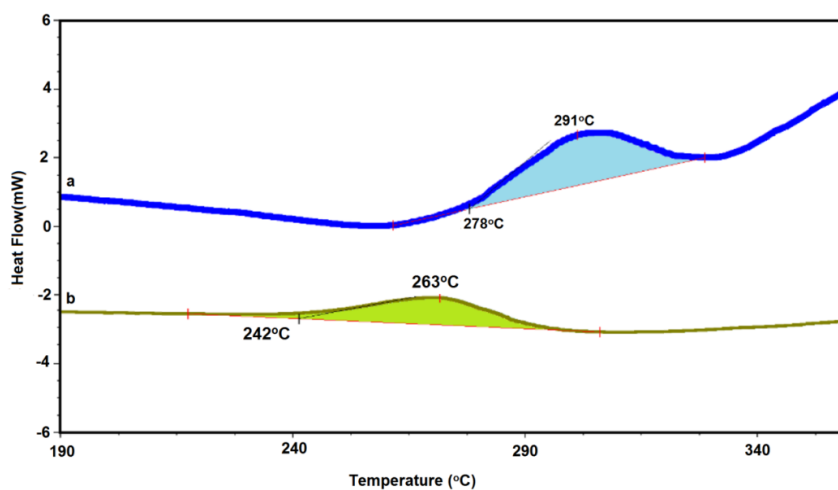
Figure 6.15: Curing profile a) C-a in presence of epoxy resin, b) neat C-a

Interestingly, the curing exotherm was found to shift to higher temperature, as shown in the **Figure 6.15**. These studies confirm that the lowering of curing temperature in the present study could be credited to the interaction of C-a monomer with hydroxyl functionalities, which in turn resulted due to the nucleophilic attack of amine on oxirane rings of epoxy resin as per the reaction depicted in **Figure 6.16.** Acidic functionalities[249] along with allylic[250] and methylol[251] etc. reportedly play an active role in catalyzing the polymerization of benzoxazines. Our studies indicate that aliphatic alcohols, although less acidic, are also capable of lowering of T_{onset} temperature of C-a ($T_{onset} = 220°C$) substantially to 179°C.
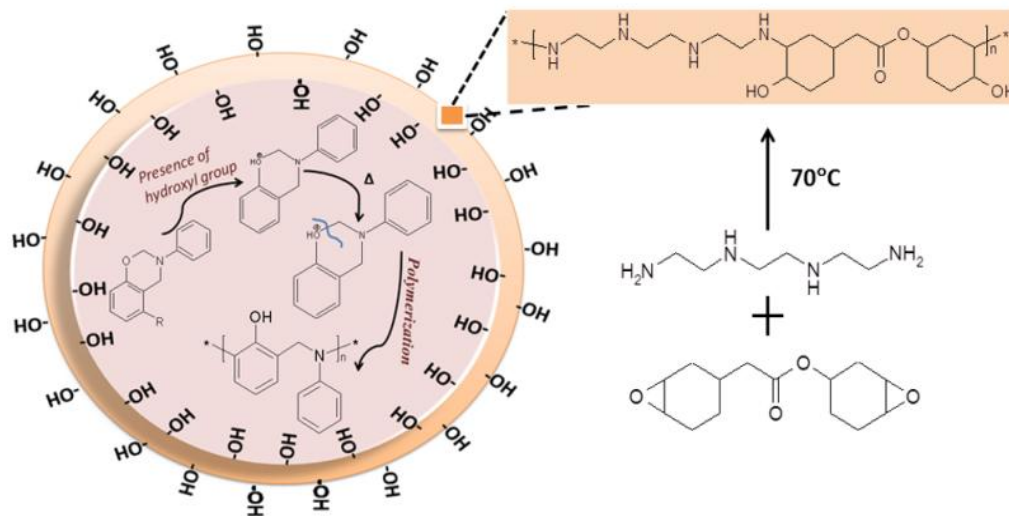
Figure 6.16: Interaction of hydroxyl groups on the inner surface with the

encapsulated benzoxazine

TG-DTG traces of C-a, before and after encapsulation in epoxy shells under air atmosphere is presented in the **Figure 6.17.** It can be seen that the polybenzoxazine formed as a result of temperature induced curing, undergoes oxidative degradation at 310°C. Encapsulation of benzoxazine in epoxy shell led to a substantial decrease in the curing temperature to 179°C, however the onset degradation temperature remained practically unaltered.
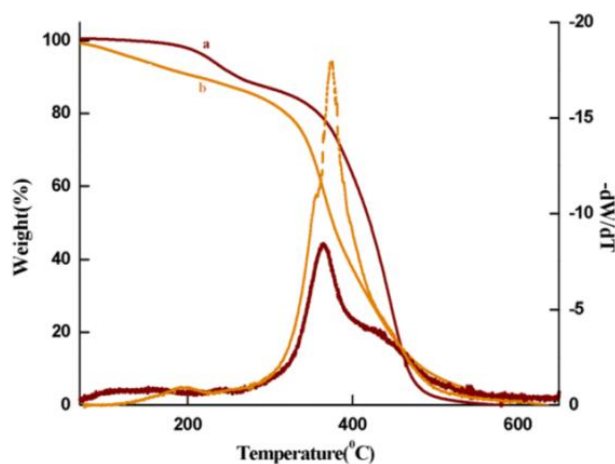
Figure 6.17: TGA traces of a) C-a b) epoxy microcapsules encapsulating C-a

142

The adhesive ability of the microcapsules encapsulating benzoxazine was quantified by evaluating the lap shear strength (LSS) using stainless steel coupons. Cardanol based benzoxazines, have been reported to exhibit LSS of 20-30 $kgcm^{-2}$ at 150°C, which advocate their calibre as healing monomers in mendable compositions[252]. The representative load–displacement curve is presented in **Figure 6.18**.
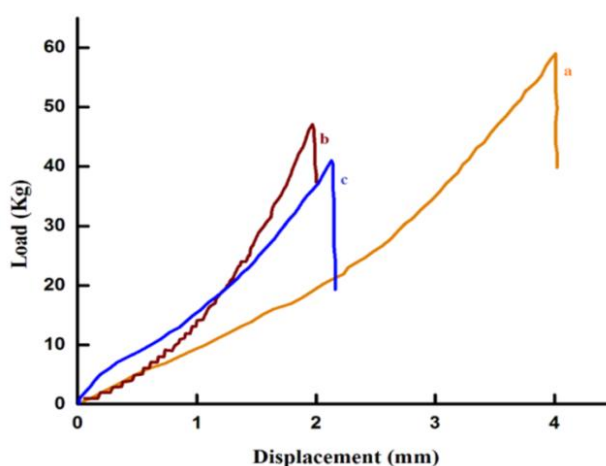
Figure 6.18: Representative load-displacement curve obtained during Lap shear strength testing of microcapsules with core content a) 37 %, b) 19.8% and c) 11.9 %.

The average values of lap shear strength exhibited by the samples are tabulated in **Table 6.5**.

Table 6.5: Lap shear strength of microcapsules with different core content

C-a: Epoxy ratio (%w/w)	Core content (%)	LSS ($kgcm^{-2}$)
1:1	11.9	13.5 ± 3
1.5:1	19.8	16.0 ± 1
2.33:1	36.0	25.3 ± 2

Subsequent to the curing of the C-a released from the microcapsules, the plates could not be separated by exposure to solvents like DMF and toluene, even for extended periods (72 h).The curing of C-a by thermally activated ring opening polymerization

results in the formation of >N- and –OH functionalities which are capable of exhibiting extensive H-bonding with the contact surface as shown in **Figure 6.19**, thereby rendering excellent adhesive properties.
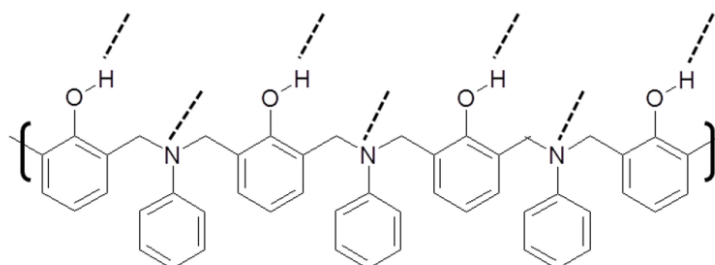
Figure 6.19: Functional groups in polybenzoxazine involved in H-bonding with the contact surface

Chapter 7
Summary & Conclusions
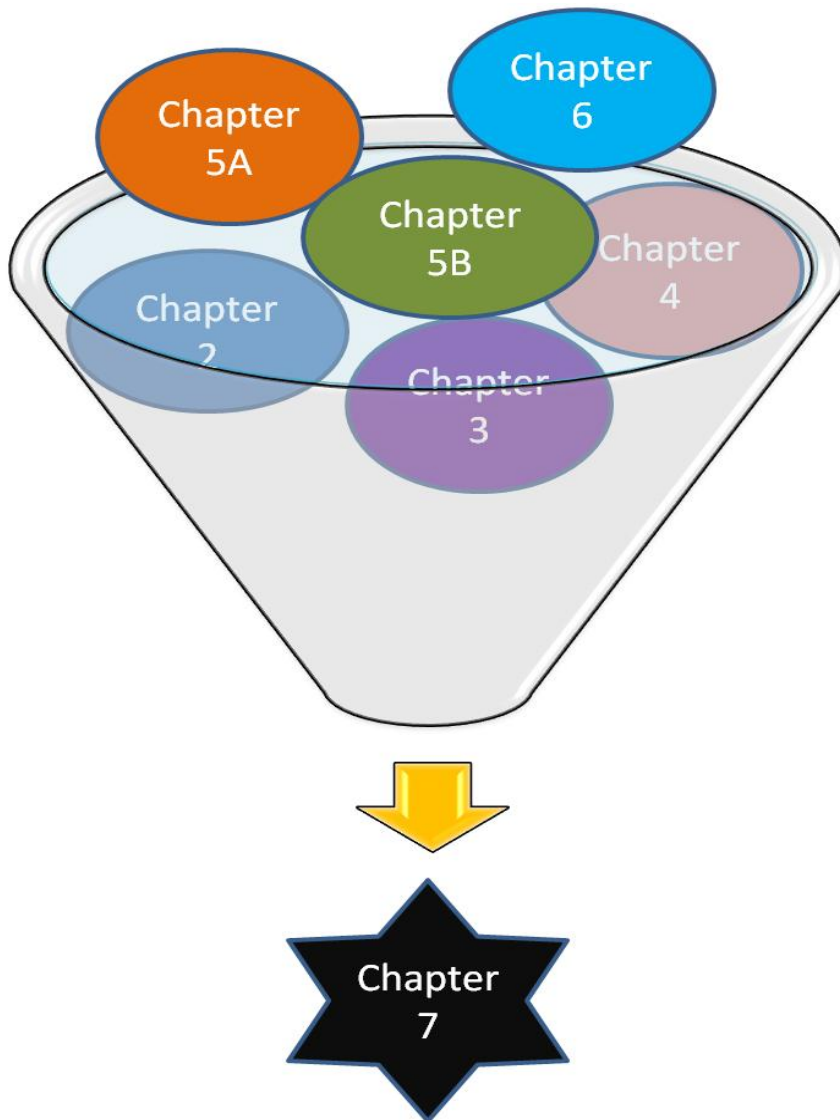
Polybenzoxazines belongs to a sub class of phenolic thermosetting resins and are bridging the gap between maleimides and epoxies. However, they are associated with a major drawback i.e., its high curing temperature, which restricts its use for practical applications. In this thesis, we have attempted to reduce the curing temperature of bio-based benzoxazines by making structural modifications in the main chain and by using curing accelerators. Benzoxazine monomers were integrated with functionalities which are intrinsically capable of lowering the polymerisation temperature and their effect on thermal and adhesive characteristics has been studied. Alternative renewable feed-stocks were explored to manage the increasing demands of petro-based chemicals.

In chapter 2, the feasibility of Microwave assisted synthesis (MAS) towards synthesis of benzoxazine monomers has been demonstrated. To ensure rapid reaction under microwave irradiation, IR active diamines were synthesised via condensation reaction of para-aminobenzoic acid (PABA) and poly(ethylene glycol)s of varying chain length, using p-TSA as a catalyst to yield amine terminated poly(ethylene glycol)s (ATPEGs). Cardanol, an agricultural waste, was chosen as a source of phenol, which undergoes microwave assisted Mannich like condensation with synthesised microwave active amines, resulting in telechelic polymers endcapped with benzoxazine moieties. Structural characterisation of the monomers was performed using FT-IR and ^{1}H-NMR. The curing behaviour was investigated using non-isothermal DSC, which revealed that the temperature associated with curing process is directly proportional to the chain length of the diamine. Rheological studies suggests that the viscosity of the benzoxazine resins was sufficiently low (C-ATPEG200 ~ 7.28 Pa.s at 30°C) to permit solvent less processing of the resin and further decreases

upon increasing the flexible segment of the telechelic polymer. The cured resins exhibited high thermal stability ($T_{5\%}$ >300 °C) and excellent lap shear strength (C-ATPEG200 = 38±0.29 kgcm^{-2}). The studies indicate that performing the synthesis of benzoxazine under microwave irradiation improves the sustainability of the process and accelerates the Mannich condensation resulting in shorter reaction times. The performance of the resin hence obtained remains unaffected in terms of end properties, processibility and applications.

Chapter 3 deals with the synthesis and chracterisation of sustainable bis-benzoxazine monomers containing amide linkages where the amine co-reactants are derived from microwave assisted tertiary recycling of PET. For this purpose, microwave assisted aminolytic depolymerization of polyethylene terephthalate (PET) in the presence of ethylene diamine (ED) was performed to yield terephthalamides which were used to prepare benzoxazine containing amide linkages. The effect of temperature and the molar ratio of PET: ED on the extent of PET conversion and relative percentage fraction of α,ω-aminoligo(ethylene terephthalamide) (AOET) and bis-(amino-ethyl) terephthalamide (BAET) was studied. Complete conversion of PET could be effected by performing the reaction at temperatures close to the melting point of PET, at PET:ED:: 1:6. Increasing the concentration of ED further, did not affect the product composition appreciably. The amine terminated terephthalamides were used to synthesize benzoxazine resins containing amide linkages in the presence of cardanol as the phenolic component using Mannich type condensation. The resins were characterized using FT-IR and ^{1}H-NMR and the curing behaviour was investigated by non-isothermal DSC. The temperature associated with the curing of C-BAET (T_{peak} = 214°C) was relatively lower than C-AOET (T_{peak} = 238°C). The cured resins exhibited

high thermal stability ($T_{5\%} > 300$ °C) and excellent lap shear strength (C-AOET = 28 kgcm^{-2}, C-BAET =38kgcm^{-2}). The study indicates that increasing oxazine functionality and presence of secondary interactions (hydrogen bonding) within the monomer alleviate the curing profile of the resin and leads to improvement in thermal and adhesive characteristics.

Further in chapter 4, we demonstrate a solventless method to integrate urea linkages in polybenzoxazines through functionalization of a model compound containing urea linkages with amine terminals and utilizing the same as a co-reactant for the preparation of bis-benzoxazine monomer containing urea linkages. The amine terminated model compound was synthesised from solventless reaction of 4,4'-methylenebis(phenyl isocyanate) (MDI) with excess ethylene diamine at room temperature. Cardanol undergoes Mannich type condensation with amine (AMDI) and paraformaldehyde, resulting in a monomer comprising of urea linkages with terminal oxazine moieties. The structural characterization of the amine and the monomer were performed using FT-IR and ^{1}H-NMR. The curing behaviour was investigated using non-isothermal DSC, which reveal that the temperature associated with the curing of synthesized monomer is ~202°C. Bidentate hydrogen bonding present in the urea linkages was credited for the observed reduction in polymerization temperature. Rheological studies suggest that initially the flowability of the monomer improves with the increase in the temperature due to reduced hydrogen bonding in the monomer and the gelation occurs at ~159°C. The cured resins exhibit high thermal stability ($T_{5\%}$ >300 °C) and excellent lap shear strength 71±0.29 kgcm^{-2}.

In chapter 5, the accelerating ability of metal organic frameworks (MOF-5) on the ring opening polymerisation of cardanol based benzoxazine(C-a) was systematically

147

studied. The presence of MOF-5 was found to decrease the curing temperature of neat benzoxazine from 263 to 229 °C (12.6 % decrease). Our studies indicate that Zn_4O nodes of atomic precision, which are available throughout the surface of the framework, are responsible for the decrease in the curing temperature. Curing studies were also performed in the presence of another zinc based metal organic framework, (ZIF-8) which exhibits high surface area but differs around the chemical environment around the central zinc atom. The potential of Cu(BDC).DMF and HKUST-1 towards lowering of curing temperature was also explored. The extent of reduction in the curing temperature was found to be much higher in the case of MOF-5. KAS method was used to determine the activation energy associated with curing, which was found to decrease from 98 kJ/mol (neat resin) to 58 kJ/mol for formulation containing MOF-5 (5%w/w). The cured resins obtained in the presence of MOF-5 exhibited relatively high thermal stability ($T_{5\%} = 416°C$) as compared to the neat cross linked resin ($T_{5\%} = 345°C$). Our studies clearly highlight the enormous scope of metal organic frameworks as curing accelerators for benzoxazine resins mandating high temperature.

In chapter 6, the accelerating ability of transition metal stearates on the ring opening polymerisation of cardanol based benzoxazine(C-a) has been systematically studied. Inclusion of 10 %w/w zinc(II) stearate was found to decrease the curing temperature of neat benzoxazine from ~263 to ~202 °C (23% decrease). This exceptional accelerating ability was attributed to the presence of acidic Zn_4O nodes in addition to the long alkyl chain of stearate, which helps in the dispersion of the accelerator within the resin. KAS method was used to determine the activation energy of polymerization, which was found to decrease from 98 kJ/mol (neat resin) to 51 kJ/mol for formulation

containing zinc(II) stearate (10 %w/w). The cured resins obtained in the presence of zinc(II) stearate exhibited relatively high thermal stability ($T_{5\%} = 351°C$) as compared to the neat cross linked resin ($T_{5\%} = 390°C$).

In chapter 7, physical and chemical microencapsulation of cardanol based benzoxazine monomer in different shell walls has been successfully demonstrated for temperature triggered healing applications. The low viscosity of cardanol facilitated the monomer as a healing agent which was subsequently encapsulated in fragile polystyrene (PS) containers by solvent evaporation technique. Microcapsules with dimensions ranging from 75-86 µm could be prepared by varying the stirring speed from 600-400 rpm. By decreasing the concentration of PS in the feed solution, it was possible to increase the core content as high as 40% (w/w).

The resin was encapsulated in cross-linked epoxy microcapsules engineered interfacially. Reaction parameters, especially benzoxazine: epoxy ratio and stirring speed were found to have a pronounced effect on the core content and particle size distribution of the microspheres. Under optimal conditions, i.e. stirring speed of 600 rpm, reaction temperature of 70°C and Bz-C:Epoxy::2.33:1, spherical microcapsules were obtained with a core content of ~37 %. The presence of hydroxyl groups formed as a result of epoxy curing was found to reduce the onset of curing temperature from 220 to 179 °C. We believe that in view of the enormous scope in modifying the structure of benzoxazines, low temperature self-healing systems can be devised in the future, which can open up novel opportunities in this field.

The work resulted in the following conclusions:

- Use of cardanol as a source of phenol allows solventless synthesis and processing of benzoxazine monomers.

- Microwave synthesis is a sustainable tool for the preparation of benzoxazine monomers which significantly reduces the reaction time without adversely affecting the yield of the reaction.

- Adhesive strength of benzoxazine monomers is strongly dependant on the Hydrogen bonding functionalities (amide, urea, hydroxyl).

- Curing profile shifts towards lower temperature as the functionality of benzoxazine monomer increases.

- The curing profile of the resin can be further shifted to lower temperature using curing accelerators which exhibit acidic moieties. The extent of acceleration is proportional to the amount of accelerator used.

- Benzoxazine monomer can be microencapsulated to bestow healing functionalities to a polymer resin. Operating parameters, namely stirring speed and feed concentration can be varied to obtain microcapsules of varying dimensions and core content .

- Dimensions of microcapsules of benzoxazine monomer decreases with increase in stirring speed. Core content of the microcapsules increased with decrease in concentration of shell wall material.

Recommendations for future work

1. Efforts should be made towards designing of curing accelerators which are more acidic but do not affect the end performance of the benzoxazines material.

2. The synthesised resin, in view of their improved adhesive strength, can be used as a matrix for fibre reinforced composites. Detailed studies on fibre reinforced composites need to be taken up in the future.

References

[1] F.W. Holly, A.C. Cope, Condensation Products of Aldehydes and Ketones with o-Aminobenzyl Alcohol and o-Hydroxybenzylamine, Journal of the American Chemical Society 66(11) (1944) 1875-1879.

[2] W.J. Burke, 3,4-Dihydro-1,3,2H-Benzoxazines. Reaction of p-Substituted Phenols with N,N-Dimethylolamines, Journal of the American Chemical Society 71(2) (1949) 609-612.

[3] W. Burke, C. Weatherbee, 3, 4-Dihydro-1, 3, 2H-Benzoxazines. Reaction of Polyhydroxybenzenes with N-Methylolamines1, Journal of the American Chemical Society 72(10) (1950) 4691-4694.

[4] W. Burke, C.W. Stephens, Monomeric products from the condensation of phenol with formaldehyde and primary amines, Journal of the American Chemical Society 74(6) (1952) 1518-1520.

[5] W. Burke, M.J. Kolbezen, C.W. Stephens, Condensation of Naphthols with Formaldehyde and Primary Amines1, Journal of the American Chemical Society 74(14) (1952) 3601-3605.

[6] W. Burke, R.P. Smith, C. Weatherbee, N, N-bis-(hydroxybenzyl)-amines: synthesis from phenols, formaldehyde and primary amines1, Journal of the American Chemical Society 74(3) (1952) 602-605.

[7] W. Burke, K. Murdock, Condensation of hydroxyaromatic compounds with formaldehyde and primary aromatic amines, Journal of the American Chemical Society 76(6) (1954) 1677-1679.

[8] W.J. Burke, E.M. Glennie, C. Weatherbee, Condensation of Halophenols with Formaldehyde and Primary Amines1, The Journal of Organic Chemistry 29(4) (1964) 909-912.

[9] W. Burke, J. Bishop, E.M. Glennie, W. Bauer Jr, A new aminoalkylation reaction. Condensation of phenols with dihydro-1, 3-aroxazines1, The Journal of Organic Chemistry 30(10) (1965) 3423-3427.

[10] H.P. Higginbottom, Polymerizable compositions comprising polyamines and poly (dihydrobenzoxazines), US4501864 A, 1985.

[11] H.P. Higginbottom, M.F. Drumm, Aqueous dispersions of polyamines and poly (dihydrobenzoxazines), US4507428 A, 1985.

[12] H.P. Higginbottom, M.F. Drumm, Process for deposition of resin dispersions on metal substrates, US4557979 A, 1985.

[13] G. Reiss, J. Schwob, G. Guth, M. Roche, B. Lande, In Advances in Polymer Synthesis; Culbertson, BM; McGrath, JE, Eds, Plenum: New York, 1985.

[14] E.T. Turpin, D.T. Thrane, Self-curable benzoxazine functional cathodic electrocoat resins and process, US4719253 A, 1988.

[15] X. Ning, H. Ishida, Phenolic materials via ring-opening polymerization: Synthesis and characterization of bisphenol-A based benzoxazines and their polymers, Journal of Polymer Science Part A: Polymer Chemistry 32(6) (1994) 1121-1129.

[16] H. Ishida, H.Y. Low, A study on the volumetric expansion of benzoxazine-based phenolic resin, Macromolecules 30(4) (1997) 1099-1106.

[17] X. Liu, Y. Gu, Study on the volumetric change during ring-opening polymerization of benzoxazines, Acta Polymerica Sinica 5 (2000) 019-029.

[18] X. Liu, Y. Gu, Study on the volumetric expansion of benzoxazine curing with different catalysts, Journal of Applied Polymer Science 84(6) (2002) 1107-1113.

[19] H. Ishida, D.J. Allen, Physical and mechanical characterization of near-zero shrinkage polybenzoxazines, Journal of Polymer Science Part B: Polymer physics 34(6) (1996) 1019-1030.

[20] S.B. Shen, H. Ishida, Development and characterization of high-performance polybenzoxazine composites, Polymer composites 17(5) (1996) 710-719.

[21] H. Ishida, Chapter 1 - Overview and Historical Background of Polybenzoxazine Research, Handbook of Benzoxazine Resins, Elsevier, Amsterdam, 2011, pp. 3-81.

[22] G. Wisanrakkit, J.K. Gillham, The glass transition temperature as a parameter for monitoring the isothermal cure of an amine-cured epoxy system, ACS Publications1990.

[23] K. Pang, J. Gillham, Anomalous behavior of cured epoxy resins: density at room temperature versus time and temperature of cure, Journal of Applied Polymer Science 37(7) (1989) 1969-1991.

[24] Y.K. Shin, Flexible bismaleimide, benzoxazine, epoxy-anhydride adduct hybrid adhesive, US9296928 B2, 2016.

[25] S. Rimdusit, H. Ishida, Development of new class of electronic packaging materials based on ternary systems of benzoxazine, epoxy, and phenolic resins, Polymer 41(22) (2000) 7941-7949.

[26] H. Ishida, Process for preparation of benzoxazine compounds in solventless systems, US5543516 A, 1996.

[27] J. Liu, Synthesis, characterization, reaction mechanism and kinetics of 3, 4-dihydro-2H-1, 3-benzoxazine and its polymer, *Thesis,* Case Western Reserve University, 1995.

[28] X. Ning, H. Ishida, Phenolic materials via ring-opening polymerization of benzoxazines: Effect of molecular structure on mechanical and dynamic mechanical properties, Journal of Polymer Science Part B: Polymer physics 32(5) (1994) 921-927.

[29] H. Ishida, J.-P. Liu, Chapter 2 - Benzoxazine Chemistry in Solution and Melt, in: H.I. Agag (Ed.), Handbook of Benzoxazine Resins, Elsevier, Amsterdam, 2011, pp. 85-102.

[30] J. Dunkers, E. Zarate, H. Ishida, Crystal structure and hydrogen-bonding characteristics of N, N-bis (3, 5-dimethyl-2-hydroxybenzyl) methylamine, a benzoxazine dimer, The Journal of Physical Chemistry 100(32) (1996) 13514-13520.

[31] X. Liu, Y. Gu, Effects of molecular structure parameters on ring-opening reaction of benzoxazines, Science in China Series B: Chemistry 44(5) (2001) 552-560.

[32] R. Huerta, R.A. Toscano, I. Castillo, 1, 4-Bis (8-tert-butyl-6-methyl-4H-1, 3-benzoxazin-3-yl) benzene, Acta Crystallographica Section E: Structure Reports Online 62(7) (2006) 02938-02940.

[33] S. Ranjith, S. Thenmozhi, R. Manikannan, S. Muthusubramanian, A. Subbiahpandi, 3, 3′-(p-Phenylene) bis (3, 4-dihydro-2H-1, 3-benzoxazine), Acta Crystallographica Section E: Structure Reports Online 65(3) (2009) 0581-0581.

[34] H. Ishida, Y. Rodriguez, Catalyzing the curing reaction of a new benzoxazine-based phenolic resin, Journal of Applied Polymer Science 58(10) (1995) 1751-1760.

[35] Y.-X. Wang, H. Ishida, Cationic ring-opening polymerization of benzoxazines, Polymer 40(16) (1999) 4563-4570.

[36] J. Dunkers, H. Ishida, Reaction of benzoxazine-based phenolic resins with strong and weak carboxylic acids and phenols as catalysts, Journal of Polymer Science Part A Polymer Chemistry 37(13) (1999) 1913-1921.

[37] J.A. Cid, Y.-X. Wang, H. Ishida, Cationic polymerization of benzoxazine monomers by boron trifluoride complex, Polymers and Polymer Composites(UK) 7(6) (1999) 409-420.

[38] T. Hayakawa, Y. Osanai, K. Niizeki, O. Haba, M. Ueda, The curing reaction of 3-aryl substituted benzoxazine, High Performance Polymers 12(1) (2000) 237-246.

[39] Y.-X. Wang, H. Ishida, Synthesis and properties of new thermoplastic polymers from substituted 3, 4-dihydro-2 H-1, 3-benzoxazines, Macromolecules 33(8) (2000) 2839-2847.

[40] A. Sudo, R. Kudoh, H. Nakayama, K. Arima, T. Endo, Selective formation of poly (N, O-acetal) by polymerization of 1, 3-benzoxazine and its main chain rearrangement, Macromolecules 41(23) (2008) 9030-9034.

[41] P. Chutayothin, H. Ishida, Cationic ring-opening polymerization of 1, 3-benzoxazines: mechanistic study using model compounds, Macromolecules 43(10) (2010) 4562-4572.

[42] Y.L. Liu, J.M. Yu, Cocuring behaviors of benzoxazine and maleimide derivatives and the thermal properties of the cured products, Journal of Polymer Science Part A: Polymer Chemistry 44(6) (2006) 1890-1899.

[43] H.Y. Low, H. Ishida, Structural effects of phenols on the thermal and thermo-oxidative degradation of polybenzoxazines, Polymer 40(15) (1999) 4365-4376.

[44] S. Wirasate, S. Dhumrongvaraporn, D.J. Allen, H. Ishida, Molecular origin of unusual physical and mechanical properties in novel phenolic materials based on benzoxazine chemistry, Journal of applied polymer science 70(7) (1998) 1299-1306.

[45] G. Lligadas, A. Tuzun, J.C. Ronda, M. Galia, V. Cadiz, Polybenzoxazines: new players in the bio-based polymer arena, Polymer Chemistry 5(23) (2014) 6636-6644.

[46] D. Pereira, P. Valentão, J. Pereira, P. Andrade, Phenolics: From Chemistry to Biology, Molecules 14(6) (2009) 2202.

[47] P. Thirukumaran, A. Shakila, S. Muthusamy, Synthesis and characterization of novel bio-based benzoxazines from eugenol, RSC Advances 4(16) (2014) 7959-7966.

[48] P. Thirukumaran, A. Shakila Parveen, M. Sarojadevi, Synthesis and Copolymerization of Fully Biobased Benzoxazines from Renewable Resources, ACS Sustainable Chemistry & Engineering 2(12) (2014) 2790-2801.

154

[49] T. Periyasamy, S.P. Asrafali, S. Muthusamy, New benzoxazines containing polyhedral oligomeric silsesquioxane from eugenol, guaiacol and vanillin, New Journal of Chemistry 39(3) (2015) 1691-1702.

[50] N.K. Sini, J. Bijwe, I.K. Varma, Renewable benzoxazine monomer from Vanillin: Synthesis, characterization, and studies on curing behavior, Journal of Polymer Science Part A: Polymer Chemistry 52(1) (2014) 7-11.

[51] N.K. Sini, J. Bijwe, I.K. Varma, Thermal behaviour of bis-benzoxazines derived from renewable feed stock 'vanillin', Polymer Degradation and Stability 109 (2014) 270-277.

[52] A. Van, K. Chiou, H. Ishida, Use of renewable resource vanillin for the preparation of benzoxazine resin and reactive monomeric surfactant containing oxazine ring, Polymer 55(6) (2014) 1443-1451.

[53] H. Xu, Z. Lu, G. Zhang, Synthesis and properties of thermosetting resin based on urushiol, RSC Advances 2(7) (2012) 2768-2772.

[54] H. Xu, W. Zhang, Z. Lu, G. Zhang, Hybrid polybenzoxazine with tunable properties, RSC Advances 3(11) (2013) 3677-3682.

[55] S. Li, T. Zou, X. Liu, M. Tao, Synthesis and characterization of benzoxazine monomers from rosin and their thermal polymerization, Designed Monomers and Polymers 17(1) (2014) 40-46.

[56] C. Wang, J. Sun, X. Liu, A. Sudo, T. Endo, Synthesis and copolymerization of fully bio-based benzoxazines from guaiacol, furfurylamine and stearylamine, Green Chemistry 14(10) (2012) 2799-2806.

[57] M. Comí, G. Lligadas, J.C. Ronda, M. Galià, V. Cádiz, Renewable benzoxazine monomers from "lignin-like" naturally occurring phenolic derivatives, Journal of Polymer Science Part A: Polymer Chemistry 51(22) (2013) 4894-4903.

[58] B. Lochab, S. Shukla, I.K. Varma, Naturally occurring phenolic sources: monomers and polymers, RSC Advances 4(42) (2014) 21712-21752.

[59] B.S. Rao, A. Palanisamy, Monofunctional benzoxazine from cardanol for bio-composite applications, Reactive and Functional Polymers 71(2) (2011) 148-154.

[60] E. Calo, A. Maffezzoli, G. Mele, F. Martina, S.E. Mazzetto, A. Tarzia, C. Stifani, Synthesis of a novel cardanol-based benzoxazine monomer and environmentally sustainable production of polymers and bio-composites, Green Chemistry 9(7) (2007) 754-759.

[61] S. Mohapatra, G.B. Nando, Cardanol: a green substitute for aromatic oil as a plasticizer in natural rubber, RSC Advances 4(30) (2014) 15406-15418.

[62] C. Voirin, S. Caillol, N.V. Sadavarte, B.V. Tawade, B. Boutevin, P.P. Wadgaonkar, Functionalization of cardanol: towards biobased polymers and additives, Polymer Chemistry 5(9) (2014) 3142-3162.

[63] P. Campaner, D. D'Amico, L. Longo, C. Stifani, A. Tarzia, S. Tiburzio, Chapter 19 - Study of a Cardanol-Based Benzoxazine as Reactive Diluent and Toughening Agent of Conventional Benzoxazines, in: H.I. Agag (Ed.), Handbook of Benzoxazine Resins, Elsevier, Amsterdam, 2011, pp. 365-375.

[64] O. A. Attanasi, M. S. Behalo, G. Favi, D. Lomonaco, S. E. Mazzetto, G. Mele, I. Pio, G. Vasapollo, Solvent Free Synthesis of Novel Mono- and Bis-Benzoxazines from Cashew Nut Shell Liquid Components, Current Organic Chemistry 16(21) (2012) 2613-2621.

[65] A. Greco, D. Brunetti, G. Renna, G. Mele, A. Maffezzoli, Plasticizer for poly (vinyl chloride) from cardanol as a renewable resource material, Polymer Degradation and Stability 95(11) (2010) 2169-2174.

[66] J. Jang, D. Seo, Performance improvement of rubber-modified polybenzoxazine, Journal of Applied Polymer Science 67(1) (1998) 1-10.

[67] P. Thirukumaran, R. Sathiyamoorthi, A. Shakila Parveen, M. Sarojadevi, New benzoxazines from renewable resources for green composite applications, Polymer Composites 37(2) (2016) 573-582.

[68] G.-m. Xu, T. Shi, J. Liu, Q. Wang, Preparation of a liquid benzoxazine based on cardanol and the thermal stability of its graphene oxide composites, Journal of Applied Polymer Science 131(11) (2014) 10.1002/app.40353.

[69] S. Li, T. Zou, L. Feng, X. Liu, M. Tao, Preparation and properties of cardanol-based polybenzoxazine/SiO2 hybrids by sol-gel technique, Journal of Applied Polymer Science 128(6) (2013) 4164-4171.

[70] C. Zhang, Y. Zhang, Q. Zhou, H. Ling, Y. Gu, Processability and mechanical properties of bisbenzoxazine modified by the cardanol-based aromatic diamine benzoxazine, 2014.

[71] B. Lochab, I.K. Varma, J. Bijwe, Cardanol-based bisbenzoxazines, Journal of Thermal Analysis and Calorimetry 107(2) (2012) 661-668.

[72] A.A. Gallo, Method for preparing polybenzoxazine, US 6376080 B1 (2002).

[73] Y.X. Wang, H. Ishida, Cationic ring-opening polymerization of benzoxazines, Polymer 40(16) (1999) 4563-4570.

[74] H. Ishida, Cationic ring-opening polymerization of benzoxazines, US6225440 B1 (2001).

[75] A. Sudo, T. Endo, A. Taden, R. Schoenfeld, T. Huver, Benzoxazine-containing formulations polymerizable/curable at low temperature, US20100144964 A1 (2010).

[76] J. Sun, W. Wei, Y. Xu, J. Qu, X. Liu, T. Endo, A curing system of benzoxazine with amine: reactivity, reaction mechanism and material properties, RSC Advances 5(25) (2015) 19048-19057.

[77] B.A. A. Rucigaj, M. Krajnc, U. Sebenik, Curing of bisphenol A-aniline based benzoxazine using phenolic, amino and mercapto accelerators, Express Polymer Letters 9(7) (2015) 647-657.

[78] A. Sudo, R. Kudoh, H. Nakayama, K. Arima, T. Endo, Selective Formation of Poly(N,O-acetal) by Polymerization of 1,3-Benzoxazine and Its Main Chain Rearrangement, Macromolecules 41(23) (2008) 9030-9034.

[79] A. Sudo, S. Hirayama, T. Endo, Highly efficient catalysts-acetylacetonato complexes of transition metals in the 4th period for ring-opening polymerization of 1,3-benzoxazine, Journal of Polymer Science Part A: Polymer Chemistry 48(2) (2010) 479-484.

[80] N.E. Leadbeater, Microwave heating as a tool for sustainable chemistry, CRC Press2010.

[81] P. Lidström, J. Tierney, B. Wathey, J. Westman, Microwave assisted organic synthesis—a review, Tetrahedron 57(45) (2001) 9225-9283.

[82] R. Hoogenboom, U.S. Schubert, Microwave-Assisted Polymer Synthesis: Recent Developments in a Rapidly Expanding Field of Research, Macromolecular Rapid Communications 28(4) (2007) 368-386.

[83] V. Pimpan, R. Sirisook, S. Chuayjuljit, Synthesis of unsaturated polyester resin from postconsumer PET bottles: Effect of type of glycol on characteristics of unsaturated polyester resin, Journal of Applied Polymer Science 88(3) (2003) 788-792.

[84] S. Watanabe, K. Hayama, K.H. Park, M.a. Kakimoto, Y. Imai, New microwave-assisted rapid synthesis of polyamides from nylon salts, Die Makromolekulare Chemie, Rapid Communications 14(8) (1993) 481-484.

[85] N. Hurduc, D. Abdelylah, J.-M. Buisine, P. Decock, G. Surpateanu, Microwave effects in the synthesis of polyethers by phase transfer catalysis, European Polymer Journal 33(2) (1997) 187-190.

[86] J.M. Lu, S.J. Ji, N.Y. Chen, Z.B. Zhang, Z.R. Sun, X.L. Zhu, W.P. Shi, Novel synthesis of polyimides of the third-order optical nonlinearities by microwave assistance, Journal of Applied Polymer Science 87(11) (2003) 1739-1747.

[87] F. Wiesbrock, R. Hoogenboom, U.S. Schubert, Microwave-Assisted Polymer Synthesis: State-of-the-Art and Future Perspectives, Macromolecular Rapid Communications 25(20) (2004) 1739-1764.

[88] F. Wiesbrock, R. Hoogenboom, C.H. Abeln, U.S. Schubert, Single-Mode Microwave Ovens as New Reaction Devices: Accelerating the Living Polymerization of 2-Ethyl-2-Oxazoline, Macromolecular Rapid Communications 25(22) (2004) 1895-1899.

[89] R. Correa, G. Gonzalez, V. Dougar, Emulsion polymerization in a microwave reactor, Polymer 39(6) (1998) 1471-1474.

[90] J. Jacob, L.H.L. Chia, F.Y.C. Boey, Microwave polymerization of poly(methyl acrylate): Conversion studies at variable power, Journal of Applied Polymer Science 63(6) (1997) 787-797.

[91] C. Zhang, L. Liao, S. Gong, Recent developments in microwave-assisted polymerization with a focus on ring-opening polymerization, Green Chemistry 9(4) (2007) 303-314.

[92] S.E. Mallakpour, A.R. Hajipour, S. Khoee, Polymerization of 4, 4′-(hexafluoroisopropylidene)-N, N′-bis (phthaloyl-L-leucine) diacid chloride with aromatic diamines by microwave irradiation, Journal of Polymer Science Part A: Polymer Chemistry 38(7) (2000) 1154-1160.

[93] S. Rimdusit, V. Jiraprawatthagool, C. Jubsilp, S. Tiptipakorn, T. Kitano, Effect of SiC whisker on benzoxazine-epoxy-phenolic ternary systems: Microwave curing and thermomechanical characteristics, Journal of Applied Polymer Science 105(4) (2007) 1968-1977.

[94] S. Rimdusit, V. Jiraprawatthagool, S. Tiptipakorn, S. Covavisaruch, T. Kitano, Characterization of SiC Whisker-Filled Polybenzoxazine Cured by Microwave Radiation and Heat, International Journal of Polymer Analysis and Characterization 11(6) (2006) 441-453.

[95] M. Akhter, S. Habibullah, S.M. Hasan, M.M. Alam, N. Akhter, M. Shaquiquzzaman, Synthesis of some new 3, 4-dihydro-2H-1, 3-benzoxazines under microwave irradiation in solvent-free conditions and their biological activity, Medicinal Chemistry Research 20(8) (2011) 1147-1153.

[96] G. Caliendo, E. Perissutti, V. Santagada, F. Fiorino, B. Severino, D. Cirillo, R.d.E. di Villa Bianca, L. Lippolis, A. Pinto, R. Sorrentino, Synthesis by microwave irradiation of a substituted benzoxazine parallel library with preferential relaxant activity for guinea pig trachealis, European Journal of Medicinal Chemistry 39(10) (2004) 815-826.

[97] W.-M. Dai, X. Wang, C. Ma, Microwave-assisted one-pot regioselective synthesis of 2-alkyl-3, 4-dihydro-3-oxo-2H-1, 4-benzoxazines, Tetrahedron 61(28) (2005) 6879-6885.

[98] T.Y. İnan, B.Y. Karaca, H. Dogan, Synthesis and characterizations of polybenzoxazines from coal-based products via microwave and conventional heat treatments, Journal of Applied Polymer Science 128(3) (2013) 2046-2055.

[99] H. Ishida, D.J. Allen, Physical and mechanical characterization of near-zero shrinkage polybenzoxazines, Journal of Polymer Science Part B: Polymer Physics 34(6) (1996) 1019-1030.

[100] S.B. Shen, H. Ishida, Development and characterization of high-performance polybenzoxazine composites, Polymer Composites 17(5) (1996) 710-719.

[101] N.N. Ghosh, B. Kiskan, Y. Yagci, Polybenzoxazines—New high performance thermosetting resins: Synthesis and properties, Progress in Polymer Science 32(11) (2007) 1344-1391.

[102] E. Calò, A. Maffezzoli, G. Mele, F. Martina, S.E. Mazzetto, A. Tarzia, C. Stifani, Synthesis of a novel cardanol-based benzoxazine monomer and environmentally sustainable production of polymers and bio-composites, Green Chemistry 9(7) (2007) 754-759.

[103] P. Sharma, B. Lochab, D. Kumar, P.K. Roy, Sustainable Bis-benzoxazines from Cardanol and PET-Derived Terephthalamides, ACS Sustainable Chemistry & Engineering 4(3) (2015) 1085-1093.

[104] P. Froimowicz, C. R. Arza, L. Han, H. Ishida, Smart, Sustainable, and Ecofriendly Chemical Design of Fully Bio-Based Thermally Stable Thermosets Based on Benzoxazine Chemistry, ChemSusChem 9(15) (2016) 1921-1928.

[105] J.H.P. Tyman, D. Wilczynski, M.A. Kashani, Compositional studies on technical cashew nutshell liquid (cnsl) by chromatography and mass spectroscopy, Journal of the American Oil Chemists' Society 55(9) (1978) 663-668.

[106] A. Minigher, E. Benedetti, O. De Giacomo, P. Campaner, V. Aroulmoji, Synthesis and characterization of novel cardanol based benzoxazines, Natural Product Communications 4(4) (2009) 521-528.

[107] S. Shukla, A. Mahata, B. Pathak, B. Lochab, Cardanol benzoxazines–interplay of oxazine functionality (mono to tetra) and properties, RSC Advances 5(95) (2015) 78071-78080.

[108] B. Lochab, I.K. Varma, J. Bijwe, Thermal behaviour of cardanol-based benzoxazines, Journal of Thermal Analysis and Calorimetry 102(2) (2010) 769-774.

[109] V.V. Namboodiri, R.S. Varma, Microwave-accelerated Suzuki cross-coupling reaction in polyethylene glycol (PEG), Green Chemistry 3(3) (2001) 146-148.

[110] G.K. Watson, N. Jones, The biodegradation of polyethylene glycols by sewage bacteria, Water Research 11(1) (1977) 95-100.

[111] R.A. Sheldon, Green solvents for sustainable organic synthesis: state of the art, Green Chemistry 7(5) (2005) 267-278.

[112] S. Chaudhary, S. Parthasarathy, D. Kumar, C. Rajagopal, P.K. Roy, Graft-interpenetrating polymer networks of epoxy with polyurethanes derived from poly(ethyleneterephthalate) waste, Journal of Applied Polymer Science 131(13) (2014) DOI: 10.1002/app.40490.

[113] D.J. Allen, H. Ishida, Physical and mechanical properties of flexible polybenzoxazine resins: Effect of aliphatic diamine chain length, Journal of Applied Polymer Science 101(5) (2006) 2798-2809.

[114] S. Ates, C. Dizman, B. Aydogan, B. Kiskan, L. Torun, Y. Yagci, Synthesis, characterization and thermally activated curing of polysulfones with benzoxazine end groups, Polymer 52(7) (2011) 1504-1509.

[115] S. Chaudhary, S. Parthasarathy, D. Kumar, C. Rajagopal, P.K. Roy, Poly (ethyleneterephthalate) glycolysates as effective toughening agents for epoxy resin, Journal of Applied Polymer Science 131(4) (2014).

[116] S. Zalipsky, Functionalized Poly(ethylene glycols) for Preparation of Biologically Relevant Conjugates, Bioconjugate Chemistry 6(2) (1995) 150-165.

[117] K.K. R J Sengwa, Microwave Absorption in oligomers of Ethylene Glycol, Indian Journal of Biochemistry and Biophysics 36 (1999) 325-329.

[118] H. Ishida, Process for preparation of benzoxazine compounds in solventless systems, US 5543516 A, 1996.

[119] D. Tiwari, A. Devi, R. Chandra, Synthesis of cardanol based phenolic resin with aid of microwaves, International Journal of Drug Development and Research (2011).

[120] P. Sharma, B. Lochab, D. Kumar, P.K. Roy, Interfacial encapsulation of bio-based benzoxazines in epoxy shells for temperature triggered healing, Journal of Applied Polymer Science 132(47) (2015).

[121] P. Sharma, S. Shukla, B. Lochab, D. Kumar, P.K. Roy, Microencapsulated cardanol derived benzoxazines for self-healing applications, Materials Letters 133 (2014) 266-268.

[122] M. Arslan, B. Kiskan, Y. Yagci, Benzoxazine-Based Thermosets with Autonomous Self-Healing Ability, Macromolecules 48(5) (2015) 1329-1334.

[123] C. Aydogan, B. Kiskan, S.O. Hacioglu, L. Toppare, Y. Yagci, Electrochemical manipulation of adhesion strength of polybenzoxazines on metal surfaces: from strong adhesion to dismantling, RSC Advances 4(52) (2014) 27545-27551.

[124] Y. Yagci, B. Kiskan, N.N. Ghosh, Recent advancement on polybenzoxazine—a newly developed high performance thermoset, Journal of Polymer Science Part A: Polymer Chemistry 47(21) (2009) 5565-5576.

[125] O.S. Taskin, B. Kiskan, A. Aksu, N. Balkis, J. Weber, Y. Yagci, Polybenzoxazine: A Powerful Tool for Removal of Mercury Salts from Water, Chemistry-A European Journal 20(35) (2014) 10953-10958.

[126] S. Shukla, A. Mahata, B. Pathak, B. Lochab, Cardanol Benzoxazines - Interplay of Oxazine Functionality (Mono to Tetra) and Properties, RSC Advances DOI:10.1039/c5ra14214h (2015).

[127] A. Chernykh, T. Agag, H. Ishida, Novel benzoxazine monomer containing diacetylene linkage: An approach to benzoxazine thermosets with low polymerization temperature without added initiators or catalysts, Polymer 50(14) (2009) 3153-3157.

[128] A. Sudo, S. Hirayama, T. Endo, Highly efficient catalysts-acetylacetonato complexes of transition metals in the 4th period for ring-opening polymerization of 1, 3-benzoxazine, Journal of Polymer Science Part A: Polymer Chemistry 48(2) (2010) 479-484.

[129] B. Kiskan, Y. Yagci, Synthesis and characterization of thermally curable polyacetylenes by polymerization of propargyl benzoxazine using rhodium catalyst, Polymer 49(10) (2008) 2455-2460.

[130] B. Lochab, I. Varma, J. Bijwe, Blends of benzoxazine monomers, Journal of Thermal Analysis and Calorimetry 111(2) (2013) 1357-1364.

[131] R. Andreu, J. Reina, J. Ronda, Carboxylic acid-containing benzoxazines as efficient catalysts in the thermal polymerization of benzoxazines, Journal of Polymer Science Part A: Polymer Chemistry 46(18) (2008) 6091-6101.

[132] H. Wang, J. Wang, X. He, T. Feng, N. Ramdani, M. Luan, W. Liu, X. Xu, Synthesis of novel furan-containing tetrafunctional fluorene-based benzoxazine monomer and its high performance thermoset, RSC Advances 4(110) (2014) 64798-64801.

[133] C.W. Chang, C.H. Lin, H.T. Lin, H.J. Huang, K.Y. Hwang, A.P. Tu, Development of an aromatic triamine-based flame-retardant benzoxazine and its high-performance copolybenzoxazines, European Polymer Journal 45(3) (2009) 680-689.

[134] A.W. Kawaguchi, A. Sudo, T. Endo, Synthesis of highly polymerizable 1,3-benzoxazine assisted by phenyl thio ether and hydroxyl moieties, Journal of Polymer Science Part A: Polymer Chemistry 50(8) (2012) 1457-1461.

[135] T. Agag, C.R. Arza, F.H. Maurer, H. Ishida, Primary amine-functional benzoxazine monomers and their use for amide-containing monomeric benzoxazines, Macromolecules 43(6) (2010) 2748-2758.

[136] T. Agag, C.R. Arza, F.H. Maurer, H. Ishida, Crosslinked polyamide based on main-chain type polybenzoxazines derived from a primary amine-functionalized benzoxazine monomer, Journal of Polymer Science Part A: Polymer Chemistry 49(20) (2011) 4335-4342.

[137] K. Fukushima, J.M. Lecuyer, D.S. Wei, H.W. Horn, G.O. Jones, H.A. Al-Megren, A.M. Alabdulrahman, F.D. Alsewailem, M.A. McNeil, J.E. Rice, J.L. Hedrick, Advanced chemical recycling of poly(ethylene terephthalate) through organocatalytic aminolysis, Polymer Chemistry 4(5) (2013) 1610-1616.

[138] C.N. Hoang, Y.H. Dang, Aminolysis of poly(ethylene terephthalate) waste with ethylenediamine and characterization of α,ω-diamine products, Polymer Degradation and Stability 98(3) (2013) 697-708.

[139] R. Soni, S. Singh, Synthesis and characterization of terephthalamides from poly (ethylene terephthalate) waste, Journal of Applied Polymer Science 96(5) (2005) 1515-1528.

[140] R. Soni, M. Teotia, K. Dutt, Studies on synthesis and characterization of a novel acrylic aromatic amide oligomer of aminolysed endproducts generated from pet waste with hydrazine monohydrate and its photocuring with acrylate monomers, Journal of Applied Polymer Science 118(2) (2010) 638-645.

[141] S. Chaudhary, P. Surekha, D. Kumar, C. Rajagopal, P.K. Roy, Microwave assisted glycolysis of poly(ethylene terepthalate) for preparation of polyester polyols, Journal of Applied Polymer Science 129(5) (2013) 2779-2788.

[142] D.S. Achilias, G.P. Tsintzou, A.K. Nikolaidis, D.N. Bikiaris, G.P. Karayannidis, Aminolytic depolymerization of poly(ethylene terephthalate) waste in a microwave reactor, Polymer International 60(3) (2011) 500-506.

[143] P.K. Roy, R. Mathur, D. Kumar, C. Rajagopal, Tertiary recycling of poly(ethylene terephthalate) wastes for production of polyurethane–polyisocyanurate foams, Journal of Environmental Chemical Engineering 1(4) (2013) 1062-1069.

[144] C. Duchesne, X. Kong, J. Brisson, M. Pezolet, R.E. Prud'Homme, Molecular orientation and relaxation of poly (ethylene terephthalate) by polarization modulation infrared spectroscopy, Macromolecules 35(23) (2002) 8768-8773.

[145] S.R. Aspinall, Ethylenediamine. IV.1 Monoalkyl Derivatives, Journal of the American Chemical Society 63(3) (1941) 852-854.

[146] R.J. Bergeron, J.R. Garlich, N.J. Stolowich, Reagents for the stepwise functionalization of spermidine, homospermidine, and bis(3-aminopropyl)amine, The Journal of Organic Chemistry 49(16) (1984) 2997-3001.

[147] A.R. Jacobson, A.N. Makris, L.M. Sayre, Monoacylation of symmetrical diamines, The Journal of Organic Chemistry 52(12) (1987) 2592-2594.

[148] Manju, P. Kumar Roy, A. Ramanan, C. Rajagopal, Post consumer PET waste as potential feedstock for metal organic frameworks, Materials Letters 106(0) (2013) 390-392.

[149] U.S. Agarwal, G. de Wit, P.J. Lemstra, A new solid-state process for chemical modification of PET for crystallization rate enhancement, Polymer 43(21) (2002) 5709-5712.

[150] Y.J. Kim, R.S. Varma, Microwave-assisted preparation of cyclic ureas from diamines in the presence of ZnO, Tetrahedron Letters 45(39) (2004) 7205-7208.

[151] B.S. Narwade, P.G. Gawali, R. Pande, G.M. Kalamse, Dielectric studies of binary mixtures ofn-propyl alcohol and ethylenediamine, Journal of Chemical Sciences 117(6) (2005) 673-676.

[152] W.H. Carothers, Polymers and polyfunctionality, Transactions of the Faraday Society 32(0) (1936) 39-49.

[153] Chapter 8 - Aliphatic Amines, in: R.A. Nyquist (Ed.), Interpreting Infrared, Raman, and Nuclear Magnetic Resonance Spectra, Academic Press, San Diego, 2001, pp. 143-148.

[154] B. Lochab, I. Varma, J. Bijwe, Thermal behaviour of cardanol-based benzoxazines, Journal of Thermal Analysis and Calorimetry 102(2) (2010) 769-774.

[155] P. Sharma, B. Lochab, D. Kumar, P.K. Roy, Interfacial encapsulation of bio-based benzoxazines in epoxy shells for temperature triggered healing, Journal of Applied Polymer Science DOI:10.1002/app.42832 (2015).

[156] P. Sharma, S. Shukla, B. Lochab, D. Kumar, P. Kumar Roy, Microencapsulated cardanol derived benzoxazines for self-healing applications, Materials Letters 133 (2014) 266-268.

[157] B. Kiskan, Y. Yagci, Self-healing of poly(propylene oxide)-polybenzoxazine thermosets by photoinduced coumarine dimerization, Journal of Polymer Science Part A: Polymer Chemistry 52(20) (2014) 2911-2918.

[158] Z. Brunovska, H. Ishida, Thermal study on the copolymers of phthalonitrile and phenylnitrile-functional benzoxazines, Journal of Applied Polymer Science 73(14) (1999) 2937-2949.

[159] K.S. Kumar, C.R. Nair, K. Ninan, Investigations on the cure chemistry and polymer properties of benzoxazine–cyanate ester blends, European Polymer Journal 45(2) (2009) 494-502.

[160] H. Ishida, D.J. Allen, Mechanical characterization of copolymers based on benzoxazine and epoxy, Polymer 37(20) (1996) 4487-4495.

[161] M. Baqar, T. Agag, H. Ishida, S. Qutubuddin, Poly (benzoxazine-co-urethane) s: a new concept for phenolic/urethane copolymers via one-pot method, Polymer 52(2) (2011) 307-317.

[162] B. Gacal, L. Cianga, T. Agag, T. Takeichi, Y. Yagci, Synthesis and characterization of maleimide (Co) polymers with pendant benzoxazine groups by photoinduced radical polymerization and their thermal curing, Journal of Polymer Science Part A: Polymer Chemistry 45(13) (2007) 2774-2786.

[163] L. Jin, T. Agag, H. Ishida, Bis (benzoxazine-maleimide) s as a novel class of high performance resin: synthesis and properties, European Polymer Journal 46(2) (2010) 354-363.

[164] Y.-J. Lee, S.-W. Kuo, Y.-C. Su, J.-K. Chen, C.-W. Tu, F.-C. Chang, Syntheses, thermal properties, and phase morphologies of novel benzoxazines functionalized with polyhedral oligomeric silsesquioxane (POSS) nanocomposites, Polymer 45(18) (2004) 6321-6331.

[165] H. Kim, Z. Brunovska, H. Ishida, Synthesis and thermal characterization of polybenzoxazines based on acetylene-functional monomers, Polymer 40(23) (1999) 6565-6573.

[166] N. Iqbal, M. Tripathi, S. Parthasarathy, D. Kumar, P. Roy, Polyurea coatings for enhanced blast-mitigation: a review, RSC Advances 6(111) (2016) 109706-109717.

[167] S. Kirschbaum, K. Landfester, A. Taden, Synthesis and Thermal Curing of Benzoxazine Functionalized Polyurethanes, Macromolecules 48(12) (2015) 3811-3816.

[168] H.-D. Kim, H. Ishida, Model compounds study on the network structure of polybenzoxazines, Macromolecules 36(22) (2003) 8320-8329.

[169] P. Sharma, B. Lochab, D. Kumar, P.K. Roy, Sustainable Bis-benzoxazines from Cardanol and PET-Derived Terephthalamides, ACS Sustainable Chemistry & Engineering 4(3) (2016) 1085-1093.

[170] P. Sharma, D. Kumar, P. Roy, Microwave-Assisted Sustainable Synthesis of Telechelic Poly(ethylene glycol)s with Benzoxazine End Groups, ChemistrySelect 1(21) (2016) 6941-6947.

[171] R. Huang, S.O. Carson, J. Silva, T. Agag, H. Ishida, J.M. Maia, Interplay between rheological and structural evolution of benzoxazine resins during polymerization, Polymer 54(7) (2013) 1880-1886.

[172] P.J. Halley, M.E. Mackay, Chemorheology of thermosets—an overview, Polymer Engineering & Science 36(5) (1996) 593-609.

[173] W.H. Awad, C.A. Wilkie, Investigation of the thermal degradation of polyurea: The effect of ammonium polyphosphate and expandable graphite, Polymer 51(11) (2010) 2277-2285.

[174] J.P. Sheth, D.B. Klinedinst, G.L. Wilkes, I. Yilgor, E. Yilgor, Role of chain symmetry and hydrogen bonding in segmented copolymers with monodisperse hard segments, Polymer 46(18) (2005) 7317-7322.

[175] A. Mallick, S. Saha, P. Pachfule, S. Roy, R. Banerjee, Selective CO 2 and H 2 adsorption in a chiral magnesium-based metal organic framework (Mg-MOF) with open metal sites, Journal of Materials Chemistry 20(41) (2010) 9073-9080.

[176] Z. Zhang, Y. Zhao, Q. Gong, Z. Li, J. Li, MOFs for CO2 capture and separation from flue gas mixtures: the effect of multifunctional sites on their adsorption capacity and selectivity, Chemical Communications 49(7) (2013) 653-661.

[177] S. Qiu, M. Xue, G. Zhu, Metal-organic framework membranes: from synthesis to separation application, Chemical Society Reviews 43(16) (2014) 6116-6140.

[178] J.-R. Li, R.J. Kuppler, H.-C. Zhou, Selective gas adsorption and separation in metal-organic frameworks, Chemical Society Reviews 38(5) (2009) 1477-1504.

[179] G. Riess, J.M. Schwob, G. Guth, M. Roche, B. Laude, Ring Opening Polymerization of Benzoxazines — A New Route to Phenolic Resins, in: B.M. Culbertson, J.E. McGrath (Eds.), Advances in Polymer Synthesis, Springer US, Boston, MA, 1985, pp. 27-49.

[180] X. Ning, H. Ishida, Phenolic materials via ring-opening polymerization: Synthesis and characterization of bisphenol-A based benzoxazines and their polymers, Journal of Polymer Science Part A: Polymer Chemistry 32(6) (1994) 1121-1129.

[181] H. Ishida, D.P. Sanders, Improved thermal and mechanical properties of polybenzoxazines based on alkyl-substituted aromatic amines, Journal of Polymer Science Part B: Polymer Physics 38(24) (2000) 3289-3301.

[182] H. Li, M. Eddaoudi, M. O'Keeffe, O.M. Yaghi, Design and synthesis of an exceptionally stable and highly porous metal-organic framework, Nature 402(6759) (1999) 276-279.

[183] N.T.S. Phan, K.K.A. Le, T.D. Phan, MOF-5 as an efficient heterogeneous catalyst for Friedel–Crafts alkylation reactions, Applied Catalysis A: General 382(2) (2010) 246-253.

[184] J. Lee, O.K. Farha, J. Roberts, K.A. Scheidt, S.T. Nguyen, J.T. Hupp, Metal-organic framework materials as catalysts, Chemical Society Reviews 38(5) (2009) 1450-1459.

[185] Z. Akimbekov, D. Wu, C.K. Brozek, M. Dinca, A. Navrotsky, Thermodynamics of solvent interaction with the metal-organic framework MOF-5, Physical Chemistry Chemical Physics 18(2) (2016) 1158-1162.

[186] J. Lee, O.K. Farha, J. Roberts, K.A. Scheidt, S.T. Nguyen, J.T. Hupp, Metal–organic framework materials as catalysts, Chemical Society Reviews 38(5) (2009) 1450-1459.

[187] S. Gao, N. Zhao, M. Shu, S. Che, Palladium nanoparticles supported on MOF-5: a highly active catalyst for a ligand-and copper-free Sonogashira coupling reaction, Applied Catalysis A: General 388(1) (2010) 196-201.

[188] A.U. Czaja, N. Trukhan, U. Müller, Industrial applications of metal–organic frameworks, Chemical Society Reviews 38(5) (2009) 1284-1293.

[189] M. Sabo, A. Henschel, H. Fröde, E. Klemm, S. Kaskel, Solution infiltration of palladium into MOF-5: synthesis, physisorption and catalytic properties, Journal of Materials Chemistry 17(36) (2007) 3827-3832.

[190] Manju, P.K. Roy, A. Ramanan, Toughening of epoxy resin using Zn_4O (1,4-benzenedicarboxylate)3 metal-organic frameworks, RSC Advances 4(94) (2014) 52338-52345.

[191] Manju, P.K. Roy, A. Ramanan, C. Rajagopal, Core-shell polysiloxane-MOF 5 microspheres as a stationary phase for gas-solid chromatographic separation, RSC Advances 4(34) (2014) 17429-17433.

[192] G. Majano, J. Pérez-Ramírez, Room Temperature Synthesis and Size Control of HKUST-1, Helvetica Chimica Acta 95(11) (2012) 2278-2286.

[193] J. Dunkers, H. Ishida, Reaction of benzoxazine-based phenolic resins with strong and weak carboxylic acids and phenols as catalysts, Journal of Polymer Science Part A: Polymer Chemistry 37(13) (1999) 1913-1921.

[194] P. Chutayothin, H. Ishida, Cationic Ring-Opening Polymerization of 1,3-Benzoxazines: Mechanistic Study Using Model Compounds, Macromolecules 43(10) (2010) 4562-4572.

[195] C. Liu, D. Shen, R.M. Sebastián, J. Marquet, R. Schönfeld, Mechanistic Studies on Ring-Opening Polymerization of Benzoxazines: A Mechanistically Based Catalyst Design, Macromolecules 44(12) (2011) 4616-4622.

[196] Y.-X. Wang, H. Ishida, Synthesis and Properties of New Thermoplastic Polymers from Substituted 3,4-Dihydro-2H-1,3-benzoxazines, Macromolecules 33(8) (2000) 2839-2847.

[197] Y. Pan, Y. Liu, G. Zeng, L. Zhao, Z. Lai, Rapid synthesis of zeolitic imidazolate framework-8 (ZIF-8) nanocrystals in an aqueous system, Chemical Communications 47(7) (2011) 2071-2073.

[198] M. Srivastava, P.K. Roy, A. Ramanan, Hydrolytically stable ZIF-8@ PDMS core–shell microspheres for gas–solid chromatographic separation, RSC Advances 6(16) (2016) 13426-13432.

[199] P. Budrugeac, E. Segal, Applicability of the Kissinger equation in thermal analysis, Journal of Thermal Analysis and Calorimetry 88(3) (2007) 703-707.

[200] H. Yee Low, H. Ishida, Structural effects of phenols on the thermal and thermo-oxidative degradation of polybenzoxazines, Polymer 40(15) (1999) 4365-4376.

[201] S.-i. Kuroda, K. Terauchi, K. Nogami, I. Mita, Degradation of aromatic polymers—I. Rates of crosslinking and chain scission during thermal degradation of several soluble aromatic polymers, European Polymer Journal 25(1) (1989) 1-7.

[202] S. Manjula, C.K.S. Pillai, V.G. Kumar, Thermal characterization of cardanol-formaldehyde resins and cardanol-formaldehyde/poly(methyl methacrylate) semi-interpenetrating polymer networks, Thermochimica Acta 159 (1990) 255-266.

[203] D. O'Connor, F.D. Blum, Thermal stability of substituted phenol-formaldehyde resins, Journal of Applied Polymer Science 33(6) (1987) 1933-1941.

[204] P. Sharma, M. Srivastava, B. Lochab, D. Kumar, A. Ramanan, P.K. Roy, Metal-Organic Frameworks as curing accelerators for benzoxazines, ChemistrySelect 1(13) (2016) 3924-3932.

[205] D. Undurraga, A. Markovits, S. Erazo, Cocoa butter equivalent through enzymic interesterification of palm oil midfraction, Process Biochemistry 36(10) (2001) 933-939.

[206] Z. Wang, Q. Li, Z. She, F. Chen, L. Li, X. Zhang, P. Zhang, Facile and fast fabrication of superhydrophobic surface on magnesium alloy, Applied Surface Science 271 (2013) 182-192.

[207] H. ısmet Gökçel, D. Balköse, U. Köktürk, Effects of mixed metal stearates on thermal stability of rigid PVC, European Polymer Journal 35(8) (1999) 1501-1508.

[208] L.M.Z. Wengong, Research on the new heat stabilizer of calcium soap and zinc soap with high efficiency and less toxicity [J], POLYVINGYI CHLORIDE 1 (2000) 010.

[209] T. Ishioka, K. Maeda, I. Watanabe, S. Kawauchi, M. Harada, Infrared and XAFS study on structure and transition behavior of zinc stearate, Spectrochimica acta. Part A, Molecular and biomolecular spectroscopy 56A(9) (2000) 1731-1737.

[210] N.U. Soriano, R. Venditti, D.S. Argyropoulos, Biodiesel synthesis via homogeneous Lewis acid-catalyzed transesterification, Fuel 88(3) (2009) 560-565.

[211] K. Jacobson, R. Gopinath, L.C. Meher, A.K. Dalai, Solid acid catalyzed biodiesel production from waste cooking oil, Applied Catalysis B: Environmental 85(1) (2008) 86-91.

[212] M. Di Serio, R. Tesser, M. Dimiccoli, F. Cammarota, M. Nastasi, E. Santacesaria, Synthesis of biodiesel via homogeneous Lewis acid catalyst, Journal of Molecular Catalysis A: Chemical 239(1) (2005) 111-115.

[213] P.K. Roy, P. Surekha, R. Raman, C. Rajagopal, Investigating the role of metal oxidation state on the degradation behaviour of LDPE, Polymer Degradation and Stability 94(7) (2009) 1033-1039.

[214] D. Lison, Human Toxicity of Cobalt-Containing Dust and Experimental Studies on the Mechanism of Interstitial Lung Disease (Hard Metal Disease), Critical Reviews in Toxicology 26(6) (1996) 585-616.

[215] H. Ishida, Y. Rodriguez, Curing kinetics of a new benzoxazine-based phenolic resin by differential scanning calorimetry, Polymer 36(16) (1995) 3151-3158.

[216] C. Jubsilp, S. Damrongsakkul, T. Takeichi, S. Rimdusit, Curing kinetics of arylamine-based polyfunctional benzoxazine resins by dynamic differential scanning calorimetry, Thermochimica acta 447(2) (2006) 131-140.

[217] C. Jubsilp, K. Punson, T. Takeichi, S. Rimdusit, Curing kinetics of benzoxazine–epoxy copolymer investigated by non-isothermal differential scanning calorimetry, Polymer Degradation and Stability 95(6) (2010) 918-924.

[218] P. Sharma, M. Srivastava, B. Lochab, D. Kumar, A. Ramanan, P.K. Roy, Metal-Organic Frameworks as curing accelerators for benzoxazines, ChemistrySelect 1(13) (2016) 3924-3932.

[219] C.A. Wilkie, A.B. Morgan, Fire retardancy of polymeric materials, CRC press2009.

[220] D.W. van Krevelen, Some basic aspects of flame resistance of polymeric materials, Polymer 16(8) (1975) 615-620.

[221] O.S. Taskin, B. Kiskan, Y. Yagci, Polybenzoxazine Precursors As Self-Healing Agents for Polysulfones, Macromolecules 46(22) (2013) 8773-8778.

[222] P. Nemeček, J. Mocák, J. Lehotay, K. Waisser, Prediction of anti-tuberculosis activity of 3-phenyl-2H-1,3-benzoxazine-2,4(3H)-dione derivatives, Chemical Papers 67(3) (2013) 305-312.

[223] A. Gharsallaoui, G. Roudaut, L. Beney, O. Chambin, A. Voilley, R. Saurel, Properties of spray-dried food flavours microencapsulated with two-layered membranes: Roles of interfacial interactions and water, Food Chemistry 132(4) (2012) 1713-1720.

[224] J. Suave, E. Dall'Agnol, A. Pezzin, D. Silva, M. Meier, V. Soldi, Microencapsulação: Inovação em diferentes áreas, Revista Saúde e Ambiente/Health and Environment Journal 7(2) (2006) 12-20.

[225] P.T.d. Silva, L.L.M. Fries, C.R.d. Menezes, A.T. Holkem, C.L. Schwan, É.F. Wigmann, J.d.O. Bastos, C.d.B.d. Silva, Microencapsulation: concepts, mechanisms, methods and some applications in food technology, Ciência Rural 44(7) (2014) 1304-1311.

[226] M. Tripathi, Rahamtullah, P.K. Roy, D. Kumar, C. Rajagopal, Influence of microcapsule shell material on the mechanical behavior of epoxy composites for self-healing applications, Journal of Applied Polymer Science 10.1002/app.40572 (2014).

[227] E.N. Brown, M.R. Kessler, N.R. Sottos, S.R. White, In situ poly(urea-formaldehyde) microencapsulation of dicyclopentadiene, Journal of Microencapsulation 20(6) (2003) 719-730.

[228] A.P. Rochmadi, W. Hasokowati, Mechanism of microencapsulation with urea-formaldehyde polymer, American. Journal of Applied Sciences 7(6) (2010) 739-745.

[229] R. Andreu, J.A. Reina, J.C. Ronda, Carboxylic acid-containing benzoxazines as efficient catalysts in the thermal polymerization of benzoxazines, Journal of Polymer Science Part A: Polymer Chemistry 46(18) (2008) 6091-6101.

[230] C. Scott, D. Wu, C.-C. Ho, C.C. Co, Liquid-Core Capsules via Interfacial Polymerization: A Free-Radical Analogy of the Nylon Rope Trick, Journal of the American Chemical Society 127(12) (2005) 4160-4161.

[231] E. Detsri, S.T. Dubas, Interfacial polymerization of polyaniline and its layer-by-layer assembly into polyelectrolytes multilayer thin-films, Journal of Applied Polymer Science 128(1) (2013) 558-565.

[232] C.N.R. Rao, G.U. Kulkarni, V.V. Agrawal, U.K. Gautam, M. Ghosh, U. Tumkurkar, Use of the liquid–liquid interface for generating ultrathin nanocrystalline films of metals, chalcogenides, and oxides, Journal of Colloid and Interface Science 289(2) (2005) 305-318.

[233] E. Koh, N.-K. Kim, J. Shin, Y.-W. Kim, Polyurethane microcapsules for self-healing paint coatings, RSC Advances 4(31) (2014) 16214-16223.

[234] X. Liu, H. Zhang, J. Wang, Z. Wang, S. Wang, Preparation of epoxy microcapsule based self-healing coatings and their behavior, Surface and Coatings Technology 206(23) (2012) 4976-4980.

[235] H. Kempe, M. Kempe, Novel Method for the Synthesis of Molecularly Imprinted Polymer Bead Libraries, Macromolecular Rapid Communications 25(1) (2004) 315-320.

[236] X. Wang, X. Ding, Z. Zheng, X. Hu, X. Cheng, Y. Peng, Magnetic Molecularly Imprinted Polymer Particles Synthesized by Suspension Polymerization in Silicone Oil, Macromolecular Rapid Communications 27(14) (2006) 1180-1184.

[237] R.W. Lenz, Experiments in polymer science, Edward A. Collins, Jan Bares, Fred W. Billmeyer, Jr., Wiley-Interscience, New York, 1973. 530 pp. $16.95, Journal of Polymer Science: Polymer Letters Edition 12(9) (1974) 535-536.

[238] L. Sánchez, P. Sánchez, A. Lucas, M. Carmona, J. Rodríguez, Microencapsulation of PCMs with a polystyrene shell, Colloid and Polymer Science 285(12) (2007) 1377-1385.

[239] S. Chaudhary, S. Parthasarathy, D. Kumar, C. Rajagopal, P.K. Roy, Amine functionalised poly(styrene) microspheres as thermoplastic toughener for epoxy resin, Polymer Composites DOI: 10.1002/pc.22927 (2014).

[240] B.J. Blaiszik, M.M. Caruso, D.A. McIlroy, J.S. Moore, S.R. White, N.R. Sottos, Microcapsules filled with reactive solutions for self-healing materials, Polymer 50(4) (2009) 990-997.

[241] K.L. Hoy, New Values of the Solubility Parameters from Vapor Pressure Data, Journal of paint technology 42 (1970) 76-118.

[242] B. Fiedler, F.H. Gojny, M.H.G. Wichmann, M.C.M. Nolte, K. Schulte, Fundamental aspects of nano-reinforced composites, Composites Science and Technology 66(16) (2006) 3115-3125.

[243] Y. Deng, G.C. Martin, Diffusion and Diffusion-Controlled Kinetics during Epoxy-Amine Cure, Macromolecules 27(18) (1994) 5147-5153.

[244] M. Tripathi, D. Kumar, C. Rajagopal, P. Roy, Curing kinetics of self-healing epoxy thermosets, Journal of Thermal Analysis and Calorimetry 119(1) (2015) 547-555.

[245] A.A. Efimova, V.N. Emel'yanenko, S.P. Verevkin, Y. Chernyak, Vapour pressure and enthalpy of vaporization of aliphatic poly-amines, The Journal of Chemical Thermodynamics 42(3) (2010) 330-336.

[246] C. Ramírez, M. Rico, A. Torres, L. Barral, J. López, B. Montero, Epoxy/POSS organic–inorganic hybrids: ATR-FTIR and DSC studies, European Polymer Journal 44(10) (2008) 3035-3045.

[247] J.M. Rallison, The Deformation of Small Viscous Drops and Bubbles in Shear Flows, Annual Review of Fluid Mechanics 16(1) (1984) 45-66.

[248] P. Sharma, S. Shukla, B. Lochab, D. Kumar, P. Kumar Roy, Microencapsulated cardanol derived benzoxazines for self-healing applications, Materials Letters 133(0) (2014) 266-268.

[249] M. Baqar, T. Agag, S. Qutubuddin, H. Ishida, Chapter 10 - Effect of Neighboring Groups on Enhancing Benzoxazine Autocatalytic Polymerization, in: H.I. Agag (Ed.), Handbook of Benzoxazine Resins, Elsevier, Amsterdam, 2011, pp. 193-210.

[250] H. Oie, A. Sudo, T. Endo, Acceleration effect of N-allyl group on thermally induced ring-opening polymerization of 1,3-benzoxazine, Journal of Polymer Science Part A: Polymer Chemistry 48(23) (2010) 5357-5363.

[251] M. Baqar, T. Agag, H. Ishida, S. Qutubuddin, Methylol-functional benzoxazines as precursors for high-performance thermoset polymers: Unique simultaneous addition and condensation polymerization behavior, Journal of Polymer Science Part A: Polymer Chemistry 50(11) (2012) 2275-2285.

[252] S. Nalakathu Kolanadiyil, J. Bijwe, I. Varma, Thermal properties of bisitaconimide and bisbenzoxazine blends, Journal of Thermal Analysis and Calorimetry 116(1) (2014) 427-434.

PUBLICATIONS

1. Microencapsulated cardanol derived benzoxazines for self-healing applications
   Pratibha Sharma, Swapnil Shukla, Bimlesh Lochab, Devendra Kumar, Prasun Kumar Roy
   Material Letters Volume 133, 2014, Pages 266-268
2. Interfacial encapsulation of bio-based benzoxazines in epoxy shells for temperature triggered healing
   Pratibha Sharma, Bimlesh Lochab, Devendra Kumar, Prasun Kumar Roy
   Journal of Applied Polymer Science, Volume 132, 2015
3. Sustainable bis-benzoxazines from Cardanol and PET-Derived Terephthalamides
   Pratibha Sharma, Bimlesh Lochab, Devendra Kumar, Prasun Kumar Roy
   ACS Sustainable Chemistry and Engineering, 2016, Volume 4, 2015, Pages 1085–1093
4. Metal-Organic Frameworks as curing accelerators for benzoxazines
   Pratibha Sharma, Manju Srivastava, Bimlesh Lochab, Devendra Kumar, Arunachalam Ramanan, Prasun Kumar Roy
   ChemistrySelect, Volume 1, 2016, Pages 3924–3932
5. Microwave-Assisted Sustainable Synthesis of Telechelic Poly(ethylene glycol)s with Benzoxazine End Groups
   Pratibha Sharma, Devendra Kumar, Prasun Kumar Roy
   ChemistrySelect, Volume 1, 2016, Pages 6941–6947
6. Poly(benzoxazine–co–urea): A Solventless Approach Towards The Introduction of Alternating Urea Linkages In Polybenzoxazine
   Pratibha Sharma, Devendra Kumar, Prasun Kumar Roy
   ChemistrySelect, Volume 2, 2017, Pages 5372–5377
7. Enhancing the processibility of high temperature polymerizing cardanol derived benzoxazines using eco-friendly curing accelerators
   Pratibha Sharma, Devendra Kumar, Prasun Kumar Roy
   Polymer, Volume 138, 2018, Pages 343-351

PATENT

Indian Patent "Process For Preparing Polybenzoxazines" (201711005289)
Prasun Kumar Roy, Pratibha Sharma, Devendra Kumar

CONFERENCE PROCEEDINGS

1. Hydrolytically stable transition metal stearates as efficient curing accelerators for ring opening polymerization of cardanol based benzoxazine" *(Oral Presentation)*
   Pratibha Sharma, Devendra Kumar, Prasun K. Roy
   Advances in Polymeric Materials, CIPET, Bhubaneswar (Feb 2-4, 2018).

2. "Introduction of urea linkages in bio-based benzoxazines via solventless approach"
   Pratibha Sharma, Prof. Devendra Kumar, Dr. Prasun K. Roy
   Study of Nanomaterials and Scientific Development in 21st Century (ICSNSDC), Jiwaji University, Gwalior (November 3-5, 2017)

3. "Metal-Organic Frameworks as curing accelerator for benzoxazines"
   Pratibha Sharma, Manju Srivastava, Bimlesh Lochab, Devendra Kumar, Arunachalam Ramanan, Prasun Kumar Roy
   MACRO 2017, VSSC, ISRO, Thiruvananthapuram, Kerala (January 8-11, 2017)

4. "Sustainable bis-benzoxazines derived from cardanol and recycled Polyethylene terephthalate"
   Pratibha Sharma, Bimlesh Lochab, Devendra Kumar, Prasun Kumar Roy
   Polymer Modification, Processing and Characterization, PEARLS, Bhaskaracharya college of applied sciences (25 January 2016) University of Delhi

5. "Sustainable bis-benzoxazines derived from cardanol and recycled Polyethylene terephthalate"
   Pratibha Sharma, Bimlesh Lochab, Devendra Kumar, Prasun Kumar Roy
   MACRO2015, Indian Association for the Cultivation of Sciences (IACS) Kolkata (January 22 2015)

6. "Cross-linkable telechelic cardanol based benzoxazines synthesized using microwave irradiation"
   Pratibha Sharma, Devendra Kumar, Prasun Kumar Roy
   Functional and Engineering Materials (FEM-2016), DMSRDE, DRDO, Kanpur

BIO-DATA

Pratibha Sharma

1/2996 Ram Nagar Loni Road Shahdara Delhi-110032

Email ID: pratibhasharma.venky@gmail.com

PERSONAL DETAILS	Female, Single
	Date of Birth: 25 November, 1990
	Languages Known: Hindi & English
EDUCATION	M.Sc (Chemistry), 2013
	Sri Venkasteswara College
	University of Delhi, Delhi
HONOURS	UGC JRF-NET qualified
	GATE qualified

Materials Letters

Microencapsulated cardanol derived benzoxazines for self-healing applications

Pratibha Sharma [a,b], Swapnil Shukla [c], Bimlesh Lochab [c,**], Devendra Kumar [b], Prasun Kumar Roy [a,*]

[a] Centre for Fire, Explosive and Environment Safety, DRDO, Timarpur, Delhi 110054, India
[b] Department of Applied Chemistry and Polymer Technology, Delhi Technological University, Delhi 110042, India
[c] Department of Chemistry, School of Natural Sciences, Shiv Nadar University, Gautam Buddha Nagar 203207, Uttar Pradesh, India

ARTICLE INFO

ABSTRACT

Benzoxazine (Bz) monomer was synthesized from renewable cardanol, a by-product from cashew-nut industry, using a solventless approach. The monomer was encapsulated in poly(styrene) (PS) shells by solvent evaporation technique to obtain spherical microcapsules. The microcapsule dimensions and core content could be tailored by optimizing the operating parameters, particularly stirring speed and PS concentration. Successful demonstration of this simple and versatile methodology widens the scope for large-scale application of benzoxazines in the field of self-healing.

© 2014 Elsevier B.V. All rights reserved.

1. Introduction

Polybenzoxazines belong to a class of phenolic thermosetting resins, which exhibit interesting properties, mainly zero-volume shrinkage, low water absorption, high thermal stability and chemical resistance, high glass transition temperature (T_g), long shelf life and self-curing characteristics. Benzoxazine precursors hold enormous potential as healing agents in self-healing compositions [1], provided they are encapsulated in fragile microcontainers, prior to their inclusion in the polymeric matrix. Surprisingly, attempts towards usage of oxazine monomers for this purpose have not been reported till date. Presently, dicyclopentadiene (DCPD) is the most common healing agent used for self-healing applications, which undergo ring opening metathesis polymerization in the presence of organometallic catalysts [2]. Although, compositions based on encapsulated DCPD have reached the stage of commercial maturity, in view of the exceptionally high cost of the organometallic catalyst, it is desirable to explore alternate healing agents.

Benzoxazines, interestingly, do not require any catalyst for their curing, and hence are ideal candidates for the aforementioned purpose. What makes these materials even more attractive is the possibility of deriving these monomers from renewable sources like cardanol; a by-product of the cashew nut processing industry [3–5]. Benzoxazines undergo thermally activated ring-opening polymerization (ROP) reaction at elevated temperatures and it is possible to alleviate the curing conditions by making structural modifications. Recently, Lochab et al. have successfully reduced the Bz–C curing temperature from 242 to 161 °C by blending with oxazines containing higher and acidic functionalities [6]. Other functional groups such as allylic [7], methylol [8] etc. has also been reported to lower the curing temperature.

Unfortunately, the possibility of curing of Bz monomers under acidic conditions imposes a restriction on the technique used for its encapsulation. The conventional micro-encapsulation procedure involves in-situ emulsion polymerization of urea or melamine with formaldehyde on the surface of the hydrophobic dispersed phase of the precursor [9]. The condensation process requires low pH (< 3); [2,10] but the acidic conditions may induce curing in Bz [11]. We believe that this issue can be addressed by encapsulating Bz in soluble polymers by solvent evaporation, which surprisingly has not been attempted till date.

In this paper, we demonstrate a technique for physical encapsulation of cardanol derived Bz in PS shells. We adopt a "green" approach for the synthesis of cardanol based benzoxazines (Bz–C), where the role of cardanol is extended to that of a reactive diluent. This is followed by its encapsulation in PS microcapsules. Of particular interest is to investigate the effect of operating parameters to arrive at optimized conditions for preparation of microcapsules.

* Corresponding author. Tel.: +911123907191; fax: +911123819547.
** Corresponding author. Tel.: + 120 2663801.
E-mail addresses: bimlesh.lochab@snu.edu.in (B. Lochab),
pk_roy2000@yahoo.com, prasunroy2000@gmail.com (P. Kumar Roy).

2. Preparation benzoxazine monomers from cardanol

Benzoxazine monomer was prepared from cardanol as per the procedure reported previously [3]. In brief, a mixture of cardanol (100 g, 0.33 mol), paraformaldehyde (19.8 g, 0.66 mol) and aniline (30.1 mL, 0.33 mol) was slowly heated and maintained under isothermal conditions at 80 °C and 90 °C for 1 h and 2 h respectively. Post-cooling, 500 mL of water was added and the organic layer was collected after extraction with chloroform (2 × 100 mL). After drying over sodium sulphate, and solvent removal under reduced pressure, the residue was dried at 70 °C under vacuum to yield Bz–C in quantitative yield as a red brown oil.

Microencapsulation of benzoxazine in poly(styrene): Bz–C was encapsulated in PS microcapsules by solvent evaporation technique using the procedure reported in the literature [12]. PS was prepared by emulsion polymerization process and the properties are presented in the supplementary section [13]. A solution of benzoxazine monomer in chloroform (20% w/v) was added drop wise to 100 mL aqueous PVA solution (2.5% w/v) under continuous stirring (500 rpm). Separately, a solution of PS in chloroform (2–10% w/v) was injected through a hypodermic syringe into the reaction vessel, maintained at 60 °C, at different stirring rates (400–600 rpm). Post-evaporation of chloroform, the reaction mixture was cooled, and the Bz–C encapsulated PS microcapsules were filtered and washed repeatedly with water followed by drying under vacuum.

Detailed characterization of the monomer and microencapsulated PS is presented in the supplementary section.

3. Results and discussion

Bz–C was prepared using solventless method, followed by its encapsulation in PS microcapsule. The effect of operating parameters, particularly stirring speed and polymer concentration on the microcapsule dimensions were investigated.
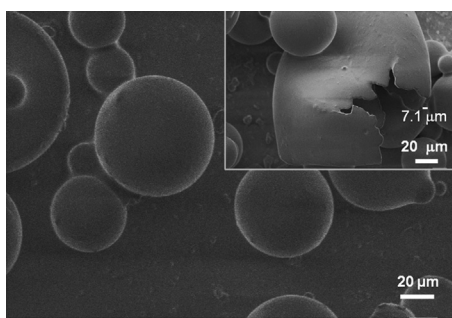
Fig. 1. SEM image of Bz–C encapsulated PS microcapsules. Inset shows the magnified image of a broken microcapsule indicating its shell wall thickness.
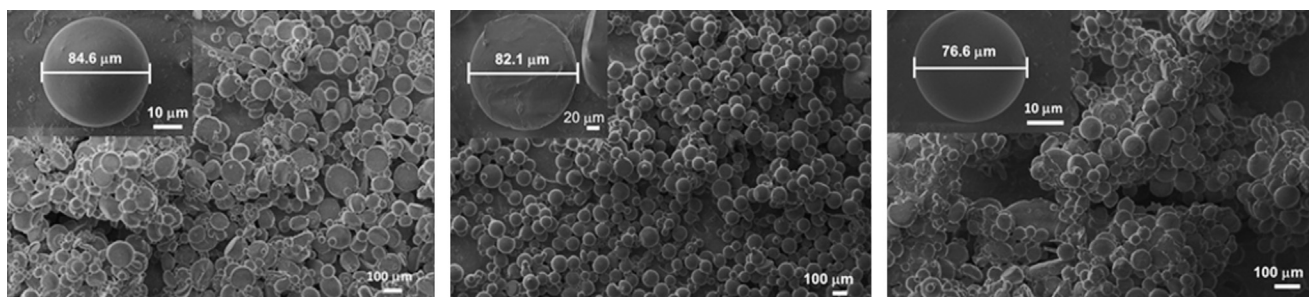
Preparation of cardanol based benzoxazine: Conventionally, the synthesis of benzoxazine monomers requires polar aprotic solvents, which have to be removed subsequently. Solvent-less synthesis of highly rigid Bz monomers results in high viscosity at higher percentage conversion which may account for incomplete conversion of reactants and poor yields. However, the low viscosity of cardanol (145 mPa s) facilitates its use as a reactive diluent and the reaction of aniline with cardanol and formaldehyde (1:1:2), post purification led to the formation of a viscous liquid (80% yield). The structure of the monomers was confirmed by ^{1}H-NMR (Fig. S1, supplementary section) and FTIR (Fig. S2, Supplementary section) spectroscopy. The ^{1}H –NMR spectra of Bz–C exhibited characteristic resonances at ~5.3 ppm (s, ArOCH$_2$N), ~4.6 ppm (s, ArCH$_2$N) suggesting conversion of hydroxyl functionalities to oxazines. The formation of oxazine ring was also substantiated by the appearance of new absorption bands at ~1250 and ~1030 cm^{-1} due to the Ar–C–O oxazine asymmetric and symmetric stretch respectively. The absence of absorption bands due to N–H stretching (3360–3442 cm^{-1}) and N–H bending (1619 cm^{-1}) in the spectra of Bz–C further suggests the absence of unreacted aniline in the Bz monomer indicating completion of reaction.

Cardanol based benzoxazines exhibit excellent adhesive properties, as indicated by lap shear strength (LSS) as high as 20–30 kg/cm^2 at 150 °C [3], which advocate their potential towards self-healing applications. The benzoxazine moieties underwent thermally activated ROP to form polymer networks containing > N- and –OH functionalities which result in extensive H-bonding with the matrix/surface and translate to strong adhesive properties.

Physical microencapsulation of benzoxazine: Bz–C was encapsulated in fragile PS containers by solvent evaporation technique to form pale yellow microcapsules, the SEM images of which are presented in Fig. 1. The microcapsules are perfectly spherical, and exhibit a smooth surface texture. The thickness of the shell wall, was found to be ~7 ± 1 μm, as can be seen in the SEM images of broken microcapsules (Fig. 1, Inset).

Effect of stirring speed: The effect of increasing stirring speed on the microcapsule dimensions is presented in Fig. 2. As expected, increasing the rate of stirring led to a decrease in the particle dimensions, which could be attributed to the shearing of the large oily droplets into smaller microspheres under higher shear rates [14,15].

Effect of concentration of encapsulating polymer: Core-content is one of the most important characteristics of microcapsules. In view of the similar solubilities of Bz–C and PS, conventional technique of core-content quantification proved unsuccessful and the ratio of heat of curing (DSC technique) of encapsulated benzoxazines to that of the neat benzoxazines was used to determine the same. The core content was found to increase from 19% to 38% by decreasing the PS content in the feed solution from 10% to 2% w/v, at a constant stirring speed of 500 rpm. However, the core content could not be increased further, due to the fragile

Fig. 2. SEM image of microcapsules prepared under different stirring speeds (a) 400, (b) 500, (c) 600 rpm. Inset shows the enlarged image of a single microcapsule. (Label a b and c in picture).

nature of the shell, which appears to be incapable of cementing higher amounts of healing agent.

The TGA traces of the resultant microcapsules in air atmosphere are presented in Fig. S7. Neat PS exhibits a mass loss of ~98% at 500 °C. The thermal decomposition of PS reportedly occurs in a single step via unzipping reaction, while polybenzoxazines exhibit a bimodal mass loss distribution centered at 448 and 558 °C [3]. Similar decomposition behaviour was observed in all the encapsulated microcapsules, suggesting polymerisation of the Bz–C during heating.

To demonstrate the potential of the Bz–C encapsulated microcapsules in the field of self healing, ~5 mg of microcapsules were placed between two glass slides, crushed by manual tapping and placed at ~240 °C for 30 min. Photographs, captured at different stages of experimentation are presented in the supplementary section. The glass slides were found to seal completely, and could not be separated by exposure to solvents even for extended periods (72 h).

It is to be noted that the system presently investigated necessitate elevated temperatures for curing. However, in view of possibility of structural modification by judicious choice of functional groups, low temperature self healing systems can be devised, which can open up novel opportunities in this field.

4. Conclusion

The low viscosity of cardanol facilitated its use as reactive diluent for the synthesis of Bz–C, which was subsequently encapsulated in PS by solvent evaporation technique. Microcapsules with dimensions ranging from 75 to 86 μm could be prepared by varying the stirring speed from 600 to 400 rpm. By decreasing the concentration of PS in the feed solution, it was possible to increase the core content as high as 38% (w/w).

Appendix A. Supporting information

Supplementary data associated with this article can be found in the online version at http://dx.doi.org/10.1016/j.matlet.2014.07.048.

References

[1] Taskin OS, Kiskan B, Yagci Y. Polybenzoxazine precursors As self-healing agents for polysulfones. Macromolecules 2013;46:8773–8.

[2] Brown EN, Kessler MR, Sottos NR, White SR. In situ poly(urea-formaldehyde) microencapsulation of dicyclopentadiene. J Microencapsul 2003;20:719–30.

[3] Lochab B, Varma I, Bijwe J. Thermal behaviour of cardanol-based benzoxazines. J Therm Anal Calorim 2010;102:769–74.

[4] Lochab B, Varma I, Bijwe J. Cardanol-based bisbenzoxazines. J Therm Anal Calorim 2012;107:661–8.

[5] Lochab B, Shukla S, Varma IK. Naturally occurring phenolic sources: monomers and polymers. RSC Adv 2014 (10.1039/C4RA00181H).

[6] Lochab B, Varma I, Bijwe J. Blends of benzoxazine monomers. J Therm Anal Calorim 2013;111:1357–64.

[7] Oie H, Sudo A, Endo T. Acceleration effect of N-allyl group on thermally induced ring-opening polymerization of 1,3-benzoxazine. J Polym Sci, Part A: Polym Chem 2010;48:5357–63.

[8] Baqar M, Agag T, Ishida H, Qutubuddin S. Methylol-functional benzoxazines as precursors for high-performance thermoset polymers: unique simultaneous addition and condensation polymerization behavior. J Polym Sci, Part A: Polym Chem 2012;50:2275–85.

[9] Tripathi M, Rahamtullah Roy PK, Kumar D, Rajagopal C. Influence of microcapsule shell material on the mechanical behavior of epoxy composites for self-healing applications. J Appl Polym Sci. 2014;10:1002.

[10] Rochmadi AP, Hasokowati W. Mechanism of microencapsulation with urea-formaldehyde polymer. Am J Appl Sci. 2010;7:739–45.

[11] Andreu R, Reina JA, Ronda JC. Carboxylic acid-containing benzoxazines as efficient catalysts in the thermal polymerization of benzoxazines. J Polym Sci, Part A: Polym Chem 2008;46:6091–101.

[12] Sánchez L, Sánchez P, Lucas A, Carmona M, Rodríguez J. Microencapsulation of PCMs with a polystyrene shell. Colloid Polym Sci. 2007;285:1377–85.

[13] Roy PK, Rawat AS, Rai PK. Synthesis, characterisation and evaluation of polydithiocarbamate resin supported on macroreticular styrene–divinylbenzene copolymer for the removal of trace and heavy metal ions. Talanta 2003;59:239–46.

[14] Chaudhary S, Parthasarathy S, Kumar D, Rajagopal C, Roy PK. Amine functionalised poly(styrene) microspheres as thermoplastic toughener for epoxy resin. Polym Compos 2014. http://dx.doi.org/10.1002/pc.22927.

[15] Roy P, Iqbal N, Kumar D, Rajagopal C. Polysiloxane-based core-shell microspheres for toughening of epoxy resins. J Polym Res 2014;21:1–9.

Interfacial encapsulation of bio-based benzoxazines in epoxy shells for temperature triggered healing

Pratibha Sharma,[1,2] Bimlesh Lochab,[3] Devendra Kumar,[2] Prasun Kumar Roy[1]

[1]Centre for Fire, Explosive and Environment Safety, DRDO, Timarpur, Delhi, India
[2]Department of Applied Chemistry and Polymer Technology, Delhi Technological University, Delhi, India
[3]Department of Chemistry, School of Natural Sciences, Shiv Nadar University, UP, India
Correspondence to: P. K. Roy (E-mail: pk_roy2000@yahoo.com) or B. Lochab (E-mail: bimlesh.lochab@snu.edu.in)

ABSTRACT: Successful application of interfacial engineering for the preparation of cross-linked epoxy microspheres containing thermally polymerizable cardanol-based benzoxazine (Bz-C) monomer in the core is demonstrated. Bz-C is facilely synthesized by Mannich type condensation of cardanol (a by-product of cashew nut industry) and aniline with formaldehyde under solventless conditions. **The encapsulation process relies on the preferential reaction of polydimethylsiloxane immiscible epoxy resin and amine-based hardener to form a cross-linked spherical shell at the interface.** The microcapsule dimensions and core content could be tailored by modulating the operating parameters, particularly stirring speed and Bz-C: epoxy ratio. Spherical microcapsules with a core content of ∼37% were obtained when the reaction was carried out at 600 rpm, while maintaining the reaction medium at 70°C with Bz-C: epoxy ratio of 2.3: 1. The simplicity and versatility of the present methodology are the forte of this technique, which widens the scope for large-scale application of benzoxazines in the field of temperature triggered healing. © 2015 Wiley Periodicals, Inc. J. Appl. Polym. Sci. **2015**, *132*, 42832.

INTRODUCTION

Polybenzoxazines belong to a class of addition cure phenolic systems which possess excellent mechanical, thermal, and flame retardant properties. The flexibility in designing the structure of benzoxazine monomers allows enormous scope in tailoring the properties of polymers for a wide range of applications in the field of polymer technology.[1] In addition, polybenzoxazines exhibit high glass transition temperature (T_g), long shelf life, chemical resistance, low water absorption, release of no by-products which translates to negligible volumetric change upon curing. Most interestingly, benzoxazines do not require any catalyst for their curing, a feature which bestow them interesting candidature as far as healing agents in mendable compositions is concerned,[2] provided they can be encapsulated in fragile microcapsules.

Currently, conventional healing agents are restricted to a class of monomers which undergo catalytic ring opening polymerization, e.g., epoxy, dicyclopentadiene (DCPD), etc., which in turn are encapsulated in the polymeric shells of melamine–formaldehyde, urea–formaldehyde (UF), and gelatin-gum arabic coacer-

vate.[3] Conformist micro-encapsulation procedures involve *in situ* emulsion polymerization of urea or melamine with formaldehyde on the surface of the hydrophobic dispersed phase of the precursor. The condensation process necessitate acidic environment (pH <3),[4,5] conditions which can induce curing in benzoxazines.[6,7] This imposes a restriction on the technique used for the encapsulation of benzoxazines in commonly used shell walls. To circumvent these issues, we have previously reported the encapsulation of benzoxazines in polystyrene shell with a core content of the order of 37%.[8]

In this article, we adopt an interfacial engineering approach to prepare epoxy microcapsules containing core of liquid benzoxazine. The potential of liquid–liquid interface toward the preparation of nanocrystals, thin films[9–11] and microcapsules[12,13] has been well reported. We believe that this concept could very well be extended to prepare microcapsules with interesting morphologies. Our aim is to elaborate this conceptually, and to elucidate this approach, we disperse epoxy–benzoxazine solution in silicone medium followed by addition of a polyamine which reacts selectively with the epoxy. In view of the preferential reaction of oxirane with amine, we engender that the reaction would be

driven to the interface, leading to the formation of cross-linked spherical shell. We adopt a "sustainable" approach for the synthesis of cardanol-based benzoxazine (Bz-C),[14,15] where the role of cardanol is extended as a reactive diluent.[16]

Conventionally, liquid paraffin is used as a dispersing phase; however, the viscosity of liquid paraffin is not high enough to maintain system stability,[17] so rapid polymerization is needed to prevent the coagulation of the polymerization droplets.[18] Polydimethylsiloxane (PDMS) was chosen as the reaction medium in view of its thermal stability and solubility differences with both the resins as well as triethylenetetramine (TETA) hardener.[18] The effect of operating parameters, particularly rate of stirring and Bz-C: epoxy ratio on the microcapsule dimensions, was established to optimize the experimental conditions for the preparation of microcapsules.

EXPERIMENTAL

Materials

Cardanol was procured from Satya Cashew Chemicals Pvt. (India), paraformaldehyde (CDH, "LR"), sodium sulfate (CDH, "AR"), aniline (Merck, "AR"), and chloroform from Rankem. Cardanol used in the current work possess double bonds in the alkylene chain at the m-position, as monoene (25%), diene (40%), and triene (34%), and unidentified product (rest) as determined by high performance liquid chromatography (HPLC). Epoxy resin (Ciba Geigy, Araldite CY 230; epoxy equivalent 200 eq g^{-1}) and hardener (HY 951; amine content 32 eq kg^{-1}) were used as received. Double distilled water was used throughout the course of study. PDMS (CDH, kinematic viscosity 300 cSt) was used without any further purification.

Characterization

Thermo scientific fourier transform infrared (FTIR) (NICOLET 8700) analyzer with an attenuated total reflectance (ATR) crystal accessory was used to perform FTIR spectra of samples in the wavelength range 4000–600 cm^{-1}, recording 32 scans at 4 cm^{-1} resolution for each spectrum. The angle of incidence of the germanium ATR crystal used was characteristically 45°. Bruker AC 300 MHz fourier transform nuclear magnetic resonance (FT-NMR) spectrometer was used to record the ^{1}H-NMR of the samples. The spectrum was recorded in CDCl$_3$ using tetramethylsilane as the internal standard.

Thermal behavior was investigated using Perkin Elmer Diamond STG-DTA under N$_2$ atmosphere (flow rate = 50 mL min^{-1}) in the temperature range of 50–700°C. A heating rate of 10°C min^{-1} and sample mass of 5.0 ± 0.5 mg were used for each experiment. Calorimetric studies were performed on a differential scanning calorimeter (TA instruments Q 20). For dynamic differential scanning calorimetry (DSC) scans, samples (10 ± 2 mg) were sealed in aluminum pans, and heated from 0°C to 300°C at 10°C min^{-1}. Nitrogen was purged at a rate of 50 mL min^{-1} to minimize the oxidation of the sample during the curing process. Prior to the experiments, the instrument was calibrated for temperature and enthalpy using standard indium and zinc. Thermal equilibrium was regained within 1 min of sample insertion, and the exothermic reaction was considered to be complete when the recorder signal leveled off to the baseline. The total area under the exothermic curve was determined to quantify the heat of curing.

Optical images of suspended micro droplets were captured using an optical microscope Motic, B3-223PL. The surface morphology of samples was studied using a scanning electron microscope (Zeiss EVO MA15) under an acceleration voltage of 1 kV. Samples were mounted on aluminium stubs and sputter-coated with gold and palladium (10 nm) using a sputter coater (Quorum-SC7620) operating at 10–12 mA for 120 s. The microsphere size distribution was determined from the scanning electron microscope (SEM) images. Image J software was used to measure the diameter of 50 spheres per image.

Lap shear strength (LSS) of bonded joints on steel plates of roughness (R_a 0.42–0.51 μm) was measured in accordance with the American standard for testing and materials (ASTM) D1002 using Universal Testing System (International equipments) at a crosshead speed of 1.3 mm min^{-1}.

Preparation of Benzoxazine Monomers from Cardanol

The synthesis of benzoxazine monomer from cardanol has been reported in our previous papers.[16] In brief, a mixture of cardanol (100 g, 0.33 mol), aniline (30.1 mL, 0.33 mol), and paraformaldehyde (19.8 g, 0.66 mol) was slowly heated to 80°C and maintained for a period of 1 h under N$_2$ atmosphere. The mixture was further heated and maintained at 90°C for additional 2 h, after which it was cooled and 500 mL of water was added to the same. The organic layer was collected after extraction with chloroform. After drying over sodium sulphate and solvent removal under reduced pressure, the residue was dried at 70°C under vacuum to yield Bz-C in quantitative yield as red brown oil.

Microencapsulation of Cardanol Benzoxazine in Epoxy

Benzoxazine was encapsulated in cross-linked epoxy shell by the preferential reaction of epoxy resin with TETA hardener at the silicone–benzoxazine interface, while keeping the mixture suspended in silicone medium by agitation. The immiscibility of the benzoxazine and epoxy resin in PDMS was first verified by capturing the optical images using computer interfaced optical microscope at a magnification of 40 of the suspensions prepared by stirring the resins vigorously (1000 rpm) for a period of 5 min.

Subsequently, epoxy was first homogenized in Bz-C in varying ratio (2.3 : 1–1.0 : 1; 10 g). The reaction was performed in reaction vessel under inert atmosphere. Silicone oil (200 mL) was purged with nitrogen over a period of 15 min. The homogenized benzoxazine–epoxy mixture was introduced into silicone, which was maintained at 70°C under continuous stirring. Stoichiometric quantity of TETA (13% w/w epoxy) was subsequently injected slowly through a hypodermic syringe and the curing reaction was allowed to continue for 8 h under varying stirring speeds (500–700 rpm), after which the reaction mixture was cooled and filtered. Epoxy microspheres were also prepared in the absence of benzoxazines under similar conditions, while maintaining a constant temperature of 70°C and a stirring speed of 600 rpm. The core content of benzoxazine-filled microcapsules was quantified as per the procedure reported previously.[8]
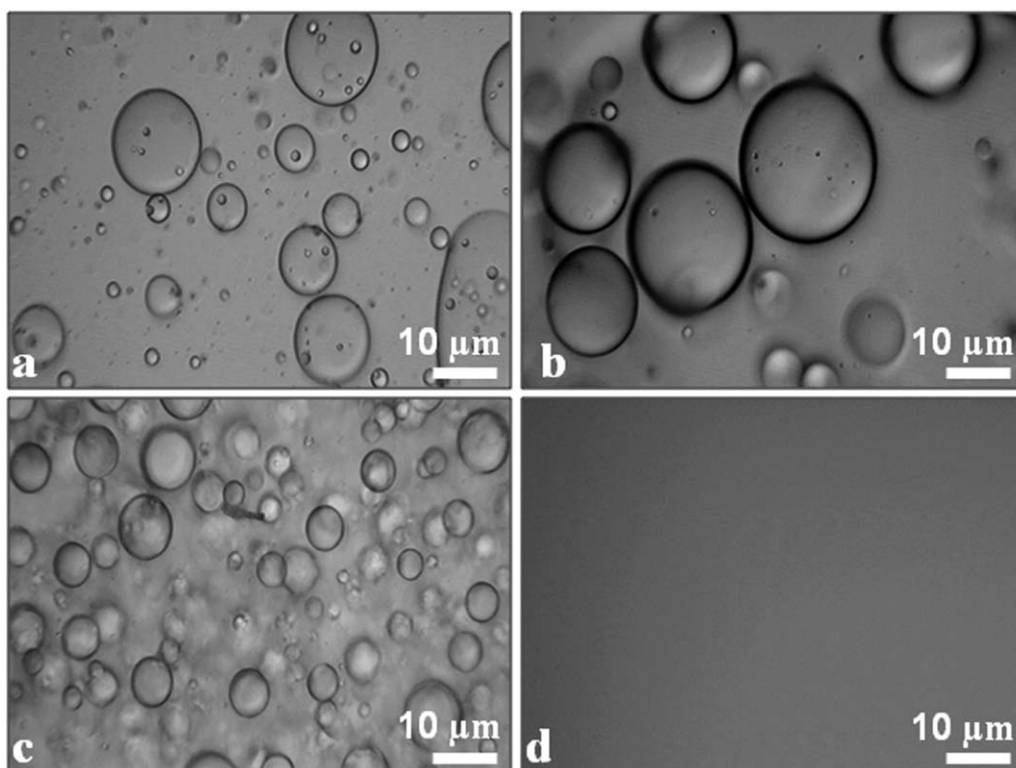
Figure 1. Optical images of (a) epoxy–PDMS, (b) epoxy–benzoxazine–PDMS mixtures, (c) benzoxazine–PDMS, and (d) epoxy–benzoxazine.

$$\text{Core content } (\%) = \frac{\Delta H_{\text{curing, encapsulated Bz–C}}}{\Delta H_{\text{curing, Bz–C}}} \times 100$$

where enthalpy of curing of neat Bz-C ($\Delta H_{\text{curing, Bz–C}}$) is 71.1 ± 1.8 J g^{-1}.

Determination of Adhesive Property of Microcapsules

To demonstrate the potential of the Bz-C encapsulated microcapsules in the context of temperature triggered healing, micro-

capsules (0.3 ± 0.01 g) with different core content were placed between two steel plates, crushed by manual tapping and placed at 216°C for a period of 1 h. A total of four replicates were tested per sample.

RESULTS AND DISCUSSION

The search for new synthetic methodologies in the context of benzoxazine microencapsulation has led us to explore the potential of interfacial engineering toward the formation of benzoxazine encapsulated epoxy microcapsules. More specifically, we studied the effect of operating parameters on the microcapsule dimensions and core content.
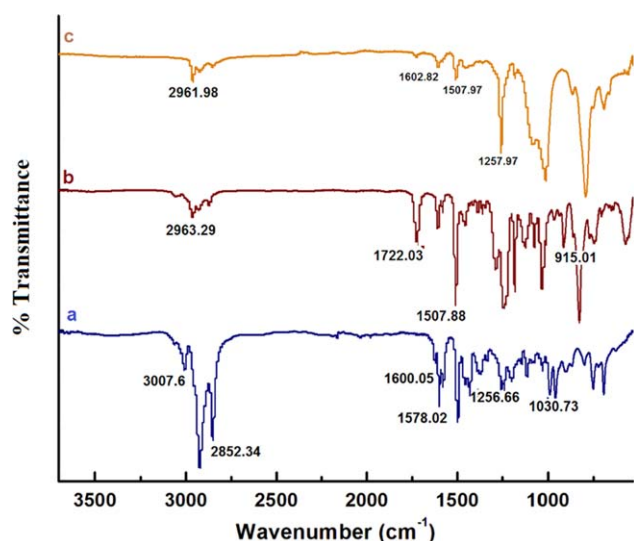
Figure 2. FTIR spectra of (a) Bz-C, (b) epoxy resin, and (c) microcapsules. [Color figure can be viewed in the online issue, which is available at wileyonlinelibrary.com.]
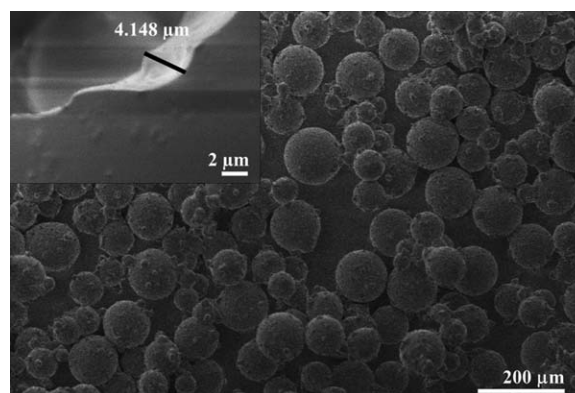
Figure 3. SEM image of Bz-C encapsulated in cross-linked epoxy shell. Inset shows the magnified image of a broken microcapsule indicating thickness of its shell wall.
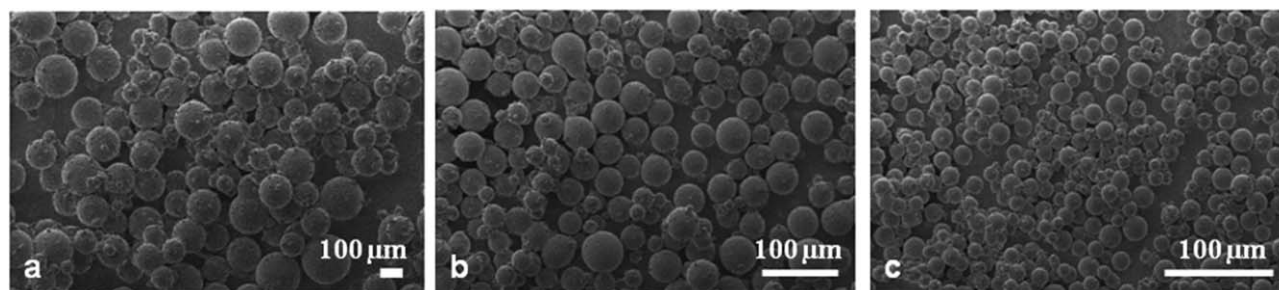
Figure 4. Effect of stirring speed on the surface morphology of microcapsules: (a) 500 rpm, (b) 600 rpm, and (c) 700 rpm.

Preparation of Cardanol-Based Benzoxazine

The synthesis of benzoxazine monomers is usually performed in the presence of polar aprotic solvents, which necessitate elaborate purification steps.[19,20] Solventless synthesis of rigid benzoxazine monomers result in extremely viscous mixtures, especially at higher conversions which in turn result in incomplete conversion of reactants leading to poor yields. A major advantage of using cardanol as the phenolic component is associated with its low viscosity (145 mPa s),[21] which permits its use as a reactive diluent. The reaction of aniline with cardanol and formaldehyde (1 : 1 : 2), post purification led to the formation of a viscous liquid in high yields (>90%). The structure of the monomers was confirmed by ^{1}H-NMR (Figure S1, Supporting Information) and FTIR spectroscopy (Figure S2, Supporting Information).

The formation of oxazine ring was confirmed by the appearance of new absorption bands at ∼1250 and ∼1030 cm^{-1} due to the Ar–C–O oxazine asymmetric and symmetric stretch, respectively.[22] The absence of absorption bands due to N–H stretching (3360–3442 cm^{-1}) and N–H bending (1619 cm^{-1}) in the spectra of Bz-C further suggests the absence of unreacted aniline in the Bz monomer, thereby indicating completion of the reaction. The formation of oxazines from hydroxyl functionalities was reconfirmed by the presence of characteristic resonances at ∼5.3 ppm (s, ArOCH$_2$N) and ∼4.6 ppm (s, ArCH$_2$N) in the ^{1}H-NMR spectra.

Microencapsulation of Cardanol-Based Benzoxazine in Cross-Linked Epoxy

The conventional *in situ* polymerization technique involves the formation of the encapsulating shell, essentially in the dispersion medium. For example, in the most commonly reported UF microencapsulation process, the monomers, namely urea and formaldehyde react in the aqueous phase to form a low molecular weight prepolymer. With increasing molecular weight of the prepolymer, deposition occurs at the healant–water interface and the cross-linking process continues to form the microcapsule shell wall.[4] The smooth inner surface of the shell basically results from the deposition of low molecular weight prepolymer at the interface while the prepolymer is still soluble. The roughness observed on the outer shell surface result from the precipitation of higher molecular weight prepolymer formed in the aqueous solution, which subsequently aggregate and deposit on the capsule surface.[23]

On the other hand, in the present study, epoxy microcapsules were prepared by the preferential reaction of the epoxy resin with TETA at the silicone–benzoxazine interface. The Hoy's solubility parameter of epoxy, TETA, and benzoxazine have been calculated

based on the group contribution models of Hoy.[24] The structure of the resins and detailed calculations are presented in the Supporting Information. It can be seen that the solubility parameter of cycloaliphatic epoxy, benzoxazine, and TETA are in the same range, i.e., 9.02 cal$^{1/2}$ cm$^{3/2}$ mL^{-1}, 9.01 cal$^{1/2}$ cm$^{3/2}$ mL^{-1} and 10.8 cal$^{1/2}$ cm$^{3/2}$ mL^{-1}, respectively. It was not possible to ascertain the Hoys parameter for PDMS in view of its inorganic–organic hybrid nature; however, the Hansen solubility parameter of TETA (22.7 MPa$^{1/2}$)[22] is markedly higher than that of PDMS (14.9 MPa$^{1/2}$).[7,25] This difference in miscibility results in their existence as phase separated droplets under agitation. To verify the same, the optical images of epoxy–PDMS, benzoxazine–PDMS, and epoxy–benzoxazine–PDMS mixtures were captured, where the presence of droplets in the medium is clearly indicative of its immiscibility (Figure 1).

Preliminary studies were performed to arrive at the optimal reaction conditions, especially reaction time and temperature. For successful encapsulation, the rate of reaction between the epoxy and amine should exceed the rate of molecular diffusion.[26] The reaction condition should be tuned so as to allow the curing process to proceed at the reactive interface till complete exhaustion of the epoxy and amine, thereby leading to the formation of a stable cross-linked shell around the unreacted benzoxazine core. The curing behavior of the cycloaliphatic epoxy resin in the presence of TETA, as established using nonisothermal calorimetry, is presented in the Supporting Information (Figure S3).[27] It can be seen that the exothermic curing process initiates at ∼61°C and reaches a peak at ∼96°C. On the basis of this curing profile,
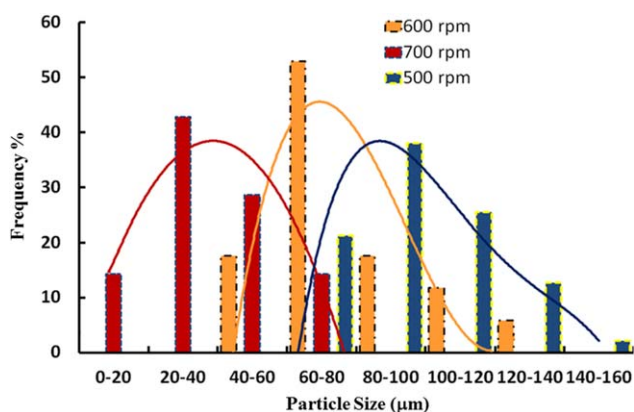
Figure 5. Effect of stirring speed on the average particle size distribution of microcapsules. [Color figure can be viewed in the online issue, which is available at wileyonlinelibrary.com.]
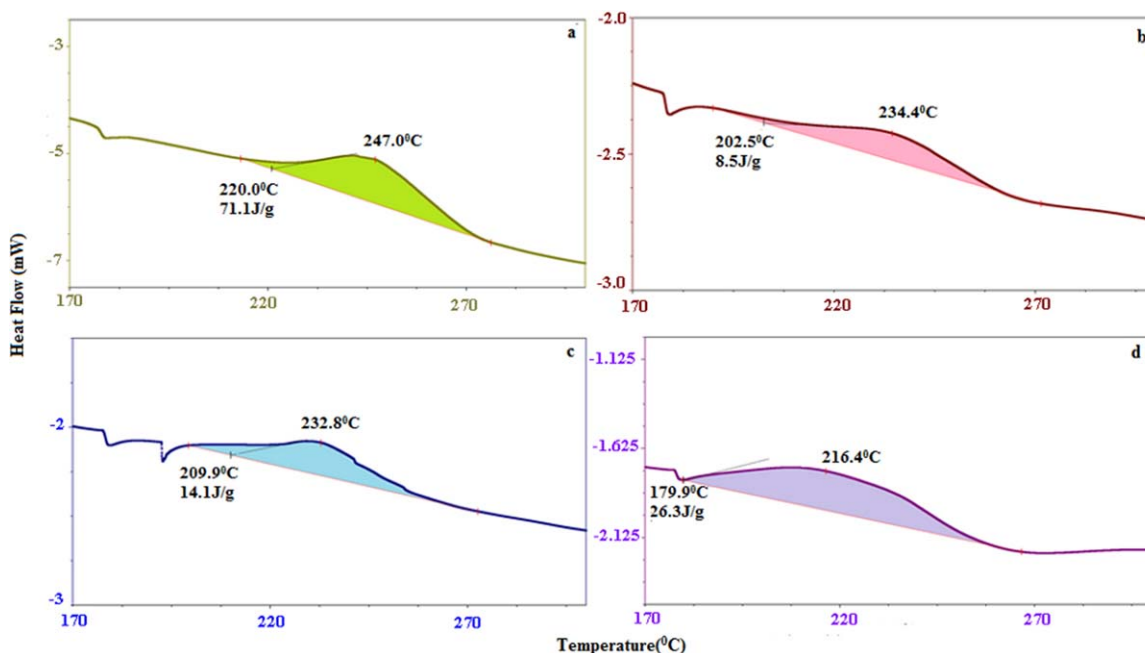
Figure 6. DSC traces of (a) Bz-C and epoxy encapsulated benzoxazine microcapsules prepared using Bz-C: Epoxy ratio of (b) 1 : 1, (c) 1.5 : 1, and (d) 2.3 : 1. [Color figure can be viewed in the online issue, which is available at wileyonlinelibrary.com.]

studies on encapsulation were performed at temperatures as low as 60°C. However, when the reaction medium was maintained at $T < 65°C$, complete curing necessitated prolonged periods (~36 h), which was too long to be of any practical significance. The rate of the curing reaction increased significantly with increasing temperature and free flowing microcapsules could be obtained within 10 h at 70°C. Further increase in temperature was impractical in view of the strong vapor pressure–temperature dependence of TETA,[28] which led to significant vaporization of the amine, thereby leading to the formation of partially cured and tacky microcapsules. In view of the above, the effects of other operating parameters were performed while maintaining the reaction medium at 70°C.

The FTIR of benzoxazine monomer, epoxy resin, and cured microcapsules is presented in Figure 2. Characteristic band at 915 cm^{-1} associated with the CO deformation due to oxirane ring is visible in the FTIR spectra of liquid epoxy resin.[29] The absence of this absorption and the peaks confirming the structure of benzoxazine in the FTIR spectra of microcapsules indicates successful encapsulation of the benzoxazine monomer in cross-linked epoxy shell.

Effect of Stirring Speed on Particle Size Distribution and Morphology

Bz-C was encapsulated in interfacially engineered cross-linked epoxy shell to form microcapsules, pale yellow in color (Figure S4), the SEM images of a representative batch being presented in Figure 3. The thickness of the shell wall was found to be ~4.1 μm, as can be seen in the SEM images of broken microcapsules (Figure 3, Inset).

The SEM images of the microcapsules prepared under varying stirring speeds are presented in Figure 4 and the related average particle size distribution is presented in Figure 5. It is interesting

to note that the high viscosity of the silicone oil employed for the purpose is proficient in stabilizing the suspended epoxy–Bz-C micro-droplets, thereby abating the necessity of a suspending agent.[18] As expected, increasing the rate of stirring led to a shift in the average particle size toward lower dimensions, which could be attributed to the extensive shearing of the large oily droplets into smaller microspheres. Among the experimental parameters: agitation rate, temperature, surfactant type and concentration, hydrodynamics, viscosity, and interfacial tension of the media are primary influential parameters on the microcapsule dimension. Stirring speed, particularly, defines the equilibrium between shear forces and interfacial tension of the discrete oil droplets.[30] It was observed that free flowing microcapsules could not be obtained upon lowering the stirring speeds to <500 rpm (SEM image presented in Supporting Information Figure S5). Increasing the stirring speed to >700 rpm is expected to lead to the formation of microcapsules of significantly lower dimensions to be of any practical value. Under optimal reactions conditions, i.e., stirring speed of 600 rpm, reaction temperature of 70°C and Bz-C: (2.3 : 1), spherical microcapsules were obtained.

Core Content

Core content refers to a quantitative estimate of the polymerizable fraction actually available in the microcapsules, which in

Table I. Effect of Bz-C: Epoxy Ratio on the Core Content of Microcapsules

Bz-C: Epoxy ratio (% w/w)	ΔH_{curing} (J/g)	Core content (%)
1 : 1	8.5	11.9
1.5 : 1	14.1	19.8
2.33 : 1	26.3	37.0
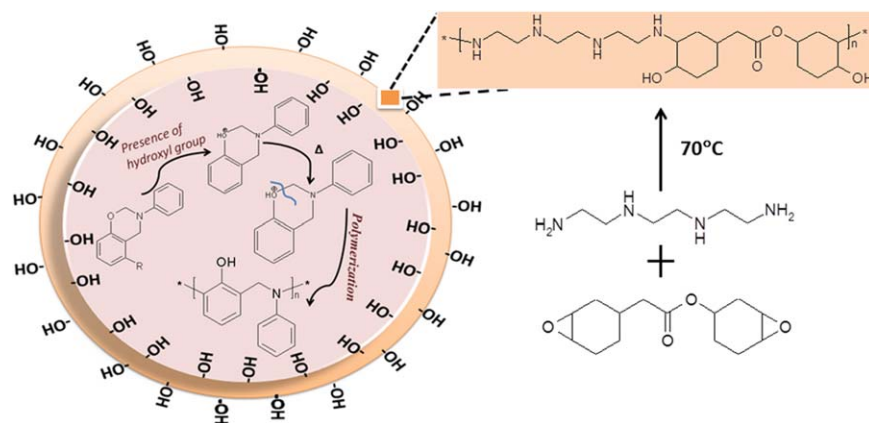
Figure 7. Interaction of hydroxyl groups on the inner surface with the encapsulated benzoxazine. [Color figure can be viewed in the online issue, which is available at wileyonlinelibrary.com.]

the present context was quantified as the ratio of heat of curing of encapsulated benzoxazine to that of the neat monomer.[8] In view of the ring strain associated with oxazine ring, Bz-C polymerizes through thermally activated ring opening polymerization and the DSC traces obtained during controlled heating are presented in Figure 6. The DSC trace of cured epoxy microsphere prepared in the absence of benzoxazine has been presented in the Supporting Information (Figure S6). As expected, the exotherm associated with the curing of benzoxazine cannot be observed in the DSC trace. The core content of the benzoxazine-filled microcapsule increased from 12% to 37% as the weight fraction of epoxy in the feed solution was lowered from 50% to 30% w/w while maintaining a constant stirring speed of 600 rpm (Table I).

Although attaining larger core content is a vital target of any encapsulation process, it was not possible to increase the core content further, probably due to high surface energy of microcapsules, which led to their agglomeration on increasing the benzoxazine content in the feed.[25] It was interesting to observe a lowering in the onset of curing behavior as the composition of the feed solution (Epoxy: Bz-C) was varied from 1 : 1 to 2.33

: 1. To gain further insight into this aspect, benzoxazine curing was also studied in the presence of liquid epoxy resin. Interestingly, the curing exotherm was found to shift to higher temperature, as shown in the Supporting Information (Figure S7). These studies confirm that the lowering of curing temperature in the present study could be credited to the interaction of Bz-C monomer with hydroxyl functionalities, which in turn resulted due to the nucleophilic attack of amine on oxirane rings of epoxy resin as per the reaction depicted in Figure 7. Acidic functionalities[31] along with allylic[32] and methylol[33], etc., reportedly play an active role in catalyzing the polymerization of benzoxazines. Our studies indicate that aliphatic alcohols, although less acidic, are also capable of lowering of T_{onset} temperature of Bz-C ($T_{onset} = 220°C$) substantially to 179°C.

TG-DTG traces of Bz-C, both before and after encapsulation in epoxy shells under air atmosphere, are presented in the Figure 8. It can be seen that the polybenzoxazine, formed as a result of temperature-induced curing, undergoes oxidative degradation at 310°C. Encapsulation of benzoxazine in epoxy shell led to a substantial decrease in the curing temperature to 179°C (Figure 6); however, the onset degradation temperature remained practically unaltered.

Adhesive Property of Microcapsules
The adhesive ability of the microcapsules encapsulating benzoxazine was quantified by evaluating the LSS using stainless steel coupons. Cardanol-based benzoxazines have been reported to exhibit LSS of 20–30 kg cm^{-2} at 150°C, which advocate their caliber as healing monomers in mendable compositions.[34] The average values of LSS exhibited by the samples are tabulated in Table II and the representative load–displacement curve is presented in Supplementary Section (Figure S8).

Figure 8. TGA traces of (a) Bz-C encapsulated epoxy microcapsules and (b) Bz-C. [Color figure can be viewed in the online issue, which is available at wileyonlinelibrary.com.]

Table II. Lap Shear Strength of Microcapsules with Different Core Content

Bz-C: Epoxy ratio (% w/w)	Core content (%)	LSS (kg cm^{-2})
1 : 1	11.9	13.5 ± 1.9
1.5 : 1	19.8	16.0 ± 2.6
2.33 : 1	37.0	25.3 ± 3.2
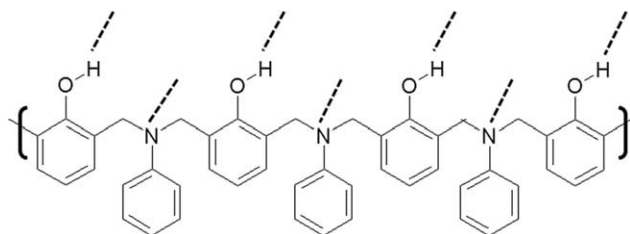
Figure 9. Functional groups in polybenzoxazine involved in H-bonding with the contact surface.

Subsequent to the curing of the Bz-C released from the microcapsules, the plates could not be separated by exposure to solvents like dimethyl formamide (DMF) and toluene, even for extended periods (72 h).The curing of Bz-C by thermally activated ring opening polymerization results in the formation of >N– and –OH functionalities as confirmed by FTIR spectroscopy [Figure S2(c)], which are capable of exhibiting extensive H-bonding with the contact surface as shown in Figure 9, thereby rendering excellent adhesive properties.

Photographs, captured at different stages of the experimentation, are presented in the Supporting Information for clear visualization (Figure S9).

CONCLUSION

The implementation of interfacial engineering for encapsulation of benzoxazine enabled the preparation of cross-linked epoxy microcapsules containing reactive monomer in the core. Reaction parameters, especially benzoxazine: epoxy ratio and stirring speed, were found to have a pronounced effect on the core content and particle size distribution of the microspheres. Under optimal conditions, i.e., stirring speed of 600 rpm, reaction temperature of 70°C, and Bz-C: Epoxyratio of 2.33: 1, spherical microcapsules were obtained with a core content of 37%. The presence of hydroxyl groups formed as a result of epoxy curing was found to reduce the onset of curing temperature from 220°C to 179°C. We believe that in view of the enormous scope in modifying the structure of benzoxazines, low temperature self-healing systems can be devised in the future, which can open up novel opportunities in this field.

REFERENCES

1. Ghosh, N. N.; Kiskan, B.; Yagci, Y. *Prog. Polym. Sci.* **2007**, *32*, 1344.

2. Taskin, O. S.; Kiskan, B.; Yagci, Y. *Macromolecules* **2013**, *46*, 8773.

3. Sun, G.; Zhang, Z. *Int. J. Pharm.* **2002**, *242*, 307.

4. Brown, E. N.; Kessler, M. R.; Sottos, N. R.; White, S. R. *J. Microencapsulation* **2003**, *20*, 719.

5. Rochmadi *Am. J. Appl. Sci.* **2010**, *7*, 739.

6. Andreu, R.; Reina, J. A.; Ronda, J. C. *J. Polym. Sci., Part A: Polym. Chem.* **2008**, *46*, 6091.

7. Ishida, H.; Rodriguez, Y. *Polymer* **1995**, *36*, 3151.

8. Sharma, P.; Shukla, S.; Lochab, B.; Kumar, D.; Kumar Roy, P. *Mater. Lett.* **2014**, *133*, 266.

9. Scott, C.; Wu, D.; Ho, C.-C.; Co, C. C. *J. Am. Chem. Soc.* **2005**, *127*, 4160.

10. Detsri, E.; Dubas, S. T. *J. Appl. Polym. Sci.* **2013**, *128*, 558.

11. Rao, C. N. R.; Kulkarni, G. U.; Agrawal, V. V.; Gautam, U. K.; Ghosh, M.; Tumkurkar, U. *J. Colloid Interface Sci.* **2005**, *289*, 305.

12. Koh, E.; Kim, N.-K.; Shin, J.; Kim, Y.-W. *RSC Adv.* **2014**, *4*, 16214.

13. Liu, X.; Zhang, H.; Wang, J.; Wang, Z.; Wang, S. *Surf. Coat. Technol.* **2012**, *206*, 4976.

14. Sethuraman, K.; Alagar, M. *RSC Adv.* **2015**, *5*, 9607.

15. Lochab, B.; Shukla, S.; Varma, I. K. *RSC Adv.* **2014**, *4*, 21712.

16. Lochab, B.; Varma, I.; Bijwe, J. *J. Therm. Anal. Calorim.* **2010**, *102*, 769.

17. Kempe, H.; Kempe, M. *Macromol. Rapid Commun.* **2004**, *25*, 315.

18. Wang, X.; Ding, X.; Zheng, Z.; Hu, X.; Cheng, X.; Peng, Y. *Macromol. Rapid Commun.* **2006**, *27*, 1180.

19. Ning, X.; Ishida, H. *J. Polym. Sci. Part A: Polym. Chem.* **1994**, *32*, 1121.

20. Wang, Y.-X.; Ishida, H. *J. Appl. Polym. Sci.* **2002**, *86*, 2953.

21. Lochab, B.; Varma, I.; Bijwe, J. *J. Therm. Anal. Calorim.* **2013**, *111*, 1357.

22. Jang, J.; Seo, D. *J. Appl. Polym. Sci.* **1998**, *67*, 1.

23. Blaiszik, B. J.; Caruso, M. M.; McIlroy, D. A.; Moore, J. S.; White, S. R.; Sottos, N. R. *Polymer* **2009**, *50*, 990.

24. Hoy, K. L. *J. Paint Technol.* **1970**, *42*, 76.

25. Fiedler, B.; Gojny, F. H.; Wichmann, M. H. G.; Nolte, M. C. M.; Schulte, K. *Compos. Sci. Technol.* **2006**, *66*, 3115.

26. Deng, Y.; Martin, G. C. *Macromolecules* **1994**, *27*, 5147.

27. Tripathi, M.; Kumar, D.; Rajagopal, C.; Roy, P. *J. Therm. Anal. Calorim.* **2015**, *119*, 547.

28. Efimova, A. A.; Emel'yanenko, V. N.; Verevkin, S. P.; Chernyak, Y. *J. Chem. Thermodyn.* **2010**, *42*, 330.

29. Ramírez, C.; Rico, M.; Torres, A.; Barral, L.; López, J.; Montero, B. *Eur. Polym. J.* **2008**, *44*, 3035.

30. Rallison, J. M. *Annu. Rev. Fluid Mech.* **1984**, *16*, 45.

31. Baqar, M.; Agag, T.; Qutubuddin, S.; Ishida, H. In Handbook of Benzoxazine Resins; Agag, H. I., Ed.; Elsevier: Amsterdam: **2011**; p 193.

32. Oie, H.; Sudo, A.; Endo, T. *J. Polym. Sci. Part A: Polym. Chem.* **2010**, *48*, 5357.

33. Baqar, M.; Agag, T.; Ishida, H.; Qutubuddin, S. *J. Polym. Sci. Part A: Polym. Chem.* **2012**, *50*, 2275.

34. Nalakathu Kolanadiyil, S.; Bijwe, J.; Varma, I. *J. Therm. Anal. Calorim.* **2014**, *116*, 427.

Sustainable Bis-benzoxazines from Cardanol and PET-Derived Terephthalamides

Pratibha Sharma,[†,‡] Bimlesh Lochab,*[,§] Devendra Kumar,[‡] and Prasun Kumar Roy*[,†]

[†]Centre for Fire, Explosive and Environment Safety, DRDO, Timarpur, Delhi 110054, India
[‡]Department of Applied Chemistry and Polymer Technology, Delhi Technological University, Delhi 110042, India
[§]Department of Chemistry, School of Natural Sciences, Shiv Nadar University, UP 203207, India

ⓢ *Supporting Information*

ABSTRACT: This paper deals with the preparation of sustainable benzoxazines that exhibit enormous potential to compete with the existing petro-based advance performance thermosets. The phenolic component used for the synthesis of benzoxazine is derived from naturally occurring cardanol, which is obtained from cashew nut tree, *Anacardium occidentale.* Polyethylene terephthalate (PET) was chosen as a sustainable feedstock for the amine fraction used to prepare the benzoxazine monomer containing amide linkages. Microwave-assisted aminolysis of PET was performed to obtain bis(amino-ethyl) terephthalamide (BAET) and α,ω-aminoligo-(ethylene terephthalamide) (AOET), which were employed as the difunctional amine for the preparation of bis-benzoxazines. In comparison to the traditional method, microwave-assisted aminolysis of PET was found to be significantly faster, and the reaction completion time could be brought

down appreciably. Mannich-like condensation of cardanol with PET-derived terephthalamides and paraformaldehyde led to the formation of bis-benzoxazines with amide linkages, the structure of which was confirmed through FT-IR and ^{1}H NMR spectroscopy. The curing behavior of the bis-benzoxazines was studied using nonisothermal differential scanning calorimetry. The presence of amide linkages in addition to the polar group formed during the ring opening of benzoxazines led to the improvement in adhesive strength, which was quantified in terms of lap shear strength.

KEYWORDS: *Sustainable, Benzoxazine, Recycling, Cardanol, Adhesive*
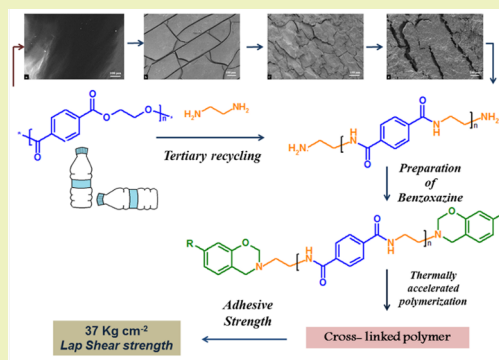
◾ INTRODUCTION

Exploring alternative renewable feedstocks to meet the ever increasing demands of the chemical industry is an essential step toward sustainable development. The generic aim of the present research is to explore the possibility of deriving economically viable and sustainable polymeric resins from renewable sources for application as advanced performance thermosets. Polybenzoxazines belong to a subclass of phenolic thermosetting resins, which exhibit extremely exciting properties, notably negligible volume shrinkage during curing,[1] low water absorption,[2] and thermal stability without compromising on excellent mechanical performance.[3,4] In fact, benzoxazines are bridging the gap between the mechanically strong polyepoxies and thermally stable maleimides. In addition, the flexibility in molecular designing made possible through the astute choice of the amine and phenolic components bestow an extremely interesting feature to these materials in terms of tunability, which opens up new vistas of application.[5-8]

In the quest to derive sustainable benzoxazines, cardanol nut shell liquid (CNSL) was chosen as the source of phenolic component for the present study. CNSL being a nonedible oil, its use as a chemical raw material does not impose any significant pressure on the food chain. Replacement of petro-

based raw material with CNSL for the chemical industry appears to be an extremely attractive proposition, in view of its low cost, relative abundance, and chemically reactivity, among other attributes.[9] CNSL is primarily composed of anacardic acid (74−77%), the rest being cardanol, cardol, and 2-methyl cardol. However, commercial-grade CNSL is obtained through roasting, which results in the decarboxylation of anacardic acid into cardanol.[10] Furthermore, the components of CNSL are themselves mixtures of another four constituents, which differ in the degree of unsaturation in the alkyl side chain, namely, saturated (5−8%), monoene (48−49%), diene (16−17%), and triene (29−30%).[11] The use of cardanol-based benzoxazines as the matrix material for fiber-reinforced composites is well reported.[8,12] The long alkyl chain present in cardanol acts as an intramolecular plasticizer,[9,13] which reduces the viscosity of the resin and renders it suitable as a reactive diluent for commercial benzoxazine resin.[14,15] The alkyl chain also increases the flexibility of molecular segments,

which reflects in their lower glass transition temperature (T_g);[16] however, the same leads to higher curing temperatures.[14]

Benzoxazines offer extremely interesting possibilities in terms of molecular design flexibility. Introduction of functional groups in addition to the oxazine ring can alter the properties of the resin appreciably.[17] In this context, the amide groups bestow flame retardance, chemical resistance, and excellent mechanical properties, due to which polyamides find extensive application in fiber and film technology. It is therefore of interest to design benzoxazine monomers containing amide groups in the chain.[18,19] Terephthalamides obtained by aminolysis of polyethylene terephthalate (PET) offer interesting candidacy to prepare diamines with amide groups for possible application as a precursor for synthesizing such bis-benzoxazines.

Bis-benzoxazine preparation usually relies on the reaction of bisphenols with amines;[20,21] however, the potential of diamines has also been explored.[3,22−24] Tertiary recycling of PET using diamines leads to terephthalamides terminated with amine functionalities.[25,26] The kinetics of PET aminolytic depolymerization is a rather slow process[27,28] due to the heterogeneous nature of the reaction medium.[29] Literature, however, supports microwave-assisted aminolysis as a propitious route toward tertiary recycling of PET wastes.[30]

We considered it of interest to reduce the energy requirements for preparation of terephthalmide-based amines by using a microwave energy source instead of the conventional heating process. This article presents an environmentally benign process to chemically recycle PET waste into benzoxazines, a value added, industrially significant, high performance material. The monomers were polymerized via thermal ring-opening polymerization to obtain polybenzoxazines with adhesive characteristics.

■ EXPERIMENTAL SECTION

Materials. Post-consumer plastic bottles were used as the source of PET. Disposed of bottles were collected, washed, dried, and used after removing the caps and labels. Bottles were cut into small pieces (6 mm × 6 mm), before microwave-assisted aminolysis in the presence of ethylene diamine (ED). Cardanol (ρ = 0.9272−0.9350 g cm^{-3}; iodine value 250; acid value max 5; hydroxyl value 180−190) was obtained from Satya Cashew Chemicals Pvt. Ltd. (India). Cardanol possess double bonds in the alkylene chain at the m-position, as monoene (25%), diene (40%), and triene (34%) and unidentified product (rest). The HPLC trace of cardanol is presented in the Supporting Information (Figure S1).[24] Paraformaldehyde, ethylene diamine, sodium sulfate, and chloroform from CDH were used as received. Double distilled water was used throughout the course of this work.

Characterization. Fourier transform infrared (FT-IR) spectra of samples were recorded using a Thermo scientific FT-IR (NICOLET 8700) analyzer with an attenuated total reflectance (ATR) crystal accessory. The angle of incidence of the germanium ATR crystal used was characteristically 45°, and the spectra were recorded in the wavelength range of 4000−500 cm^{-1}, with a resolution of 4 cm^{-1}. A Bruker AC 500 MHz Fourier transform nuclear magnetic resonance (FT-NMR) spectrometer was used to record the ^{1}H NMR of the samples. The spectrum was recorded in dueterated chloroform (CDCl$_3$) and dimethyl sulfoxide (DMSO) using tetramethylsilane (TMS) as the internal standard. Thermal behavior was investigated using a PerkinElmer Diamond STG-DTA under N$_2$ atmosphere (flow rate = 50 mL min^{-1}) in the temperature range of 50−700 °C. A heating rate of 10 °C/min and sample mass of 5.0 ± 0.5 mg were used for each experiment. Calorimetric studies were performed on a differential scanning calorimeter (DSC) (TA Instruments Q 20). A heating rate of 10 °C min^{-1} and sample mass of 5.0 ± 0.5 mg were used for each experiment. For dynamic DSC scans, samples (10 ± 2 mg) were sealed in aluminum pans and heated from 0 to 300 °C at 10

°C min^{-1} under nitrogen atmosphere to minimize oxidative degradation of the sample during curing. Prior to the experiments, the instrument was calibrated for temperature and enthalpy using standard indium and zinc. Thermal equilibrium was regained within 1 min of sample insertion, and the exothermic reaction was considered to be complete when the recorder signal leveled off to the baseline. The total area under the exothermic curve was determined to quantify the heat of curing and % crystallinity. The enthalpy of fusion associated with the melting of pristine PET ($\Delta H_{f,100\% \text{ crystalline}}$) has been reported to be 135.8 J g^{1-}.[31]

The surface morphology of samples was studied using a scanning electron microscope (Zeiss EVO MA15) under an acceleration voltage of 1 kV. Samples were mounted on aluminum stubs and sputter-coated with gold and palladium (10 nm) using a sputter coater (Quorum-SC7620) operating at 10−12 mA for 120 s.

High performance liquid chromatography analysis of the PET aminolysates was performed using an Agilent Technologies 6540 series HPLC instrument equipped with a C18 column (Grace Alltima, 150 mm long × 4.6 mm) (mobile phase: methanol; flow rate: 1.5 mL/min; UV detection at 280 nm). The mass spectra were recorded using a high resolution mass spectrometer equipped with electrospray ionization interface (ESI). Positive ion mode was used for all the analyses, and cationizing agents were not employed.

Lap shear strength (LSS) of bonded steel plates (roughness, R_a 0.42−0.51 μm) was measured in accordance with ASTM standard D1002 using the Universal Testing System (International equipment) at a crosshead speed of 1.3 mm min^{-1}.

Microwave-Assisted Aminolysis of PET. PET depolymerization was performed in a microwave reactor (Anton Paar Monowave 300) equipped with a digital temperature control and pressure monitoring system using 30 mL Teflon-coated silicone-sealed borosilicate glass reaction tube. PET flakes (1 g) together with requisite amounts of ethylene diamine were sealed under nitrogen atmosphere and allowed to react under isothermal conditions at different temperatures (100−250 °C) in a microwave synthesizer. The PET:ED molar ratio was varied from 1:2 to 1:16 to investigate the effect of the same on the PET conversion. The reaction vessel was cooled to room temperature, and the mixture was filtered through a copper wire mesh (0.5 mm × 0.5 mm pore size). The remaining PET flakes were weighed, and the extent of PET conversion was determined gravimetrically as follows:[29,32]

$$\text{PET conversion (\%)} = \left(\frac{M_{\text{PET,Initial}} - M_{\text{PET,residual}}}{M_{\text{PET,Initial}}} \right) \times 100$$

where, $M_{\text{PET, Initial}}$ and $M_{\text{PET; residual}}$ refer to the initial mass of PET and the mass of PET flakes remaining unreacted in the reaction medium, respectively.

The white product formed as a result of PET aminolysis is a mixture of terephthalamides, which can be separated on the basis of their solubility difference in ethanol.[26] For separation purposes, the aminolyzed product was refluxed in ethanol for 2 h, followed by filtration after cooling to room temperature. The ethanol-insoluble residue (Part A) was washed with acetone and dried at 50 °C for 24 h. The filtrate was concentrated and placed in an ice bath to yield crystalline powder (Part B), which was filtered and washed with acetone to remove unreacted ethylene diamine and ethylene glycol prior to drying at 40−45 °C for 6 h. Mass spectrometry, as discussed later, suggests that the ethanol-soluble fraction (part B) is bis(amino ethyl) terephthalamide (BAET, NH$_2$CH$_2$CH$_2$(NHCOC$_6$H$_4$-CONHCH$_2$CH$_2$)$_n$NH$_2$, where n = 1), while the ethanol-insoluble fraction (Part A) comprised of α,ω-aminoligo(ethylene terephthalamide) (AOET, NH$_2$CH$_2$CH$_2$(NHCOC$_6$H$_4$CONHCH$_2$CH$_2$)$_n$NH$_2$, where n ≥ 2).

Preparation of Bis-benzoxazine Containing Amide Groups. A mixture of cardanol (5 g, 16.4 mmol) BAET (2.06 g, 8.2 mmol) and paraformaldehyde (1 g, 32.9 mmol) was slowly heated to 80 °C under constant stirring for 1 h, followed by heating at 90 °C for 2 h. The reaction led to the evolution of water, and the color of the reaction medium changed from yellow to red brown. Upon cooling, water (10

Scheme 1. (A) Aminolysis of PET. (B) Oligomer Formation during PET Aminolysis
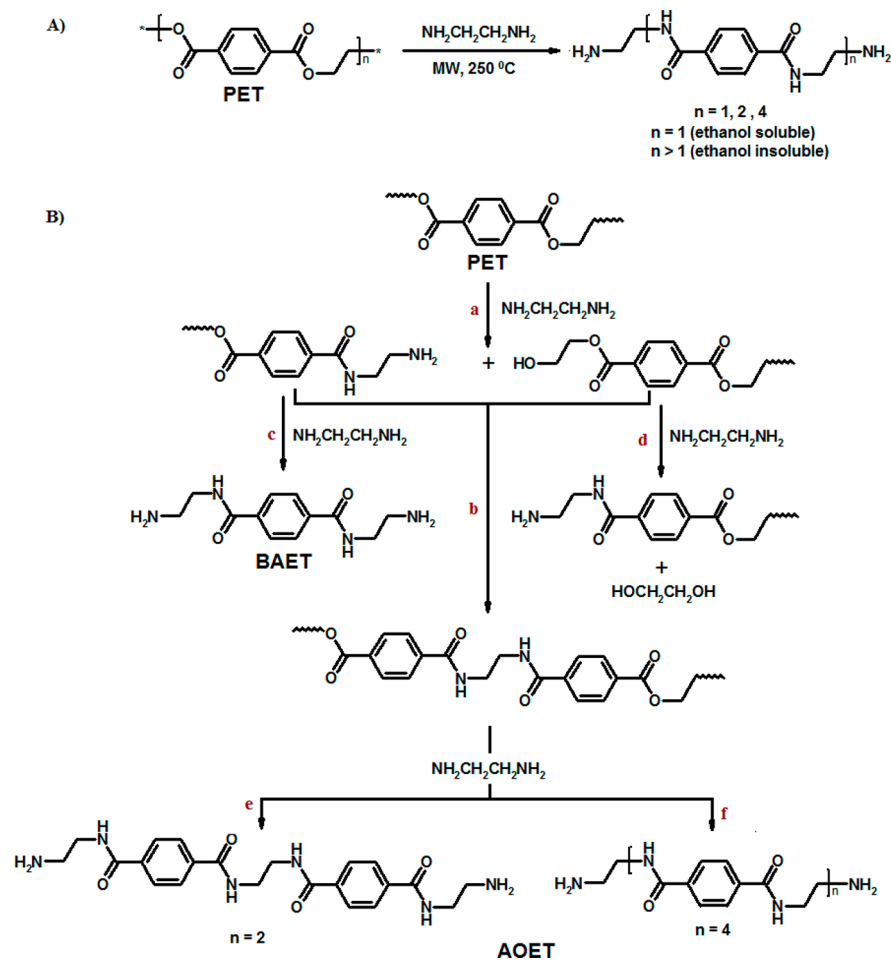
Table 1. Molecular Formula and Expected Molecular Masses of Terephthalamides

designation	molecular formula	expected molecular mass (amu)
BAET (ethanol-soluble fraction)	$NH_2CH_2CH_2NHCOC_6H_4CONHCH_2CH_2NH_2$	250.1430
AOET (ethanol-insoluble fraction)	$NH_2CH_2CH_2(NHCOC_6H_4CONHCH_2CH_2)_nNH_2$	440.2172 ($n = 2$)
		880.4348 ($n = 4$)

mL) was added, and an organic layer was extracted with chloroform (20 mL). The organic layers were combined and washed with aqueous NaOH solution (0.5 N, 100 mL) followed by washing with water (3 × 30 mL), drying over sodium sulfate, and filtration. The solvent was removed under reduced pressure to give C-BAET as a red sticky oil (yield 88%).

The method for the preparation of C-AOET is similar to that of C-BAET, except for the amount of reactants used; cardanol (5 g, 16.4 mmol), paraformaldehyde (1 g, 32.9 mmol), and AOET (3.62 g, 8.2 mmol) were slowly heated to 80 °C and maintained under stirring for a period of 1 h, followed by heating at 90 °C for 4 h. C-AOET was obtained as red sticky oil (yield 83%).

Adhesive Strength of Resin. To quantify the adhesive nature of the bis-benzoxazines, ∼ 0.05 g of the liquid resin was coated on steel plates (15 mm × 15 mm). The assembly was clamped with paper clips, kept at 80 °C for 30 min, and cured in an air oven at 80−180 °C (30 min), followed by heating at 215 °C (1 h) for the C-BAET and 238 °C (1 h) for C-AOET. The thickness of the adhesive layer was maintained at ∼0.23−0.46 mm. A total of six replicates were tested per sample, and the average value has been reported.

■ RESULTS AND DISCUSSION

Microwave-assisted aminolysis of PET in the presence of ethylene diamine was performed to yield terephthalamide, which were used to synthesize sustainable bis-benzoxazine containing amide groups by reacting with cardanol as a renewable source of phenol.

Aminolysis of PET. Detailed characterization of PET is presented in the Supporting Information (Figures S2 and S3). As is apparent from the DSC and TG traces, PET exhibits a sharp melting endotherm peaking at ∼246 °C (crystallinity = 27.2%) and undergoes a single-step pyrolytic degradation commencing at 400 °C. Aminolytic depolymerization of PET was performed under microwave irradiation with an aim to reduce the reaction time and energy as compared to the conventional process. The reaction is expected to result in the formation of terephthalamides of different molecular weights as per the reaction scheme presented in Scheme 1A, the product composition being dependent on the relative quantities of PET and ethylene diamine in the reaction medium. In the presence of excess ethylene diamine, formation of bis(2-amino ethyl) terephthalamide (BAET) is expected, as shown in Scheme
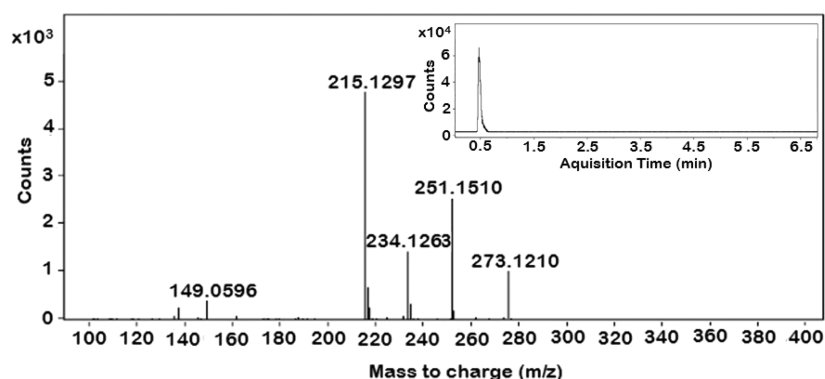
Figure 1. Mass spectra of ethanol-soluble terephthalamide fraction eluted at 0.389−0.649 min.
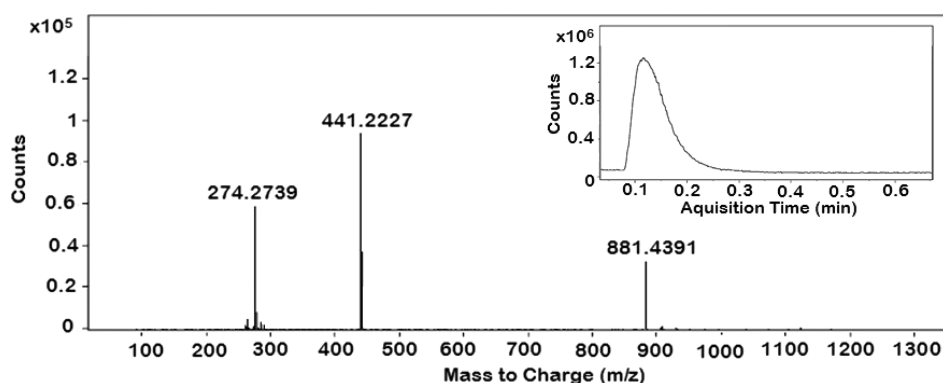
Figure 2. Mass spectra of ethanol-insoluble terephthalamide fraction eluted at 0.116 min.

1B(c). However, the condensation of the half a minolysed moiety with the terminal ester group of PET, followed by its further aminolysis results in the formation of higher oligomers, i.e., α,ω-aminoligo(ethylene terephthalamide) (AOET) as per the reaction (b−f) in Scheme 1B,[33−35] which was separated from BAET based on solubility differences in ethanol.[26] Higher molecular weight terephthalamide (AOET) is ethanol insoluble, while BAET, being ethanol-soluble, was recovered through solvent evaporation. The designated names, structural representation, and masses of the products are given in Table 1. The terephthalamides obtained through PET aminolysis were characterized using mass spectrometry.

The mass spectrum of the ethanol-soluble terephthalamide fraction (Part B) eluted at 0.389−0.649 min is presented in Figure 1. The associated chromatogram is presented in the inset. The appearance of peak at m/z 251.1510 in the spectrum is attributed to the presence of BAET ionized by H^+. The other peaks at 273.1210 are due to BAET ionized by Na^+ and fragments for $[BAET\text{-}NH_2]^+$ at m/z 234.1263 and $[BAET\text{-}2NH_2]^+$ at m/z 215.1297, which suggest the molecular formula of BAET to be $NH_2CH_2CH_2NHCOC_6H_4CONHCH_2CH_2\text{-}NH_2$.

The mass spectrum of the ethanol-insoluble fraction (Part A) eluted at 0.116 min is presented in Figure 2, and the associated chromatogram is presented in the inset. The peak profile is suggestive of the presence of more than a single component. The principal constituent terephthalamide in part A, $NH_2CH_2CH_2(NHCOC_6H_4CONHCH_2CH_2)_nNH_2$ is the dimer ($n = 2$), which is confirmed by the appearance of peak at m/z 441.2227. However, the presence of tetramer ($n = 4$) is also confirmed by the appearance of peak at m/z 881.4319 ($n = 4$) ionized by H^+ (Table 1).

Effect of Reaction Temperature on PET Conversion. The effect of increasing temperature on PET aminolysis was studied by following the extent of PET conversion; the results of which are presented in Figure 3. As expected, an increase in the
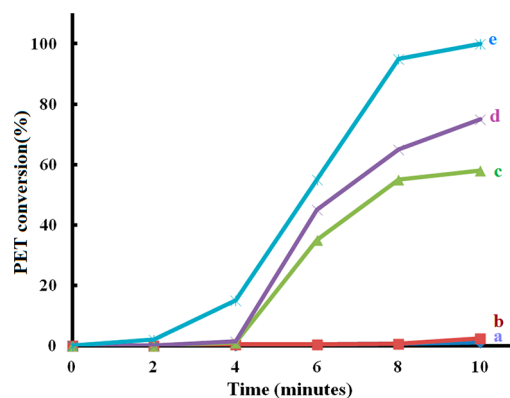
Figure 3. PET conversion as a function of the reaction temperature and time (a) 100, (b) 150, (c) 220, (d) 230, and (e) 250 °C (PET:ED::1:6).

reaction temperature led to an increase in PET conversion. At lower temperatures ($T \leq 150$ °C), PET conversion is rather negligible ($\leq 2\%$). However, as the temperature is raised to 250 °C, complete conversion can be effected within 10 min.

The notable increase in the rate can be attributed to the melting of the solid PET flakes at 246 °C, which leads to the formation of a homogeneous reaction medium. On the other hand, the solid−liquid reaction remains largely diffusion

controlled, which accounts for the slower rates of reaction at lower temperatures.[26]

Aminolysis initiates at the solid−liquid interface with the diffusion of the amine into the solid PET, resulting in the swelling of the polymer followed by its depolymerization into terephthalamides of lower molecular weight. Amorphous regions are expected to be more susceptible to degradation,[29,36] which was confirmed by morphological investigations. The SEM images of the surface of recovered PET are presented in Figure 4. As shown, the smooth surface of neat PET develops
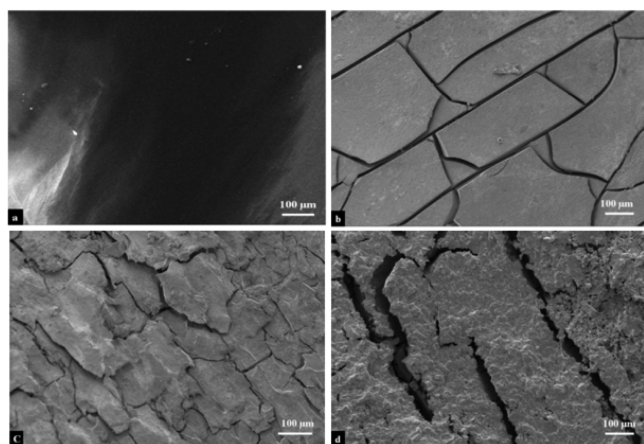
Figure 4. Scanning electron micrographs of PET films. (a) Neat PET films and residual PET after reacting with ethylene diamine for duration of (b) 4 min, (c) 6 min, and (d) 8 min (reaction temperature = 230 °C, PET:ED:: 1:6).

cracks, with the extent of corrugation increasing with time. The crystallinity of PET flakes was found to increase from 27.2% to 37.2% due to diffusion of lower terephthalamides from PET as well as solvent-induced crystallization of the polymer.[37]

Representative plots showing the variation of operating parameters during microwave-assisted PET aminolysis at two different temperatures (230 and 250 °C) are presented in the Supporting Information (Figure S4). It is shown that the temperature and pressure increase initially and remain practically constant thereafter, while the microwave power drops significantly after the rapid initial increase.

PET aminolysis has been reported to be a slow process requiring extended time periods for completion. A recent study revealed that the uncatalysed aminolytic depolymerization of

PET under electrical heating required more than 17 h in the presence of excess ED (PET:ED::1:8).[26] Our studies are clearly suggestive of the advantages associated with microwave-assisted PET aminolysis. The same is attributed to the high loss factor of ED (δ = 0.573), which is indicative of the strong ability of the diamine to convert electromagnetic energy to heat.[38,39]

Effect of Reactant Ratio on PET Conversion and Product Composition. The effect of increasing PET:ED on the extent of PET conversion is presented in Figure 5(i). It is to be noted that on the basis of stoichiometry (Scheme 1), PET:ED of 1:2 is sufficient to effect complete depolymerization of PET. However, under these conditions, only 30% conversion could be effected, which increased with increasing amounts of ED in the reactant medium. Complete PET conversion could only be effected as the PET:ED ratio increased to 1:6 under the experimental conditions employed.

The effect of varying PET: ED ratio on the relative fraction (%) of AOET and BAET is presented in Figure 5(ii). As per Carothers relation, increasing the stoichiometric imbalance between the reactants in the system precludes the formation of higher molecular weight species.[40] Assuming that all the ester linkages in PET have equal probability of undergoing aminolysis, regardless of their position in the chain and the molecular weight of the polymer, the extent of depolymerization resulting in the formation of lower molecular weight terephthalamides is expected to increase with higher amounts of ED in the reaction medium. It is shown that the product mixture obtained at lower PET:ED comprise primarily of higher species (AOET) with lesser amounts of BAET, the amount of which increases with increasing ED. Interestingly, increasing the amount of ED in the medium beyond PET:ED of 1:6 did not exert any pronounced effect on the product composition. The variation in BAET yield (%) with PET:ED ratio, as quantified in terms of the ratio of amount of BAET experimentally obtained to the theoretical prediction, is reported in the Supporting Information (Figure S5), which shows that maximum BAET yield can be obtained under PET:ED of 1:6 at a reaction temperature of 250 °C.

As expected, the FT-IR spectra of AOET and BAET (Figure S6, Supporting Information) is rather similar, with characteristic $\nu_{C=O,amide}$ at 1626 cm^{-1}, $\nu_{N-H,1°}$ at 3342 cm^{-1}, and $\nu_{N-H,2°}$ at 3280 cm^{-1}.[41] The relative intensity of the peaks associated with NH stretching of 1° and 2° amines in BAET was higher as compared to AOET, which was quantified in terms of the ratio of their absorbance. This ratio (0.57, BAET and 0.49 AOET)
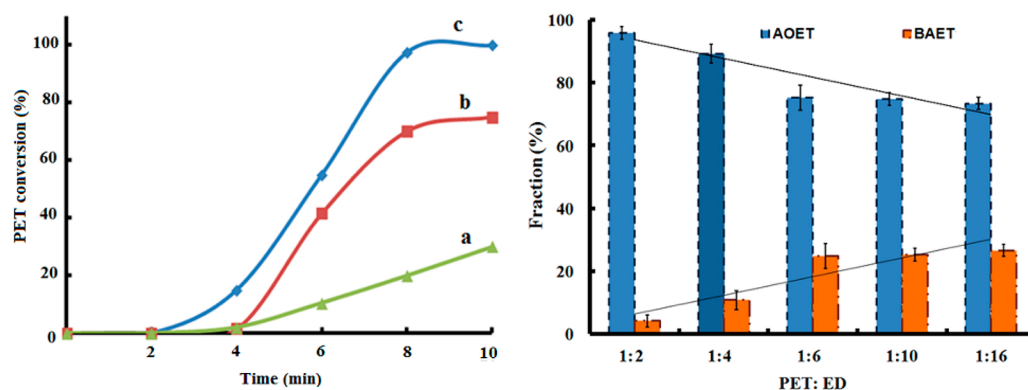
Figure 5. (i) PET conversion as a function of reaction time and PET: ED ratio (a) 1:2, (b) 1:4, and (c) 1:6. (ii) Relative fraction (%) of AOET and BAET as a function of PET:ED ratio (reaction temperature 250 °C, time = 10 min).

clearly indicates that the concentration of 1° amine in BAET is greater than in AOET, in line with the structure presented in Scheme 1.

The terephthalamides fractions were also characterized using ^{1}H NMR spectroscopy using DMSO (Figure 6). The ^{1}H NMR
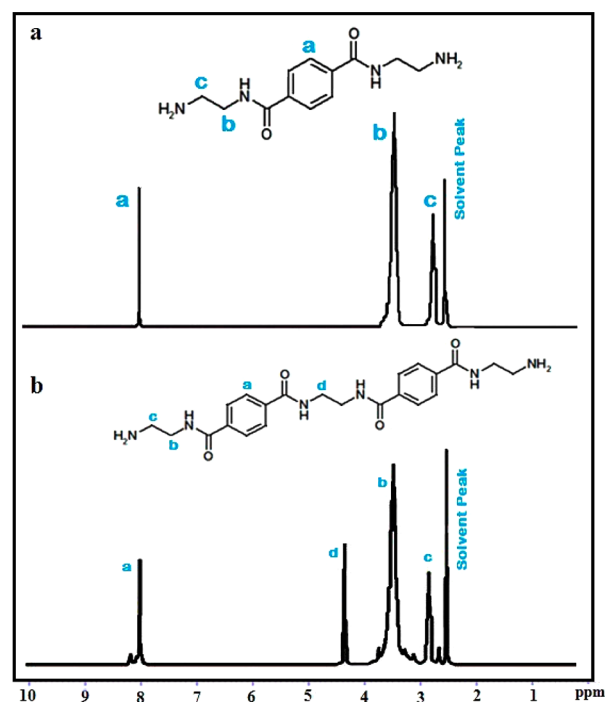
Figure 6. ^{1}H NMR spectra: (a) BAET and (b) AOET.

spectrum of BAET (Figure 6a) shows resonances at ∼8.0 ppm (4H, s, aromatic), 3.2 ppm (4H, t, CONHCH$_2$CH$_2$NH$_2$), and 2.7 ppm (4H, t, CONHCH$_2$CH$_2$NH$_2$). The ^{1}H NMR spectrum of AOET (Figure 6b) shows resonances at ∼8.0 ppm (8H, s, aromatic), 3.4 ppm (4H, t, CONHCH$_2$), 2.7 ppm (4H, t, CONHCH$_2$CH$_2$NH$_2$), and 4.3 ppm (4H, s, CONHCH$_2$CH$_2$NHCO). The appearance of a singlet centered at 4.3 ppm in the spectra of AOET is due to the symmetrical ethylene group in between two amide groups in addition to the peaks of asymmetrical ethylene group in between an amide and an amine group at 3.4 and 2.7 ppm of part B.

The DSC traces of BAET and AOET are presented in Figure 7. The sharp endotherms appearing at 181 and 298 °C are associated with the melting of BAET and AOET, respectively. It is to be noted that the melting point of the terephthalates obtained by glycolysis of PET in the presence of ethylene glycol is much lower, 110 and 160 °C for bis(hydroxyethyl) terephthalate (BHET) and oligomers, respectively.[32] This difference in the melting points of PET glycolysates and aminolysates can be attributed to the strong intermolecular H-bonding between the amide groups in terephthalamide, which is absent in the analogues esters.

Synthesis of Bis-Benzoxazines. Bis-benzoxazines containing amide linkages were prepared using a solventless route by reacting cardanol with the PET-derived terephthalamides obtained by PET aminolysis as per the reaction scheme presented in Scheme 2. The oxazine ring formed by Mannich-like condensation of cardanol with terephthalamide and paraformaldehyde (2:1:4) is capable of undergoing ring opening polymerization leading to the formation of a cross-
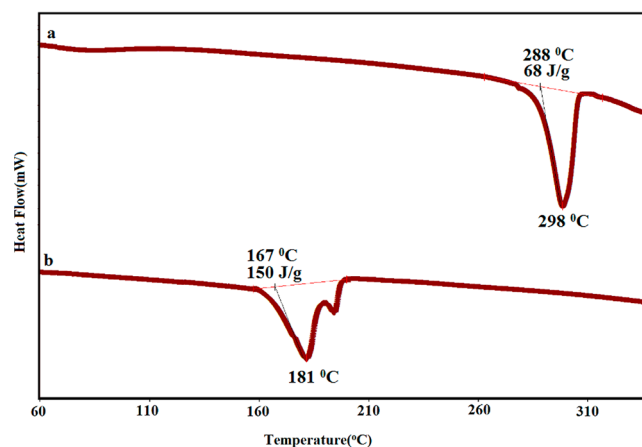
Figure 7. DSC traces: (a) AOET and (b) BAET.

Scheme 2. Bis-Benzoxazine Formation by Reaction of Terephthalamide with Cardanol and Formaldehyde
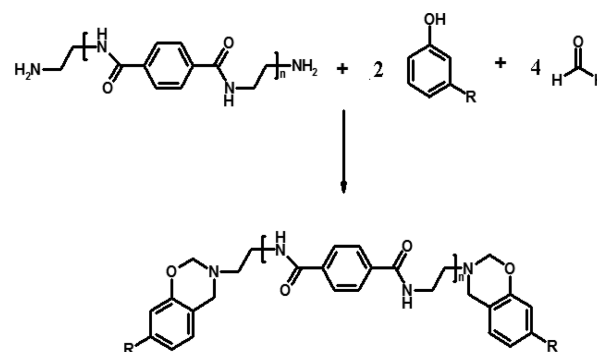
linked network. The presence of amide linkage in view of the H-bonding is expected to alter the properties of the resin appreciably. The benzoxazine resins obtained by the reaction of cardanol and formaldehyde with BAET and AOET have been referred to as C-BAET and C-AOET, respectively.

The FT-IR spectra of cardanol, C-BAET, and C-AOET are presented in Figure 8. The benzoxazine monomers showed the absence of O−H and N−H at ∼3335 and > 3161 cm^{-1}, suggestive of complete utilization of cardanol and amine toward formation of oxazine ring. In addition to the stretching bands
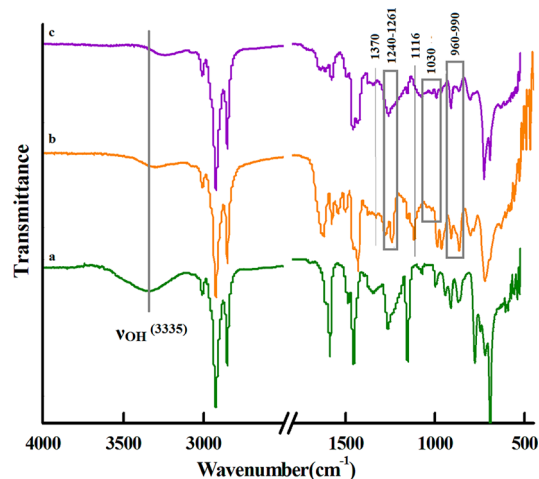
Figure 8. FT-IR spectra: a) cardanol b) C-BAET c) C-AOET.

associated with the aromatic and alkene (3008 cm^{-1}) and aliphatic (2926 and 2854 cm^{-1}) C−H vibrations, other characteristic absorption bands observed in the spectra can be attributed to the C═C (∼1600 cm^{-1}) asymmetric and symmetric stretching vibrations of C−O−C (∼1245 cm^{-1} and ∼1030 cm^{-1}), CH$_2$ wagging (1370 cm^{-1}), and asymmetric stretching vibrations of C−N−C (1116 cm^{-1}), respectively, supporting the presence of double bonds and oxazine ring in Bz monomers. In cardanol, the peak at 990 cm^{-1} can be attributed to the C═C−H vinylene C−H out-of-plane bend associated with the alkylene chain. Benzoxazine monomers showed a bimodal peak centered at 990 and 960 cm^{-1} associated with the out-of-plane bending vibrations of the C−H bond due to the alkylene double bond and oxazine ring, respectively.[42]

The ^{1}H NMR of both the bis-benzoxazine resins was recorded using CDCl$_3$ as solvent and are presented in Figure 9.
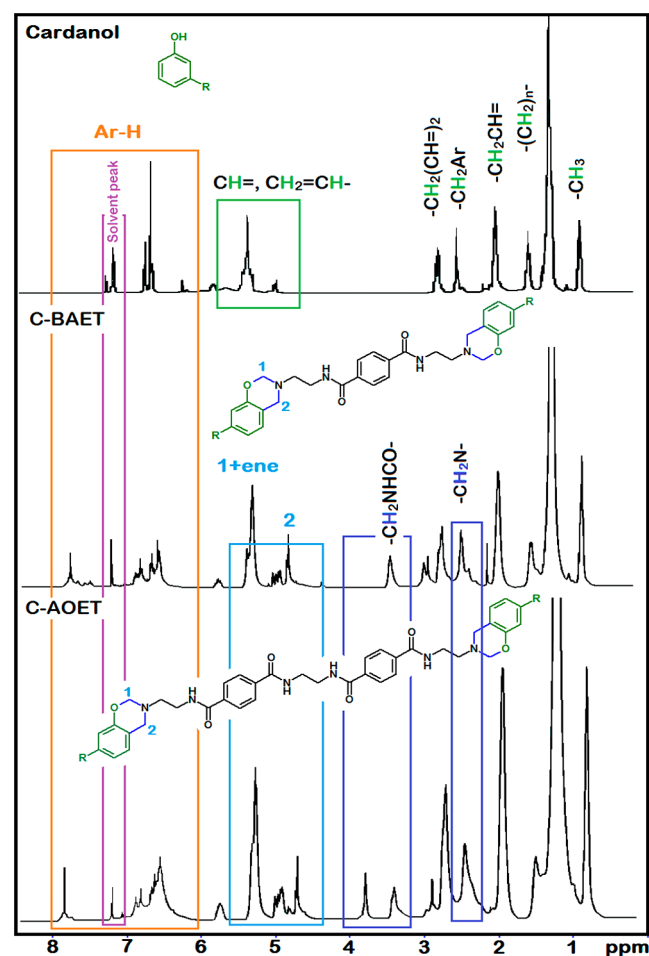
Figure 9. ^{1}H NMR spectra: (a) cardanol, (b) C-BAET, and (c) C-AOET.

C-BAET exhibits characteristic resonances at ∼5.3 ppm (4H, m, Ar**OCH$_2$N**) and ∼4.7 ppm (4H, s, Ar**CH$_2$N**), suggesting the conversion of hydroxyl to oxazine functionality (Figure 9a). Similarly, C-AOET formation was confirmed by the appearance of resonance at ∼5.4 ppm (4H, m, Ar**OCH$_2$N**) and ∼4.6 ppm (4H, s, Ar**CH$_2$N**) (Figure 9b). The intensity ratio of the signals associated with the oxazine moiety at 4.6 (singlet) and 5.4 ppm (multiplet) is expected to be 1:1. However, the same was found to be higher in the present study, which can be attributed to the resonance of alkylene protons present in cardanol (m, CH═,

CH$_2$═CH−) at the same position as Ar**OCH$_2$N** (∼5.4 ppm). In cardanol-based benzoxazines, this ratio has been reported to be 1:3.[24] This deviation from 1:1 can also be ascribed to the oligomerization of the benzoxazine resin. The protons associated with the >CH$_2$ in the mannich base formed as a result of ring opening appear in the region 3.5−4 ppm, which overlap with the peaks associated with the amine protons (BAET and AOET) in the same region as shown in the NMR spectra.

To investigate the curing behavior of the benzoxazine resins, nonisothermal calorimetric studies were performed, and the curing profiles are presented in Figure 10. It is shown that the
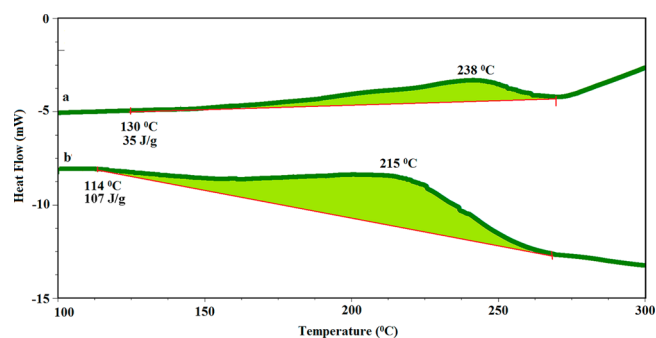
Figure 10. DSC traces: (a) C-AOET and (b) C-BAET.

temperature associated with the curing of C-BAET (T_{peak} = 214 °C) is relatively lower than C-AOET (T_{peak} = 238 °C). This is in accordance with previous studies, where increasing the chain length between benzoxazine moieties leads to an increase in curing temperature.[22] In our previous studies, we have reported the curing behavior of cardanol-based monobenzoxazine, which was found to cure at relatively higher temperature (T ∼ 242 °C).[20] Our studies clearly suggest that increasing the functionality can lead to substantial lowering of the curing temperature.[24,43] Further, the molar enthalpy associated with the polymerization for C-AOET is lower than C-BAET, which can again be credited to the larger number of oxazine rings per unit mass in the latter.

The TG-DTG traces of the cured benzoxazines (C-AOET and C-BAET) are presented in the Supporting Information (Figure S7). The benzoxazine resins prepared in the present work were found to exhibit excellent thermal stability with the temperature associated with 5% wt. loss being 298 and 380 °C for C-BAET and C-AOET, respectively, suggesting their application in demanding areas requiring high thermal stability.

Adhesive Property. The adhesive nature of the bis-benzoxazine resin was quantified as per the standard procedure. The results in terms of lap shear strength (LSS) are presented in Table 2, and the representative load−displacement curve is presented in the Supporting Information (Figure S8). It is to be noted that the LSS is dependent on several factors, particularly the ability of the resin to wet the substrate, its inherent adhesive nature, temperature, thickness of the resin, and type of failure. The presence of larger number of polymerizable molecules in

Table 2. Lap Shear Strength of Benzoxazine Resins

benzoxazine resin	lap shear strength (kgcm^{-2})
C-BAET	38.2 ± 3.9
C-AOET	28.3 ± 3.1

benzoxazines, which undergo thermally activated ring opening polymerization in the absence of catalyst, form cross-linked networks on metal surfaces.[44] The ring opening of oxazine moieties generates specific groups that are capable of undergoing H-bonding, such as −OH and >N−, as shown in the Supporting Information (Figure S9) and FTIR of cured resin (Figure S10), in addition to the amide linkages, which are already available in the main chain. Due to the presence of a larger number of polymerizable benzoxazine in C-BAET as compared to C-AOET, the lap shear strength of the former was found to be relatively higher than the latter, which advocate the use of these resins as healants for self-healing applications.[45−47]

CONCLUSION

Microwave-assisted aminolytic depolymerization of PET in the presence of ethylene diamine (ED) was performed to yield terephthalamides that were used to prepare benzoxazine containing amide linkages. The effect of temperature and the molar ratio of PET: ED on the extent of PET conversion and relative percentage fraction of AOET and BAET was studied. Complete conversion of PET could be affected by performing the reaction at a temperature close to the melting point of PET, at PET:ED:: 1:6. Increasing the concentration of ED further did not affect the product composition appreciably. The amine-terminated terephthalamides were used to synthesize benzoxazine resins containing amide linkages in the presence of cardanol as the phenolic component using Mannich-type condensation. The resins were characterized using FT-IR and ^{1}H NMR, and the curing behavior was investigated by nonisothermal DSC. The cured resins exhibited high thermal stability ($T_{5\%} > 300$ °C) and excellent lap shear strength (C-AOET = 28 kg cm^{-2}, C-BAET = 38 kg cm^{-2}). Our studies indicate that microwave irradiation can accelerate the kinetics of PET aminolysis resulting in shorter reaction times, and the products hence obtained can be transformed to a sustainable high performance resin.

ASSOCIATED CONTENT

Ⓢ Supporting Information

The Supporting Information is available free of charge on the ACS Publications website at DOI: 10.1021/acssusche-meng.5b01153.

> HPLC chromatogram of cardanol (Figure S1), character-ization of PET (Figures S2, S3), microwave profile of PET aminolysis (Figure S4), BAET yield (Figure S5), FTIR spectra of terephthalamides (Figure S6), TGA traces of cured C-AOET and C-BAET (Figure S7), representative load−displacement curve (Figure S8), functional groups in polybenzoxazine involved in H-bonding with the contact surface (Figure S9), and FTIR spectra of cured polymer (Figure S10). (PDF)

AUTHOR INFORMATION

Corresponding Authors
*Tel.: 0120-2663801. E-mail: bimlesh.lochab@snu.edu.in (B. Lochab).
*Tel.:+911123907191. Fax:+911123819547. E-mail addresses:pk_roy2000@yahoo.com (P. K. Roy).

Notes
The authors declare no competing financial interest.

REFERENCES

(1) Ishida, H.; Low, H. Y. A Study on the Volumetric Expansion of Benzoxazine-Based Phenolic Resin. *Macromolecules* **1997**, *30* (4), 1099−1106.

(2) Ishida, H.; Allen, D. J. Physical and mechanical characterization of near-zero shrinkage polybenzoxazines. *J. Polym. Sci., Part B: Polym. Phys.* **1996**, *34* (6), 1019−1030.

(3) Shen, S. B.; Ishida, H. Development and characterization of high-performance polybenzoxazine composites. *Polym. Compos.* **1996**, *17* (5), 710−719.

(4) Ghosh, N. N.; Kiskan, B.; Yagci, Y. Polybenzoxazines—New high performance thermosetting resins: Synthesis and properties. *Prog. Polym. Sci.* **2007**, *32* (11), 1344−1391.

(5) Yagci, Y.; Kiskan, B.; Ghosh, N. N. Recent advancement on polybenzoxazine—a newly developed high performance thermoset. *J. Polym. Sci., Part A: Polym. Chem.* **2009**, *47* (21), 5565−5576.

(6) Thirukumaran, P.; Shakila Parveen, A.; Sarojadevi, M. Synthesis and Copolymerization of Fully Biobased Benzoxazines from Renew-able Resources. *ACS Sustainable Chem. Eng.* **2014**, *2* (12), 2790−2801.

(7) Taskin, O. S.; Kiskan, B.; Aksu, A.; Balkis, N.; Weber, J.; Yagci, Y. Polybenzoxazine: A Powerful Tool for Removal of Mercury Salts from Water. *Chem. - Eur. J.* **2014**, *20* (35), 10953−10958.

(8) Calo, E.; Maffezzoli, A.; Mele, G.; Martina, F.; Mazzetto, S. E.; Tarzia, A.; Stifani, C. Synthesis of a novel cardanol-based benzoxazine monomer and environmentally sustainable production of polymers and bio-composites. *Green Chem.* **2007**, *9* (7), 754−759.

(9) Voirin, C.; Caillol, S.; Sadavarte, N. V.; Tawade, B. V.; Boutevin, B.; Wadgaonkar, P. P. Functionalization of cardanol: towards biobased polymers and additives. *Polym. Chem.* **2014**, *5* (9), 3142−3162.

(10) Tyman, J. H. P.; Wilczynski, D.; Kashani, M. A. Compositional studies on technical cashew nutshell liquid (cnsl) by chromatography and mass spectroscopy. *J. Am. Oil Chem. Soc.* **1978**, *55* (9), 663−668.

(11) Trevisan, M. T. S.; Pfundstein, B.; Haubner, R.; Würtele, G.; Spiegelhalder, B.; Bartsch, H.; Owen, R. W. Characterization of alkyl phenols in cashew (Anacardium occidentale) products and assay of their antioxidant capacity. *Food Chem. Toxicol.* **2006**, *44* (2), 188−197.

(12) Rao, B. S.; Palanisamy, A. Monofunctional benzoxazine from cardanol for bio-composite applications. *React. Funct. Polym.* **2011**, *71* (2), 148−154.

(13) Mohapatra, S.; Nando, G. B. Cardanol: a green substitute for aromatic oil as a plasticizer in natural rubber. *RSC Adv.* **2014**, *4* (30), 15406−15418.

(14) Campaner, P.; D'Amico, D.; Longo, L.; Stifani, C.; Tarzia, A.; Tiburzio, S. Study of a Cardanol-Based Benzoxazine as Reactive Diluent and Toughening Agent of Conventional Benzoxazines. In *Handbook of Benzoxazine Resins*, Agag, H. I., Ed.; Elsevier: Amsterdam, 2011; Chapter 19, pp 365−375.

(15) Attanasi, O. A.; Behalo, M. S.; Favi, G.; Lomonaco, D.; Mazzetto, S. E.; Mele, G.; Pio, I.; Vasapollo, G. Solvent Free Synthesis of Novel Mono- and Bis-Benzoxazines from Cashew Nut Shell Liquid Components. *Curr. Org. Chem.* **2012**, *16* (21), 2613−2621.

(16) Greco, A.; Brunetti, D.; Renna, G.; Mele, G.; Maffezzoli, A. Plasticizer for poly (vinyl chloride) from cardanol as a renewable resource material. *Polym. Degrad. Stab.* **2010**, *95* (11), 2169−2174.

(17) Kawaguchi, A. W.; Sudo, A.; Endo, T. Synthesis of highly polymerizable 1,3-benzoxazine assisted by phenyl thio ether and hydroxyl moieties. *J. Polym. Sci., Part A: Polym. Chem.* **2012**, *50* (8), 1457−1461.

(18) Agag, T.; Arza, C. R.; Maurer, F. H.; Ishida, H. Primary amine-functional benzoxazine monomers and their use for amide-containing monomeric benzoxazines. *Macromolecules* **2010**, *43* (6), 2748−2758.

(19) Agag, T.; Arza, C. R.; Maurer, F. H.; Ishida, H. Crosslinked polyamide based on main-chain type polybenzoxazines derived from a primary amine-functionalized benzoxazine monomer. *J. Polym. Sci., Part A: Polym. Chem.* **2011**, *49* (20), 4335−4342.

(20) Lochab, B.; Varma, I.; Bijwe, J. Thermal behaviour of cardanol-based benzoxazines. *J. Therm. Anal. Calorim.* **2010**, *102* (2), 769−774.

(21) Baranek, A. D.; Kendrick, L. L.; Narayanan, J.; Tyson, G. E.; Wand, S.; Patton, D. L. Flexible aliphatic-bridged bisphenol-based polybenzoxazines. *Polym. Chem.* **2012**, *3* (10), 2892−2900.

(22) Allen, D. J.; Ishida, H. Physical and mechanical properties of flexible polybenzoxazine resins: Effect of aliphatic diamine chain length. *J. Appl. Polym. Sci.* **2006**, *101* (5), 2798−2809.

(23) Allen, D. J.; Ishida, H. Polymerization of linear aliphatic diamine-based benzoxazine resins under inert and oxidative environments. *Polymer* **2007**, *48* (23), 6763−6772.

(24) Shukla, S.; Mahata, A.; Pathak, B.; Lochab, B. Cardanol Benzoxazines - Interplay of Oxazine Functionality (Mono to Tetra) and Properties. *RSC Adv.* **2015**, *5*, 78071.

(25) Fukushima, K.; Lecuyer, J. M.; Wei, D. S.; Horn, H. W.; Jones, G. O.; Al-Megren, H. A.; Alabdulrahman, A. M.; Alsewailem, F. D.; McNeil, M. A.; Rice, J. E.; Hedrick, J. L. Advanced chemical recycling of poly(ethylene terephthalate) through organocatalytic aminolysis. *Polym. Chem.* **2013**, *4* (5), 1610−1616.

(26) Hoang, C. N.; Dang, Y. H. Aminolysis of poly(ethylene terephthalate) waste with ethylenediamine and characterization of α,ω-diamine products. *Polym. Degrad. Stab.* **2013**, *98* (3), 697−708.

(27) Soni, R.; Singh, S. Synthesis and characterization of terephthalamides from poly (ethylene terephthalate) waste. *J. Appl. Polym. Sci.* **2005**, *96* (5), 1515−1528.

(28) Soni, R.; Teotia, M.; Dutt, K. Studies on synthesis and characterization of a novel acrylic aromatic amide oligomer of aminolysed endproducts generated from pet waste with hydrazine monohydrate and its photocuring with acrylate monomers. *J. Appl. Polym. Sci.* **2010**, *118* (2), 638−645.

(29) Chaudhary, S.; Surekha, P.; Kumar, D.; Rajagopal, C.; Roy, P. K. Microwave assisted glycolysis of poly(ethylene terepthalate) for preparation of polyester polyols. *J. Appl. Polym. Sci.* **2013**, *129* (5), 2779−2788.

(30) Achilias, D. S.; Tsintzou, G. P.; Nikolaidis, A. K.; Bikiaris, D. N.; Karayannidis, G. P. Aminolytic depolymerization of poly(ethylene terephthalate) waste in a microwave reactor. *Polym. Int.* **2011**, *60* (3), 500−506.

(31) Jog, J. Crystallization of polyethyleneterephthalate. *J. Macromol. Sci., Polym. Rev.* **1995**, *35* (3), 531−553.

(32) Roy, P. K.; Mathur, R.; Kumar, D.; Rajagopal, C. Tertiary recycling of poly(ethylene terephthalate) wastes for production of polyurethane−polyisocyanurate foams. *J. Environ. Chem. Eng.* **2013**, *1* (4), 1062−1069.

(33) Aspinall, S. R. Ethylenediamine. IV.1 Monoalkyl Derivatives. *J. Am. Chem. Soc.* **1941**, *63* (3), 852−854.

(34) Bergeron, R. J.; Garlich, J. R.; Stolowich, N. J. Reagents for the stepwise functionalization of spermidine, homospermidine, and bis(3-aminopropyl)amine. *J. Org. Chem.* **1984**, *49* (16), 2997−3001.

(35) Jacobson, A. R.; Makris, A. N.; Sayre, L. M. Monoacylation of symmetrical diamines. *J. Org. Chem.* **1987**, *52* (12), 2592−2594.

(36) Manju; Kumar Roy, P.; Ramanan, A.; Rajagopal, C. Post consumer PET waste as potential feedstock for metal organic frameworks. *Mater. Lett.* **2013**, *106* (0), 390−392.

(37) Agarwal, U. S.; de Wit, G.; Lemstra, P. J. A new solid-state process for chemical modification of PET for crystallization rate enhancement. *Polymer* **2002**, *43* (21), 5709−5712.

(38) Kim, Y. J.; Varma, R. S. Microwave-assisted preparation of cyclic ureas from diamines in the presence of ZnO. *Tetrahedron Lett.* **2004**, *45* (39), 7205−7208.

(39) Narwade, B. S.; Gawali, P. G.; Pande, R.; Kalamse, G. M. Dielectric studies of binary mixtures of n-propyl alcohol and ethyl-enediamine. *Proc. - Indian Acad. Sci., Chem. Sci.* **2005**, *117* (6), 673−676.

(40) Carothers, W. H. Polymers and polyfunctionality. *Trans. Faraday Soc.* **1936**, *32* (0), 39−49.

(41) Aliphatic Amines. In *Interpreting Infrared, Raman, and Nuclear Magnetic Resonance Spectra*, Nyquist, R. A., Ed.; Academic Press: San Diego, 2001; Chapter 8, pp 143−148.

(42) Lochab, B.; Shukla, S.; Varma, I. K. Naturally occurring phenolic sources: monomers and polymers. *RSC Adv.* **2014**, *4* (42), 21712−21752.

(43) Lochab, B.; Varma, I.; Bijwe, J. Blends of benzoxazine monomers. *J. Therm. Anal. Calorim.* **2013**, *111* (2), 1357−1364.

(44) Aydogan, C.; Kiskan, B.; Hacioglu, S. O.; Toppare, L.; Yagci, Y. Electrochemical manipulation of adhesion strength of polybenzox-azines on metal surfaces: from strong adhesion to dismantling. *RSC Adv.* **2014**, *4* (52), 27545−27551.

(45) Sharma, P.; Lochab, B.; Kumar, D.; Roy, P. K. Interfacial encapsulation of bio-based benzoxazines in epoxy shells for temperature triggered healing. *J. Appl. Polym. Sci.* **2015**, *132*, n/a.

(46) Sharma, P.; Shukla, S.; Lochab, B.; Kumar, D.; Kumar Roy, P. Microencapsulated cardanol derived benzoxazines for self-healing applications. *Mater. Lett.* **2014**, *133*, 266−268.

(47) Kiskan, B.; Yagci, Y. Self-healing of poly(propylene oxide)-polybenzoxazine thermosets by photoinduced coumarine dimerization. *J. Polym. Sci., Part A: Polym. Chem.* **2014**, *52* (20), 2911−2918.

Chemistry SELECT
Full Papers

| **Materials Science inc. Nanomaterials & Polymers**

Metal–Organic Frameworks as curing accelerators for benzoxazines

Pratibha Sharma,[a, b] Manju Srivastava,[a, c] Bimlesh Lochab,[d] Devendra Kumar,[b] Arunachalam Ramanan,[c] and Prasun Kumar Roy*[a]

Benzoxazine resins, although exhibiting attractive properties; particularly high thermal stability and near zero- shrinkage, suffer from a major drawback associated with its high curing temperature. In view of the Lewis acidity associated with the Zn_4O nodes in a zinc based metal organic framework [$Zn_4O(BDC)_3$, MOF5], we considered it of interest to explore its potential as a curing accelerator for a representative biobased benzoxazine resin. MOF 5 was solvothermally synthesized and characterized using different techniques including powder X-ray diffraction (PXRD), Scanning Electron Microscopy (SEM), Thermogravimetric Analysis (TGA), Fourier transform infrared spectroscopy (FT-IR) and Nitrogen physisorption measurements. Bio-based benzoxazine resin was synthesized by mannich type condensation of cardanol and aniline with formaldehyde under solventless conditions, the structure of which was confirmed using FT-IR and ^{1}H-NMR. The curing behavior of the synthesized resin was systematically investigated using non-isothermal Differential Scanning Calorimetry (DSC). Introduction of MOF 5 led to a shift in the curing profile to lower temperature, the extent of which was proportional to the amount of MOF 5 in the formulation. DSC studies were performed at different heating rates to establish the kinetic parameters associated with the curing of the resin. Activation energy, as calculated using Kissinger Akahira Sunose method, was found to concomitantly decrease from 98 kJ/mol to 58 kJ/mol upon addition of MOF 5 (5 % w/w).

Introduction

Metal organic frameworks (MOFs) are a rapidly developing class of microporous materials, which are finding increasing applications in varied fields including gas adsorption,[1] separation, chemical sensing and catalysis.[2] Inherent characteristic properties of MOFs, particularly in terms of their ultra-high surface areas, possibility of pore structure modification and a high degree of chemical and thermal stability bestow them excellent candidature for the aforementioned applications. One such application, of particular interest to our group, concerns catalytic curing of bio-based benzoxazine resins.[3]

Benzoxazines are cyclic N,O-acetal-type monomers, capable of undergoing ring-opening polymerization reaction[4] to form cross-linked networks with exceptional thermal stability.[4b, 5] However, majority of benzoxazine resins polymerize at elevated temperatures[6] which turns out to be an issue for practical applications. To overcome this drawback, several accelerators have been explored. In this context, organic acids[6a, 7] and lewis acids[8] are of particular interest, but their presence in the cured resin has been reported to reduce the chemical resistance of the polymer and adversely affect the physical properties of the resulting polymer.[9] Organic base such as amines,[10] and imidazoles[11] have also been explored as curing accelerators and the effectiveness of acid-base combination has also been reported.[12] Sudo et al[6b] studied the efficiency of acetylacetonatocomplexes of 4th period transition metals as catalysts for the ring opening polymerisation of benzoxazine. The examination revealed that acetylacetonato complexes of manganese, iron, cobalt and zinc exhibited the highest activity, which inspired us to explore the potential of zinc based MOFs in the context of curing of benzoxazine monomer.[6b] The possibility of tailoring the chemical environment around the metal centre with exceptionally high surface area of MOFs leave enormous scope for these MOFs in the context of catalysis.

MOF 5, is an archetypal robust three dimensional zinc carboxylate framework ([$Zn_4O(BDC)_3$], BDC = 1,4-benzenedicarboxylate), reported by Yaghi et.al.[13] The crystal structure of MOF 5 is comprised of oxocentered Zn_4O nodes, connected through linear BDC units forming an extended 3D cubic network with interconnected pores of 0.9 nm (Figure 1). Zinc oxide clusters

[a] P. Sharma, M. Srivastava, Dr. P. K. Roy
Centre for Fire, Explosive and Environment Safety
DRDO
Timarpur, Delhi 110054, India
+911123907191
+911123819547
E-mail: pk_roy2000@yahoo.com
pkroy@cfees.drdo.in

[b] P. Sharma, Prof. D. Kumar
Department of Applied Chemistry and Polymer Technology
Delhi Technological University
Delhi 110042, India

[c] M. Srivastava, Prof. A. Ramanan
Department of Chemistry
Indian Institute of Technology Delhi
New Delhi-16, India

[d] Dr. B. Lochab
Department of Chemistry, School of Natural Sciences
Shiv Nadar University
UP 201314, India
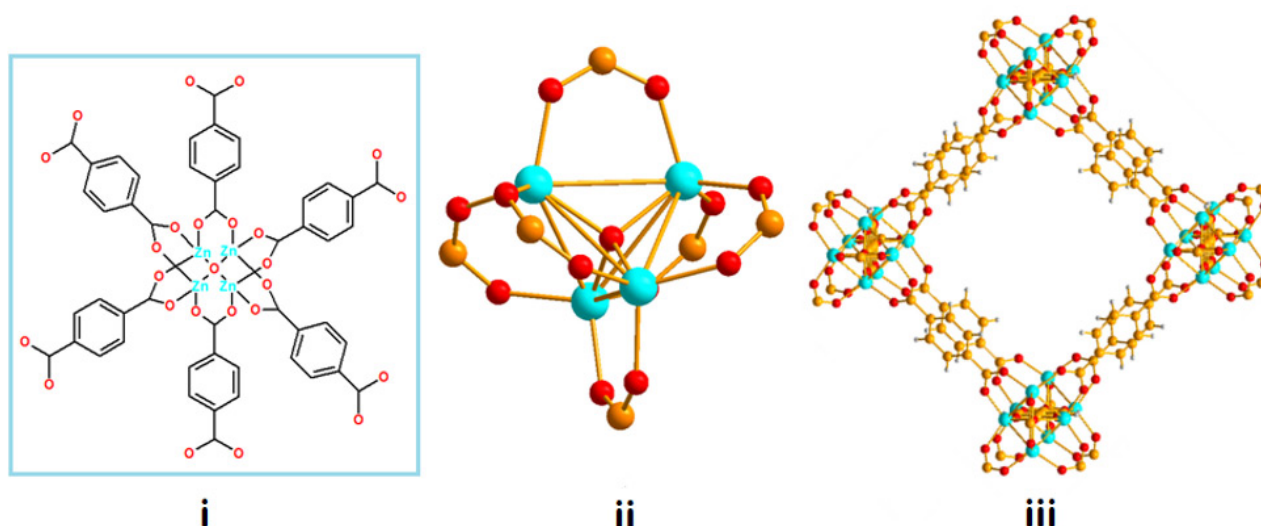
Figure 1. i) Chemical structure of secondary building unit, ii) structure of Zn$_4$O node and iii) 3 D structure of the framework of MOF 5 (Zn: cyan; C:grey; H:White and O:red).

(Zn$_4$O) of atomic precision, which are available throughout the framework confer it excellent candidature for applications where acidic catalysis is desirable which has led researchers to explore its potential in representative applications e.g. Friedel craft reaction.[14] Although applications of MOF's as heterogeneous catalyst has been well reported,[15] studies concerning their ability to accelerate the polymer curing reactions are virtually absent. It is to be noted however that the introduction of MOF 5 in polymeric matrices, both thermosetting as well as thermoplastics lead to significant improvement in their mechanical properties.[16]

Herein, we report the exploration of the potential of MOF 5 towards accelerating the ring opening polymerization of cardanol based monofunctional benzoxazine resin. Differential Scanning Calorimetric (DSC) analysis was performed to quantify the extent of acceleration in the ring opening polymerization behavior. To validate the role of Zn$_4$O nodes towards the acceleration of benzoxazine curing, calorimetric studies were also performed in the presence of ZIF 8 (Zn (MeIm)$_2$), another zinc based MOF with high surface area but lacking the acidic Zn$_4$O nodes present in MOF 5. To exclude the possible role of ligands towards acceleration of the curing process, the efficacy of another set of MOFs prepared using BDC and BTC as the ligands, i.e. Cu(BDC).DMF and[Cu$_3$(BTC)$_2$(H$_2$O)$_3$]$_n$, was also investigated.

Results and Discussions

Supramolecular assembly of MOF 5.

Zinc ions coordinate with benzene dicarboxylateligands[16–17] to result in the formation of cubic MOF 5 crystals as shown in Figure 2 (i). It is to be noted that the particle size distribution is highly dependent on the synthetic procedure adopted for its synthesis. Under the reaction conditions used for the present work, the average particle size is ca. 1–2 microns.Particle Size

distribution of MOF 5 presented in supplementary section Figure S3. Rietveld analysis of the diffraction pattern based on the structure reported in the literature (CCDC-277428) revealed the existence of the cluster core as a regular Zn$_4$O tetrahedron, linked to each other through a pair of terephthalate linkers in paddle-wheel type fashion resulting in the composition [(Zn$_4$O)(BDC)$_3$] (Figure 2(ii)). The nitrogen adsorption desorption isotherm at 77 K is presented in Figure 2(iii). Circles and triangular symbols represent adsorption and desorption data respectively. The BET surface area was found to be 1750 m^{2}g^{-1}. The TG-DTG trace of MOF 5 is presented in Figure 2 (iv). The initial mass loss of $<5\%$ at 300 °C can be attributed to the removal of DMF from the framework, which was followed by its pyrolytic decomposition at 410 °C leaving behind a char content of 51% at 600 °C.

Cardanol benzoxazine monomer

Cardanol nut shell liquid (CNSL) was chosen as the source of phenolic component to derive bio-based benzoxazine for the present study. CNSL is primarily composed of anacardic acid (74-77%), the rest being cardanol, cardol, and 2-methyl cardol. However, commercial-grade CNSL is obtained through roasting which results in the decarboxylation of anacardic acid into cardanol.[18] Furthermore, the components of CNSL are themselves mixtures of another four constituents which differ in the degree of unsaturation in the C-15 alkyl side chain attached at m-position. The long akyl chain in cardanol acts as an intramolecular plasticizer,[19] which reduces the viscosity of the resin, rendering it the characteristic of a reactive diluent for commercial benzoxazine resin,[20]thereby eliminating the use of solvent.[4b, 21]

The benzoxazine resin employed to study the effectiveness of curing accelerators, was derived by mannich like condensation reaction of cardanol, aniline and paraformaldehyde
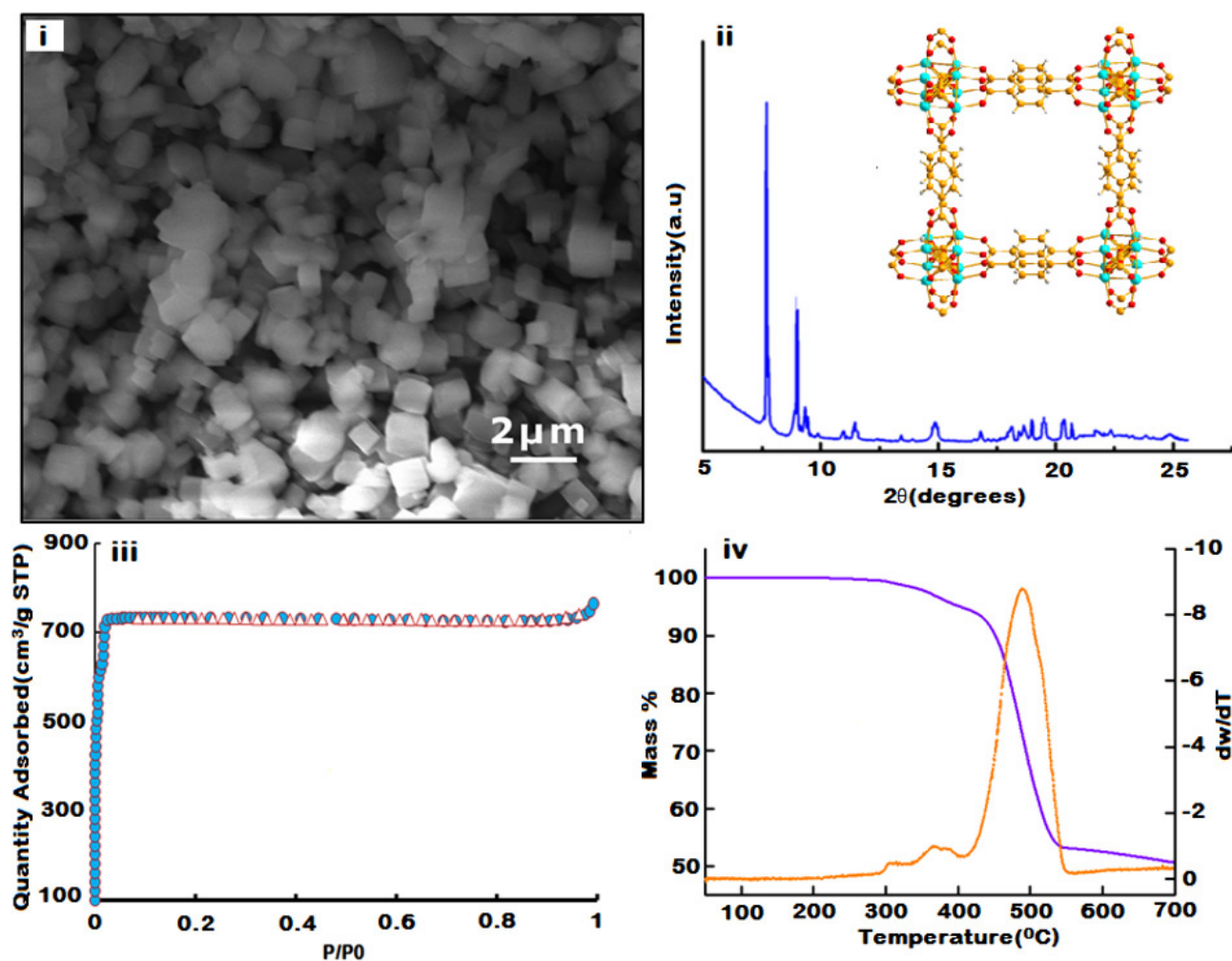
Figure 2. MOF-5 i) SEM image, ii) PXRD pattern iii) N_2 adsorption desorption isotherm and iv) TG-DTG traces.

(1:1:2),which post purification resulted in the formation of a red brown liquid in high yields (>90%). Detailed characterisation of the resin is presented in our previous paper.[22] The FT-IR and ^{1}H-NMR spectrum is presented in Figure 3. The appearance of new absorption bands at ~1250 and ~1030 cm^{-1} can be attributed to the Ar-C—O oxazine asymmetric and symmetric stretch respectively.[23] The absence of absorption bands due to N—H stretching (3360-3442 cm^{-1}) and N—H bending (1619 cm^{-1}) in the spectra of C-a further suggests the absence of unreacted aniline in the Bz monomer, thereby indicating completion of the reaction (Figure 3(i)). The formation of oxazines from hydroxyl functionalities was further confirmed by the presence of characteristic resonances at ~5.3 ppm (s, ArOC**H**$_2$N) and ~4.6 ppm (s, ArC**H**$_2$N) in the ^{1}H-NMR spectra (Figure 3(ii)).

Acceleration of benzoxazine ring opening polymerisation

Benzoxazine monomers undergo thermally accelerated cationic ring opening polymerisation leading to the formation of a thermally stable crosslinked polymer (Supplementary section, Figure S4). The ring opening polymerisation has been reported to be auto catalytic as the phenolic -OH generated in situ act as an additional initiator. Accelerators employed, alleviates the kinetics of the oxazine ring opening stage through several proposed mechanisms.[4a, 12, 24]To investigate the curing behavior of the benzoxazine resins in the presence of accelerators, non-isothermal calorimetric studies were performed and the representative curing profiles of formulations containing MOF 5 are presented in Figure 4.

It can be seen that the curing of the synthesized cardanol based benzoxazine exhibits a peak at 263 °C (Figure 4(i)). A pronounced shift in the curing profile towards lower temperature was observed, the extent of which was found to be proportional to the amount of MOF 5 in the formulation. The ability of MOF 5 to accelerate the curing process can be credited to the acidic Zn_4O nodes of the MOF 5 crystal lattice. To gain insight on the role of the chemical environment around the central zinc species, curing studies were also performed in the presence of Zn, ZnO, BDC and another zinc based metal organic framework ZIF 8, with high surface area (900 m^2/g) but differs predominantly with respect to the chemical environment around the central zinc atom.The characterization of ZIF 8 is
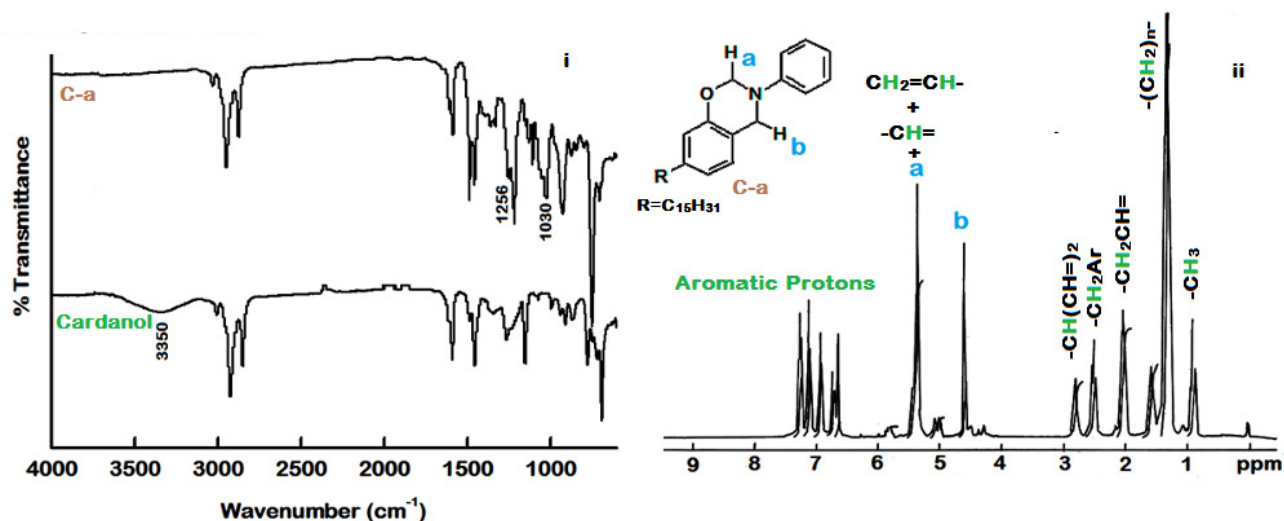
Figure 3. Cardanol based benzoxazine monomer (C-a) i) FT-IR and ii) ^{1}HNMR of C-a monomer.
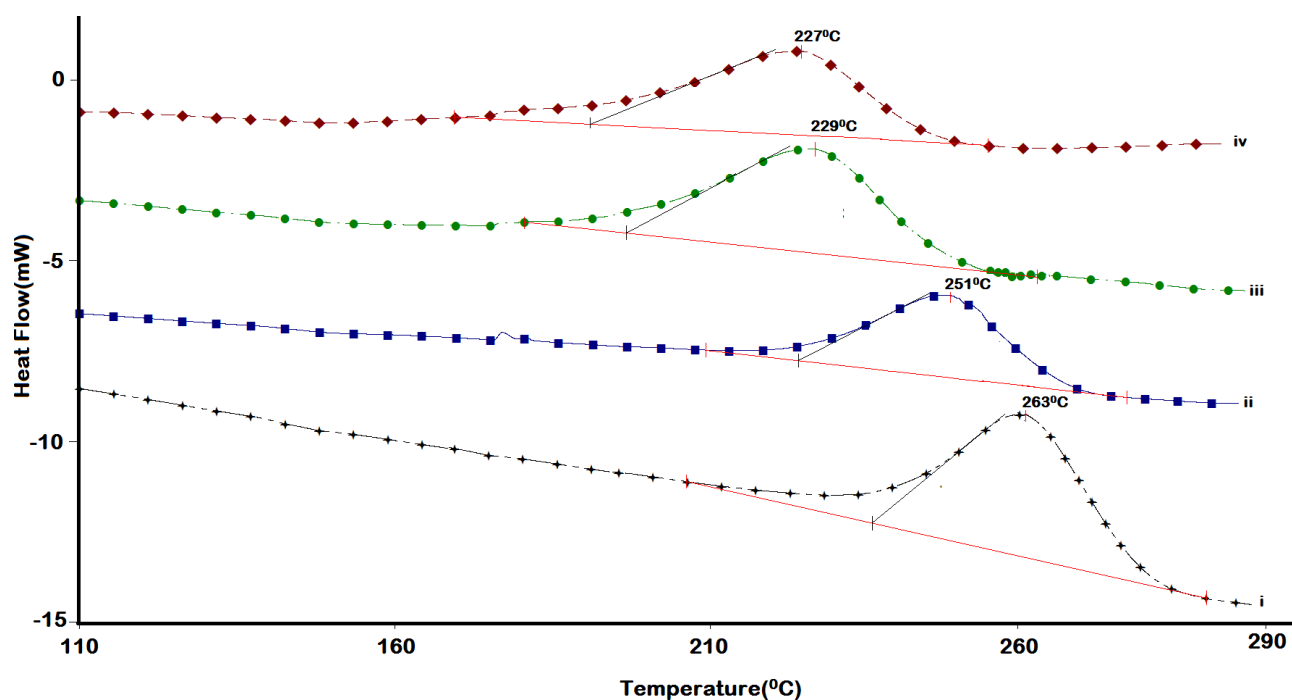
Figure 4. DSC curves for i) C-a, ii) M1C-a, iii) M5C-a and iv) M10C-a.

presented in the supplementary section (Figure S5). ZIF 8 reportedly features a sodalite topology (Si-O—Si bonds in zeolites being replaced by Zn—Im-Zn bonds) with cavities of diameter 1.16 nm, connected via 6- and 4-ring apertures.[25]

Another set of experiment was performed using two archetypal MOFs [Cu$_3$(BTC)$_2$(H$_2$O)$_3$]$_n$, HKUST-1 and Cu(BDC).DMF. The selection for the study stemming from the similarity in the nature of ligand i.e. BDC for copper terephthalate and BTC for HKUST-1. The characterization of HKUST-1 and copper terephthalate is presented in the supplementary section (Figure S6-S7). Copper terephthalate exhibits a sheet type structure in

which the Cu^{II} atoms are coordinated to the terephthalic acid linkers specific planes which are bonded through weak stacking interactions. HKUST-1 is made up of interconnected [Cu$_2$(O$_2$CR)$_4$] units (where R is an aromatic ring), creating a three dimensional network with a pore size of 1. The building block of HKUST-1 comprises of Cu^{2+} dimer coordinated with four oxygen atoms of benzene tricarboxylate forming a paddle wheel type structure. The activation of the framework reportedly leads to removal of water molecules coordinated to the exchangeable copper sites, thereby exposing the lewis acidic positions.
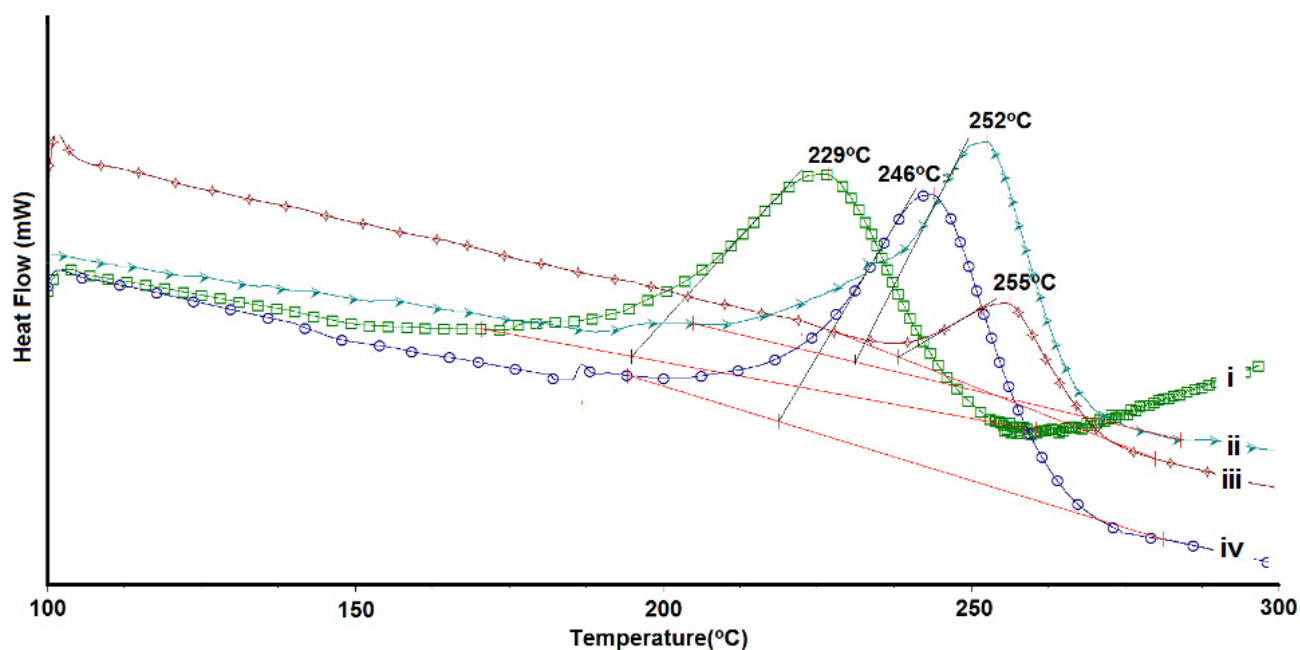
Figure 5. DSC traces i) M5C-a, ii) H5C-a, iii) CT5C-a and iv) Z5C-a.

The DSC traces associated with the curing of benzoxazine in the presence of different MOFs is presented in Figure 5. It can be seen that among all the MOFs studied, presence of MOF-5 led to the maximum decrease in the curing temperature, the results of the DSC analyses in terms of characteristic curing temperatures are summarized in Table 1.

Table 1. Effect on introduction of accelerators on characteristic curing temperatures ($\beta = 10\,°C/min$)						
Sample designation	T_o (°C)	T_{10} (°C)	T_{50} (°C)	T_{peak}(°C)	% Decrease in terms of	
					T_{peak}	T_o
C-a	240	235	250	263	–	–
BDC10C-a	231	224	240	253	2.6	3.7
ZnO10C-a	214	206	223	237	4.9	10.8
Zn10C-a	220	212	231	244	6	8.3
Z5C-a	218	197	218	246	6.5	9.1
CT5C-a	237	228	253	255	2.7	1.2
H5C-a	230	219	239	252	4.2	4.2
M1C-a	228	214	234	251	4.8	5
M5C-a	184	185	210	229	12.8	23.33
M10C-a	178	168	206	227	13.6	25.8
M15C-a	231	223	237	248	5.7	3.7

Acids, such as BDC have been reported to accelerate oxazine ring opening by the preferable protonation of oxygen atom generating a reactive species which undergoes condensation with the phenolate or other benzoxazine molecule resulting in phenolic structure (Figure 6(ii)). Metal centered accelerators such as metal oxides and MOFs accelerate benzoxazine polymerisation through the formation of aryl ether structures (Figure 6(iii)). The curing of benzoxazine in the presence

of MOF 5 as accelerator is proposed to proceed through coordination of zinc present in the Zn_4O cluster with the benzoxazine oxygen atom resulting in the formation of reactive iminium species. The electrophile generated condenses with other benzoxazine molecule resulting in unstable aryl ether structure which rearranges to more stable phenolic structures at elevated temperature (Figure 6(iv)).

As is evident from Table 1, among all the additives studied, MOF 5 leads to the most pronounced decrease in the curing temperature of C-a. However, increasing the amount of MOF 5 beyond 5 %, does not lead to any considerable decrease in the curing temperature further. In view of the same, M5C-a was chosen for establishing the kinetic parameters associated with the polymerisation reaction. It is to be noted that the dimensions of the benzoxazine resin (fully extended form, ~1.25 nm) is relatively larger than the pore diameter of MOF 5 (0.9 nm) (Supplementary section, Figure S8), which restrict the diffusion of the resin within the pores. This suggests that the accelerating ability of MOF 5 can be attributed primarily to the Zn_4O nodes available largely at the surface of the framework. In view of the possibility of tailoring the pore-dimensions of MOFs by rational choice of the organic linker, suitable framework with acidic nodes and larger pores can be designed, where the monomer can diffuse into, which can lead to further reduction in the curing temperature. It is interesting to note that ZIF 8, although containing the same metal centre (Zn) and exhibiting high surface area (900 m^2/g) did not lead to any substantial curing acceleration of the benzoxazine in terms of decrease in the curing temperature. ZIF 8, a prototypical structure with sodalite (SOD) topology comprise of individual Zn nodes as against Zn_4O nodes available throughout the MOF 5. In addition, the presence of Cu(BDC) and HKUST-1 both of which are
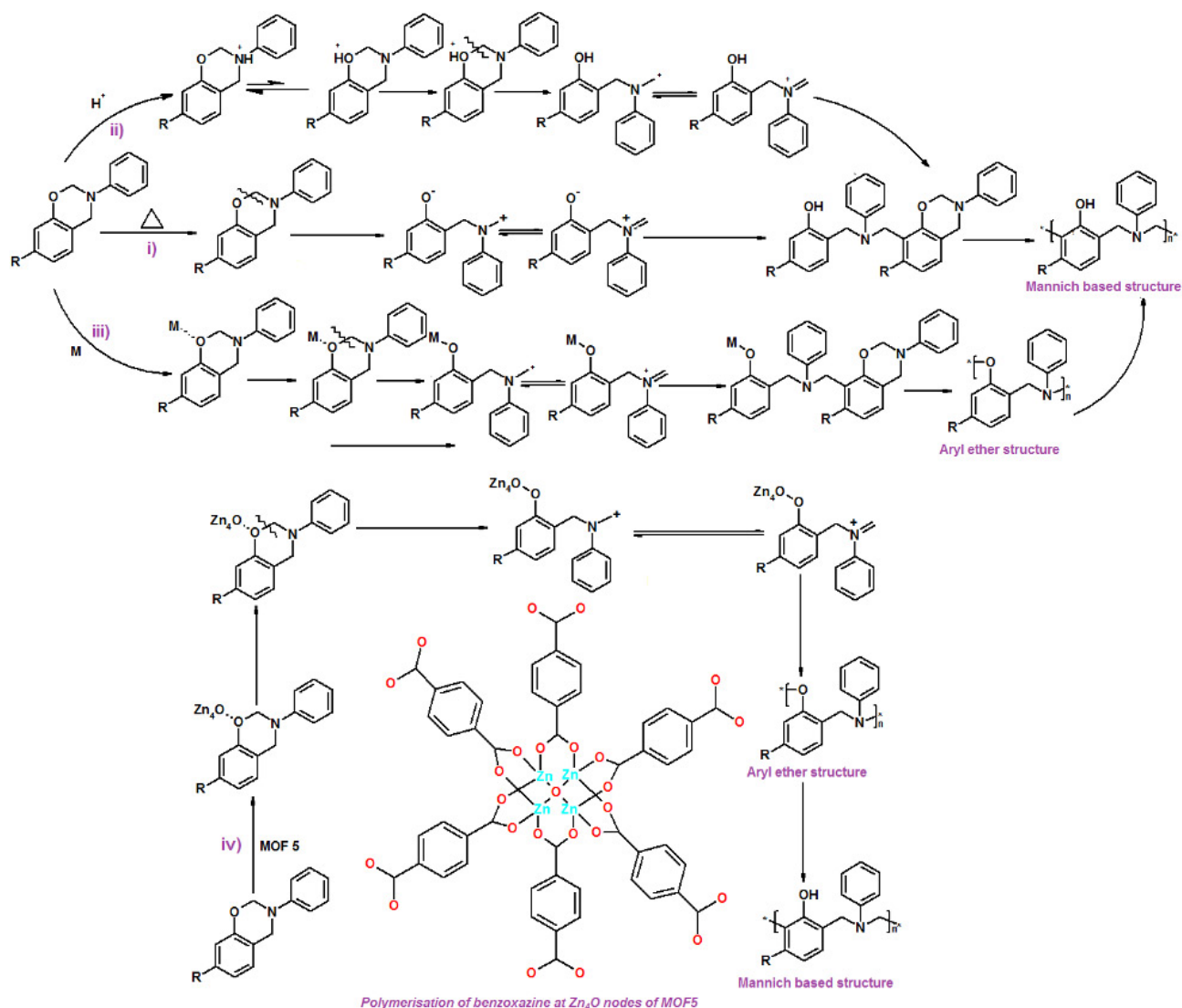
Figure 6. Probable mechanisms i) thermally accelerated polymerisation of benzoxazine resinii) polymerization by protonation iii) polymerization in the presence of metal based accelerators iv) polymerization in the presence of Lewis acidic Zn_4O nodes present in MOF 5.

synthesized using acidic ligands, does not lead to any substantial decrease in the curing temperature. Our studies lead us to believe that, it is primarily the availability of the acidic Zn_4O nodes in MOF 5, which is responsible for the acceleration of the benzoxazine curing.

One of the characteristic features of benzoxazines is "Zero-shrinkage" which implies 100% solid content. In all the cases, the benzoxazine samples exhibited high yields > 99.5%, irrespective of the presence or absence of MOF.

Curing Kinetics

The DSC traces of a representative formulation (M5C-a) at various heating rates viz. 5, 7 and 10 °C/min are presented in Figure 7. Increasing the heating rate (β) leads to systematic shift in the trace towards higher temperatures, which can be attributed to the reduced time available with the reactive molecules

upon being subjected to higher heating rates. The curing of benzoxazine resin is typically a multi-step process exhibiting complex kinetics. The process is accompanied with a dramatic change in the physical state of the reaction medium. At the early stages, the reaction medium is a liquid composed primarily of monomers. With the progress of the reaction, the molecular weight and viscosity of the polymer formed increases which in turn results in a decrease in the molecular mobility. The most dramatic decrease in the mobility occurs with the cross-linking of polymer chains, where the chains lose their ability to move past one another, and the medium turns from flowing liquid to a solid that can be either rubbery or glassy, depending upon the T_g of the cured resin. Characteristic parameters associated with the curing of the resini.e. $\triangle H_{cure}$, T_{onset} and T_{peak} are summarized in Table 2.

Figure 7. Effect of heating rate (β) on the curing profile of M5C-a a) 5, b) 7 and c) 10 °C/min.

Table 2. Characteristic curing parameters of neat benzoxazine and M5C-a				
Sample	β(°C/ min)	T_{onset} (°C)	T_{peak} (°C)	Activation energyα = 10 % (kJ/ mol)
C-a	5	224	246	98
	7	236	255	
	10	241	263	
M5C-a	5	173	196	58
	7	178	217	
	10	184	229	

The extent of conversion, α at any particular temperature (T_{α}) was calculated as the ratio of the areas under the exothermic DSC peak and expressed as:

$$\alpha = \frac{\Delta H_{T\alpha}}{\Delta H_{cure}} \qquad 1$$

where $\Delta H_{T\alpha}$ is the heat of reaction of partially cured samples (till temperature T_{α}) and $\triangle H_{cure}$ is the total heat of curing. The increase in the degree of conversion with temperature for C-a and M5C-a at a particular heating rate (5 °C/min) is presented in Figure 8.

It can be seen that the complete curing of neat monomer is achieved at 280 °C while in the presence of MOF 5 the same is attained at 230 °C, which is indicative of the ability of MOF 5 as an accelerator for curing of benzoxazines.

In view of its simplicity, Kissinger-Akahira-Sunoseequation[26] was applied for determination of activation energies (E_{α}) from the plot of $ln\left(\frac{\beta_i}{T_{\alpha,i}^2}\right)$ against $1/T_{\alpha}$.

$$ln\left(\frac{\beta_i}{T_{\alpha,i}^2}\right) = \text{Constant} - \frac{E_{\alpha}}{RT_{\alpha,i}} \qquad 2$$
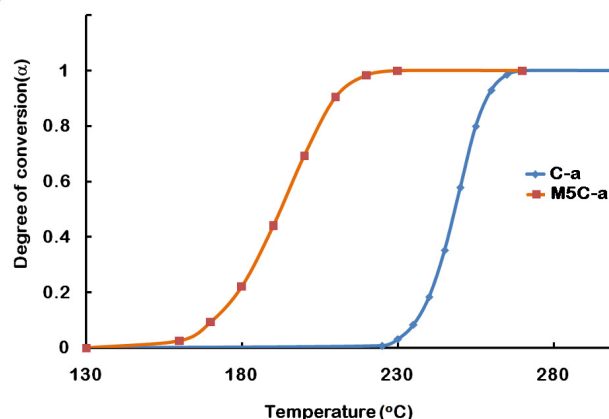
Figure 8. Effect of temperature on the degree of conversion of cardanol based benzoxazine in the presence and absence of MOF 5 (β = 5 °C/min).

Where, β is the heating rate, T_{α} is the temperature associated with a particular conversion (α) at the corresponding heating rate, E_{α} is the activation energy at that α and R is the gas constant. The linear plots at few representative conversions for M5C-a are presented in the supplementary section, (Figure S9) which were in turn used to arrive at the activation energy. The presence of MOF 5 led to a substantial decrease in the activation energy from 98 kJ/mol for neat resin to 58 kJ/mol (M5C-a).

Thermal properties

Thermogravimetric analysis was performed to investigate the effect of introducing MOF 5 on the thermal stability of polybenzoxazine. The TG and DTG traces of poly(C-a) and poly(M5C-a) are presented in Figure 9. The thermal decomposition of cardanol based benzoxazines is a multi-step process occur-
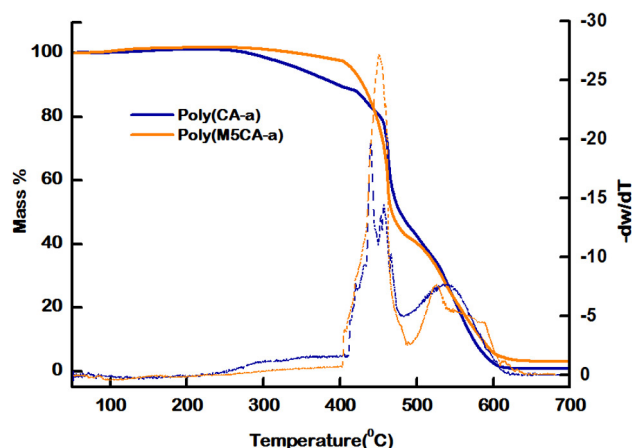
Figure 9. TG-DTG traces of Poly(C-a) and Poly(M5C-a).

ring through the degradation of the phenolic linkages and of the Mannich bridges in the polybenzoxazine.[27] The double bond α-carbon of the cardanol undergoes scission at ~ 200 °C[28] and the methylene linkages in the cured polymer have been reported to undergo cleavage at 440–500 °C.[29]

Decomposition temperatures associated with characteristic mass loss at 5%, 10% and char content (at 600 °C) are presented in Table 3. An appreciable increase in the $T_{5\%}$ and $T_{10\%}$

Table 3. Characteristic thermo-oxidative degradation parameters

Sample Designation	$T_{5\%}(°C)$	$T_{10\%}(°C)$	Char content at 600 °C (%)
Poly (C-a)	345	393	1.6
Poly (M5C-a)	416	429	5.9

values is evident from the traces, and the increase in the char content can be attributed to the presence of zinc oxide formed during the oxidative degradation of the cured formulation.

Adhesive property

The effect of MOF−5 inclusion on the adhesive strength of the benzoxazine resin was studied on steel plates as per the standard procedure. The results in terms of LSS are tabulated in Table 4 and the representative load−displacement curve is presented in Figure S10. The LSS of adhesive to any substrate is dependent on several factors, particularly substrate wetting, in-

Table 4. Lap Shear Strength values of benzoxazines

Resin	Lap Shear Strength (Kg cm^{-2})
C-a	27±2
M5C-a	25±3

herent adhesive strength, temperature, resin thickness and type of failure. The adhesive thickness for C-a was maintained between 0.23–0.46 mm. The curing of benzoxazine lead to generation of sites which are involved in hydrogen bonding such as -OH and >N-. It can be seen from the table that the presence of MOF 5 does not lead to any appreciable decrease in the LSS of the resin.

Conclusions

The accelerating ability of MOF 5 on the ring opening polymerisation of a representative bio based cardanol based benzoxazine(C-a) was systematically studied. The presence of MOF 5 was found to decrease the curing temperature of neat benzoxazine from 263 °C to 229 °C (12.6% decrease). Our studies indicate that Zn_4O nodes of atomic precision, which are available throughout the surface of the framework, are responsible for the decrease in the curing temperature. To validate the same, curing studies were also performed in the presence of another zinc based metal organic framework, (ZIF 8) which exhibits high surface area but differs around the chemical environment around the central zinc atom. In addition, the potential of Cu(BDC).DMF and HKUST-1 towards lowering of curing temperature were also explored. The extent of reduction in the curing temperature was found to be much higher in the case of MOF 5. KAS method was used to determine the activation energy of polymerization, which was found to decrease from 98 kJ/mol (neat resin) to 58 kJ/mol for formulation containing MOF 5 (5%w/w). The cured resins obtained in the presence of MOF 5 exhibited relatively high thermal stability ($T_{5\%}$ = 416 °C) as compared to the neat crosslinked resin ($T_{5\%}$ = 345 °C). Our studies clearly highlight the enormous scope of metal organic frameworks as accelerators for polymerisation of benzoxazine resins mandating high temperature. In view of the flexibility in designing and controlling the architecture of these hybrid structures, novel benzoxazine systems with low curing temperatures and improved performance can be formulated in the future.

[1] A. Mallick, S. Saha, P. Pachfule, S. Roy, R. Banerjee, *J. Mater. Chem.* **2010**, *20*, 9073–9080.

[2] a) Z. Zhang, Y. Zhao, Q. Gong, Z. Li, J. Li, *Chem. Commun.* **2013**, *49*, 653–661; b) S. Qiu, M. Xue, G. Zhu, *Chem. Soc. Rev.* **2014**, *43*, 6116–6140; c) J.-R. Li, R. J. Kuppler, H.-C. Zhou, *Chem. Soc. Rev.* **2009**, *38*, 1477–1504.

[3] a) P. Sharma, B. Lochab, D. Kumar, P. K. Roy, *J. Appl. Polym. Sci.* **2015**, *132*; b) P. Sharma, S. Shukla, B. Lochab, D. Kumar, P. Kumar Roy, *Mater. Lett.* **2014**, *133*, 266–268; c) M. Arslan, B. Kiskan, Y. Yagci, *Macromolecules* **2015**, *48*, 1329–1334.

[4] a) G. Riess, J. M. Schwob, G. Guth, M. Roche, B. Laude, in *Adv. Polym. Syn.* (Eds.: B. M. Culbertson, J. E. McGrath), Springer US, Boston, MA, **1985**,

pp. 27–49;b) X. Ning, H. Ishida, *J. Polym. Sci., Part A: Polym. Chem.***1994**, *32*, 1121–1129;c) Y. Yagci, B. Kiskan, N. N. Ghosh, *J. Polym. Sci., Part A: Polym. Chem.***2009**, *47*, 5565–5576.

[5] a) H. Ishida, D. J. Allen, *J. Polym. Sci., Part B: Polym. Phys.***1996**, *34*, 1019–1030;b) H. Ishida, D. P. Sanders, *J. Polym. Sci., Part B: Polym. Phys.***2000**, *38*, 3289–3301.

[6] a) H. Ishida, Y. Rodriguez, *J. Appl. Polym. Sci.***1995**, *58*, 1751–1760;b) A. Sudo, S. Hirayama, T. Endo, *J. Polym. Sci., Part A: Polym. Chem.***2010**, *48*, 479–484.

[7] A. A. Gallo, *US 6376080 B1***2002**.

[8] a) Y. X. Wang, H. Ishida, *Polymer***1999**, *40*, 4563–4570;b) H. Ishida, *US6225440 B1***2001**.

[9] A. Sudo, T. Endo, A. Taden, R. Schoenfeld, T. Huver, *US20100144964 A1***2010**.

[10] J. Sun, W. Wei, Y. Xu, J. Qu, X. Liu, T. Endo, *RSC Adv.***2015**, *5*, 19048–19057.

[11] B. A. A. Rucigaj, M. Krajnc, U. Sebenik, *Exp. Polym. Lett.***2015**, *9*, 647–657.

[12] A. Sudo, R. Kudoh, H. Nakayama, K. Arima, T. Endo, *Macromolecules***2008**, *41*, 9030–9034.

[13] H. Li, M. Eddaoudi, M. O'Keeffe, O. M. Yaghi, *Nature***1999**, *402*, 276–279.

[14] a) N. T. S. Phan, K. K. A. Le, T. D. Phan, *Applied Catalysis A: General***2010**, *382*, 246–253;b) J. Lee, O. K. Farha, J. Roberts, K. A. Scheidt, S. T. Nguyen, J. T. Hupp, *Chemical Society Reviews***2009**, *38*, 1450–1459;c) Z. Akimbekov, D. Wu, C. K. Brozek, M. Dinca, A. Navrotsky, *PCCP***2016**, *18*, 1158–1162.

[15] a) J. Lee, O. K. Farha, J. Roberts, K. A. Scheidt, S. T. Nguyen, J. T. Hupp, *Chem. Soc. Rev.***2009**, *38*, 1450–1459;b) S. Gao, N. Zhao, M. Shu, S. Che, *Appl. Catal. A***2010**, *388*, 196–201;c) A. U. Czaja, N. Trukhan, U. Müller, *Chem. Soc. Rev.***2009**, *38*, 1284–1293;d) M. Sabo, A. Henschel, H. Fröde, E. Klemm, S. Kaskel, *J. Mater. Chem.***2007**, *17*, 3827–3832.

[16] Manju, P. K. Roy, A. Ramanan, *RSC Adv.***2014**, *4*, 52338–52345.

[17] a) Manju, P. Kumar Roy, A. Ramanan, C. Rajagopal, *Mater. Lett.***2013**, *106*, 390–392;b) Manju, P. K. Roy, A. Ramanan, C. Rajagopal, *RSC Adv.***2014**, *4*, 17429–17433.

[18] J. H. P. Tyman, D. Wilczynski, M. A. Kashani, *J. Am. Oil. Chem. Soc.***1978**, *55*, 663–668.

[19] a) S. Mohapatra, G. B. Nando, *RSC Adv.***2014**, *4*, 15406–15418;b) C. Voirin, S. Caillol, N. V. Sadavarte, B. V. Tawade, B. Boutevin, P. P. Wadgaonkar, *Polym. Chem.***2014**, *5*, 3142–3162.

[20] a) P. Campaner, D. D'Amico, L. Longo, C. Stifani, A. Tarzia, S. Tiburzio, in *Handbook of Benzoxazine Resins* (Ed.: H. I. Agag), Elsevier, Amsterdam, **2011**, pp. 365–375;b) O. A. Attanasi, M. S. Behalo, G. Favi, D. Lomonaco, S. E. Mazzetto, G. Mele, I. Pio, G. Vasapollo, *Curr. Org. Chem.***2012**, *16*, 2613–2621.

[21] Y. X. Wang, H. Ishida, *J. Appl. Polym. Sci.***2002**, *86*, 2953–2966.

[22] B. Lochab, I. K. Varma, J. Bijwe, *J. Therm. Anal. Calorim.***2010**, *102*, 769–774.

[23] J. Jang, D. Seo, *J. Appl. Polym. Sci.***1998**, *67*, 1–10.

[24] a) J. Dunkers, H. Ishida, *J. Polym. Sci., Part A: Polym. Chem.***1999**, *37*, 1913–1921;b) P. Chutayothin, H. Ishida, *Macromolecules***2010**, *43*, 4562–4572;c) C. Liu, D. Shen, R. M. Sebastián, J. Marquet, R. Schönfeld, *Macromolecules***2011**, *44*, 4616–4622;d) Y.-X. Wang, H. Ishida, *Macromolecules***2000**, *33*, 2839–2847.

[25] a) Y. Pan, Y. Liu, G. Zeng, L. Zhao, Z. Lai, *Chem. Commun.***2011**, *47*, 2071–2073;b) M. Srivastava, P. K. Roy, A. Ramanan, *RSC Adv.***2016**, *6*, 13426–13432.

[26] P. Budrugeac, E. Segal, *J. Therm. Anal. Calorim.***2007**, *88*, 703–707.

[27] a) H. Yee Low, H. Ishida, *Polymer***1999**, *40*, 4365–4376;b) S.-i. Kuroda, K. Terauchi, K. Nogami, I. Mita, *Eur. Polym. J.***1989**, *25*, 1–7.

[28] S. Manjula, C. K. S. Pillai, V. G. Kumar, *Thermochim. Acta***1990**, *159*, 255–266.

[29] D. O'Connor, F. D. Blum, *J. Appl. Polym. Sci.***1987**, *33*, 1933–1941.

| Sustainable Chemistry

Microwave-Assisted Sustainable Synthesis of Telechelic Poly(ethylene glycol)s with Benzoxazine End Groups

Pratibha Sharma,[a, b] Devendra Kumar,[b] and Prasun Kumar Roy*[a]

A microwave assisted synthetic route was explored as a sustainable tool for the preparation of cross-linkable telechelic poly(ethylene glycol)s endcapped with benzoxazine functionality. In comparison to the conventional methodology, the reaction completion time could be significantly reduced using MAS technique and the sustainability of the procedure was improved. Microwave active bifunctional amines were prepared by the condensation reaction of p-aminobenzoic acid and poly(ethylene glycol)s of different chain lengths to yield amine terminated poly(ethylene glycol)s (ATPEGs). Cardanol, an agro-waste was chosen as the phenolic source, which was reacted with ATPEG to undergo Mannich like condensation resulting in reactive thermoplastic of telechelic nature. The structure of the resulting polymer was confirmed through FT-IR and ^{1}H-NMR spectroscopy. Benzoxazine moieties present at the terminals undergo thermally accelerated ring opening polymerization to form cross-linked networks which was studied using non-isothermal differential scanning calorimetry (DSC). The rheological behavior of the resulting polymer suggests that the viscosity of the benzoxazine-endcapped telechelic poly (ethylene glycol)s is sufficiently low to permit solventless processing which can be credited to the presence of flexible polyether linkages. The adhesive properties of the cross-linked benzoxazine endcapped telechelic poly(ethylene glycol)s have also been studied.

1. Introduction

Microwave assisted synthesis (MAS) has emerged as a sustainable tool for organic synthesis which offers a simple, efficient and economic route towards the preparation of industrially important chemicals.[1] Microwave assisted heating is a rather rapid process, which does not mandate any contact between the energy source and the reaction vessel. The acceleration in the rate of reaction is primarily due to thermal effects, which is essentially due to rapid heating of the reactants.[2] Possible existence of "non-thermal microwave effects" that could rationalize the difference in 'thermal' and 'microwave assisted' heating has always been a topic of much debate.[2] In general, the essential criterion behind the success of MAS technique is the polarity of the reaction media. In the field of polymers, the application of microwaves for process development has led to apt solutions for several intriguing technical problems.[3] For example, MAS has been adopted for the synthesis of several industrially important polymeric resins like unsaturated polyesters,[4] polyamides,[5] polyethers,[6] polyimides[7] etc. and microwave radiation has also been reported to facilitate the curing process of various polymeric systems.[8]

Several benzoxazine derivatives have also been prepared using MAS,[9] which are generally used in the field of pharmacological sciences. Inan et. al.[10] reported the microwave synthesis of polybenzoxazine precursor using humic acid as a source of phenol from coal. However, literature on the exploration of MAS technique towards synthesis of polymeric benzoxazine resins is relatively scarce, the reason probably being the low microwave activity of the reactants involved, i.e. amine, formaldehyde and phenol. 1,3-benzoxazine monomer is synthesized by Mannich like condensation of these reactants in solution or through melt processing. Polybenzoxazines, formed by the thermal curing of this monomer, exhibit interesting properties, particularly negligible volume shrinkage during curing,[11] low water absorption[12] and excellent thermal stability in combination with excellent mechanical performance.[13] As is clear, there is enormous design flexibility in benzoxazine synthesis, due to the large library of precursors available. In view of the potential of benzoxazines in different areas, all endeavors towards reduction in the reaction time for the preparation of these resins are highly desirable.

Development of benzoxazines, especially those based on renewable raw materials using alternative sustainable processes, has been receiving the attention of academicians and industrialists.[14] In the context of sustainable benzoxazines, there is enormous literature to support the candidature of agro-waste cardanol as a phenolic source. Cardanol possess a long alkyl chain which can lead to intramolecular plasticization,[15] resulting in the lowering of glass transition temperature (T_g) of the cured specimen[16] but higher polymerisation temperatures.[17] What makes cardanol particularly interesting in the context of benzoxazine preparation, is its ability to render the synthetic process solventless. The Mannich like condensa-

[a] P. Sharma, Dr. P. K. Roy
     Centre for Fire, Explosive and Environment Safety, DRDO, Timarpur, Delhi
     110054, India.Tel.: +911123907191Fax: +911123819547
     E-mail: pk_roy2000@yahoo.com
              pkroy@cfees.drdo.in
[b] P. Sharma, Prof. D. Kumar
     Department of Applied Chemistry and Polymer Technology, Delhi Technological University, Delhi 110042, India.

tion reaction of cardanol with amines and formaldehyde has been extensively studied,[14a, b, 18] which reveal that the reaction requires about 3 h at 90 °C. We hypothesize that the sustainability of this process can be further improved by using MAS technology, which has the additional advantage of reducing the reaction time.

As already mentioned, both the raw materials for benzoxazine synthesis i.e. phenols and amines, are not sufficiently microwave active to ensure rapid reaction under microwave irradiation. Poly(ethylene glycol)s (PEGs), on the other hand, are considered effective solvents for the microwave assisted synthesis.[19] It is worth mentioning that PEGs are employed as green solvents for sustainable organic synthesis as they are relatively inexpensive, nontoxic and biodegradable.[20] We considered it of interest to functionalize PEGs to yield microwave active amine-terminated poly(ethylene glycol)s (ATPEGs), which can subsequently be used as a reactant for the preparation of monomer. The resulting benzoxazine is expected to contain repeating ether functionalities, and the length of the polyether chain affects the flexibility of the resultant polymer.[21] The presence of oxazine moieties at the terminal positions lead to the formation of benzoxazine-endcapped telechelic poly(ethylene glycol)s, which are cross-linkable macro-monomers combining the thermoplastic properties associated with the flexible segment in addition to the dimensional, high-temperature stability and chemical resistance offered by the benzoxazine units.[22]

Most of the commercial benzoxazines are solids at room temperature and require liquification prior to the processing step. By judicious choice of reactants and using organic solvents, the resin viscosity can be optimized, the latter route being less preferred due to environmental concerns.[23]The aim of the present work is to perform solvent less microwave assisted synthesis of cross-linkable telechelic poly(ethylene glycol)s with benzoxazine end groups, which exhibit sufficiently low viscosity due to the presence of flexible polyether chains.

2. Results and Discussion

The potential of MAS technology towards the sustainable synthesis of telechelic poly(ethylene glycol) endcapped with benzoxazine moieties has been explored. Microwave active amines ATPEG were prepared, which were reacted with cardanol and formaldehyde under solventless conditions to result in telechelic polymer with terminal benzoxazine moieties, which are capable of undergoing ring opening polymerisation to form crosslinked polymers with excellent thermal stability.

Amine terminated poly(ethylene glycol) (ATPEG)

The most common approach for the conversion of hydroxyl functionality into primary amine involves a multiple stage protocol, where the hydroxyls are first converted to sulphonates or halides followed by the nucleophilic substitution by azide anion, which are subsequently reduced.[24] It is to be noted that, commercially, only high molecular weight amines terminated poly(ethylene glycol) ($M_w > 2000$) are available,

which too are rather expensive. We have previously reported a single step process for the amine termination of poly(ethylene glycol), which involves condensation reaction with PABA in the presence of catalyst as per Scheme 1.[25]
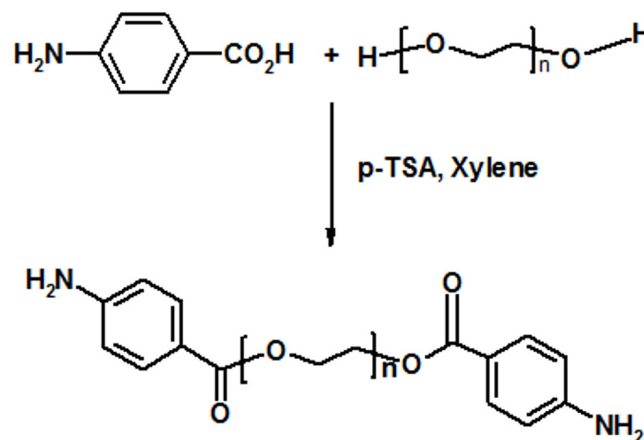
Scheme 1. Amine functionalization of poly(ethylene glycol).

The FT-IR spectra of amine-terminated poly(ethylene glycol)s (ATPEGs) is presented inFigure 1(i) and that of PEGs is shown in supplementary section Figure S2. The spectra of both PEG and ATPEG exhibit characteristic peaks associated with $\nu_{C-H, stretch}$ at ~ 2875 cm^{-1}, $\nu_{C-H, bend}$ at ~ 1466 cm^{-1} and $\nu_{C-O, stretch}$ at ~ 1060 cm^{-1}. The amine derivative exhibits additional peaks associated with $\nu_{N-H, stretch}$at ~ 3357 cm^{-1}, $\nu_{N-H, bend}$ at ~ 1603 cm^{-1}, $\nu_{C=O, stretch}$ at ~ 1698 cm^{-1}, and $\nu_{C-N,stretch}$ at ~ 1341 cm^{-1}.

The ATPEGs were also characterized using ^{1}H-NMR spectroscopy using CDCl$_3$ solvent and the ^{1}H-NMR spectra of the amines are also presented in Figure 1(ii). As expected, the spectra of all the amines were found to be similar irrespective of the molecular weight of the polyether glycol used for synthesis. Characteristic resonances at ~6.5 ppm (4H, **aromatic**), 7.5 ppm (4H, **aromatic**), 4.2 ppm (4H, s, ArN**H$_2$**) and 3.4 ppm (m, OCH$_2$**CH$_2$**O) can be seen in spectra of ATPEG.

Poly(ethylene glycol) are microwave active species with PEG 200 having a loss factor of ~7.08 (2GHz and 25 °C).[26] Since, it is the terminal hydroxyl groups, which contribute towards the polarity of PEG, the microwave activity of the reactants decreases with increasing molecular mass. The presence of ethereal oxygen and terminal –**NH$_2$**is also expected to confer microwave activity to ATPEGs, which form the basis of selection of the latter for microwave assisted synthesis of benzoxazines. The ability of the reactants to convert microwave energy into heat was evidenced in terms of increase in the temperature of the ATPEG, upon being exposed to uniform microwave radiation. The temperature-time profiles for a few representative reactants are presented in Figure S3, supplementary section.
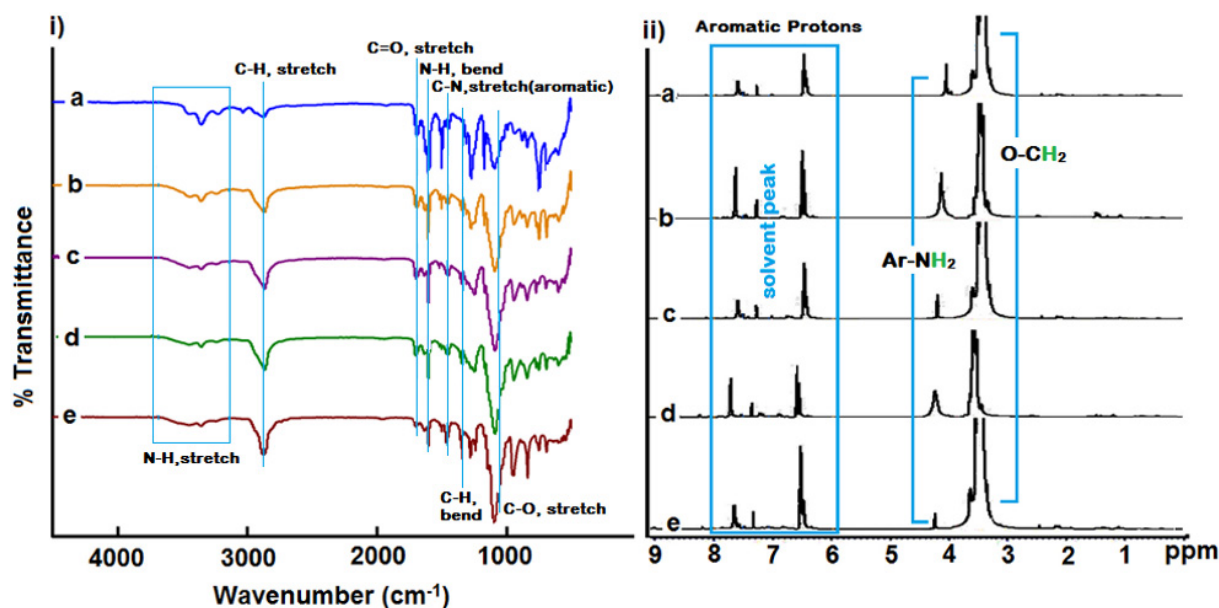
Figure 1. i) FT-IR and ii) ^{1}H-NMR spectra of a) ATPEG200 b) ATPEG400 c) ATPEG600 d) ATPEG1000 e) ATPEG1500.

MAS for synthesis of telechelic poly(ethylene glycol)s endcapped with benzoxazine

Thermally cross-linkable telechelic poly(ethylene glycol)s with benzoxazine end groups were synthesized through solvent-less Mannich like condensation reaction of cardanol with the ATPEG using conventional as well as microwave route as per the reaction presented in Scheme 2. The microwave assisted syn-
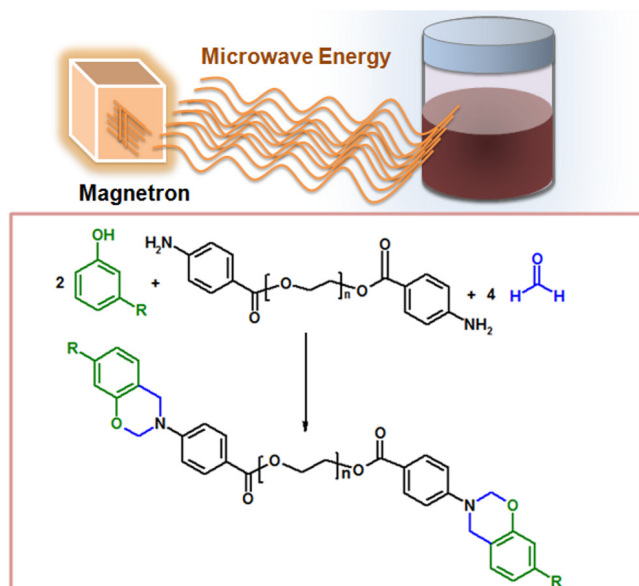
Scheme 2. Telechelic poly(ethylene glycol) endcapped with benzoxazines from cardanol and amine terminated poly(ethylene glycol) (ATPEG).

thesis of benzoxazine-endcapped telechelic polymers was relatively easy, and more energy efficient than the conventional route without compromising on the performance, properties and application of the end product.

In view of the suitable viscosity of cardanol (145 mPa.s),[18c] solventless synthesis was feasible.[14a, b, 18b, 27] However, under conventional heating, the reaction took approximately 180 mins (at 90 °C) to reach completion (yield ~90±5%). As with most chemical reactions, raising the reaction temperature increases the reaction rate and the extent of acceleration was evidenced in terms of the reduction in reaction completion time. At 150 °C, the reaction completion time concomitantly reduced to 120 mins, without affecting the reaction yield (~90±5%), however the elevated temperature leads to oligomerization of the monomer, which was observed in the ^{1}H-NMR spectra. The ^{1}H-NMR spectra of the benzoxazine-endcapped polymer is presented in Figure 2, where the reaction was performed at 90 °C and 150 °C.

In view of the presence of alkylene protons associated with cardanol (m, $CH=$, $CH_2=CH-$),which resonates at the same position as $ArOCH_2N$ (~5.4 ppm),the intensity ratio of the signals associated with the oxazine moiety in cardanol based benzoxazines at 4.6 (singlet) and 5.4 ppm (multiplet) is expected to be 1:3.[18b] However, it can be seen that the ratio of intensities of the signals deviates largely in the product obtained when the reaction was performed at 150 °C. This deviation from 1:3 can be ascribed to the oligomerization in the oxazine moiety. This leads to the appearance of an additional peak in the region 3.5-4.5 ppm, which is associated with $-CH_2-$ protons of mannich base formed during the ring opening of the oxazine moiety (Figure 2).

Liu and Ishida have proposed the mechanism and studied the kinetics of the solventless synthesis of Bisphenol A and

Figure 2. ^{1}H-NMR spectra of C-ATPEG200 prepared at a) 90 °C and b) 150 °C.

Scheme 3. Possible mechanism of benzoxazine formation using solvent less route at higher temperature.

toluidine based benzoxazine.[28] It has been suggested that at temperatures between 90–100 °C, the overall reaction rate is controlled by the formation of mannich base, which follows third order kinetics. With the progress of the reaction, the concentration of mannich base reaches maxima, which subsequently convert to benzoxazine. On increasing the temperature further, and/or with extended time, the 1,3, benzoxazine undergoes ring opening to form oligomers. In view of the possibility of oligomerization, it is suggested that under conventional heating, it is not advisable to increase the reaction temperature beyond 90 °C, in congruence with previous studies.[29]

It is to be noted that under conventional conditions, paraformaldehyde remains in the solid phase, which renders this reaction practically diffusion controlled. Increasing the reaction temperature beyond the melting point of paraformaldehyde (120 °C), leads to the formation of a homogeneous media, where the reaction is expected to proceed more rapidly. We hypothesize that using microwaves, it is possible to increase the temperature of the reactants to reach > 120 °C, following which the reaction can be maintained isothermally for adequate time durations to result in formation of benzoxazines monomer avoiding the formation of oligomers, as shown in Scheme 3.

In view of the microwave activity of ATPEG and cardanol,[30] it was observed that the reaction took significantly lesser periods (25 min as opposed to 120 min at 150 °C) to reach completion (yield ~95 ± 5%) under microwave assisted conditions. The microwave profile is presented in supplementary

section Figure S4. It can be seen that the reactants reach 150 °C in less than a minute under microwave irradiation, a phenomenon unaccomplishable using conventional heating. This rapid heating of the reactants is primarily responsible for the reduction in the reaction time under microwave conditions. In view of the possibility of opening of the oxazine moiety at higher temperatures (T > 150 °C), the temperature of the reaction media was not increased further.

The FT-IR spectra of the benzoxazine monomers are presented in Figure 3(i). The absence of absorption due to O—H and N—H stretching at > 3161 cm^{-1} suggests that the unreacted amine terminated poly(ethylene glycol) and cardanol are completely removed from the resin. The appearance of absorption bands at ~1250 and ~1030 cm^{-1} can be attributed to the Ar-C—O oxazine asymmetric and symmetric stretch respectively.[31] In addition to the stretching bands associated with the alkene and aromatic groups (3008 cm^{-1}), aliphatic C—H vibrations (2926 and 2854 cm^{-1}), other characteristic absorption bands include C=C (~1600 cm^{-1}), CH$_2$ wagging (1370 cm^{-1}), and asymmetric stretching vibrations of C—N-C (1116 cm^{-1}) respectively. A bimodal peak centered at 990 and 960 cm^{-1} associated with the out-of-plane bending vibrations of C—H bond due to alkylene double bond and oxazine ring respectively is also present.[32]

The ^{1}H-NMR spectra of benzoxazine-endcapped polymer prepared is presented in Figure 3(ii). C-ATPEG exhibit characteristic resonances at ~ 5.3 ppm (m, ArO**CH$_2$**N) and ~ 4.7 ppm (s, Ar**CH$_2$**N), which confirms the formation of oxazine functionality. Interestingly, oligomerization is practically absent, when the reaction is performed under microwave conditions. This can be attributed to the lower residence time available with the resin under the experimental conditions maintained during microwave synthesis.

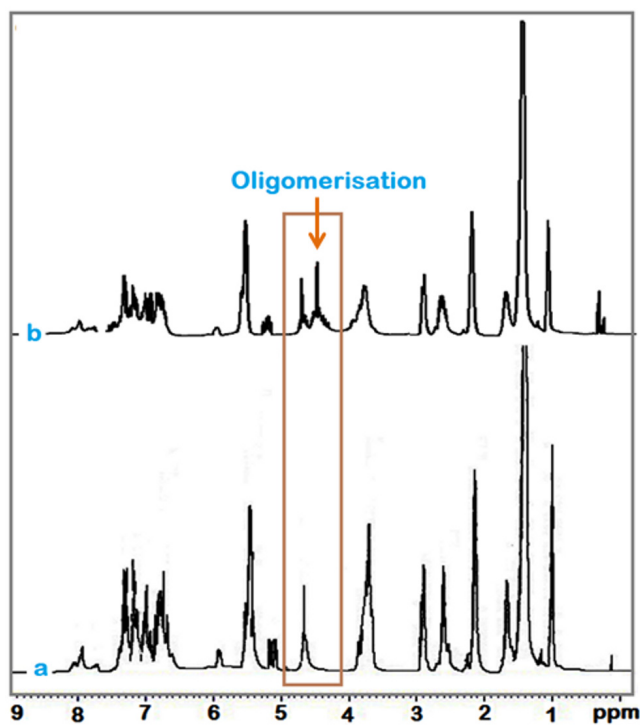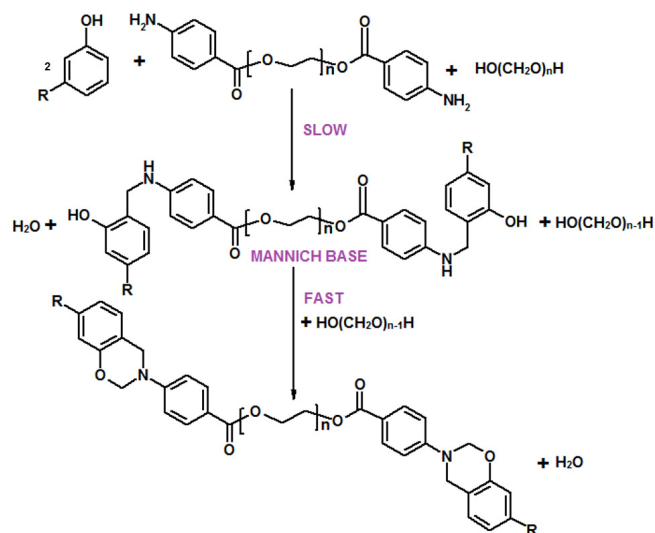The curing behavior was studied using non-isothermal calorimetry, and the DSC profiles are presented in Figure 4. The
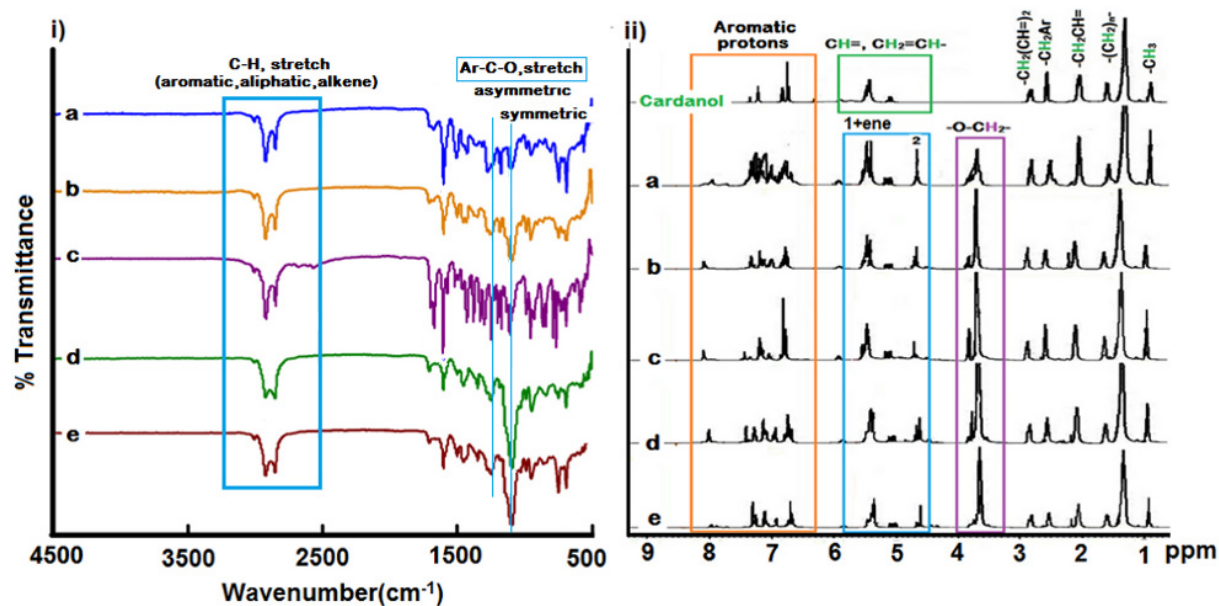
Figure 3. i) FT-IR and ii) ^{1}H-NMR spectra ofa) C-ATPEG200 b) C-ATPEG400 c) C- ATPEG600 d) C-ATPEG1000 e) C-ATPEG1500.
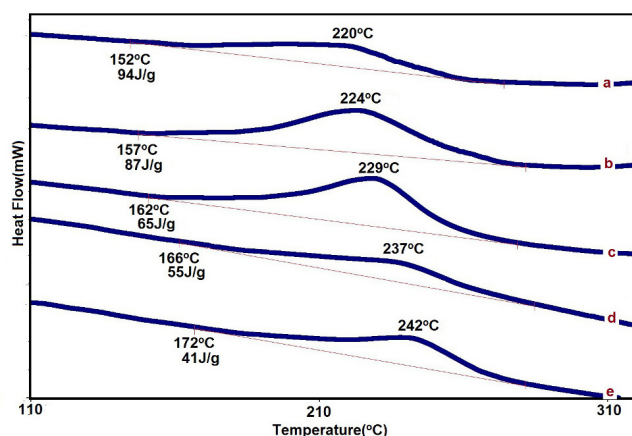

Figure 4. DSC traces a) C-ATPEG200 b) C-ATPEG400 c) C-ATPEG600 d) C-ATPEG1000 e) C- ATPEG1500.

polymerisation of benzoxazine, being autocatalytic in nature is strongly influenced by the adjacency of the reactive oxazine terminals. The temperature associated with the cross linking of benzoxazine-endcapped polymer was found to increase with increasing chain length of the ATPEG used for its preparation; a feature attributable to the dilution of the oxazine functionalities.[21b] The broad exothermic peaks as observed in the DSC profiles are a result of the dispersity associated with the polyether chains of ATPEGs. In addition, the molar enthalpy associated with the polymerization of C-ATPEG was found to decrease with increasing chain length, which can again be credited to the lower oxazine ring concentration per unit mass.

In view of the telechelic nature of the synthesized benzoxazine-endcapped poly(ethylene glycol)s, several possibilities in terms of molecular architecture can be envisaged in the

cross-linked polymer, the extreme ones being pictorially represented in the supplementary section (Figure S5). However, their formation mandates the alignment of reactive species.The telechelics prepared in the present work exhibit low liquefaction temperatures, suggestive of the absence of strong molecular interactions, thereby eliminating the possibility of formation of regular structures.

The TG-DTG traces of the cured benzoxazines are presented in the Supporting Information (Figure S6). The benzoxazine resins prepared in the present work were found to exhibit excellent thermal stability with the temperature associated with 5 % mass loss to be higher than 300 °C, suggesting their application in demanding areas requiring high thermal stability.

The practical applicability of a polymer is governed by its ease of processibility, where viscosity turns out to be a controlling parameter. The difference in the liquefaction and gelation temperatures is indicative of the processing window available with the polymer, as it is only within this range that the polymer can be molded or compounded. Rheological behavior of C-ATPEG was analyzed to study the effect of increasing flexible segments of amines on processibility of resin (Figure 5) and studies indicated that the viscosity of the resin was sufficiently low to allow solventless processing.

Cardanol based benzoxazine precursors are liquids at room temperature, and therefore liquefying point is not observed in the complex viscosity curve. As expected, telechelic polymers with relatively smaller flexible segment exhibit marginally higher viscosity, which is noticeable only at the gelation point (Inset, Figure 5). Due to early onset of oligomerization, the benzoxazine-endcapped polymers with lower cross-linking temperature exhibited higher viscosity buildup at gelation temperature. It is interesting to note that the complex viscosity of the C-ATPEG200 (~7.28 Pa.s at 30 °C) is substantially lower
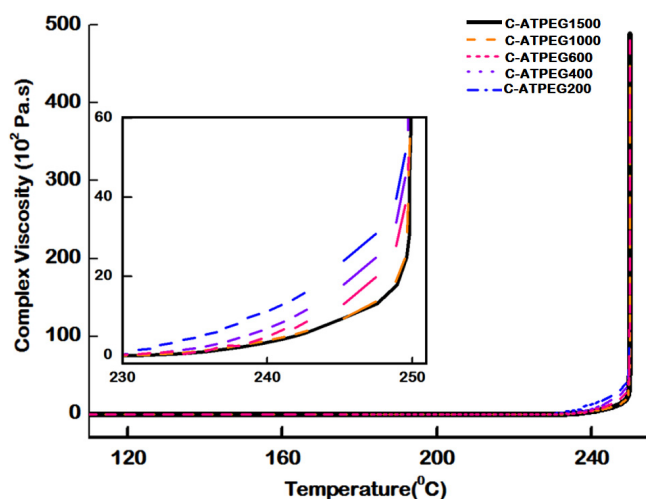
Figure 5. Variation of complex viscosity with temperature of the monomer.

than that of cardanol-aniline monofunctional benzoxazine (~ 26.4 Pa.s under the same conditions).[18b] This decrease in the complex viscosity can be credited to the presence of flexible ether linkages, in addition to the long alkyl chain in cardanol.

Adhesive Property

The adhesion of the crosslinked telechelic poly(ethylene glycol)s endcapped with benzoxazine over stainless steel coupons was quantified as per the standard procedure. The results in terms of lap shear strength (LSS) are presented in Table 1, and

Table 1. Lap shear Strength of polybenzoxazines	
Benzoxazine–endcapped poly(ethylene glycol)s	**Lap Shear Strength (MPa)**
Poly(C-ATPEG1500)	0.98 ± 0.09
Poly(C-ATPEG1000)	1.47 ± 0.09
Poly(C-ATPEG600)	1.76 ± 0.09
Poly(C-ATPEG400)	2.05 ± 0.19
Poly(C-ATPEG200)	3.70 ± 0.29

the representative load − displacement curve is presented in Figure S7. Benzoxazine moiety undergoes thermally accelerated ring opening polymerization to form crosslinked networks on metal surfaces,[33]resulting in functional groups that are capable of undergoing H-bonding, such as − OH and > N − , as shown in the FT-IR of cured resin (Supplementary Section, Figure S8). It can be seen from the table that cross-linked benzoxazine-endcapped polymer with shortest chain length (Poly(C-ATPEG200) exhibit highest LSS, which can be attributed to the relatively larger number of crosslinks in the polybenzoxazine network and highlight the potential of these resins as adhesives and healants for healing applications.[34]

3. Conclusions

Thermally cross-linkable telechelic poly(ethylene glycol)s with benzoxazine end groupswere prepared under solvent-less conditions using both conventional as well as microwave heating. The microwave assisted synthesis took substantially lower time (25 mins) as compared to the conventional heating process which required ~ 120 mins at the same temperature. Microwave active diamines were prepared by condensation of PABA and poly(ethylene glycol)s of different chain length, using p-TSA as a catalyst to yield amine terminated poly(ethylene glycol)s (ATPEGs). Cardanol, a natural source of phenol, acts a reactive diluent thereby rendering the process green. Cardanol undergoes Mannich type condensation with microwave active amines, resulting in telechelic polymers endcapped with benzoxazine groups, which were characterized using FT-IR and ^{1}H-NMR. The curing behavior was investigated using non-isothermal DSC, which reveal that temperature associated with crosslinking decreases with decreasing chain length of the diamine. Rheological studies suggests that the viscosity of the benzoxazine resins was sufficiently low (C-ATPEG200 ~ 7.28 Pa.s at 30 °C) to permit solvent less processing of the resin and further decreases on increasing the flexible segment of the telechelic polymer. The cured resins exhibited high thermal stability ($T_{5\%} > 300$ °C) and excellent lap shear strength (C-ATPEG200 = 3.70 ± 0.29 MPa). The studies indicate that performing the synthesis of benzoxazine under microwave irradiation improves the sustainability of the process and accelerates the Mannich condensation resulting in shorter reaction completion times.The performance of the resin hence obtained remains unaffected in terms of end properties, processibility and applications.

Supplementary Information

Experimental Section, HPLC chromatogram of cardanol (Figure S1), Designations and yield of amine terminated poly (ethylene glycol)s (Table S1), FT-IR spectra of Poly(ethylene glycol)s(Figure S2), Microwave activity (Figure S3), Microwave Profile (Figure S4), Probable arrangement of repeating unit in telechelic polybenzoxazines (Figure S5), TGA Traces of polybenzoxazine (Figure S6), Load Displacement curve of polybenzoxazines(Figure S7) FT-IR of polybenzoxazines (Figure S8)

Conflict of Interest

The authors declare no conflict of interest.

[1] N. E. Leadbeater, Microwave heating as a tool for sustainable chemistry, CRC Press, **2010**

[2] P. Lidström, J. Tierney, B. Wathey, J. Westman, *Tetrahedron* **2001**, *57*, 9225–9283.

[3] R. Hoogenboom, U. S. Schubert, *Macromol. Rapid Commun.* **2007**, *28*, 368–386.

[4] V. Pimpan, R. Sirisook, S. Chuayjuljit, *J. Appl. Polym. Sci.* **2003**, *88*, 788–792.

[5] S. Watanabe, K. Hayama, K. H. Park, M. a. Kakimoto, Y. Imai, *Die Makromolekulare Chemie, Rapid Communications* **1993**, *14*, 481–484.

[6] N. Hurduc, D. Abdelylah, J.-M. Buisine, P. Decock, G. Surpateanu, *Eur. Polym. J.* **1997**, *33*, 187–190.

[7] a) J. M. Lu, S. J. Ji, N. Y. Chen, Z. B. Zhang, Z. R. Sun, X. L. Zhu, W. P. Shi, *J. Appl. Polym. Sci.* **2003**, *87*, 1739–1747;b) F. Wiesbrock, R. Hoogenboom, U. S. Schubert, *Macromol. Rapid Commun.* **2004**, *25*, 1739–1764.

[8] a) F. Wiesbrock, R. Hoogenboom, C. H. Abeln, U. S. Schubert, *Macromol. Rapid Commun.* **2004**, *25*, 1895–1899;b) R. Correa, G. Gonzalez, V. Dougar, *Polymer* **1998**, *39*, 1471–1474;c) J. Jacob, L. H. L. Chia, F. Y. C. Boey, *J. Appl. Polym. Sci.* **1997**, *63*, 787–797;d) C. Zhang, L. Liao, S. Gong, *Green Chem.* **2007**, *9*, 303–314;e) S. E. Mallakpour, A. R. Hajipour, S. Khoee, *J. Polym. Sci., Part A: Polym. Chem.* **2000**, *38*, 1154–1160;f) S. Rimdusit, V. Jiraprawatthagool, C. Jubsilp, S. Tiptipakorn, T. Kitano, *J. Appl. Polym. Sci.* **2007**, *105*, 1968–1977;g) S. Rimdusit, V. Jiraprawatthagool, S. Tiptipakorn, S. Covavisaruch, T. Kitano, *Int. J. Polym. Anal. Charact.* **2006**, *11*, 441–453.

[9] a) M. Akhter, S. Habibullah, S. M. Hasan, M. M. Alam, N. Akhter, M. Shaquiquzzaman, *Med. Chem. Res.* **2011**, *20*, 1147–1153;b) G. Caliendo, E. Perissutti, V. Santagada, F. Fiorino, B. Severino, D. Cirillo, R. d. E. di Villa Bianca, L. Lippolis, A. Pinto, R. Sorrentino, *Eur. J. Med. Chem.* **2004**, *39*, 815–826;c) W.-M. Dai, X. Wang, C. Ma, *Tetrahedron* **2005**, *61*, 6879–6885.

[10] T. Y. İnan, B. Y. Karaca, H. Dogan, *J. Appl. Polym. Sci.* **2013**, *128*, 2046–2055.

[11] H. Ishida, H. Y. Low, *Macromolecules* **1997**, *30*, 1099–1106.

[12] H. Ishida, D. J. Allen, *J. Polym. Sci., Part B: Polym. Phys.* **1996**, *34*, 1019–1030.

[13] a) S. B. Shen, H. Ishida, *Polym. Compos.* **1996**, *17*, 710–719;b) N. N. Ghosh, B. Kiskan, Y. Yagci, *Prog. Polym. Sci.* **2007**, *32*, 1344–1391.

[14] a) E. Calò, A. Maffezzoli, G. Mele, F. Martina, S. E. Mazzetto, A. Tarzia, C. Stifani, *Green Chem.* **2007**, *9*, 754–759;b) P. Sharma, B. Lochab, D. Kumar, P. K. Roy, *ACS Sus. Chem. Eng.* **2015**, *4*, 1085–1093;c) P. Thirukumaran, A. Shakila, S. Muthusamy, *RSC Adv.* **2014**, *4*, 7959–7966;d) P. Thirukumaran, A. Shakila Parveen, M. Sarojadevi, *ACS Sus. Chem. Eng.* **2014**, *2*, 2790–

2801;e) P. Froimowicz, C. R. Arza, L. Han, H. Ishida, *ChemSusChem* **2016**, *9*, 1921–1928.

[15] a) S. Mohapatra, G. B. Nando, *RSC Adv.* **2014**, *4*, 15406–15418;b) C. Voirin, S. Caillol, N. V. Sadavarte, B. V. Tawade, B. Boutevin, P. P. Wadgaonkar, *Polym. Chem.* **2014**, *5*, 3142–3162.

[16] A. Greco, D. Brunetti, G. Renna, G. Mele, A. Maffezzoli, *Polym. Degrad. Stab.* **2010**, *95*, 2169–2174.

[17] P. Campaner, D. D'Amico, L. Longo, C. Stifani, A. Tarzia, S. Tiburzio, in Handb. Benzoxazine Resins (Ed.: H. I. Agag), Elsevier, Amsterdam, **2011**, pp. 365–375.

[18] a) A. Minigher, E. Benedetti, O. De Giacomo, P. Campaner, V. Aroulmoji, *Nat. Prod. Commun.* **2009**, *4*, 521–528;b) S. Shukla, A. Mahata, B. Pathak, B. Lochab, *RSC Adv.* **2015**, *5*, 78071–78080;c) B. Lochab, I. K. Varma, J. Bijwe, *J. Therm. Anal. Calorim.* **2010**, *102*, 769–774.

[19] V. V. Namboodiri, R. S. Varma, *Green Chem.* **2001**, *3*, 146–148.

[20] a) G. K. Watson, N. Jones, *Water Res.* **1977**, *11*, 95–100;b) R. A. Sheldon, *Green Chem.* **2005**, *7*, 267–278.

[21] a) S. Chaudhary, S. Parthasarathy, D. Kumar, C. Rajagopal, P. K. Roy, *J. Appl. Polym. Sci.* **2014**, *131*, n/a-n/a;b) D. J. Allen, H. Ishida, *J. Appl. Polym. Sci.* **2006**, *101*, 2798–2809.

[22] S. Ates, C. Dizman, B. Aydogan, B. Kiskan, L. Torun, Y. Yagci, *Polymer* **2011**, *52*, 1504–1509.

[23] B. Kiskan, Y. Yagci, *Polymer* **2005**, *46*, 11690–11697.

[24] S. Zalipsky, *Bioconjugate Chem.* **1995**, *6*, 150–165.

[25] S. Chaudhary, S. Parthasarathy, D. Kumar, C. Rajagopal, P. K. Roy, J. Appl. Polym. Sci. **2014**, *131*.

[26] K. K. R J Sengwa, *Indian J. Biochem. Biophys.* **1999**, *36*, 325–329.

[27] H. Ishida, US 5543516 A, **1996**

[28] H. Ishida, J.-P. Liu, in Handb. Benzoxazine Resins (Ed.: H. I. Agag), Elsevier, Amsterdam, **2011**, pp. 85–102.

[29] ⟩H. Ishida, in Handb. Benzoxazine Resins (Ed.: H. I. Agag), Elsevier, Amsterdam, **2011**, pp. 3–81.

[30] D. Tiwari, A. Devi, R. Chandra, *Int. J. Drug Dev. Res.* **2011**.

[31] J. Jang, D. Seo, *J. Appl. Polym. Sci.* **1998**, *67*, 1–10.

[32] B. Lochab, S. Shukla, I. K. Varma, *RSC Adv.* **2014**, *4*, 21712–21752.

[33] C. Aydogan, B. Kiskan, S. O. Hacioglu, L. Toppare, Y. Yagci, *RSC Adv.* **2014**, *4*, 27545–27551.

[34] a) P. Sharma, B. Lochab, D. Kumar, P. K. Roy, *J. Appl. Polym. Sci.* **2015**, *132*;b) P. Sharma, S. Shukla, B. Lochab, D. Kumar, P. K. Roy, *Mater. Lett.* **2014**, *133*, 266–268;c) M. Arslan, B. Kiskan, Y. Yagci, *Macromolecules* **2015**, *48*, 1329–1334.

Sustainable Chemistry

Poly(benzoxazine–co–urea): A Solventless Approach Towards The Introduction of Alternating Urea Linkages In Polybenzoxazine

Pratibha Sharma,[a, b] Devendra Kumar,[b] and Prasun K. Roy*[a]

In this paper, an alternative approach towards synthesis of phenolic/urea copolymers has been explored via benzoxazine chemistry. Biobased poly(benzoxazine-co-urea) has been prepared through ring opening polymerisation of a benzoxazine monomer containing urea linkages. The amine co-reactant for the benzoxazine synthesis was derived by the additive rearrangement of 4,4′-methylenebis(phenyl isocyanate) (MDI) with ethylene diamine, which underwent Mannich like condensation with cardanol and paraformaldehyde to yield biobased benzoxazine monomer containing urea linkages. The structure of the amine and the benzoxazine has been characterized by Fourier transform infrared spectroscopy (FT-IR) and nuclear magnetic resonance spectroscopy (¹H-NMR). Benzoxazine monomer undergoes thermally accelerated ring opening polymerization to form cross-linked networks, which has been demonstrated using rheometry and non-isothermal differential scanning calorimetry (DSC). The presence of alternating urea linkages in the benzoxazine network is expected to improve the adhesive properties of the resin, which was quantified in terms of Lap shear strength. Thermal degradation of the crosslinked copolymer has also been studied by thermogravimetric analysis (TGA).

1. Introduction

Polybenzoxazines, belonging to a class of advanced high performance polymers, are gaining a lot of attention lately in view of their potential to bridge the gap between mechanically robust polyepoxies and thermally stable maleimides.[1] These materials, in view of their excellent mechanical properties,[2] low moisture absorption,[3] inherent flame retardancy,[4] and dimensional stability,[5] are excellent candidates for demanding applications particularly in aerospace. The possibility of molecular designing, by choosing the raw materials astutely, allows structural tenability, which in turn can be used to develop different materials with wide ranging properties.[6] Benzoxazine monomers undergo cationic ring opening polymerization upon heating and the curing process does not mandate the presence of curing initiators or catalyst.[7]

Blending and copolymerization are undoubtedly the most extensively explored routes towards preparing of materials with intermediary properties. In this context, benzoxazines moieties have been integrated into other polymeric networks, especially where improvement in thermal and mechanical properties is required e.g. polybenzoxazine precursor has been copolymerized with ester,[8] epoxy,[9] urethanes, siloxane,[12] acetylene,[13] nitriles.[14] Surprisingly, the potential of benzoxazines has not been explored towards improving the property of polyurea, the latter being reported of exhibiting exceptional blast resistance,[15] but relatively inferior thermal stability.

A general flow chart, illustrating possible routes for preparation of benzoxazine copolymers is presented in Figure 1. Self polymerizable monomers can be integrated in the polymeric network by functionalizing the benzoxazine with the co-monomer, followed by thermal treatment (Figure 1, Approach 1).[14] Blending/reaction of benzoxazine with co-monomer is usually performed, where the monomer mandates a curing agent (Figure 1, Approach 2).[16] Baqar et al.[10] reported a route where benzoxazine is first substituted and subsequently reacted with the curing agent of the co-monomer, followed by the thermal polymerization of oxazine moiety, resulting in cross-linked alternating copolymer (Figure 1, Approach 3).

The present work deals with another alternative for preparation of benzoxazine-urea copolymers by Mannich like condensation of cardanol with amine terminated model compound containing urea linkages. These terminal oxazine moieties are expected to undergo ring-opening polymerisation leading to the formation of cross-linked polymer with alternating benzoxazine-urea linkages. The phenolic moieties thus generated are preserved and will be involved in formation of intramolecular six-membered ring hydrogen bonding responsible for bestowing unique properties of polybenzoxazines.[7a,b] The effect of introducing urea linkages on the adhesive and thermal properties of the resin is discussed.

[a] P. Sharma, Dr. P. K. Roy
     Centre for Fire, Explosive and Environment Safety, DRDO, Timarpur, Delhi
     110054, India.
     Tel.:+911123907191
     Fax:+911123819547
     E-mail: pk_roy2000@yahoo.com
[b] P. Sharma, Prof. D. Kumar
     Department of Applied Chemistry and Polymer Technology, Delhi Technological University, Delhi 110042, India.
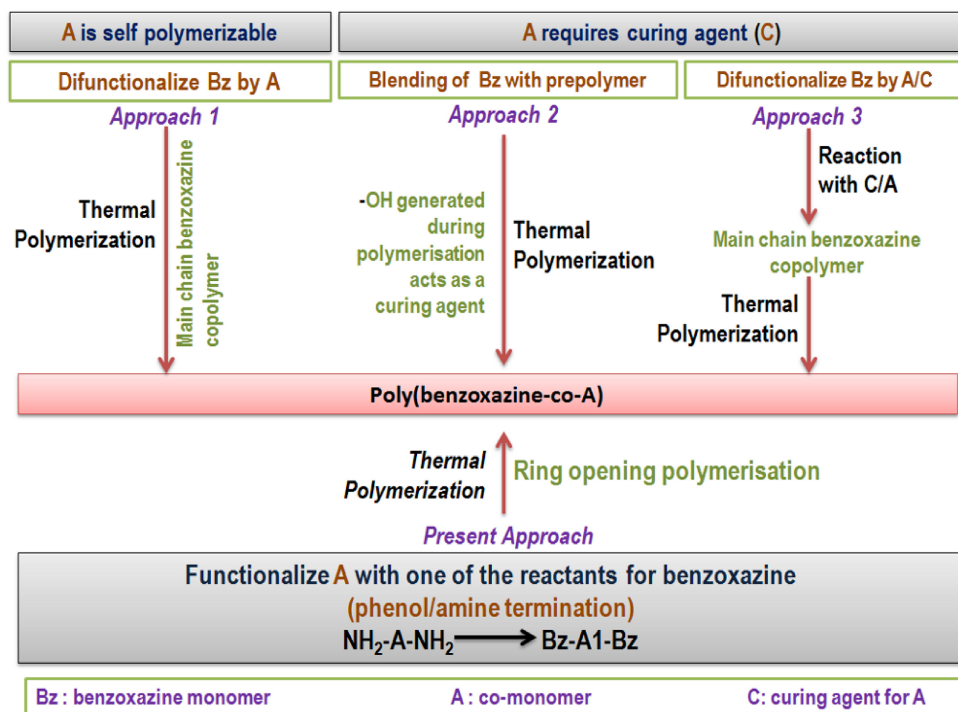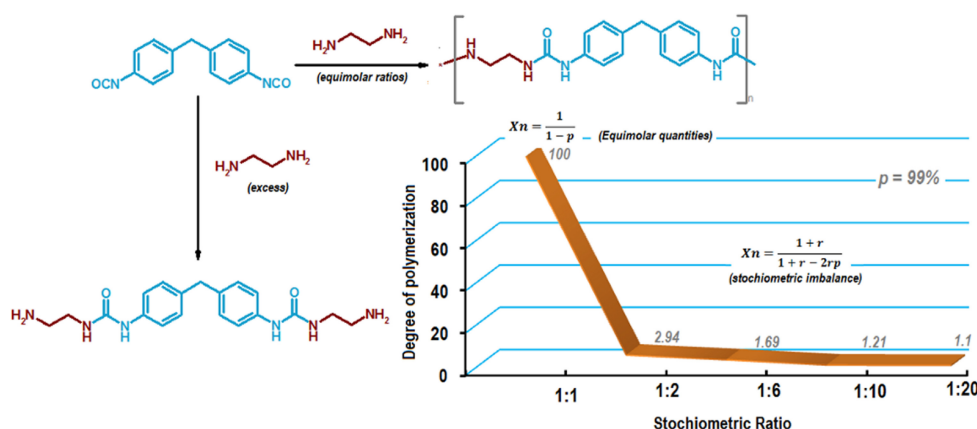
Figure 1. Varied approaches behind benzoxazine copolymer preparation.

Scheme 1. Synthesis of 4,4′-methylene-bis(3-ethylamine-1-phenylurea) (AMDI).

2. Result and Discussion

2.1 4,4′-Methylenebis(3-ethylamine-1-phenylurea), AMDI

The additive rearrangement of diisocyanate with diamine exhibit rapid reaction kinetics, and under stoichiometric conditions (1:1) leads to the formation of polyurea as shown in Scheme 1. However, performing the reaction in the presence of excess of any one of the reactants, a drastic reduction in degree of polymerization is expected (Inset, Scheme 1), as predicted by the Carothers relation.[17] The detailed calculations are presented in supplementary section (Table S1). In the present work, the ratio of isocyanate: amine was maintained at 1:6, to arrive at 4,4′-methylenebis(3-ethylamine-1-phenylurea) which could be used subsequently as the source of amine for benzoxazine monomer.

HPLC-MS of the obtained product was performed and the mass spectrum of amine eluted at 0.37 min is presented in Figure 2. The appearance of peak at m/z 372.4580 in the spectrum is due to the presence of AMDI ionized by $2H^+$. The other peaks at m/z 398.2002 and 355.3349 can be attributed to AMDI ionized by Na^+ and fragments for $[AMDI-NH_2]^+$, which suggest the formation of AMDI with molecular formula of NH_2 $CH_2CH_2NHCONHC_6H_4CH_2C_6H_4NHCONHCH_2CH_2NH_2$.

The FT-IR spectra of AMDI and MDI is presented in Figure 3(i(a,b)). The presence of a sharp absorption band at 3298 cm^{-1} ($\nu_{N-H,1°}$), 1633 cm^{-1} ($\nu_{C=O, urea}$) and the absence of $\nu_{N=C=O}$ at 2274 cm^{-1} in the spectra of AMDI indicate complete conversion of isocyanate to form urea linkages.[18]

The structure of AMDI was further confirmed using ^{1}H-NMR spectroscopy where DMSO is used as the solvent (Figure 3(ii)). The spectrum shows resonances at ~ 7.1 ppm (4H, aromatic), 7.5 (4H, aromatic), 6.3 ppm (4H, t, -NHCONH-CH$_2$CH$_2$NH$_2$), 3.8 ppm (2H, -C$_6$H$_4$-CH$_2$-C$_6$H$_4$-), 3.2 ppm (4H, -NHCONH-CH$_2$CH$_2$ NH$_2$) and 1.8 ppm (4H, CONHCH$_2$CH$_2$NH$_2$).
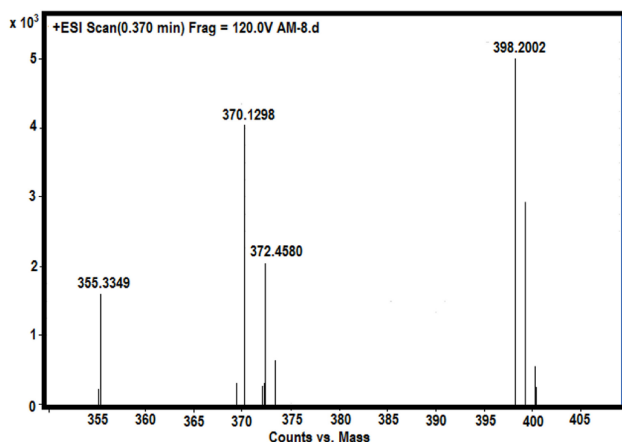
Figure 2. Mass spectra of AMDI eluted at 0.370 min.

A sharp endothermic peak at 129°C, associated with the melting of AMDI was observed in the DSC trace (Figure 4). The
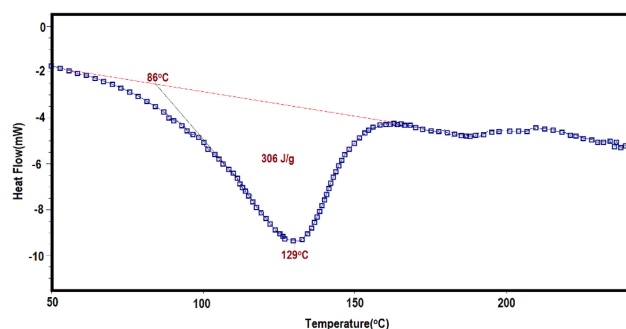

Figure 4. DSC trace of AMDI.

difference in the melting point of AMDI and MDI from which it is derived (42-45°C), can be attributed to the strong intermolecular H–bonding between the urea linkages.

TG-DTG trace of AMDI is presented in supplementary section (Figure S2). The amine exhibits negligible mass loss at

T < 200°C, which confirms the stability of the structure under the conditions employed for the synthesis of benzoxazine.

2.2 Cardanol bis–benzoxazine with urea linkages, C-amdi

Benzoxazine monomer possessing urea linkages was derived through Mannich like condensation of cardanol, AMDI and paraformaldehyde (2:1:4), which resulted in the formation of a red brown liquid in high yields (>80%) as per the reaction sequence presented in Scheme 2. A schematic representation of the preparation of benzoxazine containing urea linkages is presented in supplementary section (Scheme S1). Cardanol, an agricultural source of phenol, exhibit sufficiently low viscosity (145 mPa.s),[19] acting as a reactive diluent, so as to permit solventless synthesis of the benzoxazine.[6d, g, 20] The oxazine moieties available at the terminal position can undergo ring opening polymerization reaction resulting in the formation of a polymeric network with alternating benzoxazine/urea linkages.

The FT-IR and ^{1}H-NMR spectrum of the bis-benzoxazine resin (C-amdi) is presented in Figure 5. The absence of peaks due to O−H and N−H at ~3335 and 3298 cm^{-1} in the FT-IR of the monomer is indicative of complete utilization of cardanol and amine towards formation of the oxazine ring. The characteristic absorption bands associated with asymmetric and symmetric stretching vibrations of C−O-C (~1270 cm^{-1} and ~1030 cm^{-1}), CH$_2$ wagging (1368 cm^{-1}), and asymmetric stretching vibrations of C−N-C (1117 cm^{-1}) supports the formation of oxazine ring in the monomer. Stretching bands associated with the aromatic and alkene (3008 cm^{-1}), and aliphatic (2852 cm^{-1}) C–H vibrations, C≡C (~1583 cm^{-1}) were also observed.[21] (Figure 5(i)).

The formation of oxazine was further confirmed by the presence of characteristic resonances at ~5.3 ppm (s, ArOCH$_2$N) and ~4.6 ppm (s, ArCH$_2$N) in the ^{1}H-NMR spectra of the resin using CDCl$_3$ as a solvent (Figure 5(ii)).

Understanding the rheological response of C-amdi is essential in order to gain insight into the conditions required for processing of the resin. During polymerization, structural changes take place as the material gradually builds up and
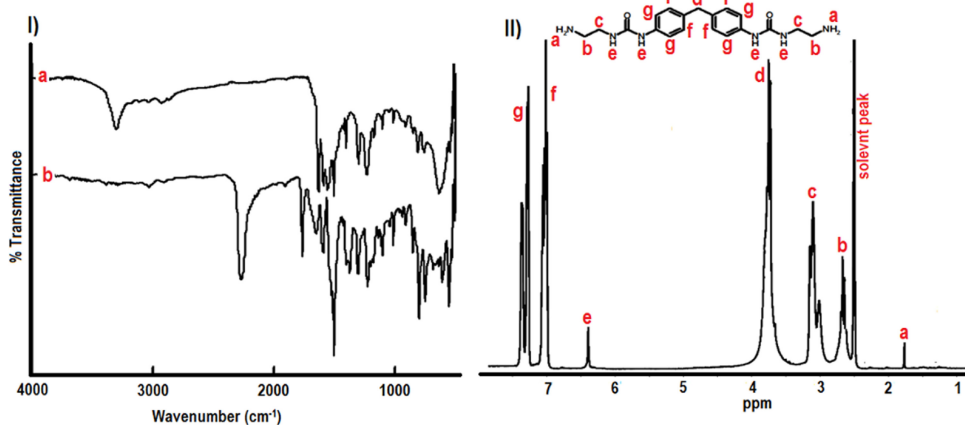
Figure 3. i) FT-IR and ii)^{1}H-NMR of AMDI.
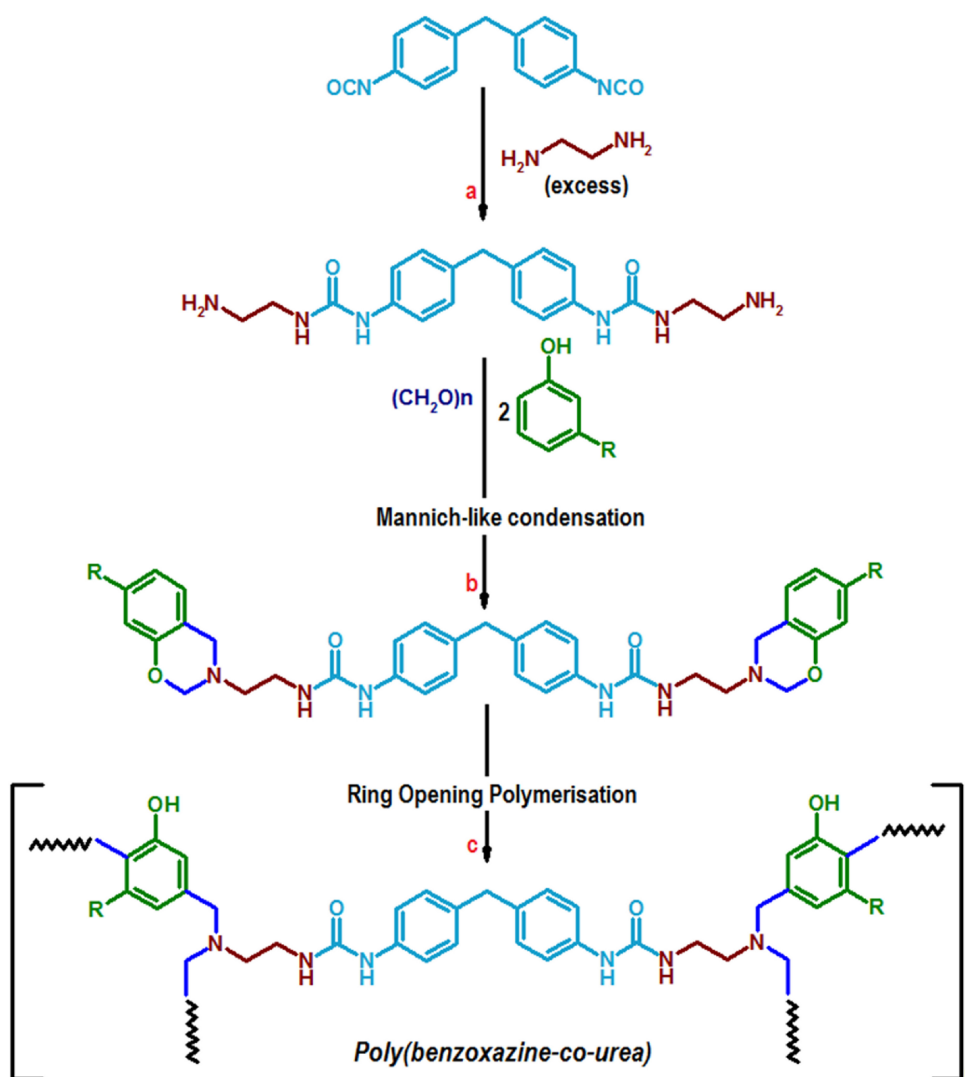
Scheme 2. Bis-benzoxazine formation by reaction of AMDI with cardanol and para formaldehyde.
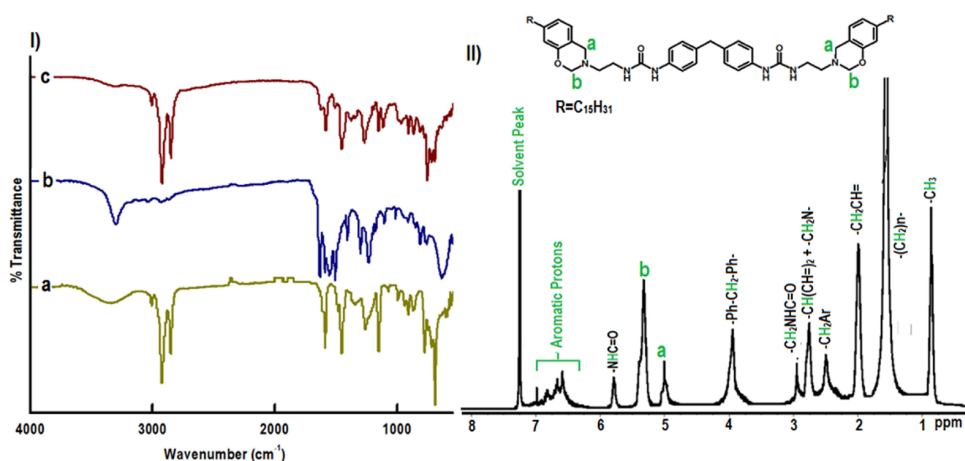
Figure 5. i)FT-IR of a) Cardanol, b) AMDI, c) C-amdi and ii) ^{1}H-NMR of C-amdi.

converts from monomer to oligomer and finally into a rigid crosslinked polymer.

Temperature sweep experiments is the most conventional techniques for studying the rheological behavior of any resin during polymerization, and the variation in terms of complex viscosity and loss-storage modulus is presented in Figure 6. It can be seen that an increase in the temperature lead to a continuous decrease in the viscosity of the resin which is expected in view of the reduced hydrogen bonding interactions between urea linkages available in the monomer. The
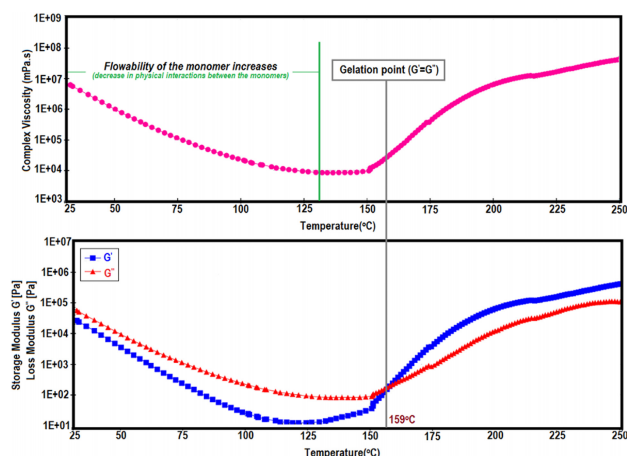
Figure 6. Rheological behavior of C-amdi during polymerisation.

ring-opening of oxazine moieties leads to the formation of opened Mannich bases, having hydrogen bonding interactions. At this stage, the degree of polymerization and the viscosity buildup is practically negligible.[22] Subsequently, polymerisation is initiated where the linear chains associate with each other leading to a buildup of viscosity. The phenolic hydroxyl groups generated act as polymerization catalysts and gelation is achieved at ~159°C where a crossover of loss and storage modulus can be seen.[22–23] Further increase in temperature lead to an increase in the viscosity as well as the moduli which finally levels off.

Non-isothermal calorimetry was also performed to understand the enthalpy associated with the curing of the benzoxazine resin, and the resulting curing profiles are presented in Figure 7. The curing of cardanol based bis-benzoxazines
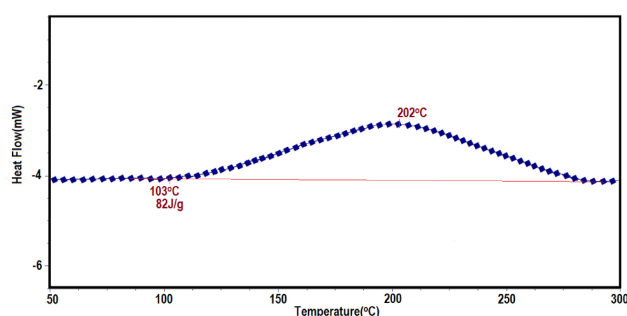
Figure 7. DSC trace of C-amdi.

containing amide linkages has been reported to initiate at T_{onset} ~114°C peaking at T_{peak} ~215°C.[20a] It is interesting to observe that the introduction of urea linkages lead to further decrease in the curing temperature, with the initiation temperature being reduced to T_{onset} ~103°C and peak temperature at T_{peak} ~202°C. The bidentate hydrogen bonds within the urea linkages in the resin, is responsible for bringing the benzox-

azine moieties closer to each other and the proximity of the oxazine rings tend to accelerate the ring opening polymerisation.

TG-DTG trace of the poly(benzoxazine-co-urea) is presented in the supplementary section (Figure S3). The benzoxazine resins prepared in the present work was found to exhibit excellent thermal stability with the temperature associated with 5 and 10% mass loss being ~322 and 369°C respectively. Polyureas, due to the presence of urea linkages, degrades at relatively lower temperatures.[15,24] It can be seen that copolymerization with benzoxazine tends to improve the thermal stability of the polyureas, thereby suggesting its use in applications mandating thermal stability.

2.3 Lap shear strength studies

The adhesive property of the poly(benzoxazine-co-urea) was quantified as per the standard procedure and a representative load-displacement curve obtained is presented in supplementary section (Figure S4). The lap shear strength (LSS) of the developed benzoxazine-urea copolymer is 5.98 ± 0.29 MPa which is relatively higher than the bi-functional benzoxazine resin containing amide linkages.[20a] It is to be noted that the adhesive strength of the adhesive is a function of several parameters, particularly wetting ability of the substrate with the resin, its inherent adhesive nature, temperature, thickness of the resin, mode of failure, hydrogen bonding interactions and cross link density. The ring opening polymerisation of oxazine moieties generate functional group which are capable of undergoing H-bonding, such as –OH and >N- as shown in the FT-IR spectra of poly(benzoxazine-co-urea) presented in the supplementary section (Figure S5). Moreover, the three dimensional network formed herein comprises of urea linkages, which exhibit bi-dentate hydrogen bonding (bond strength ~21.8 kJ/mol)[25] as shown in Figure 8, which is an additional factor
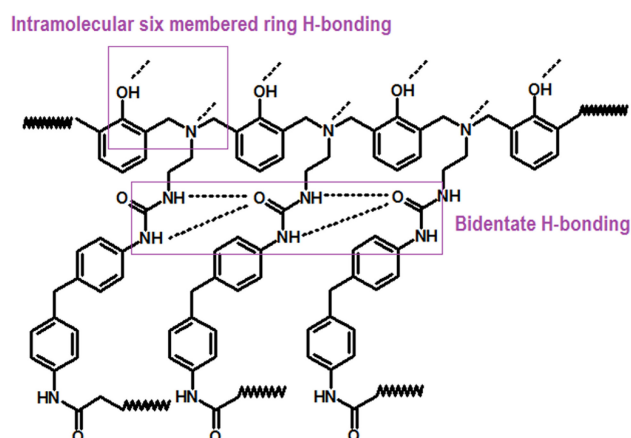

Figure 8. Hydrogen bonding in the poly(benzoxazine-co-urea).

responsible for the adhesive strength of the resin. Fractographic analysis on the cracked surface (obtained post-lap

shear strength studies) was performed to gain an insight into the micro-mechanisms behind the failure of sample. For this purpose, the fracture surface of the sample was examined by SEM and a representative SEM image is presented in the supplementary section (Figure S6). The fracture surface of benzoxazine shows uninterrupted crack propagation, which in turn is characteristic of brittle failure.

3. Conclusion

Thermally accelerated ring opening polymerization of bis-benzoxazine containing urea linkages led to the formation of poly(benzoxazine-co-urea). 4,4′methylenebis(phenyl isocyanate) (MDI) was reacted with ethylene diamine resulting in the formation of AMDI, which was further used to synthesize bis-benzoxazine. Cardanol, an agro waste, was chosen as the phenolic source, undergoes Mannich type condensation with amine (AMDI) and paraformaldehyde, resulting in a monomer comprising of urea linkages with terminal oxazine moieties. The structural characterization of the amine and the monomer were performed using FT-IR and ^{1}H-NMR. The curing behavior was investigated using non-isothermal DSC, which reveal that the cross linking temperature associated with the synthesized monomer is ~202 °C. Bidentate hydrogen bonding present in the urea linkages was credited for the observed reduction in polymerisation temperature. Rheological studies suggest that initially the flowability of the monomer improves with the increase in the temperature due to reduced hydrogen bonding in the monomer and the gelation occurs at ~159 °C. The cured resins exhibit high thermal stability ($T_{5\%} > 300$ °C) and excellent lap shear strength 5.98 ± 0.29 MPa. The performance of the copolymer hence obtained remains unaffected in terms of end properties, processibility and applications.

Supporting Information Summary

Experimental Section, HPLC chromatogram of cardanol (Figure S1), Predicting the effect of isocyanate: amine on degree of polymerisation: Carothers relation, Degree of polymerisation X_n, for different values of r (Table S1), TG-DTG of 4,4′-methylenebis (3-ethylamine-1-phenylurea) (Figure S2), Schematic representing preparation of benzoxazine containing urea linkages (Scheme S1), TG-DTG of poly(benzoxazine-co-urea) (Figure S3), Load-displacement plot of poly(benzoxazine-co-urea) (Figure S4), FT-IR spectra of poly(benzoxazine-co-urea) (Figure S5), SEM image of the fractured poly(benzoxazine-co-urea) (Figure S6).

[1] a) G. Wu, J. Li, K. Wang, Y. Wang, C. Pan, A. Feng, *J. Mater. Sci.: Mater. Electron.* **2017**, *28*, 6544–6551; b) G. Wu, Y. Cheng, Z. Wang, K. Wang, A. Feng, *J. Mater. Sci.: Mater. Electron.* **2017**, *28*, 576–581.

[2] a) S. B. Shen, H. Ishida, *Polym. Comp.* **1996**, *17*, 710–719; b) N. Ghosh, B. Kiskan, Y. Yagci, *Prog. Polym. Sci.* **2007**, *32*, 1344–1391.

[3] H. Ishida, D. J. Allen, *J. Poly. Sci. B Poly. Phy* **1996**, *34*, 1019–1030.

[4] R. Tietze, M. Chaudhari, in *Handbook of Benzoxazine Resins* (Ed.: H. I. Agag), Elsevier, Amsterdam, **2011**, pp. 595–604.

[5] H. Ishida, H. Y. Low, *Macromolecules* **1997**, *30*, 1099–1106.

[6] a) Y. Yagci, B. Kiskan, N. N. Ghosh, *J. Poly. Sci. A Poly. Chem.* **2009**, *47*, 5565–5576; b) P. Thirukumaran, A. Shakila Parveen, M. Sarojadevi, *ACS Sustain. Chem. Eng.* **2014**, *2*, 2790–2801; c) O. S. Taskin, B. Kiskan, A. Aksu, N. Balkis, J. Weber, Y. Yagci, *Chem. Eur. J* **2014**, *20*, 10953–10958; d) E. Calò, A. Maffezzoli, G. Mele, F. Martina, S. E. Mazzetto, A. Tarzia, C. Stifani, *Green Chem.* **2007**, *9*, 754–759; e) P. Sharma, S. Shukla, B. Lochab, D. Kumar, P. K. Roy, *Mater. Lett.* **2014**, *133*, 266–268; f) P. Sharma, B. Lochab, D. Kumar, P. K. Roy, *J. Appl. Polym. Sci.* **2015**, *132*; g) S. Shukla, A. Mahata, B. Pathak, B. Lochab, *RSC Adv.* **2015**, *5*, 78071–78080.

[7] a) A. Sudo, R. Kudoh, H. Nakayama, K. Arima, T. Endo, *Macromolecules* **2008**, *41*, 9030–9034; b) H.-D. Kim, H. Ishida, *Macromolecules* **2003**, *36*, 8320–8329; c) R. Andreu, J. Reina, J. Ronda, *J. Poly. Sci. A Poly. Chem.* **2008**, *46*, 3353–3366; d) T. Agag, T. Takeichi, *Macromolecules* **2001**, *34*, 7257–7263; e) J. Dunkers, H. Ishida, *J Poly. Sci. A Poly. Chem.* **1999**, *37*, 1913–1921; f) P. Sharma, M. Srivastava, B. Lochab, D. Kumar, A. Ramanan, P. K. Roy, *ChemistrySelect* **2016**, *1*, 3924–3932.

[8] K. S. Kumar, C. R. Nair, K. Ninan, *Eur. Polym. J* **2009**, *45*, 494–502.

[9] H. Ishida, D. J. Allen, *Polymer* **1996**, *37*, 4487–4495.

[10] M. Baqar, T. Agag, H. Ishida, S. Qutubuddin, *Polymer* **2011**, *52*, 307–317.

[11] a) B. Gacal, L. Cianga, T. Agag, T. Takeichi, Y. Yagci, *J. Poly. Sci. A Poly. Chem.* **2007**, *45*, 2774–2786; b) L. Jin, T. Agag, H. Ishida, *Eur. Polym. J* **2010**, *46*, 354–363.

[12] Y.-J. Lee, S.-W. Kuo, Y.-C. Su, J.-K. Chen, C.-W. Tu, F.-C. Chang, *Polymer* **2004**, *45*, 6321–6331.

[13] H. Kim, Z. Brunovska, H. Ishida, *Polymer* **1999**, *40*, 6565–6573.

[14] Z. Brunovska, H. Ishida, *J. Appl. Polym. Sci.* **1999**, *73*, 2937–2949.

[15] N. Iqbal, M. Tripathi, S. Parthasarathy, D. Kumar, P. Roy, *RSC Adv.* **2016**, *6*, 109706–109717.

[16] S. Kirschbaum, K. Landfester, A. Taden, *Macromolecules* **2015**, *48*, 3811–3816.

[17] W. H. Carothers, *Trans. Faraday Soc.* **1936**, *32*, 39–49.

[18] in *Interpreting Infrared, Raman, and Nuclear Magnetic Resonance Spectra* (Ed.: R. A. Nyquist), Academic Press, San Diego, **2001**, pp. 143–148.

[19] B. Lochab, I. K. Varma, J. Bijwe, *J. Therm. Anal. Calorim.* **2010**, *102*, 769–774.

[20] a) P. Sharma, B. Lochab, D. Kumar, P. K. Roy, *ACS Sustain. Chem. Eng.* **2016**, *4*, 1085–1093; b) P. Sharma, D. Kumar, P. Roy, *ChemistrySelect* **2016**, *1*, 6941–6947.

[21] B. Lochab, S. Shukla, I. K. Varma, *RSC Adv.* **2014**, *4*, 21712–21752.

[22] R. Huang, S. O. Carson, J. Silva, T. Agag, H. Ishida, J. M. Maia, *Polymer* **2013**, *54*, 1880–1886.

[23] P. J. Halley, M. E. Mackay, *Polym. Eng. Sci.* **1996**, *36*, 593–609.

[24] W. H. Awad, C. A. Wilkie, *Polymer* **2010**, *51*, 2277–2285.

[25] J. P. Sheth, D. B. Klinedinst, G. L. Wilkes, I. Yilgor, E. Yilgor, *Polymer* **2005**, *46*, 7317–7322.
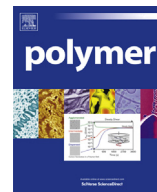
Enhancing the processibility of high temperature polymerizing cardanol derived benzoxazines using eco-friendly curing accelerators

Pratibha Sharma [a, b], Devendra Kumar [b], Prasun Kumar Roy [a, *]

[a] Centre for Fire, Explosive and Environment Safety, DRDO, Timarpur, Delhi 110054, India
[b] Department of Applied Chemistry and Polymer Technology, Delhi Technological University, Delhi 110042, India

ARTICLE INFO

ABSTRACT

The advent of bio-based benzoxazine in the field of polybenzoxazines is a major breakthrough towards their sustainable development. Cardanol derived benzoxazine offers solvent less synthesis and processing benefits over the petro based resin, however these mandate high curing temperatures. The polymerization temperature can be alleviated through structural modifications or physical blending with curing accelerators; the latter approach being preferred in view of its economic viability. Most of the curing accelerators are moisture sensitive, which adversely affect the end performance of the polymer. In this paper, the potential of eco-friendly stearates based on transition metals as curing accelerators for the polymerization of cardanol based benzoxazine resin has been demonstrated. Metal stearates were formulated with bio-based monomer which leads to significant lowering of the curing profiles, the extent of which was proportional to the amount of accelerator. The hydrophobicity associated with the long alkyl chain in stearate bestows it hydrolytic stability, which allows its use under ambient conditions without special caution. Zinc(II) stearate exhibit highest activity towards acceleration and its inclusion does not alter the viscosity of the formulation offering a processing advantage. Kinetic parameters associated with polymerization of the resin were established using Kissinger Akahira Sunose method.

© 2018 Elsevier Ltd. All rights reserved.

1. Introduction

Polybenzoxazines is a new class of phenolic-like thermosetting resins based on the ring opening polymerization of the benzoxazine monomer, which exhibit extremely interesting properties, notably negligible volume shrinkage during curing [1], low water absorption [2] and thermal stability [3,4]. In addition, molecular designing flexibility through the astute choice of the amine and phenolic components bestow an extremely interesting feature to these materials in terms of tunablity, thereby opening up new vistas of application [5–9].

Biobasedbenzoxazine monomers appear to be proficient in satisfying the increasing demands of polymer industry. However, a major drawback associated with bio-based benzoxazine resin is its high curing temperature [10,11], which restricts its usage for widespread applications [12,13]. It is extremely desirable to develop sustainable benzoxazine formulations with low curing temperatures. Temperature associated with the curing process can

be alleviated through structural modifications [14–16] or addition of curing accelerators [11,17–19]; the latter methodology being preferred in view of its economic viability. In this context, accelerators for curing of petro-based as well as bio-based benzoxazines are commercially available with Huntsman (DT300 and DT310), however the chemical composition is not available in public domain.

Several accelerators, based on organic acids [10,20] and Lewis acids [21,22]have been reported for accelerating polymerization, but their presence in the resin reportedly affect the chemical resistance of the polymer and deteriorate the physical properties of the resulting cross-linked product [17]. Organic bases such as amines [23], and imidazoles [24]have also been explored, and the effectiveness of acid-base combination has also been studied [25]. Sudo et al. [11] studied the efficiency of acetylacetonato complexes of 4th period transition metals as catalysts, and reported that the complexes of manganese, iron, cobalt and zinc exhibited the highest activity. Due to high surface area and acidic sites, metal organic frameworks (MOFs) based on zinc have also been explored as curing accelerators [26]. The studies indicate that Lewis acidic Zn_4O nodes of atomic precision, which are available throughout the

surface of the framework, are responsible for the decrease in the curing temperature.

Inopportunely, metal complexes are relatively intolerant towards moisture, which deteriorate the mechanical performance of the material. Acetylacetonato complexes with hexafluoroacetylacetonate ligand (F_6-acac)are relatively more efficient accelerators, in view of their enhanced Lewis acidity of the metal center due to the presence of strong electron-withdrawing group [11]. In addition, the replacement of acetylacetonate with the hexafluoroacetylacetonate also improved the moisture tolerance of the accelerator. However, fluorinated compounds are toxic which imposes operability issues and are relatively expensive. This motivated us to consider the possibility of tailoring the chemical environment around the metal center and explore the potential of stearates based on transition metals, which proves to be efficient, ecofriendly and economically viable, in the context of curing of bio-based benzoxazine monomer.

Metal stearates, coordination complexes of long chain fatty acids with transition metals, are of greatest commercial importance. The organic ligand, i.e. stearic acid is derived from saponification of the triglycerides obtained from natural sources (cocoa butter and shea butter) [27]. Among the many interesting properties of metallic stearates, the most important are water repellence [28], gelling capacity, and stabilizing effect [29]. The LD_{50}values of zinc compounds are high (186–623 mg zinc/kg/day) which is indicative of its low toxicity [30]. Most of the metal stearates, undergo solid to liquid transition ca ~150 °C; conditions under which cardanol based benzoxazine curing is negligible [8]. In addition, metal stearates do not undergo thermal degradation during processing of the resin, rendering them excellent candidature as curing accelerators.

The present work deals with the preparation of a series of transition metal stearates and to explore their potentialas curing accelerators for cardanol-aniline benzoxazine, a value added, industrially significant high performance material.

2. Experimental

2.1. Materials

Cardanol ($\rho = 0.927$–0.935 g/cm^3; Iodine value 250; Acid Value Max 5; Hydroxyl Value 180–190) was obtained from Satya Cashew Chemicals Pvt. Ltd. (India). The HPLC chromatogram of cardanol is presented in the supplementary section (Fig. S1) [14]. Aniline, paraformaldehyde was purchased from CDH chemicals. Cardanol-aniline benzoxazine was synthesized as reported previously [13,14,26] and is used as resin for the screening of curing accelerators. Manganous chloride, ferric chloride, cobaltous chloride, nickel sulphate, cuprous chloride, zinc sulphate, and stearic acid were purchased from CDH were used as received. Zinc acetate anhydrous ('AR', E. Merck), was used without further purification. Double distilled water was used throughout the course of this work.

2.2. Characterization methods

Fourier Transform Infrared (FT-IR) spectra of samples were recorded using a Thermo scientific FT-IR (NICOLET 8700) analyzer with an attenuated total reflectance (ATR) crystal accessory. The angle of incidence of the germanium ATR crystal used was characteristically 45° and the spectra was recorded in the wavelength range 4000–500 cm^{-1}, with a resolution of 4 cm^{-1}. Thermal behavior was investigated using Perkin Elmer Diamond STG-DTA under N_2 atmosphere (flow rate $= 50$ ml min^{-1}) in the temperature range 50–700 °C. A heating rate of 10 °C/min and sample mass of 5.0 ± 0.5 mg was used for each experiment. Calorimetric studies

were performed on a Differential Scanning Calorimeter (TA instruments Q 20). For dynamic DSC scans, the sample (5 ± 2 mg) was sealed in aluminum pans using T_{zero} press, and heated from 30 to 300 °C at three different rates 5, 7 and 10 °C/min. N_2 was purged at rate of 50 ml/min to minimize oxidation of the sample during the curing process. Prior to the experiments, the instrument was calibrated for temperature and enthalpy using standard Indium and Zinc. Thermal equilibrium was regained within 1 min of sample insertion, and the exothermic reaction was considered to be complete when the recorder signal leveled off to the baseline. The total area under the exothermic curve was determined to quantify the heat of curing.

Anton Paar Rheometer MCR-102 was used to study the rheological behavior of the resin. Temperature-sweep experiment was performed by applying oscillatory mode in three intervals: 30–150°C at 5°C min^{-1}, 150–250°C at 3°C min^{-1} followed by isothermal at 250°C for 1 h. A constant strain of 0.5% and constant angular frequency of 10 rad/s was maintained during each interval (parallel plate size of diameter 8 mm and gap thickness was maintained at 1.00 mm).

2.3. Synthesis of metal stearates

Transition metal stearates were synthesized using double decomposition technique of sodium stearate with metal salt as per the procedure reported in the literature [31]. Sodium stearate was prepared by the reaction of stearic acid with stoichiometric amount of sodium hydroxide. Subsequently, the temperature was increased to 75 °C, and the desired aqueous metal salt solution was added dropwise till complete precipitation of the metal stearates was observed. The metal stearates formed were filtered, washed repeatedly with hot water and finally dried under vacuum at 60 °C.

2.4. Polymerization of cardanol based benzoxazine (C-a) using metal stearates

To an accurately weighed amount of the cardanol-derived benzoxazine (C-a), varying amount of metal stearates (1–10 %w/ w) were added and stirred at room temperature; conditions under which no polymerization was perceptible. The details of the formulations prepared along with their sample designations have been mentioned in supplementary section (Table S1). Neat benzoxazine has been referred to as C-a and the compositions containing metal stearates have been referred to as MStXC-a where X indicates the mass percent of metal stearate present in the sample. For e.g. C-a containing 10% w/w zinc(II) stearate has been designated as ZnSt10C-a. A control set of curing studies were also performed on benzoxazine resin containing stearic acid and zinc acetate anhydrous. Sample was placed in a DSC aluminium pan and heated at a uniform rate of 10 °C/min, while measuring the heat flow associated with polymerization. The corresponding DSC profiles of formulations were used to quantify characteristic curing parameters.

3. Results and discussions

The potential of stearates based on transition metals as curing accelerator for benzoxazine resins has been explored. Non-isothermal calorimetric studies were performed to study the curing behavior of benzoxazine in the presence of stearates.

3.1. Transition metal stearates

Metallic stearates were synthesized by double decomposition process involving formation of sodium stearate followed by the

$$C_{17}H_{35}COOH + NaOH \longrightarrow C_{17}H_{35}COONa + H_2O$$

$$C_{17}H_{35}COONa + M^{2+}_{(aq)} \longrightarrow (C_{17}H_{35}COO)_2M + 2Na^+$$
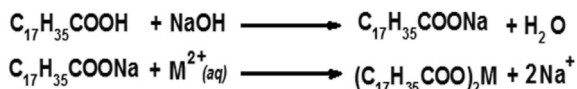
Scheme 1. Double decomposition method for metal stearate preparation.

replacement of the sodium cation with transition metal to form an insoluble metal stearate (Scheme 1).

FT-IR spectra of all the stearates exhibited absorbance at $1545\,cm^{-1}$; attributable to asymmetric vibration stretching of the carboxylic group coordinated to the metal ion (Fig. 1 (i)). Three intense bands in the $1300-1600\,cm^{-1}$ region were also observed. The $1545\,cm^{-1}$ band is assigned to the carboxylate antisymmetric stretch and $1465\,cm^{-1}$ to the CH_2 bending. The $1399\,cm^{-1}$ band may be assigned to the C_xH_{2x} bending and/or the carboxylate symmetric stretch, both of which should be observed in the infrared spectrum. DSC traces presented in Fig. 1(ii), reveal that all the stearates undergo melting prior to the onset of the polymerization of the benzoxazine monomer (~242 °C). This is expected to result in homogeneous blending of the stearate with the monomer, thereby enhancing their candidature as accelerators. Thermo gravimetric analysis (Fig. 1(iii)) revealed that all metal stearates are thermally stable within the processing window of the benzoxazine monomer ca~ 250 °C.

All the metal stearates were found to be insoluble in water and soluble in THF, DMF, xylene and toluene. The contact angle of zinc(II) stearate powder has been reported to be $154.6 \pm 1.5°$ [28], which is a direct evidence of its super hydrophobic surface. The same was confirmed from the mobile water drops over surface of zinc(II) stearate powder as can be seen in digital images presented in supplementary section (Fig. S2). In this context, it is imperative to

mention that zinc stearate find extensive use as a lubricant additive which improves filler dispersion in hydrophobic plastic media [32]. The hydrolytic stability of the metal stearates is an extremely interesting feature, which bestow them ideal candidature as curing accelerator for benzoxazine curing. Characteristic thermal properties like non-volatile content (%) and ash content (%) of metal stearates were determined as per the standard procedure (supplementary section) and the results are tabulated in supplementary section (Table S2). All metal stearates exhibited a nonvolatile content >95% and ash content of 12−15%. The ash content has been reported to be dependent on the oxidation state of the central metal [31]. As per theoretical calculations, the metal content corresponding to all the stearates should be $6.25 \pm 0.21\%$. However, this figure is not in concordance with the char content obtained during TGA, which can be attributed to the conversion of the metal to its oxide form during the thermal decomposition process.

The acidic co-reactants were completely consumed during the formation of metal stearate, which was confirmed from the negligible free fatty acid content, as determined using established procedure presented in supplementary section.

3.2. Screening of accelerators based on DSC analysis of polymerization of cardanol benzoxazine monomer

Benzoxazine monomers undergo thermally accelerated cationic ring opening polymerization and results in thermally stable polymer. The presence of curing accelerators in the formulation is expected to shift the curing profile towards lower temperatures and alter the kinetics of the oxazine ring opening stage through several reported mechanisms [25,33−37]. Non-isothermal calorimetric studies were performed to assess the potential of metal stearates
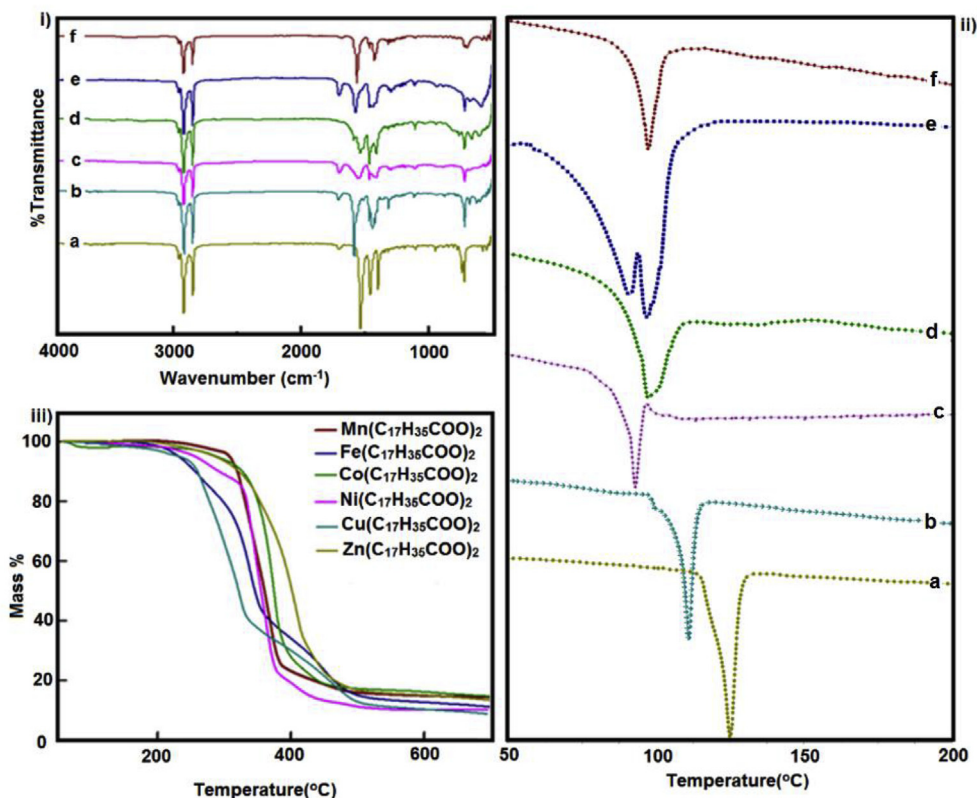

Fig. 1. Characterization of metal stearates i) FT-IR ii) DSC and iii) TGA traces of a) zinc(II) b) copper(II)c) nickel(II) d) cobalt(II) e) iron(II) f) manganous(II)stearate.

Table 1
Effect on introduction of accelerators on characteristic curing temperatures (β = 10 °C/min).

Sample designation	T_o (°C)	T_{peak} (°C)	% Reduction		Enthalpy of polymerization (J/g)
			T_o	T_{peak}	
C-a	242	263	—	—	63
St10C-a	223	244	7.8	7.2	88
MnSt10C-a	187	226	22.7	14.0	97
FeSt10C-a	206	225	14.8	14.4	94
CoSt10C-a	183	213	24.3	19.0	97
NiSt10C-a	205	236	15.2	10.2	97
CuSt10C-a	212	234	12.3	11.0	73
ZnSt1C-a	226	247	6.6	6.0	79
ZnSt5C-a	193	222	20.2	15.5	82
ZnSt10C-a	169	202	30.1	23.1	92
ZnAc10C-a	218	222	9.9	15.5	68

towards acceleration in polymerization of benzoxazine resins. The results of the DSC analyses in terms of characteristic curing temperatures and enthalpy are summarized in Table 1 [38].

The presence of metal stearates based on manganese(II), iron(II), cobalt(II) and zinc(II) in the formulation led to a remarkable decrease in the curing parameters, with copper(II) and nickel(II) stearate being relatively less effective. Cobalt(II) complexes have been reported to exhibit high levels of toxicity and pose adverse effect on the environment [39]. In view of these concerns, zinc(II) stearate, was selected as the most suitable accelerator and representative curing profiles of formulations containing varying amounts of zinc stearate are presented in Fig. 2. The enthalpy of polymerization associated with the prepared formulations is listed in Table 1. An increased enthalpy of polymerization was observed in formulations containing curing accelerators. A similar increase in the enthalpy of polymerization has been reported earlier [18]. The increase in the heat of polymerization can be attributed to the destabilization of the oxazine moiety due to interaction with the Lewis acidic accelerators. This interaction results in a strained benzoxazine molecule with relatively higher potential energy, which leads to a larger potential energy difference between the reactant and product.

It has already been mentioned that the ring opening polymerization of cardanol based benzoxazine initiates at 242 °C with a peak at 263 °C (Fig. 2(i)). It can be seen from the figure that the curing profile shifts towards lower temperature in the presence of

zinc(II) stearate, the extent of which was found to be proportional to its amount in the formulation. Inclusion of zinc(II) stearate (10% w/w) in the formulation was found to decrease the curing temperature of neat benzoxazine from ~263 °C to ~202 °C (23% decrease) (Fig. 2(ii)-(iv)). Acetylacetonate complexes have been previously reported to decrease the curing temperature of BA-a (bisphenol-aniline benzoxazine) by 23% [11]. Commercially available accelerators DT310 and DT300 (Huntsman), post addition in BA-a have been reported to decrease the curing temperature by 16.8 and 7.2% respectively.

Extensive characterization studies on zinc(II) stearate [40] confirm the presence of acidic Zn_4O nodes, which are coordinatively linked to four carboxylate moieties with a Zn-O distance of 0.195 nm (Fig. 3). It is the presence of these Lewis acidic Zn_4O nodes, which is responsible for accelerating activity of zinc(II) stearate [26]. As the temperature is increased, a solid−liquid phase transition occurs in zinc(II) stearate at ~130 °C, however the coordination structure reportedly remains unaffected [40].

To understand the importance of the chemical environment around the central zinc species, curing studies were also performed in the presence of zinc(II) acetate anhydrous, which also has been reported to possess Zn_4O nodes [40], and the results are included in Table 1. It can be speculated that the synergistic combination of acidic Zn_4O nodes and the uniform dispersion due to the hydrophobic stearate chains (Fig. 4(i)) result in the observed acceleration of the curing reaction.
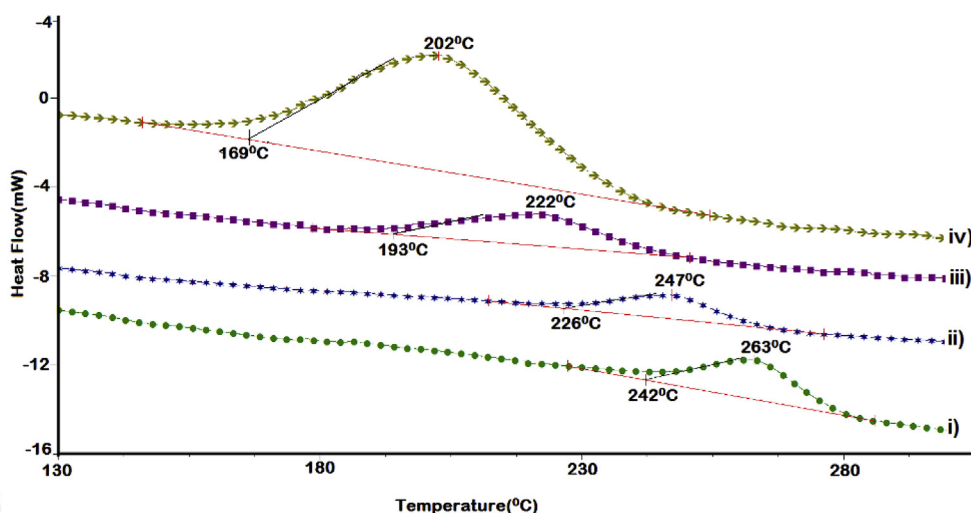

Fig. 2. DSC profile i) C-a, ii) ZnSt1C-a, iii) ZnSt5C-a and iv) ZnSt10C-a.
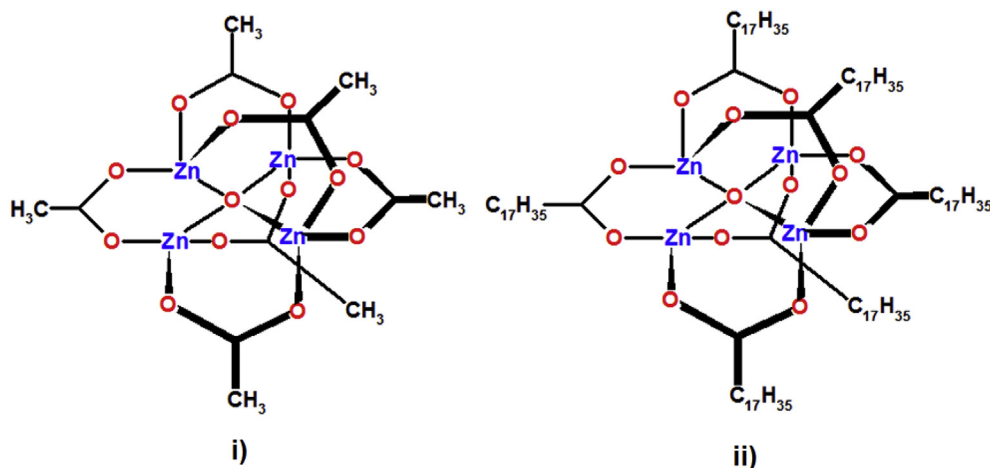
Fig. 3. Chemical Structures of i) anhydrous zinc(II) acetate and ii) zinc(II) stearate.

The proposed mechanism of zinc(II) stearate accelerated polymerization of benzoxazine is presented in Fig. 4(ii). The Zn_4O nodes available in zinc(II) stearate interact with the oxygen to form a cyclic oxonium cationic species, which is followed by an electronic rearrangement leading to the formation of a resonance stabilized iminium cation. Subsequently, benzoxazine monomer adds to the cationic imine moiety, forming another electron deficient cyclic oxonium species. Repetitive electrophilic substitutions result in a polymeric network with thermally unstable aryl ether structure, which undergoes rearrangement resulting in a polymer with phenolic structure.

To gain an insight into this aspect, the rheological behavior of the resin post-introduction of zinc(II) stearate has been investigated by temperature sweep experiments. The variation of complex viscosity and loss-storage modulus with respect to temperature is presented in Fig. 5. It can be seen that at room temperature, viscosity of the formulation (ZnSt10C-a) is higher than that of the neat resin (C-a). However, increasing the temperature to 130 °C leads to a precipitous drop in the viscosity of the formulation, which is accompanied by a concomitant decrease in storage and loss modulus, a phenomenon that can be attributed to the melting of zinc(II) stearate. Our studies indicate that the introduction of accelerator does not lead to any increase in the viscosity of the formulation. The ring-opening of oxazine moieties leads to the formation of open Mannich bases, possessing hydrogen bonding interactions, however till ~220 °C, the viscosity buildup is practically negligible [41]. Subsequently, polymerization is initiated where the linear chains associate with each other leading to a sudden increase in viscosity. The phenolic hydroxyl groups generated, act as polymerization catalysts which leads to gelation at ~220 °C, observed as a crossover of loss and storage modulus [41,42] (Fig. 5(ii)), while the same is achieved at ~257 °C (for the neat resin) as shown in Fig. 5(i), which further confirms the accelerating activity of zinc(II) stearate. Further increase in temperature leads to an increase in the viscosity as well as the moduli, which finally levels off.

3.3. Kinetics of metal stearate accelerated polymerization

DSC traces of a representative formulation (ZnSt10C-a) at various heating rates viz. 5, 7 and 10 °C/min are presented in Fig. 6. Increasing the heating rate (β) leads to systematic shift in the trace towards higher temperatures, which can be attributed to the reduced time available with the reactants at higher heating rates. The curing of cardanol based benzoxazine resin is typically a multi-step process, which exhibits complex reaction kinetics [43–45]. The process is accompanied with a dramatic change in the physical state of the reaction medium. At the early stages, the reaction medium is a liquid composing primarily of monomers. With the progress of the reaction, the molecular weight and viscosity of the polymer formed increases, which in turn results in a decrease in the molecular mobility. The sudden decrease in the mobility however occurs with the cross-linking of polymer chains, where the chains lose their ability to move past one another, and the medium turns to a solid that can be either rubbery or glassy, depending upon the T_g of the cured resin. Characteristic parameters associated with the curing of the resin i.e. ΔH_{cure}, T_{onset} and T_{peak} are summarized in Table 2.

The extent of conversion, α at any particular temperature (T_α) was calculated as the ratio of the areas under the exothermic DSC peak and expressed as:

$$\alpha = \frac{\Delta H_{T_\alpha}}{\Delta H_{cure}} \tag{1}$$

where ΔH_{T_α} is the heat of reaction of partially cured samples (till temperature T_α) and ΔH_{cure} is the total heat of curing. The increase in the degree of conversion with temperature for ZnSt10C-a at different heating rates is presented in Fig. 7(i).

It can be seen that in the presence of zinc(II) stearate, complete curing is attained at ~203 °C while the same for a neat monomer is achieved at 280 °C [26], clearly demonstrating the effectiveness of zinc(II) stearate as an curing accelerator for benzoxazine.

In view of its simplicity, Kissinger–Akahira–Sunose equation [46] was applied for determination of activation energies (E_α) from the plot of $ln\left(\frac{\beta_i}{T_{\alpha,i}^2}\right)$ against $1/T_\alpha$.

$$ln\left(\frac{\beta_i}{T_{\alpha,i}^2}\right) = \text{Constant} - \frac{E_\alpha}{RT_{\alpha,i}} \tag{2}$$

Where, β is the heating rate, T_α is the temperature associated with a particular conversion (α) at the corresponding heating rate, E_α is the activation energy at that α and R is the gas constant. The linear plots at few representative conversions for ZnSt10C-a are presented in Fig. 7(ii), which were used to arrive at the activation energy. The variation in E_α with degree of conversion for ZnSt10C-a is presented
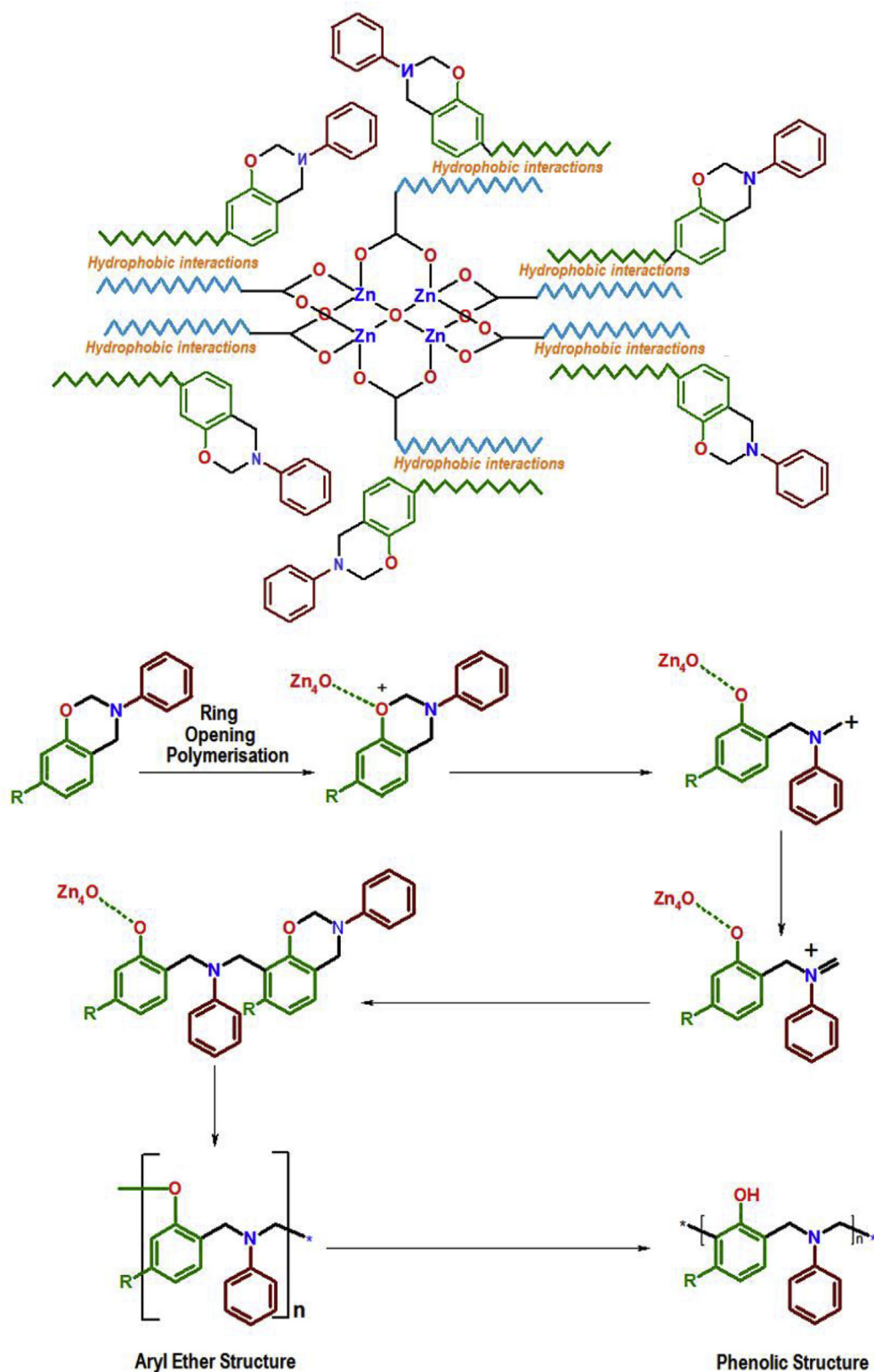
Fig. 4. i) Hydrophobic interactions present within zinc(II) stearate and C-a resulting in uniform dispersion of accelerator in the resin. ii) Proposed mechanism for ring opening polymerization of C-a in the presence of zinc(II) stearate as curing accelerator.

in supplementary section (Fig. S3) and the average value is reported in Table 2. The presence of zinc(II) stearate led to a substantial decrease in the activation energy from 98 kJ/mol for neat resin to 51 kJ/mol (ZnSt10C-a).

3.4. Thermal properties of polybenzoxazines

Thermogravimetric analysis was performed on the cured resins, to investigate the effect of introducing zinc(II) stearate on the
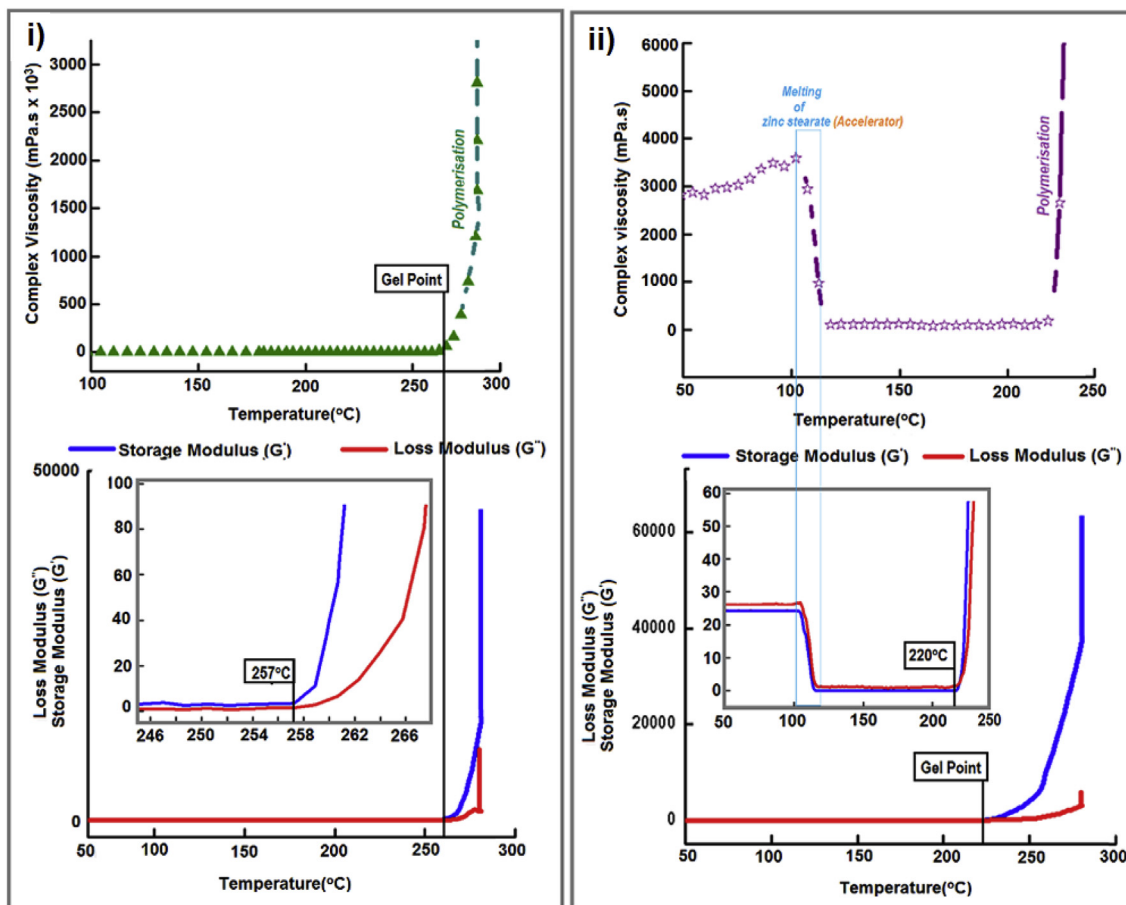
Fig. 5. Rheological behavior of i) C-a and ii) ZnSt10C-a during polymerization.
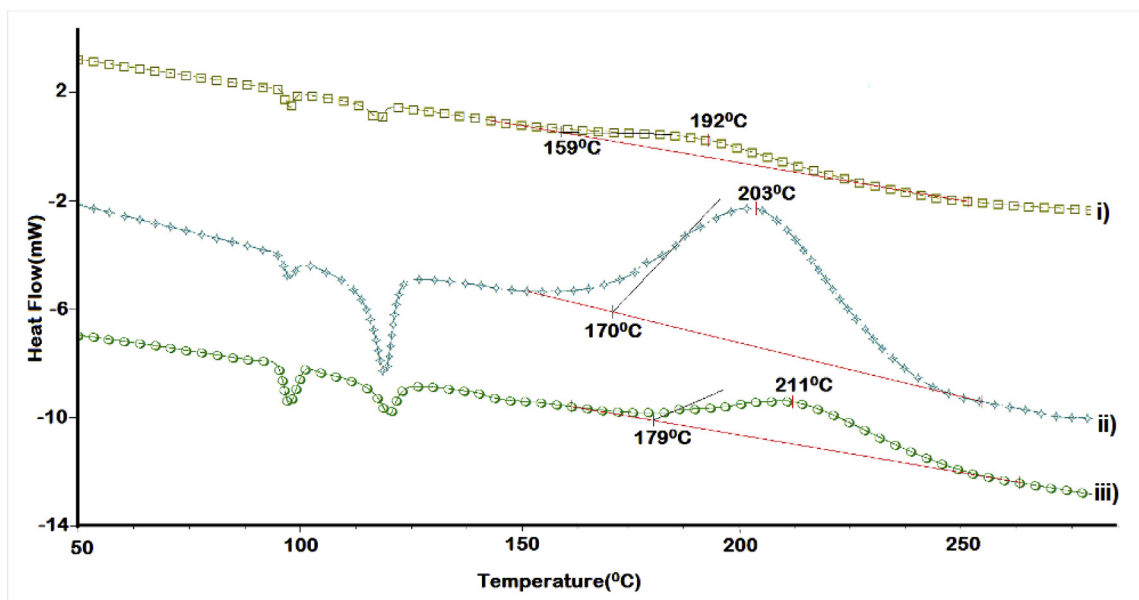
Fig. 6. Effect of heating rate(β) on the curing profile of ZnSt10C-a i) 5, ii) 10 and iii) 15 °C/min.

thermal stability of cardanol based polybenzoxazine. The TG and DTG traces of poly(C-a) and poly(ZnSt10C-a) are presented in Fig. 8. The thermal decomposition of cardanol based benzoxazines is a multi-step process occurring through the degradation of the phenolic linkages and of the Mannich bridges in the poly-benzoxazine [47,48]. The double bond α-carbon of the cardanol

Table 2
Characteristic curing parameters of C-a (neat benzoxazine)and ZnSt10C-a.

Sample	β(°C/min)	T_{onset}(°C)	T_{peak}(°C)	Activation energy (kJ/mol)
C-a	5	224	246	98
	10	236	255	
	15	241	263	
ZnSt10C-a	5	159	192	51
	10	170	203	
	15	179	211	

undergoes scission at ~200 °C [49] and the methylene linkages in the cured polymer have been reported to undergo cleavage at 440—500 °C [50].

Decomposition temperatures associated with characteristic mass loss at 5%, 10% and char content (at 600 °C) are presented in Table 3. An appreciable increase in the $T_{5\%}$ and $T_{10\%}$ values is evident from the traces, and the increase in the char content can be attributed to the presence of zinc oxide formed during the thermal degradation of the cured formulation. Polybenzoxazines have been reported to exhibit excellent fire, smoke and toxicity (FST) properties, which can be preliminarily adjudged through Limiting oxygen index (LOI) studies. The same refers to the minimum amount of oxygen (%) in an oxygen-nitrogen mixture that is just sufficient to maintain combustion (post-ignition) of the material [51]. A significant correlation between the char residue (CR) and LOI has been reported, LOI = 17.5 + 0.4 × CR [52]. The LOI for poly(C-a) was calculated to be 24, which is considered to be suitable for application of these polymers in areas necessitating flame retardance [14]. The same was found to increase substantially to 28 upon addition of 10 %w/w zinc stearate indicating superior flame retardancy of the developed formulation.

4. Conclusions

The accelerating ability of zinc(II) stearate on the ring opening polymerization of a representative bio-based cardanol based benzoxazine(C-a) has been systematically studied. Addition of zinc(II) stearate(10%w/w) in the resin, was found to decrease the curing temperature of neat benzoxazine from ~263 °C to ~202 °C (23% decrease). This exceptional accelerating ability has been attributed to the presence of acidic Zn_4O nodes in addition to the long alkyl chain of stearate, which helps in the dispersion of the
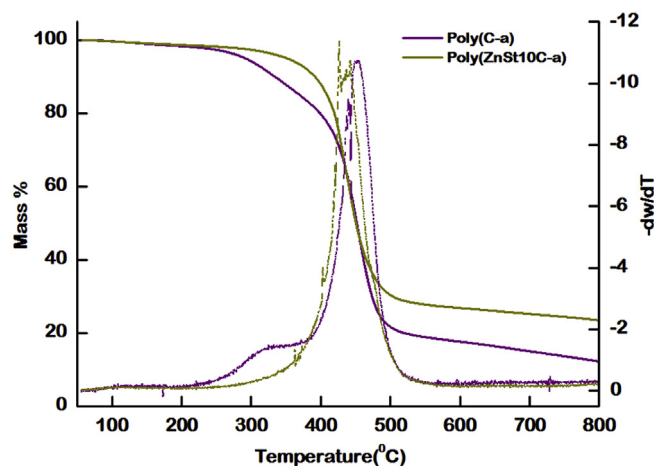

Fig. 8. TG-DTG traces of Poly(C-a) and Poly(ZnSt10C-a).

Table 3
Characteristic thermo-oxidative degradation parameters.

Sample Designation	$T_{5\%}$ (°C)	$T_{10\%}$(°C)	Char content at 600 °C (%)	LOI
Poly (C-a)	292	331	18	24
Poly(ZnSt10C-a)	351	390	27	28

accelerator in the resin. KAS method was used to determine the activation energy of polymerization, which was found to decrease from 98 kJ/mol (neat resin) to 51 kJ/mol for formulation containing zinc(II) stearate (10%w/w). The cured resins obtained in the presence of zinc(II) stearate exhibited relatively high thermal stability ($T_{5\%}$ = 351 °C) as compared to the neat polymer ($T_{5\%}$ = 292 °C). Our studies clearly highlight the enormous scope of metal stearates as eco-friendly accelerators for polymerization of bio-based benzoxazine resins, which requires high temperatures for curing. In view of the flexibility in designing and controlling the architecture of these hybrid structures, sustainable benzoxazine systems with low curing temperatures and improved performance can be formulated in the future.

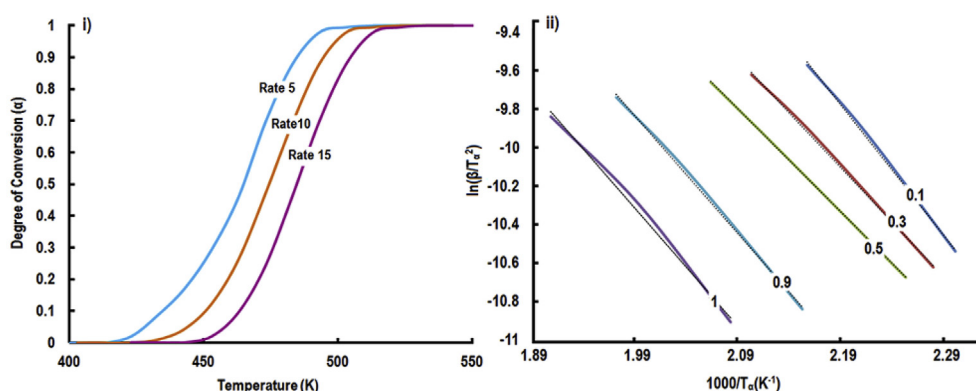

Fig. 7. i) Effect of temperature on the degree of conversion of cardanol based benzoxazine in the presence and absence of zinc(II) stearate (β = 5, 10 and 15 °C/min) ii) Iso-conversion plots associated with various degree of conversions (α).

Acknowledgements

Appendix A. Supplementary data

Supplementary data related to this article can be found at https://doi.org/10.1016/j.polymer.2018.01.084.

References

[1] H. Ishida, H.Y. Low, A study on the volumetric expansion of benzoxazine-based phenolic resin, Macromolecules 30 (4) (1997) 1099–1106.

[2] H. Ishida, D.J. Allen, Physical and mechanical characterization of near-zero shrinkage polybenzoxazines, J. Polym. Sci. B Polym. Phys. 34 (6) (1996) 1019–1030.

[3] S.B. Shen, H. Ishida, Development and characterization of high-performance polybenzoxazine composites, Polym. Compos. 17 (5) (1996) 710–719.

[4] N.N. Ghosh, B. Kiskan, Y. Yagci, Polybenzoxazines—new high performance thermosetting resins: synthesis and properties, Prog. Polym. Sci. 32 (11) (2007) 1344–1391.

[5] Y. Yagci, B. Kiskan, N.N. Ghosh, Recent advancement on polybenzoxazine—a newly developed high performance thermoset, J. Polym. Sci. Polym. Chem. 47 (21) (2009) 5565–5576.

[6] P. Thirukumaran, A. Shakila Parveen, M. Sarojadevi, Synthesis and copolymerization of fully biobased benzoxazines from renewable resources, ACS Sustain. Chem. Eng. 2 (12) (2014) 2790–2801.

[7] O.S. Taskin, B. Kiskan, A. Aksu, N. Balkis, J. Weber, Y. Yagci, Polybenzoxazine: a powerful tool for removal of mercury salts from water, Chem. A Eur. J. 20 (35) (2014) 10953–10958.

[8] E. Calo, A. Maffezzoli, G. Mele, F. Martina, S.E. Mazzetto, A. Tarzia, C. Stifani, Synthesis of a novel cardanol-based benzoxazine monomer and environmentally sustainable production of polymers and bio-composites, Green Chem. 9 (7) (2007) 754–759.

[9] P. Sharma, B. Lochab, D. Kumar, P.K. Roy, Sustainable bis-benzoxazines from cardanol and PET-derived terephthalamides, ACS Sustain. Chem. Eng. 4 (3) (2015) 1085–1093.

[10] H. Ishida, Y. Rodriguez, Catalyzing the curing reaction of a new benzoxazine-based phenolic resin, J. Appl. Polym. Sci. 58 (10) (1995) 1751–1760.

[11] A. Sudo, S. Hirayama, T. Endo, Highly efficient catalysts-acetylacetonato complexes of transition metals in the 4th period for ring-opening polymerization of 1,3-benzoxazine, J. Polym. Sci. Polym. Chem. 48 (2) (2010) 479–484.

[12] P. Sharma, B. Lochab, D. Kumar, P.K. Roy, Interfacial encapsulation of bio-based benzoxazines in epoxy shells for temperature triggered healing, J. Appl. Polym. Sci. 132 (47) (2015), https://doi.org/10.1002/app.42832.

[13] P. Sharma, S. Shukla, B. Lochab, D. Kumar, P. Kumar Roy, Microencapsulated cardanol derived benzoxazines for self-healing applications, Mater. Lett. 133 (2014) 266–268.

[14] S. Shukla, A. Mahata, B. Pathak, B. Lochab, Cardanol benzoxazines - interplay of oxazine functionality (mono to tetra) and properties, RSC Adv. 5 (95) (2015) 78071–78080.

[15] P. Sharma, D. Kumar, P.K. Roy, Poly(benzoxazine–co–urea): a solventless approach towards the introduction of alternating urea linkages in polybenzoxazine, ChemistrySelect 2 (19) (2017) 5372–5377.

[16] P. Sharma, D. Kumar, P.K. Roy, Microwave-assisted sustainable synthesis of telechelic poly(ethylene glycol)s with benzoxazine end groups, ChemistrySelect 1 (21) (2016) 6941–6947.

[17] A. Sudo, T. Endo, A. Taden, R. Schoenfeld, T. Huver, Benzoxazine-containing formulations polymerizable/curable at low temperature, US20100144964 A1 (2010).

[18] L. Zhang, J. Mao, S. Wang, Y. Yang, Y. Chen, H. Lu, Meta-phenylenediamine formaldehyde oligomer: a new accelerator for benzoxazine resin, React. Funct. Polym. 121 (Supplement C) (2017) 51–57.

[19] W. Chow, S. Grishchuk, T. Burkhart, J. Karger-Kocsis, Gelling and curing behaviors of benzoxazine/epoxy formulations containing 4, 4′-thiodiphenol accelerator, Thermochim. Acta 543 (2012) 172–177.

[20] A.A. Gallo, Method for preparing polybenzoxazine, US 6376080 B1 (2002).

[21] Y.X. Wang, H. Ishida, Cationic ring-opening polymerization of benzoxazines, Polymer 40 (16) (1999) 4563–4570.

[22] H. Ishida, Cationic ring-opening polymerization of benzoxazines, US6225440 B1 (2001).

[23] J. Sun, W. Wei, Y. Xu, J. Qu, X. Liu, T. Endo, A curing system of benzoxazine with amine: reactivity, reaction mechanism and material properties, RSC Adv. 5 (25) (2015) 19048–19057.

[24] B.A.A. Rucigaj, M. Krajnc, U. Sebenik, Curing of bisphenol A-aniline based benzoxazine using phenolic, amino and mercapto accelerators, Express

[25] A. Sudo, R. Kudoh, H. Nakayama, K. Arima, T. Endo, Selective formation of poly(N,O-acetal) by polymerization of 1,3-benzoxazine and its main chain rearrangement, Macromolecules 41 (23) (2008) 9030–9034.

[26] P. Sharma, M. Srivastava, B. Lochab, D. Kumar, A. Ramanan, P.K. Roy, Metal-Organic Frameworks as curing accelerators for benzoxazines, ChemistrySelect 1 (13) (2016) 3924–3932.

[27] D. Undurraga, A. Markovits, S. Erazo, Cocoa butter equivalent through enzymic interesterification of palm oil midfraction, Process Biochem. 36 (10) (2001) 933–939.

[28] Z. Wang, Q. Li, Z. She, F. Chen, L. Li, X. Zhang, P. Zhang, Facile and fast fabrication of superhydrophobic surface on magnesium alloy, Appl. Surf. Sci. 271 (2013) 182–192.

[29] H. ısmet Gökçel, D. Balköse, U. Köktürk, Effects of mixed metal stearates on thermal stability of rigid PVC, Eur. Polym. J. 35 (8) (1999) 1501–1508.

[30] L.M.Z. Wengong, Research on the new heat stabilizer of calcium soap and zinc soap with high efficiency and less toxicity [J], Polyvingyi chloride 1 (2000) 010.

[31] P.K. Roy, P. Surekha, R. Raman, C. Rajagopal, Investigating the role of metal oxidation state on the degradation behaviour of LDPE, Polym. Degrad. Stabil. 94 (7) (2009) 1033–1039.

[32] E. Richard, C. Anandan, S.T. Aruna, Fabrication of superhydrophobic zinc stearate hierarchical surfaces from different precursors, Mater. Manuf. Process. 31 (9) (2016) 1171–1176.

[33] J. Dunkers, H. Ishida, Reaction of benzoxazine-based phenolic resins with strong and weak carboxylic acids and phenols as catalysts, J. Polym. Sci. Polym. Chem. 37 (13) (1999) 1913–1921.

[34] P. Chutayothin, H. Ishida, Cationic ring-opening polymerization of 1,3-benzoxazines: mechanistic study using model compounds, Macromolecules 43 (10) (2010) 4562–4572.

[35] C. Liu, D. Shen, R.M. Sebastián, J. Marquet, R. Schönfeld, Mechanistic studies on ring-opening polymerization of benzoxazines: a mechanistically based catalyst design, Macromolecules 44 (12) (2011) 4616–4622.

[36] G. Riess, J.M. Schwob, G. Guth, M. Roche, B. Laude, Ring opening polymerization of benzoxazines — a new route to phenolic resins, in: B.M. Culbertson, J.E. McGrath (Eds.), Advances in Polymer Synthesis, Springer US, Boston, MA, 1985, pp. 27–49.

[37] Y.-X. Wang, H. Ishida, Synthesis and properties of new thermoplastic polymers from substituted 3,4-Dihydro-2H-1,3-benzoxazines, Macromolecules 33 (8) (2000) 2839–2847.

[38] P.K. Roy, P. Sharma, D. Kumar, Process for preparation of polybenzoxazines, Indian Patent 201711005289 (2017).

[39] D. Lison, Human toxicity of cobalt-containing dust and experimental studies on the mechanism of interstitial lung disease (hard metal disease), Crit. Rev. Toxicol. 26 (6) (1996) 585–616.

[40] T. Ishioka, K. Maeda, I. Watanabe, S. Kawauchi, M. Harada, Infrared and XAFS study on structure and transition behavior of zinc stearate, Spectrochim. Acta Mol. Biomol. Spectrosc. 56A (9) (2000) 1731–1737.

[41] R. Huang, S.O. Carson, J. Silva, T. Agag, H. Ishida, J.M. Maia, Interplay between rheological and structural evolution of benzoxazine resins during polymerization, Polymer 54 (7) (2013) 1880–1886.

[42] P.J. Halley, M.E. Mackay, Chemorheology of thermosets—an overview, Polym. Eng. Sci. 36 (5) (1996) 593–609.

[43] H. Ishida, Y. Rodriguez, Curing kinetics of a new benzoxazine-based phenolic resin by differential scanning calorimetry, Polymer 36 (16) (1995) 3151–3158.

[44] C. Jubsilp, S. Damrongsakkul, T. Takeichi, S. Rimdusit, Curing kinetics of arylamine-based polyfunctional benzoxazine resins by dynamic differential scanning calorimetry, Thermochim. Acta 447 (2) (2006) 131–140.

[45] C. Jubsilp, K. Punson, T. Takeichi, S. Rimdusit, Curing kinetics of benzoxazine–epoxy copolymer investigated by non-isothermal differential scanning calorimetry, Polym. Degrad. Stabil. 95 (6) (2010) 918–924.

[46] P. Budrugeac, E. Segal, Applicability of the Kissinger equation in thermal analysis, J. Therm. Anal. Calorim. 88 (3) (2007) 703–707.

[47] H. Yee Low, H. Ishida, Structural effects of phenols on the thermal and thermo-oxidative degradation of polybenzoxazines, Polymer 40 (15) (1999) 4365–4376.

[48] S.-i. Kuroda, K. Terauchi, K. Nogami, I. Mita, Degradation of aromatic polymers—I. Rates of crosslinking and chain scission during thermal degradation of several soluble aromatic polymers, Eur. Polym. J. 25 (1) (1989) 1–7.

[49] S. Manjula, C.K.S. Pillai, V.G. Kumar, Thermal characterization of cardanol-formaldehyde resins and cardanol-formaldehyde/poly(methyl methacrylate) semi-interpenetrating polymer networks, Thermochim. Acta 159 (1990) 255–266.

[50] D. O'Connor, F.D. Blum, Thermal stability of substituted phenol-formaldehyde resins, J. Appl. Polym. Sci. 33 (6) (1987) 1933–1941.

[51] C.A. Wilkie, A.B. Morgan, Fire Retardancy of Polymeric Materials, CRC press, 2009.

[52] D.W. van Krevelen, Some basic aspects of flame resistance of polymeric materials, Polymer 16 (8) (1975) 615–620.